NASA TECHNICAL NOTE

NASA TN D-7856

NASA TN D-7856

FLAPPING RESPONSE CHARACTERISTICS OF HINGELESS ROTOR BLADES BY A GENERALIZED HARMONIC BALANCE METHOD

David A. Peters and Robert A. Ormiston

Ames Research Center

and

U.S. Army Air Mobility R&D Laboratory

Moffett Field, Calif. 94035

NATIONAL AERONAUTICS AND SPACE ADMINISTRATION • WASHINGTON, D. C. • FEBRUARY 1975

1. Report No.	2. Government Accession No.	3. Recipient's Catalog No.
NASA TN D-7856		

4. Title and Subtitle	5. Report Date
FLAPPING RESPONSE CHARACTERISTICS OF HINGELESS ROTOR BLADES BY A GENERALIZED HARMONIC BALANCE METHOD	February 1975
	6. Performing Organization Code

7. Author(s)	8. Performing Organization Report No.
David A. Peters and Robert A. Ormiston	A-5494
	10. Work Unit No.

9. Performing Organization Name and Address	11. Contract or Grant No.
Ames Research Center, NASA and U. S. Army Air Mobility R&D Laboratory Moffett Field, Calif., 94035	
	13. Type of Report and Period Covered
12. Sponsoring Agency Name and Address	Technical Note
National Aeronautics and Space Administration Washington, D. C. 20546	14. Sponsoring Agency Code

15. Supplementary Notes

16. Abstract

Linearized equations of motion for the flapping response of flexible rotor blades in forward flight are derived in terms of generalized coordinates. The equations are solved using a matrix form of the method of linear harmonic balance, yielding response derivatives for each harmonic of the blade deformations and of the hub forces and moments. Numerical results and approximate closed-form expressions for rotor derivatives are used to illustrate the relationships between rotor parameters, modeling assumptions, and rotor response characteristics. Finally, basic hingeless rotor response derivatives are presented in tabular and graphical form for a wide range of configuration parameters and operating conditions.

17. Key Words (Suggested by Author(s))	18. Distribution Statement
Hingeless rotor Helicopter Stability and control	Unclassified - Unlimited STAR Category 02

19. Security Classif. (of this report)	20. Security Classif. (of this page)	21. No. of Pages	22. Price*
Unclassified	Unclassified	140	$4.75

*For sale by the National Technical Information Service, Springfield, Virginia 22151

TABLE OF CONTENTS

NOMENCLATURE

a	nominal lift curve slope, rad^{-1}, equation (22)
a_n, A_n	Fourier coefficients of $\cos(n\psi)$, equation (B11)
$(a_n)_f$	Fourier coefficient for $f(\psi)$, equation (B1)
$\bar{a}(r,\psi)$	local lift curve slope, rad^{-1}, equation (18)
$[A(\psi)], A_{jm}$	Floquet modal function matrix, equation (34)
b	number of blades, equation (50)
b_n, B_n	Fourier coefficients of $\sin(n\psi)$, equation (B11)
$(b_n)_f$	Fourier coefficient for $f(\psi)$, equation (B1)
B	tip loss factor, equation (56)
c	nominal blade chord, m, equation (22)
c_ℓ	lift coefficient, equation (18)
$\bar{c}(r)$	local blade chord, m, equation (18)
C	hingeless rotor parameter $= \frac{8(P^2 - 1)}{\gamma} = \frac{8K_\beta}{\Omega^2 \rho a c R^4}$ for centrally hinged rigid blade, equations (52) and (53)
$C(k)$	Theodorsen function, equation (A8)
$\bar{C}_{L_{\alpha_c}}$	roll moment coefficient derivative with respect to α_c, $\frac{\partial (a_o)\bar{C}_L}{\partial \alpha_c}$
$\bar{C}_{L_{\theta_c}}$	roll moment coefficient derivative with respect to θ_c, $\frac{\partial (a_o)\bar{C}_L}{\partial \theta_c}$
$\bar{C}_{L_{\theta_o}}$	roll moment coefficient derivative with respect to θ_o, $\frac{\partial (a_o)\bar{C}_L}{\partial \theta_o}$
$\bar{C}_{L_{\theta_s}}$	roll moment coefficient derivative with respect to θ_s, $\frac{\partial (a_o)\bar{C}_L}{\partial \theta_s}$
$\bar{C}_{M_{\alpha_c}}$	pitch moment coefficient derivative with respect to α_c, $\frac{\partial (a_o)\bar{C}_M}{\partial \alpha_c}$

$\overline{C}_{M_{\theta_c}}$ pitch moment coefficient derivative with respect to θ_c, $\frac{\partial(a_o)\overline{C}_M}{\partial\theta_c}$

$\overline{C}_{M_{\theta_o}}$ pitch moment coefficient derivative with respect to θ_o, $\frac{\partial(a_o)\overline{C}_M}{\partial\theta_o}$

$\overline{C}_{M_{\theta_s}}$ pitch moment coefficient derivative with respect to θ_s, $\frac{\partial(a_o)\overline{C}_M}{\partial\theta_s}$

$\overline{C}_{S_{\theta_o}}$ root moment coefficient derivative with respect to θ_o, $\frac{\partial(a_o)\overline{C}_S}{\partial\theta_o}$

$\overline{C}_{S2_{\theta_o}}$ second harmonic root moment coefficient with θ_o, equation (54d),

$$= \sqrt{\left[\frac{\partial(a_2)\overline{C}_S}{\partial\theta_o}\right]^2 + \left[\frac{\partial(b_2)\overline{C}_S}{\partial\theta_o}\right]^2}$$

C_S, C_L, C_M root, roll, and pitch moment coefficients, $\frac{S,L,M}{\rho(\Omega R)^2\pi R^3}$, equation (13)

$\overline{C}_{T_{\alpha_c}}$ thrust coefficient derivative with respect to α_c, $\frac{\partial(a_o)\overline{C}_T}{\partial\alpha_c}$

$\overline{C}_{T_{\theta_c}}$ thrust coefficient derivative with respect to θ_c, $\frac{\partial(a_o)\overline{C}_T}{\partial\theta_c}$

$\overline{C}_{T_{\theta_o}}$ thrust coefficient derivative with respect to θ_o, $\frac{\partial(a_o)\overline{C}_T}{\partial\theta_o}$

$\overline{C}_{T_{\theta_s}}$ thrust coefficient derivative with respect to θ_s, $\frac{\partial(a_o)\overline{C}_T}{\partial\theta_s}$

C_V, C_T — shear and thrust coefficients, $\frac{V,T}{\rho(\Omega R)^2 \pi R^2}$, equations (13) and (50)

$\left.\begin{matrix}\bar{C}_V, \bar{C}_T, \bar{C}_S \\ \bar{C}_L, \bar{C}_M\end{matrix}\right\}$ rotor coefficients = $\frac{C_V, C_T, C_S, C_L, C_M}{\sigma a} = \frac{V,T}{\rho acR^3\Omega^2}, \frac{S,L,M}{\rho acR^4\Omega^2}$, equations (13), (50), and (51)

$\left.\begin{matrix}D^C, D^K, \\ D^A, D^V\end{matrix}\right\}$ aerodynamic integrals, equations (30) and (A15)

e — dimensionless hinge offset $\frac{\varepsilon}{R}$, equation (9)

e_{ac} — aerodynamic center offset, distance aerodynamic center lies forward of elastic axis divided by $\bar{c}$, equation (A8)

e_{rc} — dimensionless root cutout, equation (56)

EI — beam cross-sectional bending stiffness, N-m^2, equation (1)

f_ε — nonintegral portion of Lagrangian, N-m, equation (1)

f,n — complex Fourier coefficients, equation (B1)

f(r) — integrand of Lagrangian, N, equation (1)

$\left.\begin{matrix}f(\psi), g(\psi), \\ h(\psi)\end{matrix}\right\}$ general periodic functions of azimuth, equation (B11)

F(r) — aerodynamic loading, equation (2)

$\bar{F}(r)$ — dimensionless aerodynamic loading $\frac{F(r)}{\Omega^2 \rho acR^3}$, equation (9)

g — vertical component of local inertial force field, m/sec^2, equation (A1)

g_o, g_s, g_c — generalized inertial forces, equation (A4)

$\left.\begin{matrix}[H_q], [H_V], \\ [H_S]\end{matrix}\right\}$ harmonic balance multiplier matrices, equations (45) and (47)

i — $\sqrt{-1}$, equation (38); or an index if used as a subscript, c.f. equation (7)

I	number of inflow harmonics, equation (A11)
$\mathrm{Im}(\ )$	imaginary part of complex number, equation (B24)
$[I_m]$	mth order identity matrix, equation (32)
IN	number of azimuthal increments used to determine Fourier series
I_y	flapping inertia of centrally hinged blade = $\int_o^R mr^2\,dr$, kg-m^2, equation (53)
j	index, equation (5)
J	number of modal coordinates, equation (5)
J_L	Lagrangian, equations (1) and (A1)
k	reduced frequency = $\frac{\bar{c}(\omega \pm n)}{2U_y}$, equation (A8); or an index when used as a subscript or exponent, c.f. equations (26) and (39)
K	number of control variables, equation (27); or order of derivative, equation (B10)
K_β	root flapping spring restraint stiffness, N-m/rad, equation (1)
$K_{ij}, [K]$	generalized stiffness, equation (9) or (33)
ℓ	lift on blade element, N, equation (18)
L	roll moment for b blades (right side down), N-m, equation (48)
m	mass per unit blade length, kg/m, equation (1); or an index when used as a subscript
$\bar{m}$	dimensionless blade mass, equation (A4)
$m_{ij}, [m]$	generalized mass, equation (9)
$m_{yo}, m_{yy}, m_{yj}, \langle m_y \rangle$	modal parameters, $\langle m_y \rangle = \langle m_{y1}, \ldots, m_{yJ} \rangle$, equations (13b) and (A4)

M	pitch moment for b blades (nose-up), N-m, equation (48)
$M(r,\psi)$	local Mach number, equation (23)
n	harmonic number, equation (38)
N	number of harmonics, equation (38)
P	first flapping natural frequency divided by rotational frequency
$P_{ij}, [P]$	generalized centrifugal stiffness, equation (9)
P_j	inflow polynominals, equation (A11)
P_{oi}	centrifugal restoring force of built-in blade preshape, equation (A4)
$P_t(r)$	pretwist polynomial, equation (A9a)
$[P^{++}], [P^{+-}], [P^{--}], [P^{-+}]$	Fourier matrices, equation (B13)
$q_j, \bar{q}_j, \{q\}, \{\bar{q}\}$	generalized coordinates, equations (5) and (31)
q_o	amount of built-in blade preshape, equation (A3b)
Q^C, Q^K, Q^A, A^V	aerodynamic integrals, equations (30) and (A15)
r	radial distance along blade, m, equation (1), figure 1
$\bar{r}$	dimensionless distance $\frac{r}{R}$, equation (9)
$\vec{r}$	unit vector along undeformed blade, figure 2
R	blade radius, m, equation (1), figure 1
$Re(\ )$	real part of complex number, equation (B24)
s, s_θ, s_u, s_w	correction to lift-curve slope, equations (22) and (A7)
S	root bending moment for one blade, N-m, equations (10) and (11)
$S_y, S_j, \langle S \rangle$	blade inertial parameters, $\langle S \rangle = \langle S_1, \ldots, S_J \rangle$, equations (13b) and (A4)

t	time, sec, equation (1)
T	thrust for b blades, N, equation (48)
T_r	tension force in blade, N, equation (4)
$U_m, \{U\}$	Floquet coefficients, equation (37)
$U_x, U_y, U_z, \bar{U}_z$	airspeed in blade element axis system, m/sec, equations (17) and (A9b), figure 3
V	root shear for one blade, N, equations (10) and (11)
V_∞	freestream velocity, equation (16)
V_C, V_K, V_j	aerodynamic functions, equations (28) and (A13)
V_x, V_y, V_z	components of V_∞ in shaft-fixed axis system, m/sec, equation (16)
w	vertical displacement of blade element, m, equation (1), figure 1
w_o	built-in blade preshape, m, equation (A3b)
$\left.\begin{matrix} W^C, W^K \\ W^A, W^V \end{matrix}\right\}$	aerodynamic integrals, equations (30) and (A15)
$x_i, \{x\}$	general variables, equation (36)
$\vec{x}\ \vec{y}\ \vec{z}$	blade-fixed coordinates, figure 2
$\vec{X}\ \vec{Y}\ \vec{Z}$	shaft-fixed coordinates, figure 2
z	hub plunge displacement, positive down, m, equation (A1)
$[Z]$	combined stiffness matrix, equation (33)
α	blade element angle of attack, rad, equation (19), figure 3
α_c	shaft tilt in pitch (nose-up), rad, equation (16)
α_n	Fourier coefficients of $\cos(n\psi)$, equation (B11c)
α_s	shaft tilt in roll (right side down), rad, equation (A1)

β	flapping angle for rigid hinged blade, $\phi_1 = \bar{r} - e$, $q_1 = \beta$, rad, table 1
β_n	Fourier coefficients of $\sin(n\psi)$, equation (B11c)
γ	Lock number = $\frac{\rho a c R^4}{I_y}$, equations (53) and (A4)
γ_m	constants depending on initial conditions, equation (34)
δ	variational, equation (2)
Δ	phase angle, rad, equation (B5)
ε	flapping hinge offset, m, equation (9), figure 1
η	dummy integration variable, equation (4)
η_m	complex eigenvalues, equation (34)
θ	blade feathering angle, rad, equations (19) and (24), figure 3
$\theta_j, \{\theta\}$	generalized control vector for rotor, equations (27) and (A12)
$\theta_o, \theta_s, \theta_c$	collective and cyclic pitch, rad, equation (24)
θ_{q_j}	pitch-flap coupling of jth mode, equation (24)
θ_t	amount of pretwist, rad, equation (A9a)
$[\Theta_q], [\Theta_V], [\Theta_S], [\Theta_T], [\Theta_L], [\Theta_M]$	partial derivative matrices, equations (44), (46), and (49)
$\lambda_{js}, \lambda_{jc}$	Fourier components of λ, equation (A11)
$\lambda(r,\psi)$	inflow ratio, equation (A10)
μ	advance ratio, equation (25b)
$\nu(r,\psi)$	induced inflow, equation (A10c)

$[\Pi], [\overline{\Pi}]$	Fourier product matrix, modified matrix, equations (B14) and (B15)
ρ	density of air, kg/m^3, equation (18)
σ	rotor solidity $\frac{bc}{\pi R}$, equation (13a)
ϕ	inflow angle in blade coordinates, rad, equation (19), figure 3
ϕ_j	modal functions, equation (5)
ϕ_o	built-in blade preshape, equation (A3b)
$[\Phi]$	Fourier phase change matrix, equation (B6)
ψ	azimuth angle, rad, equation (4), figure 2
ω	frequency of control input, per rev, equations (A16) and (B17)
Ω	rotational frequency of blade, rad/sec, equation (4)
$[\square]$	Fourier derivative matrix, equation (B10)
$( )'$	$\frac{d}{d\bar{r}}$, equation (9)
$(\dot{})$	$\frac{d}{d\psi}$, equation (8)
$(\tilde{})$	corrected for reduced frequency variation between harmonics, equation (B22)
$[\ ]$	matrix
$\{\ \}$	column vector
$< >$	row vector

FLAPPING RESPONSE CHARACTERISTICS OF HINGELESS ROTOR BLADES BY A GENERALIZED HARMONIC BALANCE METHOD

David A. Peters
and
Robert A. Ormiston

Ames Research Center, NASA
and
U. S. Army Air Mobility R&D Laboratory

SUMMARY

Linearized equations of motion for the flapping response of flexible rotor blades in forward flight are derived and used for calculating thrust and moment response derivatives of hingeless rotors. The equations are based on linear, quasi-steady, strip-theory aerodynamics neglecting induced downwash but including the effects of reversed flow and compressibility. Lead-lag bending, torsional deformations of the blade, and unsteady hub motions are not included in the basic equations. The blade equations are extended in an appendix, however, to include unsteady aerodynamics, nonuniform inflow, unsteady hub motions, and unsteady control inputs. The differential equations of motion for the generalized coordinates of the blade bending modes are solved using a harmonic balance method. The method is generalized in matrix form so that the system of differential equations may be transformed by appropriate Fourier operators into algebraic equations for the harmonics of the blade flapping response. Analytical and numerical results are presented for use in determining rotor response derivatives for the thrust, pitch moment, and roll moment with respect to collective and cyclic pitch and rotor shaft angle of attack for a variety of different system parameters. Simple analytical expressions for the derivatives are presented that are valid at low advance ratios for a rigid, spring restrained, centrally hinged blade representation. A series of numerical results are presented for a typical hingeless rotor configuration to illustrate the basic response behavior as a function of each of the four main system parameters. Results are also presented to indicate the range of validity of a series of approximations for the blade equations of motion. Truncation errors, reversed flow, compressibility, and approximate mode shapes are examined in detail. Supplementary charts and tables of the rotor response derivatives are presented in an appendix to facilitate rapid estimation of the derivatives for preliminary design purposes.

INTRODUCTION

The hingeless rotor, although not a recent development, is finding increasing application for helicopters and low disk-loading VTOL aircraft. Because of its special configuration, it offers several advantages over

conventional articulated rotors. The basic difference between hingeless and articulated rotors is in the attachment of the blades to the hub. The blades of the hingeless rotor (also called the rigid rotor or nonarticulated rotor) are attached directly to the hub without the flapping and lead-lag hinges of articulated rotors. The feathering hinge, or bearing, is usually retained to control the blade pitch angle. Eliminating hinges simplifies the rotor mechanically and can potentially reduce weight and aerodynamic drag. Furthermore, the cantilever blades transfer aerodynamic bending moments to the hub and thus, unlike hinged rotors, produce large rotor hub moments. This hub moment capability provides the hingeless rotor with much higher control power and angular damping than is available with articulated rotors; as a result, the flying qualities of a hingless rotor helicopter may be improved substantially. However, the increased hub moments of the hingeless rotor can also produce undesirable effects. For example, pitch and roll cross-coupling, lift-roll coupling, static angle-of-attack instability (pitch-up), gust sensitivity, and rotor vibratory moments are all increased, especially at high speeds and for configurations having blades with high flap bending stiffness.

This report presents a detailed and comprehensive study of the basic hingeless rotor response characteristics. The properties noted above influence mainly the stability and control characteristics or flying qualities of hingeless rotor helicopters. Therefore, the response characteristics of interest are the rotor derivatives (also called stability and control derivatives), which are defined as the partial derivatives of the steady-state force and moment response of the rotor taken with respect to control inputs or changes in the rotor operating condition. In the present context, response characteristics can also include derivatives of the harmonics of rotor forces and moments and also frequency response from harmonic control inputs. This report does not deal with the stability of transient rotor responses.

The purpose of the report is to provide a basic understanding of hingeless rotor response characteristics and to improve the accuracy of calculating these response characteristics. Linear partial differential equations are presented for the flapping motion, thrust, and root flap bending moment of an elastic rotor blade using linear aerodynamic theory that is valid for forward flight. The equations are reduced to modal form by the Rayleigh-Ritz method and solved by a generalized matrix formulation of a harmonic balance method. The basic response behavior of typical hingeless rotor configurations is described in terms of the basic system parameters: advance ratio, fundamental blade flapping frequency, Lock number, and pitch-flap coupling. The sensitivity of hingeless rotor response to approximations in mathematical and structural modeling is examined in detail and the limits of accuracy for commonly used assumptions are established. Finally, tabulations of several important rotor derivatives are included for a range of typical hingeless rotor configurations. Only the basic derivatives for thrust, pitch moment, and roll moment in response to collective pitch, longitudinal and lateral cyclic pitch, and angle of attack are considered. It is not intended to provide all force and moment derivatives necessary for a quasistatic flight dynamics analysis.

The need for the present study is based on the following: First, the stability and control derivatives for hingeless rotors are larger and more

sensitive to configuration parameters and operating conditions than are the derivatives for articulated rotors. These properties are therefore crucial to the design of hingeless rotor helicopters, and it is particularly important to have a comprehensive and general understanding of them. Second, several different approximate mathematical models of the hingeless rotor have been developed. The validity of these methods has not been adequately established and further attention is required. Third, no published references contain a comprehensive description or tabulation of the primary hingeless rotor derivatives for a broad range of basic configuration parameters. Most available references are limited to the development of methods for estimating derivatives or evaluating the accuracy of various approximate methods. Several proprietary methods have been developed for predicting hingeless rotor derivatives for design purposes, but these sophisticated techniques usually yield only limited information and are not practical for producing sufficient results to illustrate the basic properties of hingeless rotor derivatives.

Several previous investigations of hingeless rotor response characteristics are available in the literature. A significant part of these investigations pertains to the development of approximate mathematical models for the hingeless rotor. A brief review of this literature illustrates the factors involved in these approximate mathematical models and will help to introduce the subject of this report.

In one of the earliest investigations (ref. 1), at low advance ratios, Payne described some general features of a centrally hinged, rigid blade with hinge restraint, a configuration similar in many respects to the hingeless rotor. The high control power and damping were noted and the variation of moment response with hinge restraint was studied.

Young (ref. 2) developed a simplified theory for use in preliminary design, where the flapping motion of an elastic blade was approximated by a rigid blade with an offset flapping hinge and spring restraint. The offset distance and spring stiffness were determined by the fundamental nonrotating and rotating frequencies, respectively, of the elastic blade. Young also described the increased control power, angular damping, and pitch/roll coupling of the hingeless rotor.

Sissingh (ref. 3) investigated the response characteristics of the hingeless rotor at high forward speeds. A centrally hinged, spring-restrained, rigid blade model was used and the effects of reversed flow on the periodic coefficients of the flapping equation of motion were included. Solutions obtained with an analog computer showed the sensitivity of response for various values of Lock number and blade flapping frequency at high advance ratios.

Bramwell (ref. 4) developed a simplified method for determining the stability derivatives of a hingeless rotor helicopter. A rigid blade with an offset flapping hinge was used and charts were presented for obtaining the rotor force and moment derivatives. Unlike Young, Bramwell chose the hinge offset based on the fundamental flap bending mode shape of the elastic blade; that is, the rigid blade was assumed tangent to the elastic blade at the rotor

blade tip. Little discussion on hingeless rotor properties was given except to note the typical high moment response.

Shupe (ref. 5) and Curtiss (ref. 6) investigated additional refinements of the mathematical modeling. It was found that nonuniform downwash created by rotor hub moments could substantially influence the control power and damping. Shupe also showed that the offset hinge, rigid blade model of Young would lead to moderate inaccuracies as a result of aerodynamic approximations inherent in the choice of the blade mode shape, and that the rotor hub moments should be expressed in terms of integrated aerodynamic and inertial forces rather than the local internal elastic moment in the blade. Finally, using the elastic blade equations, Shupe studied the effects of the second flap bending mode (neglecting coupling with first mode bending) and found a significant effect at moderate advance ratios ($\mu \leq 0.5$).

Ormiston and Peters (ref. 7) investigated further the effects of approximate blade flapping mode shapes and higher flap bending modes using methods developed here. These results show that approximate modes are less accurate as the flapping frequency is reduced and that the effects of second mode flap bending are unimportant for low and moderate advance ratios.

Sissingh and Kuczynski (ref. 8) investigated the effects of torsion on the stability and flapping response of hingeless rotor blades. Except at very high advance ratios or for configurations with low torsional frequency or nearly resonant flap and torsion frequencies, the effects of flapping/torsion coupling were found to be small.

Hohenemser and Yin (ref. 9) showed that the importance of the second flapping mode found by Shupe was due to the neglect of the coupling terms between modes. In addition, a few results for blades with tapered mass distribution were presented.

Huber (ref. 10) investigated the combined effects of torsion, lead-lag bending, and flap bending on the stability and control characteristics of hingeless rotor helicopters. A rigid blade with offset hinges was used and the equations of motion were solved by numerical integration because of the nonlinear coupling of bending and torsion as well as nonlinear airfoil aerodynamics. It was found that the torsion and lead-lag degrees of freedom can be important for hingeless rotor response. However, the usual procedures for linearizing the nonlinear torsion terms permit them to be expressed as effective pitch-flap and pitch-lag couplings, of which the predominant effect on the rotor response is produced by the pitch-flap coupling.

The mathematical model used here is simplified with respect to certain structural and aerodynamic details. This simplification is necessary to provide comprehensive results for a range of configuration parameters without obscuring the basic results with less important details or causing the number of independent variables to increase unreasonably. The structural model considers the elastic blade flapping deflections (perpendicular to the plane of rotation) in terms of an arbitrary number of elastic modes. The rigid blade with offset hinge is included as a special case. Coupled lead-lag

(parallel to the plane of the rotation) and torsional deflections can be important for hingeless rotor response, but they are not included here. The principal effect of this bending/torsion coupling can be obtained from the present results if an equivalent linear pitch-flap coupling is determined following reference 10. The aerodynamic forces are based on linear, two-dimensional, steady airfoil theory, including reversed flow and compressibility but neglecting aerodynamic drag, pitching moments, and nonlinear airfoil stall. These effects are important only for extreme operating conditions and are not required to study the basic response characteristics of hingeless rotors.

The blade flapping equations are solved by first expressing each generalized coordinate of the elastic blade flapping motion by a Fourier series. Since the periodic coefficients of the equations and the forcing functions can be expressed as known Fourier series, equating terms of like harmonic content results in a set of linear algebraic equations for the unknown coefficients of the assumed Fourier series. This method, referred to here as the harmonic balance method, has traditionally been used to solve for articulated rotor blade flapping response. Usually only one or two harmonics were used for the flapping motion of a rigid, hinged blade (refs. 11 to 15) (although ref. 16 treats the flap, lead-lag, and pitch motion of a rigid blade), so that closed-form expressions for first harmonic flapping response could be obtained. These results are useful for low advance ratios, and illustrate the basic dependence of rotor response on the system parameters. For higher advance ratios, reversed flow effects are important, the second and higher harmonics of the flapping motion are required, and numerical solutions become necessary.

For hingeless rotors, the number of unknown coefficients to be determined by the harmonic balance can be substantially increased by the generalized coordinates of higher bending modes and by the higher harmonics required at moderate to high advance ratios. The harmonic balance method presented here is generalized through matrix techniques. This allows a practical and efficient numerical solution of the blade equations even when the number of unknown coefficients is large. The method is also applicable to other linear systems that have nonanalytic periodic coefficients, with an arbitrary number of harmonic control inputs or forcing functions. In this form, the method could be applied, for example, to the flap, lead-lag, and torsional motions of several rotor blades (as well as the dynamics of fuselage motion and feedback control systems), including unsteady aerodynamics.

BLADE FLAPPING EQUATIONS

Linear equations are derived for the flapping motion of a rotating elastic blade including the aerodynamic forces for forward flight conditions. The equations represent a simplified model of the hingeless rotor, but one that is sufficiently accurate to illustrate its fundamental response characteristics. Not included are lead-lag and torsional deflections, nonlinear airfoil aerodynamics (such as stall), and nonlinearities due to large deflection amplitudes.

The derivation of the equations is performed in two steps. First, the energy equation for a rotating beam with distributed forces is derived and then reduced by the Rayleigh-Ritz method to a system of ordinary differential equations in terms of the generalized coordinates of elastic bending modes. Since these equations are available in the literature (cf. ref. 17), only a brief derivation is given. The present treatment is sufficiently general to accommodate both cantilever blades and hinged blades with spring restraint about the hinge. A rigid blade with the hinged boundary condition is often used to approximate an elastic cantilever blade.

Second, the aerodynamic forces acting on the blade are derived. Linear, thin airfoil theory is used; velocity components parallel to the blade radial axis, unsteady aerodynamics, and wake-induced downwash are neglected. Reversed flow effects and Prandtl-Glauert compressibility corrections are included.

Rotating Beam Equations

Description of model— The physical model adopted for the helicopter rotor blades is a beam rotating with angular velocity Ω as illustrated in figure 1. The beam is taken to be infinitely rigid inboard of the flapping hinge ($r < \varepsilon$) and flexible outboard of the hinge. Only deflections normal to the plane of rotation (w) are considered. The beam is restrained at the flapping hinge by a root spring K_β. For a completely hingeless rotor, $K_\beta \to \infty$. The beam has variable section properties (e.g., EI, m, $\bar{c}$) and may also have a root cutout ($r < Re_{rc}$) where aerodynamic forces are negligible

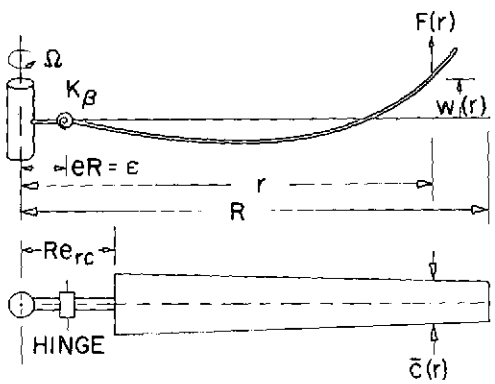

Figure 1.- Rotating beam geometry.

Lagrangian— The Lagrangian for a beam that performs small vertical motions is given by the kinetic energy of the system minus the potential energy in the strain field, tension field, and external spring. If the beam is taken to be infinitely rigid for $r < \varepsilon$ the Lagrangian may be expressed as

$$J_L = \int_\varepsilon^R \left[\frac{1}{2} m \left(\frac{d\psi}{dt} r \right)^2 + \frac{1}{2} m \left(\frac{\partial w}{\partial t} \right)^2 - \frac{1}{2} EI \left(\frac{\partial^2 w}{\partial r^2} \right)^2 \right.$$

$$\left. - \frac{1}{2} T_r \left(\frac{\partial w}{\partial r} \right)^2 \right] dr - \frac{1}{2} K_\beta \left(\frac{\partial w}{\partial r} \right)_{r=\varepsilon}^2$$

$$\equiv \int_\varepsilon^R f(r)\,dr - f_\varepsilon \qquad (1)$$

where J_L is the Lagrangian; r, the radial distance along the blade; R, the tip radius; m, the mass per unit length; w, the vertical displacement from the static position; t, time; EI, the bending stiffness; T_r, the radial tension force; ψ, the azimuth angle; and K_β, a root spring. The function f(r) is defined as the integrand of equation (1), and is the difference between the potential and kinetic energy per unit length. The function f_ε, defined as $(1/2)K_\beta(\partial w/\partial r)^2_{r=\varepsilon}$, is the potential energy in the root spring.

The equations of motion are obtained by adding the first variational (including time) of the Lagrangian and the work done by external forces, setting the sum to zero, and integrating by parts:

$$\int_\varepsilon^R \left[\frac{\partial f}{\partial w} - \frac{\partial}{\partial t}\frac{\partial f}{\partial(\partial w/\partial t)} - \frac{\partial}{\partial r}\frac{\partial f}{\partial(\partial w/\partial r)} + \frac{\partial^2}{\partial r^2}\frac{\partial f}{\partial(\partial^2 w/\partial r^2)} + F(r) \right] dr\ \delta w$$

$$+ \frac{\partial f}{\partial(\partial w/\partial r)}\delta w\Big|_\varepsilon^R + \frac{\partial f}{\partial(\partial^2 w/\partial r^2)}\delta\left(\frac{\partial w}{\partial r}\right)\Big|_\varepsilon^R - \frac{\partial}{\partial r}\frac{\partial f}{\partial(\partial^2 w/\partial r^2)}\delta w\Big|_\varepsilon^R - \delta(f_\varepsilon) = 0 \qquad (2)$$

where F represents the external aerodynamic forces in the direction of w. The integral term in equation (2) yields a partial differential equation for the blade motion w. The nonintegral (or trailing) terms, on the other hand, supply the appropriate boundary conditions of any particular problem. Applying the definition of f(r) in equation (1) to the first variational in equation (2) yields

$$\int_\varepsilon^R \left[-m\frac{\partial^2 w}{\partial t^2} + \frac{\partial}{\partial r}\left(T_r\frac{\partial w}{\partial r}\right) - \frac{\partial^2}{\partial r^2}\left(EI\frac{\partial^2 w}{\partial r^2}\right) + F(r) \right] dr\ \delta w - T_r\frac{\partial w}{\partial r}\delta w\Big|_\varepsilon^R$$

$$- EI\frac{\partial^2 w}{\partial r^2}\delta\left(\frac{\partial w}{\partial r}\right)\Big|_\varepsilon^R + \frac{\partial}{\partial r}\left(EI\frac{\partial^2 w}{\partial r^2}\right)\delta w\Big|_\varepsilon^R - K_\beta\frac{\partial w}{\partial r}\delta\left(\frac{\partial w}{\partial r}\right)_{r=\varepsilon} = 0 \qquad (3)$$

For a beam rotating with constant angular velocity Ω and having a free tip:

$$T_r = \Omega^2\int_r^R m\eta\, d\eta\ , \qquad \frac{dT_r}{dr} = -mr\Omega^2\ , \qquad \Omega = \frac{d\psi}{dt} \qquad (4)$$

Setting the integrand of equation (3) to zero yields the differential equation for the small vertical oscillations of a rotating beam under the influence of general external forces; setting the trailing terms to zero yields the appropriate boundary conditions.

Rayleigh-Ritz method– The Rayleigh-Ritz method uses the expansion theorem for linear systems (ref. 18), which implies that the response $w(r,t)$ can be separated into a sum of products of functions of r only and functions of t only:

$$w = R \sum_{j=1}^{J} \phi_j(r) q_j(t) \tag{5}$$

where $\phi_j(r)$ are modal functions and $q_j(t)$ are generalized coordinates. Although this formulation does not necessarily uncouple the solution for each q_j, the linearity does ensure that the series will converge as J becomes large. The modal functions ϕ_j are chosen as any complete set of linearly independent functions (provided they satisfy certain geometric boundary conditions and are piecewise twice differentiable). For solution by the Rayleigh-Ritz method, equations (4) and (5) are substituted into equation (3). Since

$$\left.\begin{aligned} \delta w &= R \sum_{j=1}^{J} \phi_j(r) \delta q_j \\ \delta\left(\frac{\partial w}{\partial r}\right) &= R \sum_{j=1}^{J} \frac{d\phi_j}{dr} \delta q_j \end{aligned}\right\} \tag{6}$$

and because equation (3) must vanish for arbitrary δq_j, there will be J equations for the unknown generalized coordinates q_j (one equation for each δq_j coefficient). The J equations are

$$\begin{aligned} R^2 \sum_{j=1}^{J} \Bigg\{ & \int_{\varepsilon}^{R} \left[\phi_i \frac{d^2}{dr^2}\left(EI \frac{d^2\phi_j}{dr^2}\right) + \Omega^2 m r \phi_i \frac{d\phi_j}{dr} - \Omega^2 \phi_i \frac{d^2\phi_j}{dr^2} \int_{r}^{R} m\eta \, d\eta \right] dr \, q_j \\ & + \int_{\varepsilon}^{R} m\phi_i\phi_j \, dr \frac{d^2 q_j}{dt^2} + \Omega^2 \left[\phi_i \frac{d\phi_j}{dr} \int_{r}^{R} m\eta \, d\eta \right] \Bigg|_{\varepsilon}^{R} q_j + EI \frac{d\phi_i}{dr} \frac{d^2\phi_j}{dr^2} \Bigg|_{\varepsilon}^{R} q_j \\ & - \phi_i \frac{d}{dr}\left(EI \frac{d^2\phi_j}{dr^2}\right) \Bigg|_{\varepsilon}^{R} q_j + K_\beta \frac{d\phi_i}{dr} \frac{d\phi_j}{dr} \Bigg|_{r=\varepsilon} q_j \Bigg\} = R \int_{\varepsilon}^{R} \phi_i F(r) dr \, , \quad i = 1, J \end{aligned} \tag{7}$$

and when the coefficients of q_j are collected, equation (7) can be expressed as

$$\sum_{j=1}^{J} [m_{ij}\ddot{q}_j + (P_{ij} + K_{ij})q_j] = \int_e^1 \phi_i \bar{F}(r)d\bar{r} , \qquad i = 1, J \tag{8}$$

where

$$\left.\begin{aligned}
m_{ij} &\equiv \frac{1}{\rho acR} \int_e^1 m\phi_i\phi_j \, d\bar{r} \\
P_{ij} &\equiv \frac{1}{\rho acR} \left\{ \int_e^1 \left[m\bar{r}\phi_i\phi_j' - \phi_i\phi_j'' \int_{\bar{r}}^1 m\eta \, d\eta \right] d\bar{r} + \left[\phi_i\phi_j' \int_{\bar{r}}^1 m\eta \, d\eta \right] \Bigg|_e^1 \right\} \\
&= \frac{1}{\rho acR} \int_e^1 \left[\phi_i'\phi_j' \int_{\bar{r}}^1 m\eta \, d\eta \right] d\bar{r} \\
K_{ij} &\equiv \frac{1}{\rho acR^5\Omega^2} \left\{ \int_e^1 [\phi_i(EI\phi_j'')'']d\bar{r} + K_\beta R(\phi_i'\phi_j')_{\bar{r}=e} + [-\phi_i(EI\phi_j'')' \right. \\
&\quad \left. + EI\phi_i'\phi_j''] \Big|_e^1 \right\} \\
&= \frac{1}{\rho acR^5\Omega^2} \int_e^1 EI\phi_i''\phi_j'' \, d\bar{r} + \frac{K_\beta}{\rho acR^4\Omega^2} (\phi_i'\phi_j')_{\bar{r}=e} \\
\bar{F} &\equiv \frac{F}{\Omega^2\rho acR^3} , \qquad e \equiv \frac{\varepsilon}{R}
\end{aligned}\right\} \tag{9}$$

Equation (8) gives the linearized, dimensionless flapping equations of motion for a rotating beam written in terms of the generalized coordinates q_j. The matrices defined in equations (9) have been simplified by placing all terms within the integral. This yields the same result as applying Galerkin's method (with trailing terms) to equation (1). The coefficients m_{ij} and K_{ij} form the generalized mass and stiffness matrices for a nonrotating beam. The coefficients P_{ij} form the centrifugal stiffness matrix due to rotation. The function $\bar{F}(r)$ is the dimensionless aerodynamic force acting on the blade.

Root shear and moment— The thrust and moment response of a rotor is determined by summing the root shears and moments of each individual blade. The root shear and moment (V and S) for each blade in the rotating coordinate system can be expressed either in terms of internal elastic forces or as integrals of the blade aerodynamic and inertial loading. In terms of the elastic forces,

$$\left.\begin{aligned} V &= \frac{\partial}{\partial r}\left(EI\,\frac{\partial^2 w}{\partial r^2}\right)_{r=\varepsilon} + \int_0^{\varepsilon} F(r)\,dr \\ S &= \left\{\begin{array}{c}\left(EI\,\dfrac{\partial^2 w}{\partial r^2}\right)_{r=\varepsilon} \\ \text{or} \\ \left(K_\beta\,\dfrac{\partial w}{\partial r}\right)_{r=\varepsilon}\end{array}\right\} + \varepsilon\,\frac{\partial}{\partial r}\left(EI\,\frac{\partial^2 w}{\partial r^2}\right)_{r=\varepsilon} + \int_0^{\varepsilon} F(r)\,r\,dr \end{aligned}\right\} \tag{10}$$

In terms of the integrated loading, the shear and moment are

$$\left.\begin{aligned} V &= -\int_{\varepsilon}^{R} m\,\frac{\partial^2 w}{\partial t^2}\,dr + \int_0^{R} F(r)\,dr \\ S &= -\int_{\varepsilon}^{R} m\left(\frac{\partial^2 w}{\partial t^2} + \Omega^2 w\right) r\,dr + \int_0^{R} F(r)\,r\,dr \end{aligned}\right\} \tag{11}$$

The two formulations given in equations (10) and (11) can differ in accuracy when w is approximated by a truncated orthogonal expansion such as equation (5). In general, the accuracy of equations (10) can be increased by choosing the actual mode shapes of the beam as the modal functions; but the accuracy of equations (10) is generally not as good as that of equations (11). This difference in accuracy can be attributed to two factors: (1) equations (11) contain $F(r)$ explicitly while equations (10) contain $F(r)$ implicitly as a series expansion and (2) the errors involved in truncating $d^3\phi/dr^3$ and $d^2\phi/dr^2$ in equations (10) are greater than the errors involved in truncating the lower derivates ϕ and $d\phi/dr$ in equations (11). For this reason, the integrated loading equations (11) for the root shear and moment is used.

The shear and moment may also be expressed in terms of the generalized coordinates q_j by substituting equation (5) into (11):

$$\left.\begin{aligned} V &= -\sum_{j=1}^{J}\left[\Omega^2 R\int_{\varepsilon}^{R} m\phi_j\,dr\right]\frac{d^2q_j}{dt^2} + \int_0^R F(r)dr \\ S &= -\sum_{j=1}^{J}\left[\Omega^2 R\int_{\varepsilon}^{R} mr\phi_j\,dr\right]\left(\frac{d^2q_j}{dt^2} + \Omega^2 q\right) + \int_0^R F(r)r\,dr \end{aligned}\right\} \tag{12}$$

After the terms are made dimensionless, the shear and moment expressions become

$$\left.\begin{aligned} \bar{C}_V &\equiv \frac{C_V}{\sigma a} = -\sum_{j=1}^{J} S_j\ddot{q}_j + \int_0^1 \bar{F}\,d\bar{r} \\ \bar{C}_S &\equiv \frac{C_S}{\sigma a} = -\sum_{j=1}^{J} m_{yj}(\ddot{q}_j + q_j) + \int_0^1 \bar{F}\bar{r}\,d\bar{r} \end{aligned}\right\} \tag{13a}$$

where

$$\left.\begin{aligned} \bar{C}_V &\equiv \frac{V}{\rho acR^3\Omega^2} \\ \bar{C}_S &\equiv \frac{S}{\rho acR^4\Omega^2} \\ S_j &\equiv \frac{1}{\rho acR}\int_e^1 m\phi_j\,d\bar{r} \\ m_{yj} &\equiv \frac{1}{\rho acR}\int_e^1 m\bar{r}\phi_j\,d\bar{r} \end{aligned}\right\} \tag{13b}$$

and σ is the solidity for one blade only ($\sigma = c/\pi R$). Equations (13) thus give the shear and moment coefficients as functions of the generalized coordinates and generalized forces.

Boundary conditions– To apply the above equations to a particular blade configuration (hingeless or articulated), the boundary conditions implied by the trailing terms in equation (3) must be considered carefully. They must vanish independently from the integral term in equation (3) because the variational δw is arbitrary. It follows that four boundary conditions must hold:

$$\left.\begin{aligned}
\left[\frac{\partial}{\partial r}\left(EI\,\frac{\partial^2 w}{\partial r^2}\right) - T_r\,\frac{\partial w}{\partial r}\right]\delta w &= 0 \qquad (r = \varepsilon, R)\\
\left[K_\beta\,\frac{\partial w}{\partial r} - EI\,\frac{\partial^2 w}{\partial r^2}\right]\delta\left(\frac{\partial w}{\partial r}\right) &= 0 \qquad (r = \varepsilon)\\
\left[EI\,\frac{\partial^2 w}{\partial r^2}\right]\delta\left(\frac{\partial w}{\partial r}\right) &= 0 \qquad (r = R)
\end{aligned}\right\} \tag{14}$$

For each condition in equations (14) to be fulfilled, either the variational (δw, $\delta(\partial w/\partial r)$) must vanish (a geometric boundary condition) or the bracketed term must vanish (a natural boundary condition). For articulated rotors, the only geometric boundary condition is the vertical displacement constraint at the root, $\delta w\big|_{r=\varepsilon} = 0$. Three natural boundary conditions remain (note that $T_r(R) = 0$):

$$\left.\begin{aligned}
\frac{\partial}{\partial r}\left(EI\,\frac{\partial^2 w}{\partial r^2}\right)_{r=R} &= 0\\
\left(EI\,\frac{\partial^2 w}{\partial r^2}\right)_{r=R} &= 0\\
\left(K_\beta\,\frac{\partial w}{\partial r} - EI\,\frac{\partial^2 w}{\partial r^2}\right)_{r=\varepsilon} &= 0
\end{aligned}\right\} \tag{15a}$$

These conditions imply that the shear and moment at the free tip must vanish and that moments about the hinge must be in equilibrium. For hingeless rotors, an additional geometric boundary condition,

$$\left(\frac{\partial w}{\partial r}\right)_{r=\varepsilon} = 0 \tag{15b}$$

is imposed and the natural boundary condition on the moment about the hinge is relaxed.

The modal functions, ϕ_j, must satisfy all geometric boundary conditions, but not necessarily all natural boundary conditions. The trailing terms in equation (3) will force the solution to minimize the integral and trailing terms in equation (7). Thus, when the trailing terms are retained, ϕ_j need not satisfy natural boundary conditions. If the trailing terms are not retained in equation (7), then ϕ_j must satisfy all boundary conditions.

Generalized Forces

The aerodynamic force acting on the rotor blade is derived from inviscid, linear, quasi-steady strip-theory. The effects of drag, induced downwash, and stall are neglected. In this theory, the relative air velocities experienced by each blade element determine the aerodynamic lift on that element.

Two sets of rotor axis systems are used to determine the relative air velocities for each blade element. The first axis system $(\vec{X}, \vec{Y}, \vec{Z})$ is a nonrotating, shaft-fixed system figure 2a. The rotor shaft is assumed to lie along the $-\vec{Z}$ axis, and the free stream velocity V_∞ is assumed to lie in the $\vec{X}\,\vec{Z}$ plane. The angle between V_∞ and the $\vec{X}$ axis is α_c, the shaft angle of attack. The shaft-fixed velocity components are therefore given by

$$V_x = -V_\infty \cos \alpha_c$$

$$V_y = 0$$

$$V_z = -V_\infty \sin \alpha_c \qquad (16)$$

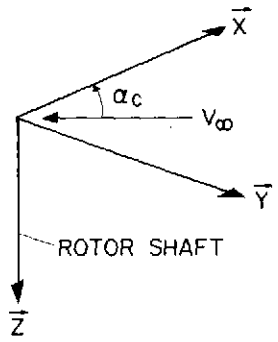

(a) Nonrotating axes.

The second axis system $(\vec{x}, \vec{y}, \vec{z})$ is a rotating, blade-fixed system, figure 2b. The position of this coordinate system is defined by two rotations of the shaft-fixed system. First, the shaft-fixed system is given a rotation through an angle $\psi + \pi$ about the $-\vec{Z}$ axis. This aligns $\vec{X}$ with the undeformed blade axis $\vec{r}$. The $\vec{X}$, $\vec{Y}$, $\vec{Z}$ axis system is then given a small angle rotation dw/dr about the new $\vec{Y}$ axis. This rotation aligns $\vec{X}$ with the local blade element. The axis system generated by these two rotations is defined as the rotating, blade-fixed system $(\vec{x}, \vec{y}, \vec{z})$.

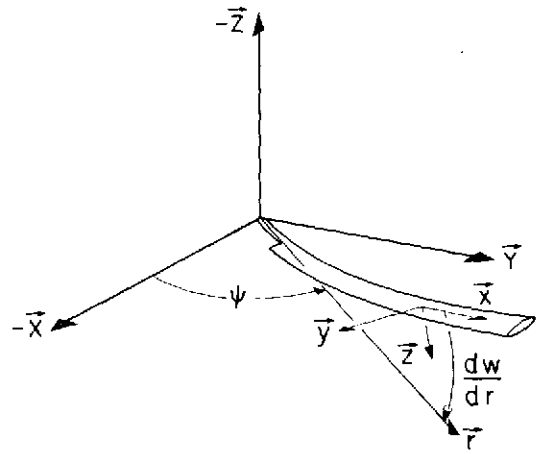

(b) Rotating axes.

Figure 2.- Rotor coordinate systems.

The relative fluid velocities experienced by each local blade element are found by transforming the V_x, V_y, V_z velocity components to the blade fixed axis and adding the velocity components due to blade rotation and vertical motion.

$$U_x = -V_x \cos \psi - V_z \, dw/dr$$

$$U_y = \Omega r - V_x \sin \psi$$

$$U_z = dw/dt + V_z - V_x \cos \psi dw/dr \tag{17}$$

According to strip theory, the blade lift is independent of the spanwise velocity component U_x, and the lift per unit span is given by

$$\ell = \frac{\rho \bar{c}(r)}{2} \left[U_y^2 + U_z^2\right] c_\ell \tag{18a}$$

where c_ℓ is the lift coefficient, $\bar{c}(r)$ is the local blade chord, and ρ is the density of air. The two-dimensional lift coefficient c_ℓ given by inviscid thin-airfoil theory is

$$c_\ell = \text{sgn}(U_y)\bar{a}(r,\psi) \sin \alpha \tag{18b}$$

where $\bar{a}(r,\psi)$ is the local lift-curve slope (2π for a flat plate), and the $\text{sgn}(U_y)$ provides for proper lift force direction in the region of reversed flow ($U_y < 0$). The angle of attack, α, is defined as the difference of the geometric pitch angle θ and the resultant inflow angle ϕ, as shown in figure 3. The quantity $\sin \alpha$ in Eq. (18b) can be evaluated as follows

$$\alpha = \theta - \phi$$

$$\phi \equiv \tan^{-1} (U_z/U_y)$$

$$\sin \alpha = \sin \theta \cos \phi - \cos \theta \sin \phi \tag{19}$$

where

$$\cos \phi = \frac{U_y}{\sqrt{U_y^2 + U_z^2}}$$

$$\sin \phi = \frac{U_z}{\sqrt{U_y^2 + U_z^2}}$$

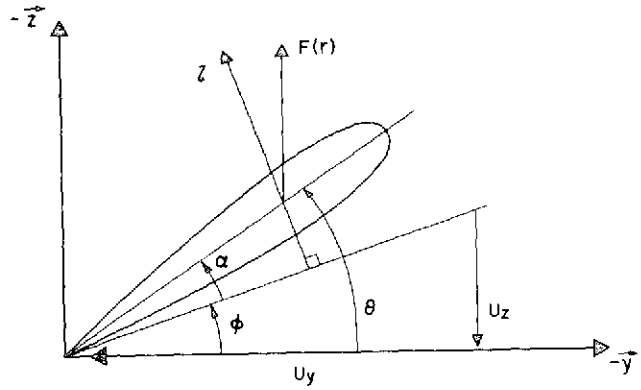

Figure 3.- Blade element geometry.

The rotor blade force component in equations (7) and (11) is shown in figure 3 and is given by

$$F = \ell \cos \phi \tag{20}$$

The effect of the cosine of the small angle dw/dr can be neglected because w has been assumed to be an infinitesimal quantity (making the equations linear in w and its derivatives).

Combining equations (18) and (20)*, the vertical component of ℓ can be written

$$F = \operatorname{sgn}(U_y) \frac{\rho \bar{a}(r,\psi)\bar{c}(r)}{2} [U_y^2 \sin \theta - U_y U_z \cos \theta] \tag{21}$$

For small pitch angle, θ, the aerodynamic load may be written as

$$\left.\begin{aligned} F &= \frac{\rho a c}{2} s(r,\psi)[U_y^2 \theta - U_y U_z] \\ s(r,\psi) &= \operatorname{sgn}(U_y) \frac{\bar{a}(r,\psi)\bar{c}(r)}{ac} \end{aligned}\right\} \tag{22}$$

where a and c are nominal values for the lift-curve slope and chord. The term $s(r,\psi)$, as defined in equations (22), can be used to account for reversed flow, tip loss, root cutout, compressibility, and other parameters that affect the blade lift-curve slope. Reversed flow is defined as the condition in which a portion of the blade encounters airflow directed toward the trailing edge of the blade (U_y negative). In addition to the nonanalytic switching of sign associated with $\operatorname{sgn}(U_y)$, reversed flow can also result in an abrupt change in the magnitude of $\bar{a}(r,\psi)$ since the blade lift characteristics near $\alpha = 180°$ may be different from the lift characteristics near $\alpha = 0°$. The change in sign and possible change in $\bar{a}$ are accounted for by $s(r,\psi)$. Similarly, blade tip loss (loss of lift near the tip due to effects of three-dimensional flow) and root cutout (incomplete airfoil sections near the blade root) are treated by setting $s(r,\psi) = 0$ near the blade root and tip. For compressibility corrections, the simple Prandtl-Glauert correction factor can be included with

$$s = \operatorname{sgn}(U_y) \frac{\bar{c}(r,\psi)}{c} \frac{1}{\sqrt{1 - M^2(r,\psi)}} \tag{23}$$

where M is the local Mach number.

Final equations— The final rotor equations are obtained by: first, substituting the velocity expressions (16) and (17) into (21); second, writing

*Note that the usual small angle assumption for $\phi \cong \tan \phi$ (or $\phi \cong U_z/U_y$) has not been invoked.

the pitch angle θ in terms of the physical controls; and third, substituting the resultant force expressions into equations (7) and (11). The blade pitch angle, θ, is written in terms of collective pitch θ_o, cyclic pitch θ_s and θ_c, and the pitch-flap coupling θ_{q_j}:

$$\theta = \theta_o + \theta_s \sin\psi + \theta_c \cos\psi + \sum_{j=1}^{J} \theta_{q_j} q_j \tag{24}$$

The pitch-flap coupling θ_{q_j} can result from the kinematics of the pitch change mechanism (for which θ_{q_j} is proportional to the modal deflection ϕ_j at the pitch horn), or it can result from a flapping mode shape that includes some torsional deformation (for which θ_{q_j} is taken to be some average value of the torsional component of ϕ_j). Combining these equations and making them dimensionless gives the following expression for the aerodynamic force:

$$\bar{F} = \frac{s}{2}\left\{(\bar{r} + \mu \sin\psi)^2\left[\theta_o + \theta_s \sin\psi + \theta_c \cos\psi + \sum_{j=1}^{J} \theta_{q_j} q_j\right]\right.$$
$$\left. - (\bar{r} + \mu \sin\psi)\left[-\mu\alpha_c + \phi_j \dot{q}_j + \mu \cos\psi \sum_{j=1}^{J} (\phi_j' q_j)\right]\right\} \tag{25a}$$

where

$$\mu \equiv \frac{V_\infty \cos\alpha_c}{\Omega r} \tag{25b}$$

In more compact notation, the dimensionless aerodynamic force is

$$\bar{F} = s(r,\psi) \sum_{k=1}^{K} V_k \theta_k - s(r,\psi) \sum_{j=1}^{J} \left[V_C \phi_j \dot{q}_j + (V_K \phi_j' + \theta_{q_j} V_1) q_j\right] \tag{26}$$

where

$$K = 4\,, \quad \theta_1 \equiv \theta_o\,, \quad \theta_2 \equiv \theta_s\,, \quad \theta_3 \equiv \theta_c\,, \quad \theta_4 \equiv \alpha_c \tag{27}$$

and

$$
\left.
\begin{aligned}
V_C &\equiv \frac{\bar{r}}{2} + \frac{\mu \sin(\psi)}{2} \\
V_K &\equiv \frac{\mu \bar{r} \cos(\psi)}{2} + \frac{\mu^2 \sin(2\psi)}{4} \\
V_1 &\equiv \frac{\bar{r}^2}{2} + \frac{\mu^2}{4} + \mu \bar{r} \sin(\psi) - \frac{\mu^2 \cos(2\psi)}{4} \\
V_2 &\equiv \frac{-\mu \bar{r}}{2} - \left(\frac{\bar{r}^2}{2} + \frac{3\mu^2}{8}\right)\sin(\psi) - \frac{\mu \bar{r} \cos(2\psi)}{2} + \frac{\mu^2 \sin(3\mu)}{8} \\
V_3 &\equiv -\left(\frac{\bar{r}^2}{2} + \frac{\mu^2}{8}\right)\cos(\psi) + \mu \bar{r} \sin(2\psi) + \frac{\mu^2 \cos(3\psi)}{8} \\
V_4 &\equiv \mu\left[\frac{\bar{r}}{2} + \frac{\mu^2 \sin(\psi)}{2}\right]
\end{aligned}
\right\} \qquad (28)
$$

The final equations for the blade deformations and the root shear and moment can now be written in matrix form:

$$
[m]\{\ddot{q}\} + [D^C]\{\dot{q}\} + [P + K + D^K - D^A]\{q\} = [D^V]\{\theta\} \qquad (29a)
$$

$$
\bar{C}_S = -\langle m_y \rangle \{\ddot{q}\} - \langle Q^C \rangle \{\dot{q}\} - \langle m_y + Q^K - Q^A \rangle \{q\} + \langle Q^V \rangle \{\theta\} \qquad (29b)
$$

$$
\bar{C}_V = -\langle S \rangle \{\ddot{q}\} - \langle W^C \rangle \{\dot{q}\} - \langle W^K - W^A \rangle \{q\} + \langle W^V \rangle \{\theta\} \qquad (29c)
$$

where

$$
\left.
\begin{aligned}
D^C_{ij} &\equiv \int_e^1 s V_C \phi_i \phi_j \, d\bar{r} \\
D^K_{ij} &\equiv \int_e^1 s V_K \phi_i \phi_j' \, d\bar{r} \\
D^A_{ij} &\equiv \theta_{q_j} \int_e^1 s V_1 \phi_i \, d\bar{r}, \qquad j = 1, 4 \\
D^V_{ij} &\equiv \int_e^1 s V_j \phi_i \, d\bar{r}
\end{aligned}
\right\} \qquad (30)
$$

(Continued)

$$
\left.
\begin{aligned}
Q_j^C &\equiv \int_e^1 sV_C\phi_j\bar{r}\,d\bar{r} \\
Q_j^K &\equiv \int_e^1 sV_K\phi_j'\bar{r}\,d\bar{r} \\
Q_j^A &\equiv \theta_{q_j}\int_0^1 sV_1\bar{r}\,d\bar{r} \\
Q_j^V &\equiv \int_0^1 sV_j\bar{r}\,d\bar{r}\,, \qquad j = 1, 4 \\
W_j^C &\equiv \int_e^1 sV_C\phi_j\,d\bar{r} \\
W_j^K &\equiv \int_e^1 sV_K\phi_j'\,d\bar{r} \\
W_j^A &\equiv \theta_{q_j}\int_0^1 sV_1\,d\bar{r} \\
W_j^V &\equiv \int_0^1 sV_j\,d\bar{r}\,, \quad j = 1, 4
\end{aligned}
\right\} \tag{30}
$$

These blade equations are generalized in appendix A to include harmonic control inputs, unsteady aerodynamics, nonuniform downwash, and rotor hub motion.

GENERALIZED HARMONIC BALANCE

The flapping equations of motion in terms of the generalized coordinates (eq. (29)) are linear ordinary differential equations with periodic coefficients and may be solved in several ways. The formal solution, which is periodic in time, is given by Floquet theory. Although the solution may be determined directly from Floquet theory, the linear and periodic properties imply that a specialized method may be more efficient computationally. The harmonic balance is, in this sense, a specialized method. The generalized coordinates are first expressed in terms of Fourier series and these series are substituted in the equations of motion. This process involves multiplication of the Fourier series that represents each generalized coordinate by the Fourier series of the time-varying coefficients, thereby yielding a new series of harmonic terms. The coefficients of each sine and cosine harmonic are equated to the coefficients of corresponding harmonics of the periodic

aerodynamic forcing functions in the equations of motion. This "harmonic balance" gives a system of linear algebraic equations in the Fourier coefficients of each of the blade flapping generalized coordinates.

The harmonic balance method has traditionally been used to obtain analytical solutions for the response of rigid, articulated, helicopter rotor blades with a single flapping degree of freedom. For the elastic hingeless rotor blade, however, several generalized coordinates for the blade flapping deflection are often required. If each coordinate is represented by even as few as two Fourier coefficients, the harmonic balance method can become algebraically cumbersome. Therefore, a matrix formulation is developed to generalize the harmonic balance method so that the analysis of systems having many coupled degrees of freedom can be performed efficiently. In this matrix form, the generalized harmonic balance method is a practical and efficient means of solving for the forced response of a system of linear differential equations with periodic coefficients. This report therefore includes an outline of the derivation of the matrix formulation of the method. The method is then applied to the rotor blade flapping equations derived in the previous section. The derivation begins with a review of the formal solution from Floquet theory.

Floquet Theory

The classical solution of linear differential equations with periodic coefficients is given by Floquet theory. To apply the theory, equation (29a) is first converted to state variable form with the definition

$$\{\bar{q}\} \equiv \begin{Bmatrix} \{q\} \\ \{\dot{q}\} \end{Bmatrix} \tag{31}$$

which yields

$$\{\dot{\bar{q}}\} + \begin{bmatrix} 0 & -I_J \\ [m]^{-1}[Z] & [m]^{-1}[D^C] \end{bmatrix} \{\bar{q}\} = \begin{bmatrix} 0 \\ [m]^{-1}[D^V] \end{bmatrix} \{\theta\} \tag{32}$$

where

$$[Z] \equiv [P] + [K] + [D^K] - [D^A] \tag{33}$$

Because the coefficients of equation (32) are periodic, Floquet's theorem states that the homogeneous solution to the equations ($\theta_i = 0$) has the form

$$\{\bar{q}\} = [A(\psi)] \left\{ \gamma_m e^{\eta_m \psi} \right\} \tag{34}$$

The complex periodic matrix [A] and the complex eigenvalues η_m can be determined from the Floquet transition matrix, and the coefficients γ_m can be determined from initial conditions (ref. 19). It follows that equation (32) can be reduced to a system of uncoupled constant coefficient equations by a change of variable:

$$\{\bar{q}\} = [A(\psi)]\{x\} \tag{35}$$

which yields

$$\{\dot{x}\} - \left[\begin{array}{c} \\ \eta_j \\ \\ \end{array}\right]\{x\} = \{U\} \tag{36}$$

where

$$\{U\} = [A(\psi)]^{-1}\left[\begin{array}{c} 0 \\ \\ [m]^{-1}[D^V] \end{array}\right]\{\theta\} \tag{37}$$

The solution for the x_m can be obtained by inspection:

$$x_m = \sum_{n=-N}^{+N} \frac{U_{m,n}\, e^{ni\psi}}{n - \eta_m}, \quad m = 1, 2J \tag{38}$$

where $U_{m,n}$ are the complex Fourier coefficients of U_m. The particular solution to equation (32) can then be found by substituting equation (38) into (35) to yield

$$q_j = \sum_{m=1}^{2\cdot J} \sum_{k=-N}^{+N} \sum_{n=-N}^{+N} \frac{A_{jm,k} U_{m,n}\, e^{i(n+k)\psi}}{n - \eta_m}, \qquad j = 1, J \tag{39}$$

where $A_{jm,k}$ are the complex Fourier coefficients of A_{jm}. Thus the solution is a periodic function with no subharmonics.

Floquet theory can therefore be applied directly to calculate the forced response of equation (29a) by first solving for the transient response (eq. (34)) and then applying it to equation (32). In this case it is computationally more efficient to solve directly for the forced response by taking advantage of the form of the solution. Equation (39) shows that the solution for the generalized coordinates is periodic with 2π and can therefore be expressed as

$$q_j = \sum_{n=0}^{N} (a_n)_{q_j} \cos(n\psi) + (b_n)_{q_j} \sin(n\psi), \qquad j = 1, J \tag{40}$$

The harmonic balance method involves first substituting equation (40) into (29a), second expanding the coefficients of equation (29a) into their Fourier series, third forming appropriate derivatives and products, and fourth, collecting coefficients of like harmonics. This process results in $(2N+1)J$ linear algebraic equations for the unknown harmonics of the generalized coordinates $(a_n)_{q_j}$ and $(b_n)_{q_j}$. Although Floquet theory implies that, in general, N approaches infinity in equations (39) and (40), in practice the Fourier series for q_j must be truncated at a finite value for N. The truncation error associated with restricting N in equation (40) must therefore be established in each particular case.

Matrix Formulation

Example of matrix operations— The basic principles of the harmonic balance method are cumbersome when applied to systems with many degrees of freedom. Furthermore, when the equation coefficients are nonanalytic functions, the Fourier series for these coefficients must be evaluated numerically. The harmonic balance method presented here is formulated in matrix notation so that operations involving derivatives, products, and the collection of terms are done symbolically. The definitions and rules of manipulation for these symbolic operations are developed in appendix B. As an example of the application of these operations, consider the assumed solution of equation (40) substituted into (29a) for $J = 1$, $K = 1$. The resulting system of algebraic equations is

$$\left[[\Pi(m_{11})][\Box]^2 + [\Pi(D_{11}^C)][\Box] + [\Pi(Z_{11})]\right]\begin{Bmatrix} a_n \\ b_n \end{Bmatrix}_{q_1} = \begin{Bmatrix} a_n \\ b_n \end{Bmatrix}_{D_{11}^V} \theta_1 \qquad (41)$$

where $[\Pi]$ is the Fourier product matrix (defined as a simple algorithm of the Fourier coefficients of its argument), $[\Box]$ is the Fourier derivative matrix, and $\langle a_n b_n \rangle_{D_{11}^V}$ are the Fourier coefficients of D_{11}^V

$$D_{11}^V = \sum_{n=0}^{N} (a_n)_{D_{11}^V} \cos(n\psi) + (b_n)_{D_{11}^V} \sin(n\psi) \qquad (42)$$

The coefficients b_0, although unobservable because they multiply $\sin(0\psi)$, are retained in the equations for reasons of symmetry. Thus, the Fourier operators $[\Pi]$ and $[\Box]$ may be used to transform a periodic coefficient differential equation into a system of algebraic equations.

Equation (39) shows that if $\mathrm{Im}(\eta_m)$ is an integer and $\mathrm{Re}(\eta_m) = 0$, the forced solution will increase without bound. Thus, if the left-hand side of equation (41) is singular, it can be assumed that $\mathrm{Re}(\eta_m) = 0$ which implies

from equation (39) that the system is neutrally stable. The existence of a solution to equation (41) is therefore a necessary condition for stability. Note, however, that solutions to equation (41) will exist even when $\mathrm{Im}(\eta_m)$ is not an integer or when $\mathrm{Re}(\eta_m) > 0$. Thus, the existence of a solution to equation (41) is not a sufficient condition for stability.

Application to rotor equations— The Fourier operations applied to a single equation in equation (41) may easily be applied to the complete set of rotor equations, equation (29a), transforming them into 2J(N+1) algebraic equations:

$$\begin{bmatrix} [\Pi(m_{11})] & \cdots & [\Pi(m_{1J})] \\ \vdots & & \vdots \\ [\Pi(m_{J1})] & \cdots & [\Pi(m_{JJ})] \end{bmatrix} \begin{bmatrix} [\Box]^2 & & \\ & \ddots & \\ & & [\Box]^2 \end{bmatrix} \begin{Bmatrix} \begin{Bmatrix} a_n \\ b_n \end{Bmatrix}_{q_1} \\ \vdots \\ \begin{Bmatrix} a_n \\ b_n \end{Bmatrix}_{q_J} \end{Bmatrix}$$

$$+ \begin{bmatrix} \vdots \\ \cdots [\Pi(D^C_{ij})] \cdots \\ \vdots \end{bmatrix} \begin{bmatrix} \ddots & & \\ & [\Box] & \\ & & \ddots \end{bmatrix} \begin{Bmatrix} \vdots \\ \begin{Bmatrix} a_n \\ b_n \end{Bmatrix}_{q_j} \\ \vdots \end{Bmatrix} + \begin{bmatrix} \vdots \\ \cdots [\Pi(Z_{ij})] \cdots \\ \vdots \end{bmatrix} \begin{Bmatrix} \vdots \\ \begin{Bmatrix} a_n \\ b_n \end{Bmatrix}_{q_j} \\ \vdots \end{Bmatrix}$$

$$= \begin{bmatrix} \vdots \\ \cdots \begin{Bmatrix} a_n \\ b_n \end{Bmatrix}_{D^V_{ik}} \cdots \\ \vdots \end{bmatrix} \begin{Bmatrix} \vdots \\ \theta_k \\ \vdots \end{Bmatrix}, \qquad \begin{matrix} i = 1, J & n = 0, N \\ j = 1, J & k = 1, K \end{matrix} \tag{43}$$

The solution for the $\langle a_n b_n \rangle_{q_j}$ follows directly:

$$\begin{Bmatrix} \vdots \\ \begin{Bmatrix} a_n \\ b_n \end{Bmatrix}_{q_j} \\ \vdots \end{Bmatrix} = [H_q]^{-1} \begin{bmatrix} \vdots \\ \cdots \begin{Bmatrix} a_n \\ b_n \end{Bmatrix}_{D^V_{ik}} \cdots \\ \vdots \end{bmatrix} \{\theta\} \Bigg\}$$

$$\equiv [\theta_q]\{\theta\} \Bigg\} \tag{44}$$

where

$$[H_q] \equiv \begin{bmatrix} & \vdots & \\ \cdots & [\Pi(m_{ij})][\square]^2 + [\Pi(D^C_{ij})][\square] + [\Pi(Z_{ij})] & \cdots \\ & \vdots & \end{bmatrix} \tag{45}$$

Shear and moment— In addition to obtaining the solution for the blade motions (i.e., for q_j), it is also useful to obtain the solution for the shear and moment at the blade root in the rotating coordinate system. The root shear and moment coefficients, $\overline{C}_V$ and $\overline{C}_S$, are obtained as functions of time by substituting the solution for q_j (eq. (44)) directly into equations (29b) and (29c). The Fourier coefficients (i.e., harmonics) of $\overline{C}_V$ and $\overline{C}_S$ may then be obtained by Fourier analysis of the equations. The substitution of equation (44) into (29b) and (29c) and the subsequent Fourier analysis can be performed by straightforward application of the Fourier product and derivative rules to equations (29b) and (29c). The resulting expressions for the shear and moment coefficients are

$$\left.\begin{aligned} \begin{Bmatrix} a_n \\ b_n \end{Bmatrix}_{\overline{C}_V} &= -[H_V][\Theta_q]\{\theta\} + \begin{bmatrix} \cdots \begin{Bmatrix} a_n \\ b_n \end{Bmatrix}_{W_j{}^V} \cdots \end{bmatrix}\{\theta\} \equiv [\Theta_V]\{\theta\} \\ \begin{Bmatrix} a_n \\ b_n \end{Bmatrix}_{\overline{C}_S} &= -[H_S][\Theta_q]\{\theta\} + \begin{bmatrix} \cdots \begin{Bmatrix} a_n \\ b_n \end{Bmatrix}_{Q_j{}^V} \cdots \end{bmatrix}\{\theta\} \equiv [\Theta_S]\{\theta\} \end{aligned}\right\} \tag{46}$$

where

$$\left.\begin{aligned} [H_V] &\equiv \left[\cdots [\Pi(S_j)][\square]^2 + [\Pi(W_j{}^C)][\square] + [\Pi(W_j{}^K - W_j{}^A)] \cdots\right] \\ [H_S] &\equiv \left[\cdots [\Pi(m_{yj})][\square]^2 + [\Pi(Q_j{}^C)][\square] + [\Pi(m_{yj} + Q_j{}^K - Q_j{}^A)] \cdots\right] \end{aligned}\right\} \tag{47}$$

The Fourier coefficient matrices for W^V and Q^V in equation (46) give the portion of $\overline{C}_V$ and $\overline{C}_S$ due directly to control inputs, not including the indirect effect that blade elastic deformations have on the shear and moment (i.e., they give $\overline{C}_V$ and $\overline{C}_S$ for an infinitely rigid rotor). The H_V and H_S matrices, on the other hand, give the contribution of each of the generalized blade deformations to $\overline{C}_V$ and $\overline{C}_S$. Thus, $[\Theta_V]$ and $[\Theta_S]$ in equation (46) give the total shear and moment due to control inputs, including the effect of structural deformations caused by those inputs.

Hub forces and moments— The hub forces and moments in the nonrotating coordinate system may be directly obtained from the blade root shear and moment in the rotating coordinate system. For a single-bladed rotor, the expressions are

$$\left.\begin{aligned} T &= V \\ L &= -S \sin \psi \\ M &= -S \cos \psi \end{aligned}\right\} \tag{48}$$

where T is the rotor thrust, L is the rolling moment (positive with right side down), and M is the pitching moment (positive with nose-up). The harmonic coefficients of T, L, and M are obtained by use of the Fourier product operator:

$$\left.\begin{aligned} \begin{Bmatrix} a_n \\ b_n \end{Bmatrix}_{\overline{C}_T} &= [\Theta_V]\{\theta\} \equiv [\Theta_T]\{\theta\} \\ \begin{Bmatrix} a_n \\ b_n \end{Bmatrix}_{\overline{C}_L} &= -[\Pi(\sin \psi)][\Theta_S]\{\theta\} \equiv [\Theta_L]\{\theta\} \\ \begin{Bmatrix} a_n \\ b_n \end{Bmatrix}_{\overline{C}_M} &= -[\Pi(\cos \psi)][\Theta_S]\{\theta\} \equiv [\Theta_M]\{\theta\} \end{aligned}\right\} \tag{49}$$

The harmonic content of T, L, and M for a rotor with b blades is obtained by first summing the contributions of each blade and second dividing by the blade number b, since b appears in the definition of $\overline{C}_T$ through σ. The result for $\overline{C}_T$ is

$$\overline{C}_T(\Omega t)\Big|_{b\text{-blades}} = \frac{1}{b} \sum_{j=1}^{b} \overline{C}_I\left(\Omega t + [j - 1]\,\frac{2\pi}{b}\right)\Big|_{1\text{-blade}} \tag{50}$$

From the relation in equation (B2), it is seen that equation (50) cancels all harmonics of $\overline{C}_T$ which are not integer multiples of b ($n = 0, b, 2b, \ldots$), but leaves unchanged harmonics that are integer multiples of b. The same cancellation is also true for $\overline{C}_L$ and $\overline{C}_M$; therefore, the single-bladed results for $\overline{C}_T$, $\overline{C}_L$, and $\overline{C}_M$ are valid for rotors with any number of blades so long as the appropriate solution harmonics are set to zero.

Response derivatives— The absolute magnitudes of the blade deflections, root shear, root moment, thrust, roll moment, and pitch moment are obtained by multiplying the appropriate $[\Theta]$ matrices by the control vector $\{\theta\}$. This linear dependence on θ_j gives the elements of $[\Theta]$ direct physical significance as the partial derivatives of each response harmonic taken with respect to each generalized control θ_j. For example, the elements of $[\Theta_T]$ (with $N = 2$) are

$$[\Theta_T] = \begin{bmatrix} \partial(a_0)\overline{C}_T/\partial\theta_o & \partial(a_0)\overline{C}_T/\partial\theta_s & \partial(a_0)\overline{C}_T/\partial\theta_c & \partial(a_0)\overline{C}_T/\partial\alpha_c \\ \partial(a_1)\overline{C}_T/\partial\theta_o & \partial(a_1)\overline{C}_T/\partial\theta_s & \partial(a_1)\overline{C}_T/\partial\theta_c & \partial(a_1)\overline{C}_T/\partial\alpha_c \\ \partial(a_2)\overline{C}_T/\partial\theta_o & \partial(a_2)\overline{C}_T/\partial\theta_s & \partial(a_2)\overline{C}_T/\partial\theta_c & \partial(a_2)\overline{C}_T/\partial\alpha_c \\ 0 & 0 & 0 & 0 \\ \partial(b_1)\overline{C}_T/\partial\theta_o & \partial(b_1)\overline{C}_T/\partial\theta_s & \partial(b_1)\overline{C}_T/\partial\theta_c & \partial(b_1)\overline{C}_T/\partial\alpha_c \\ \partial(b_2)\overline{C}_T/\partial\theta_o & \partial(b_2)\overline{C}_T/\partial\theta_s & \partial(b_2)\overline{C}_T/\partial\theta_c & \partial(b_2)\overline{C}_T/\partial\alpha_c \end{bmatrix} \tag{51}$$

This same partial derivative structure exists for all $[\Theta]$ matrices ($[\Theta_q]$, $[\Theta_V]$, $[\Theta_S]$, $[\Theta_M]$, $[\Theta_L]$). For simplicity of notation, the elements of the first row of $[\Theta_T]$ (the steady portion of $\overline{C}_T$) are abbreviated as $< \overline{C}_{T_{\theta_o}} \; \overline{C}_{T_{\theta_s}} \; \overline{C}_{T_{\theta_c}} \; \overline{C}_{T_{\alpha_c}} >$. Similar abbreviations are used for the a_o (steady) components of $\overline{C}_S$, $\overline{C}_L$, and $\overline{C}_M$. These a_o components of the partial derivatives are called the rotor response derivatives.

HINGELESS ROTOR RESPONSE CHARACTERISTICS

The basic characteristics of the rotor derivatives will be examined for a typical hingeless rotor configuration. Twelve dimensionless derivatives will be included: rotor thrust, pitching moment, and rolling moment, with respect to collective pitch θ_o, longitudinal cyclic pitch θ_s, lateral cyclic pitch θ_c, and shaft angle of attack α_c. The response behavior is first examined with the aid of simplified closed-form expressions for these response derivatives. And second, the variation of the derivatives with respect to the parameters that define the configuration and operating condition will be discussed. A more comprehensive series of graphical and tabular results are presented in appendix C.

With certain simplifications and assumptions, the harmonic balance solution of the flapping equations can be used to obtain analytical expressions

for the response derivatives. To obtain these simplified expressions, the centrally hinged, rigid blade model is used, only the first harmonic flapping response is retained, and the effects of reversed flow aerodynamics are neglected. The expressions, given in table 1, correspond directly to the classical expressions for steady-state blade flapping response β found in reference 13 (for the articulated rotor) and in reference 1 (for hinge spring restraint). The results are reasonably accurate at low advance ratio and they readily illustrate the dependence of response behavior on the system parameters.

Characteristics of the Simplified Derivative Expressions

The most fundamental hingeless rotor behavior is manifest in the rotor pitch and roll moment derivatives with respect to cyclic pitch. The magnitude of the hub moment, the relative magnitude of the pitch and roll moment components, and the influence of flap frequency and Lock number are all significant. This fundamental behavior can be demonstrated with the simple expressions for the dimensionless control power derivatives in hover given in table 1. Since the control power derivatives are symmetric in hover, only the response derivatives for lateral cyclic pitch are considered. From table 1,

$$\left.\begin{aligned} \frac{\partial (a_o)\overline{C}_M}{\partial \theta_c} \equiv \overline{C}_{M_{\theta_c}} &= -\frac{1}{16}\frac{C^2}{1+C^2} \\ \frac{\partial (a_o)\overline{C}_L}{\partial \theta_c} \equiv \overline{C}_{L_{\theta_c}} &= -\frac{1}{16}\frac{C}{1+C^2} \end{aligned}\right\} \tag{52}$$

where

$$C = \frac{8(P^2 - 1)}{\gamma}$$

The control power derivatives are wholly determined by the parameter C that is determined by the flap frequency and Lock number. This parameter arises from the definition of the dimensionless moment coefficients, $\overline{C}_M$ and $\overline{C}_L$. The dimensional hub moment is proportional to the product of blade flapping amplitude and hinge spring stiffness K_β. The introduction of the dimensionless coefficients then results in the above expressions with C defined in terms of P and γ. For a centrally hinged, rigid blade, C can also be written in another form:

TABLE 1.- SIMPLIFIED FORMULAS FOR RESPONSE DERIVATIVES; $\partial x/\partial y$.

y \ x	$\overline{C}_T$	$(a_0)_\beta$*	$(a_1)_\beta$*	$(b_1)_\beta$*
θ_o	$\frac{1}{6}(1 + \mu^2)$	$\frac{\gamma}{8P^2}(1 + \mu^2)$	$\frac{-(8/3)\mu[1 + C(\gamma/16P^2)]}{1 + C^2}$	$\frac{(8/3)\mu[C - (\gamma/16P^2)]}{1 + C^2}$
θ_s	$\frac{\mu}{4}$	$\frac{\gamma}{6P^2}\mu$	$\frac{-(1 + 2\mu^2) - (2/9)\mu^2 C(\gamma/P^2)}{1 + C^2}$	$\frac{C[1 + (3/2)\mu^2] - (2/9)\mu^2(\gamma/P^2)}{1 + C^2}$
θ_c	0	0	$\frac{C(1 + \mu^2/2)}{1 + C^2}$	$\frac{1}{1 + C^2}$
α_c	$\frac{\mu}{4}$	$\frac{\gamma}{6P^2}\mu$	$\frac{-\mu^2[2 + (2/9)C(\gamma/P^2)]}{1 + C^2}$	$\frac{\mu^2[2C - (2/9)(\gamma/P^2)]}{1 + C^2}$

*Note that $\overline{C}_S = (C/8)a_0$, $\overline{C}_M = -(C/16)a_1$, and $\overline{C}_L = -(C/16)b_1$.

$$\left.\begin{aligned} p^2 &= \frac{1 + K_\beta}{I_y \Omega^2} \\ \gamma &= \frac{\rho a c R^4}{I_y} \\ C &= \frac{8K_\beta}{\rho a c \Omega^2 R^4} \end{aligned}\right\} \qquad (53)$$

This form of C shows that the blade root elastic restraint is the most significant factor for the dimensionless hub moment derivatives. In addition, the blade flapping inertia I_y has no influence on the hub moment derivatives even though it influences both P and γ. (Note in table 1 that blade inertia (through γ) influences blade coning deflections a_o, which does affect the control power derivatives in forward flight.)

The simple relations for pitch and roll moment derivatives with respect to lateral cyclic pitch in hover (eq. (52)) are shown in figure 4. The parametric variation of the pitch and roll derivatives as a function of C takes the form of a semicircle tangent to the origin with a diameter of 1/16.

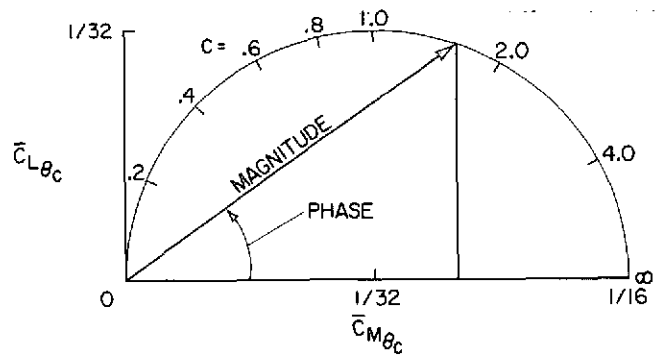

Figure 4.- Moment derivatives with respect to cyclic pitch in hover.

The phase, $\tan^{-1}(\bar{C}_{L_{\theta_c}}/\bar{C}_{M_{\theta_c}})$, between the pitch and roll derivatives ranges from 0° to 90° as C ranges from ∞ to 0, respectively. The phase angle of the classical articulated rotor without hinge offset (P = 1, C = 0) is 90°. For a typical hingeless rotor with P = 1.15 and γ = 8, C = 0.3225 and the phase angle is about 72°. For typical variations of P and γ, the phase angle varies from about 60° to 84°. Any phase angle not equal to 0° or 90° introduces pitch-roll cross-coupling of the primary response derivatives, and the amount of coupling depends on the particular configuration parameters. Although this coupling is easily eliminated in hover by biasing the control input phasing, additional phase variations and hence pitch-roll coupling occur due to forward flight.

The magnitude of the hub moment response to cyclic pitch in hover $\left(\sqrt{\bar{C}^2_{M_{\theta_c}} + \bar{C}^2_{L_{\theta_c}}}\right)$ is given by $C/\left(16\sqrt{1 + C^2}\right)$, which is the product of hinge spring restraint (included in C) and the blade cyclic flapping amplitude

$1/\sqrt{1 + C^2}$ (i.e., the spring rate times the deflection). An increase in rotor flap frequency P produces opposite effects in these two components of the hub moment expression. As P increases, the spring restraint is increased but the blade deflection is consequently reduced. For low values of P, typical of most hingeless rotors, the effect of elastic restraint term is most important and the cyclic blade deflection is only slightly reduced. For the limiting case of the classical articulated rotor, $P = 1$, $C = 0$, the flapping amplitude is maximum but the hub moment is zero. As P increases above 1, the hub moment increases nearly in proportion to C until the flapping amplitude begins to diminish significantly. For high values of P, the opposing contributions cancel one another and the hub moment magnitude approaches a constant value of 1/16 as P and C approach infinity. This is the limiting case of a completely rigid rotor blade. For convenience, figure 5 is provided to quickly estimate the parameter C and the magnitude and phase of the hover control power derivatives for different combinations of P and γ.

The general magnitude and phase response characteristics of the hub moment control power derivatives in hover also hold for forward flight. However, these characteristics are increasingly modified as the advance ratio μ increases. The contribution of the advance ratio terms is included in the simplified rotor derivative expressions given in table 1. The μ dependence generally (except for the θ_c derivatives) takes the form of two terms - one due to μ and another to coning. The latter term depends on both μ and the configuration parameters P and γ. The thrust derivatives are independent of the configuration parameters and are functions only of advance ratio. The lateral cyclic (θ_c) derivatives exhibit a very weak dependence on advance ratio, containing only higher-order terms in μ. This is expected since blade pitch angle changes due to θ_c are largest at the front and rear portions ($\psi = 0°$, $180°$) of the rotor disk where the blade tangential velocity U_y is independent of advance ratio.

Influence of System Parameters on Hingeless Rotor Response

The response characteristics for a typical hingeless rotor configuration, presented graphically in figures 6 to 9, directly illustrate the influence of the four main system parameters: advance ratio μ, fundamental flap frequency P, Lock number γ, and pitch-flap coupling θ_{q_j}. This concise presentation of all 12 primary derivatives clearly shows the relative magnitude and the parameter sensitivity of each derivative. The results in figures 6 to 9 are calculated numerically using the centrally hinged, rigid blade, with two harmonics of flapping, and full reversed flow. This representation gives reasonable accuracy for the range of parameters shown. The baseline configuration and advance ratio are $P = 1.15$, $\gamma = 8$, $\theta_{q_1} = 0$, $e_{rc} = 0$, $B = 1.0$, and $\mu = 0.6$.

The variation of the derivatives as a function of advance ratio is shown in figure 6; results from the simplified expressions in table 1 are given by the dotted lines. The thrust derivatives are very sensitive to μ (except for the θ_c derivative) and follow the simple formulas reasonably

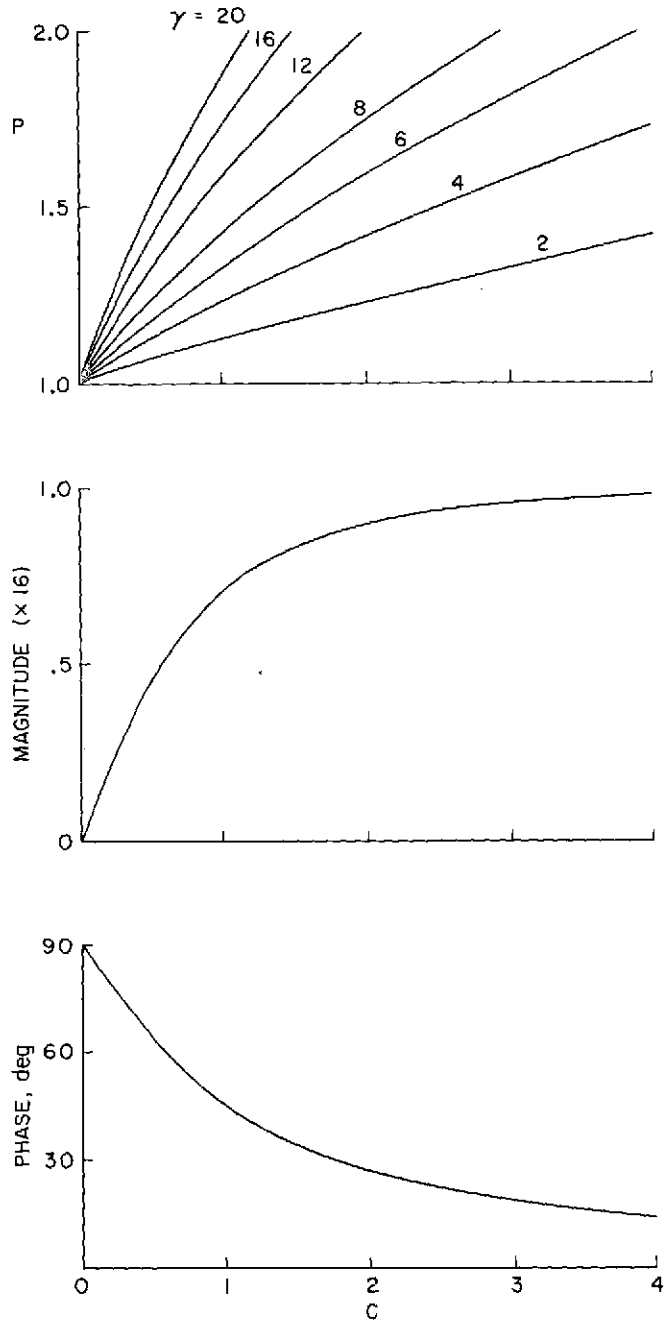

Figure 5.- Effect of P and γ on moment response in hover.

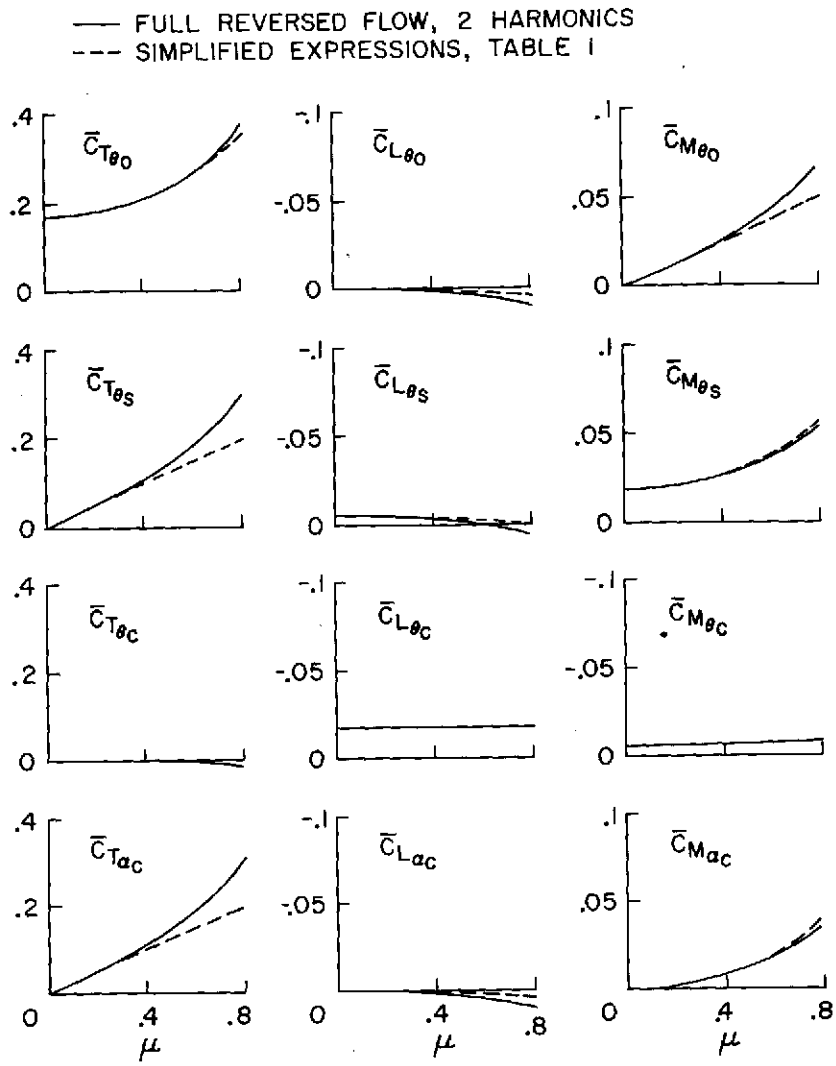

Figure 6.- Effect of advance ratio on response derivatives; P = 1.15, γ = 8, $\theta_{q_1} = 0$.

well. Since the thrust derivatives are not configuration-dependent, these results are not essentially different from articulated rotor behavior. The rolling moment response for collective pitch and angle of attack is relatively low in magnitude and therefore lift-roll coupling is small. Cross-coupling of pitch and roll control power increases substantially with advance ratio, particularly for the longitudinal cyclic derivatives, $\bar{C}_{M_{\theta_s}}$ and $\bar{C}_{M_{\theta_c}}$. The static angle-of-attack stability $\bar{C}_{M_{\alpha_c}}$ is considerable larger than would be expected for an articulated rotor and tends to produce pitch-up divergence at high forward speed.

The most important hingeless rotor configuration parameter is the flapping frequency. The sensitivity of the rotor derivatives to this parameter is shown in figure 7. For a centrally hinged articulated rotor, the flapping frequency P is equal to unity. With typical hinge offsets of a few percent of the blade radius, P increases to about 1.03. For typical hingeless rotor blades of low flapwise stiffness, P ranges from about 1.08 to 1.15. For blades of high flapwise stiffness P can be as high as 1.5. As noted above, the thrust derivatives are insensitive to P but the magnitude and phase of the moment derivatives are strongly influenced by P. When P is equal to zero, no hub moments are generated in response to cyclic flapping. Four of the moment derivatives become zero in the limit as $P \to \infty$: $\bar{C}_{M_{\theta_o}}$, $\bar{C}_{M_{\theta_s}}$, $\bar{C}_{L_{\theta_c}}$, and $\bar{C}_{M_{\alpha_c}}$.

For intermediate values of P the varying magnitude and phase of the blade flapping response produces a corresponding variation in the moment response derivatives. For the typical configuration of P = 1.15 at $\mu = 0.6$, an increase in P increases the pitching moment responses significantly. In particular, the static pitch-up derivative $\bar{C}_{M_{\alpha_c}}$ becomes more unstable as

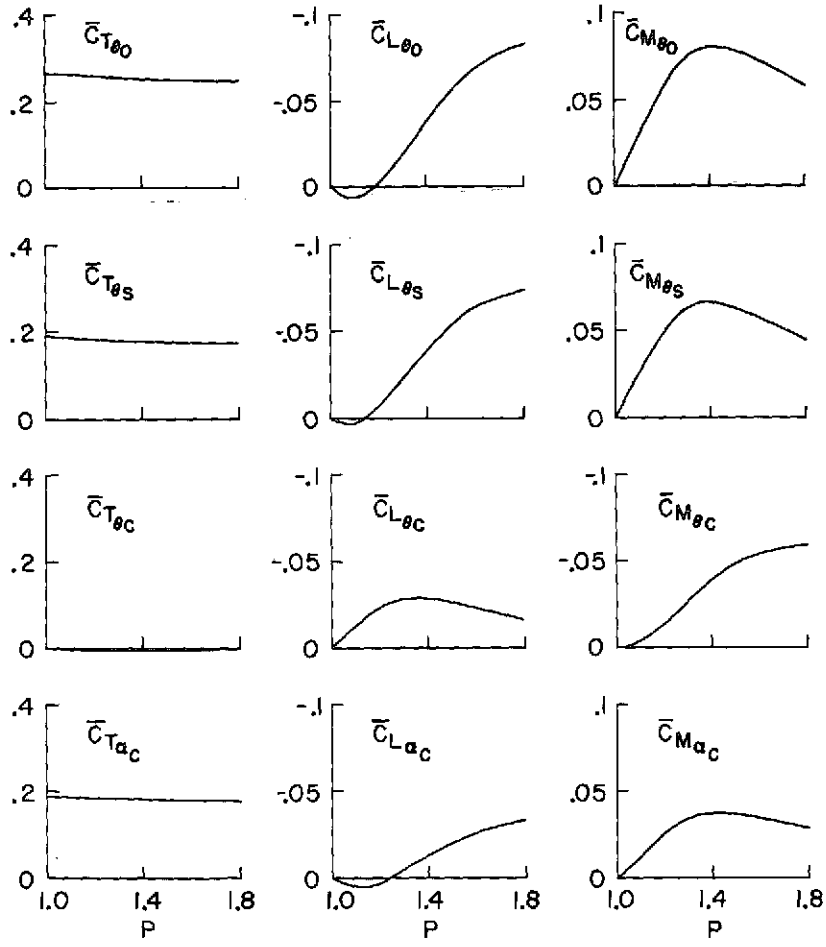

Figure 7.- Effect of flap frequency on response derivatives; $\mu = 0.6$, $\gamma = 8$, $\theta_{q_1} = 0$.

P increases. For relatively large values of P (i.e., 1.3 to 1.4), the pitching moment derivatives are generally large, with several approaching asymptotic values. For $\mu = 0.6$, the roll moment coupling with collective, longitudinal cyclic, and angle of attack is relatively small at the typical value $P = 1.15$; but all these couplings increase significantly with P.

Trends for Lock number variations are shown in figure 8. Since Lock number and flapping frequency are inversely related through the parameter C, the results of figure 8 bear an inverse resemblance to the results for flap frequency variation in figure 7. In other words, an increase in Lock number has the same qualitative effect as a decrease in flap frequency. This effect is clearly evident in the limiting behavior of the control power derivatives as $\gamma \to 0$ and $P \to \infty$. Lock number variations have a significant effect on the derivatives. Note that parameters included in the definition of Lock number are also used to normalize the derivatives. For example, a reduction in blade chord c will reduce Lock number and increase the normalized control power cross-coupling derivatives $\bar{C}_{L_{\theta_s}}$ and $\bar{C}_{M_{\theta_c}}$. However, the reduction in rotor

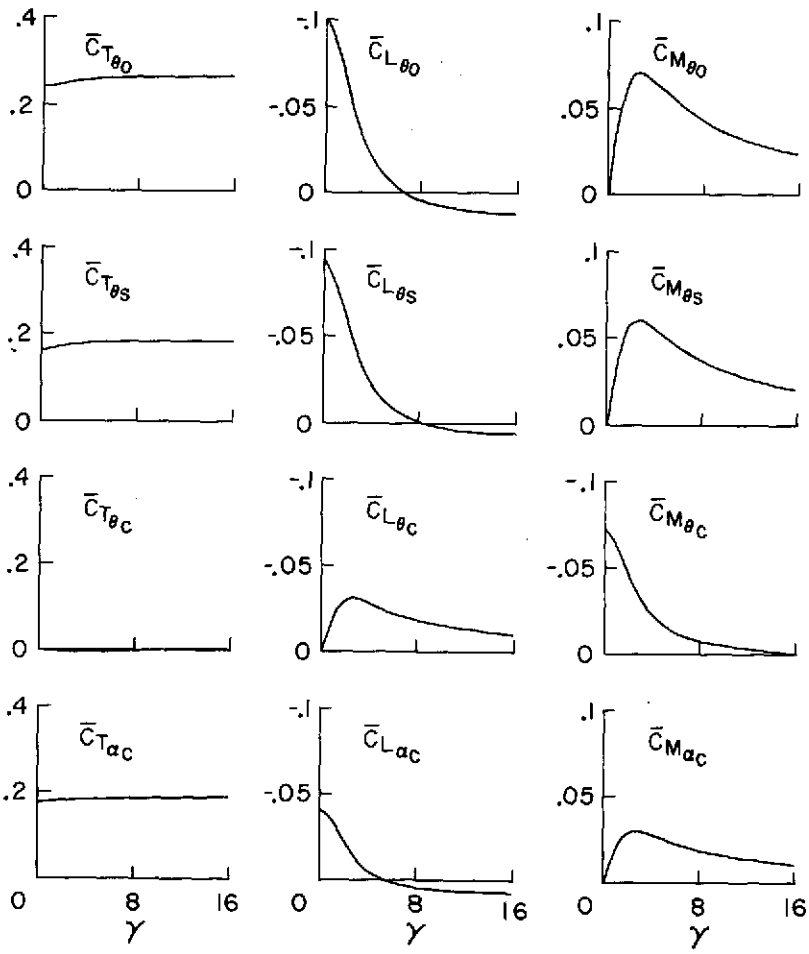

Figure 8.- Effect of Lock number on response derivatives; $\mu = 0.6$, $P = 1.15$, $\theta_{q_1} = 0$.

solidity σ accounts for a significant part of the increase (since $\overline{C}_{(\ )} \equiv C_{(\ )}/a\sigma$).

The final parameter is pitch-flap coupling, θ_{q_j} - commonly used for articulated rotors to reduce flapping sensitivity at high advance ratios. It has a significant effect on the stability and control properties of the rotor, primarily by modifying the effective flapping frequency. (The fundamental flapping frequency P is defined only in terms of the inertial and stiffness properties of the blade. The basic effects are shown in figure 9 with P held constant.) Positive θ_{q_1} (also called negative delta-3) produces positive blade pitch with increased flap deflection (i.e., statically destabilizing). Negative θ_{q_1} is statically stabilizing and reduces flapping and hence moment response. It is evident that pitch-flap coupling can be a powerful design parameter in modifying control power, cross-coupling, thrust sensitivity to angle-of-attack changes, and pitch-up instability.

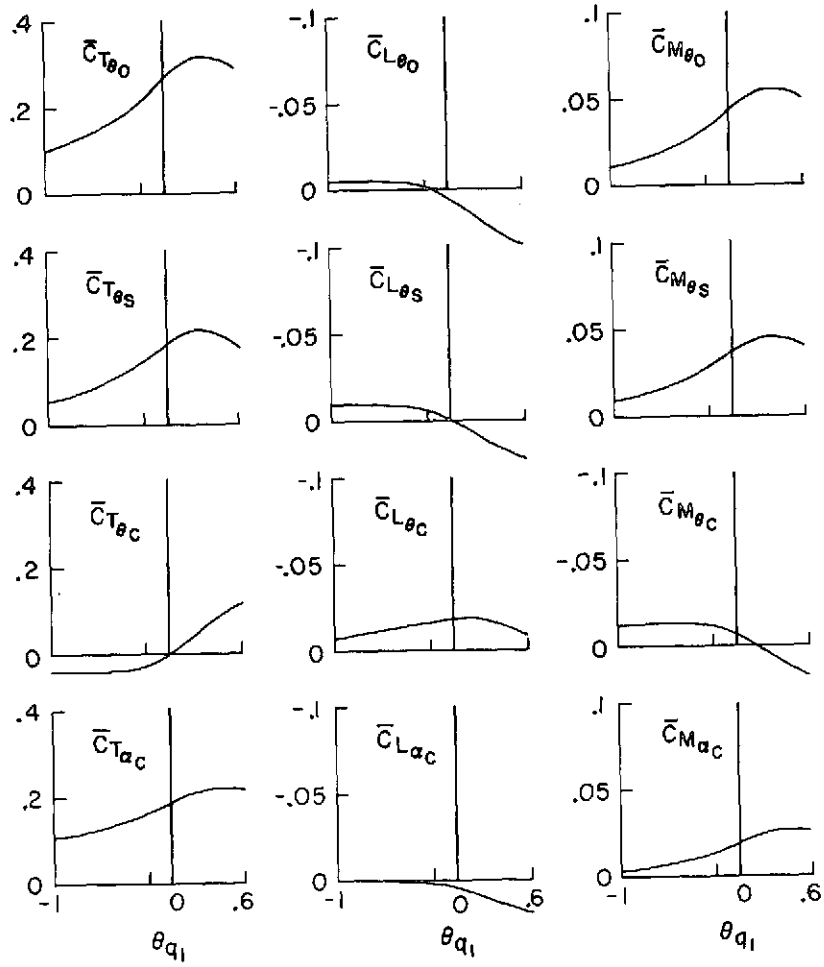

Figure 9.- Effect of pitch-flap coupling on response derivatives; $\mu = 0.6$, $P = 1.15$, $\gamma = 8$.

SENSITIVITY TO THE MATHEMATICAL MODEL

The basic properties of hingeless rotor flapping response are described in the previous section. The sensitivity of these results to various approximations of the mathematical model is now examined. The approximations are organized into three basic groups: numerical, aerodynamic, and structural.

Several forms of the blade root moment $\overline{C}_S$ are chosen as a basis for comparing the different approximations. The blade root moment provides a common basis for comparison for different representations of the hingeless rotor. For a centrally hinged, spring restrained blade, the root moment of the blade is directly proportional to the flapping angle. For a centrally hinged blade, therefore, the root moment, flapping angle, and tip deflection parameters are equally meaningful. For a flexible blade, there is no general relation between root moment and tip deflection, and a flapping angle cannot be uniquely defined. The root moment, however, can be uniquely defined for all hingeless rotor models; and it provides a common basis for comparing the various mathematical models of either rigid or elastic blades.

The blade collective pitch angle θ_o is chosen as the independent generalized control variable. The collective pitch is a basic control variable and is appropriate for the present purpose. Therefore, derivatives of the type $\partial(\,)\overline{C}_S/\partial\theta_o$ (which form the first column of $[\theta_S]$) are considered. In particular, results are presented in terms of the zeroth, the first, and the second harmonics of $\overline{C}_S$. For convenience, they are presented in the following forms: First, the zeroth harmonic blade root moment derivative is presented. (This derivative is also an indication of blade coning.) In compact form, it is written as:

$$\overline{C}_{S_{\theta_o}} \equiv \frac{\partial(a_o)\overline{C}_S}{\partial\theta_o} \tag{54a}$$

Next, the zeroth harmonics of the rotor pitch moment and roll moment derivatives (in the nonrotating coordinate system) are presented. These derivatives, directly proportional to the first sine and cosine components of the blade root moment in the rotating coordinate system, are written in compact form as:

$$\overline{C}_{L_{\theta_o}} \equiv \frac{\partial(a_o)\overline{C}_L}{\partial\theta_o} = -\frac{1}{2}\frac{\partial(b_1)\overline{C}_S}{\partial\theta_o} \tag{54b}$$

$$\overline{C}_{M_{\theta_o}} \equiv \frac{\partial(a_o)\overline{C}_M}{\partial\theta_o} = -\frac{1}{2}\frac{\partial(a_1)\overline{C}_S}{\partial\theta_o} \tag{54c}$$

Finally, the combined magnitude of the second harmonic (sine and cosine) of the blade root moment derivative is presented. The compact notation for this magnitude is

$$\bar{C}_{S2_{\theta_o}} \equiv \sqrt{\left[\frac{\partial(a_2)\bar{C}_S}{\partial\theta_o}\right]^2 + \left[\frac{\partial(b_2)\bar{C}_S}{\partial\theta_o}\right]^2} \tag{54d}$$

A typical hingeless rotor configuration is used as a baseline for comparisons: $P = 1.15$, $\gamma = 4$, $B = 0.97$, $e_{rc} = 0$, $\theta_{q_1} = 0$, $N = 3$, and $IN = 32$ with full reversed flow. For the comparisons of numerical and aerodynamic approximations, a centrally hinged, rigid blade representation is used. For the structural comparisons, a uniform elastic blade representation is used. When the elastic blade model is used with rotating mode shapes as modal functions, the eigenvalues of the equations (with $\gamma = 0$) correspond exactly to the natural frequencies of the modeled blade (in a vacuum). When the modal functions are not chosen to be the rotating modes, however, the eigenvalues of the equations only approach the blade frequencies as the number of modal coordinates increases. To discriminate between elastic mode shape effects and flap frequency effects, the similarity parameter $EI/m\Omega^2R^4$ is therefore chosen so that the first eigenvalue of the equations corresponds to the desired flap frequency P.

Numerical Approximations

Harmonic number— The coefficients and the aerodynamic forcing functions in the equations of motion are periodic functions of the independent variable ψ, the azimuth angle. In the harmonic balance method, these functions are expanded in Fourier series. Since the functions are not analytic, an exact Fourier representation is not possible and they must be approximated by truncated Fourier series. One of the modeling parameters in a rotor response analysis is therefore the number of harmonics, N, retained in the Fourier analysis.

Although previous investigators considered only one or two harmonics, the accuracy of this Fourier truncation has not been systematically examined. Figure 10 represents the effects of this truncation. For $\bar{C}_{S_{\theta_o}}$, one harmonic is adequate up to $\mu = 1.0$; two harmonics are required for higher advance ratios. For the rotor pitch and roll hub moments $\bar{C}_{M_{\theta_o}}$ and $\bar{C}_{L_{\theta_o}}$, however, one harmonic is adequate only to $\mu = 0.4$; two harmonics are adequate up to $\mu = 1.0$ and three harmonics are required for higher advance ratios. This is not surprising since the zeroth harmonics of the hub moments are proportional to the first harmonics of the blade root moment. As might be expected, the effects of Fourier truncation are more pronounced for the higher harmonic responses. Further evidence is given by the second harmonic root moment where one harmonic is adequate only up to $\mu = 0.2$, two harmonics are adequate up to $\mu = 0.8$, and three harmonics are required for higher advance ratios. Investigations using up to 15 harmonics for advance ratios up to 3.5 (including collective and cyclic pitch derivatives) indicate the following general conclusions. For the nth harmonic of response derivatives in the rotating reference frame (i.e., blade deformations, root shears, root moments, and

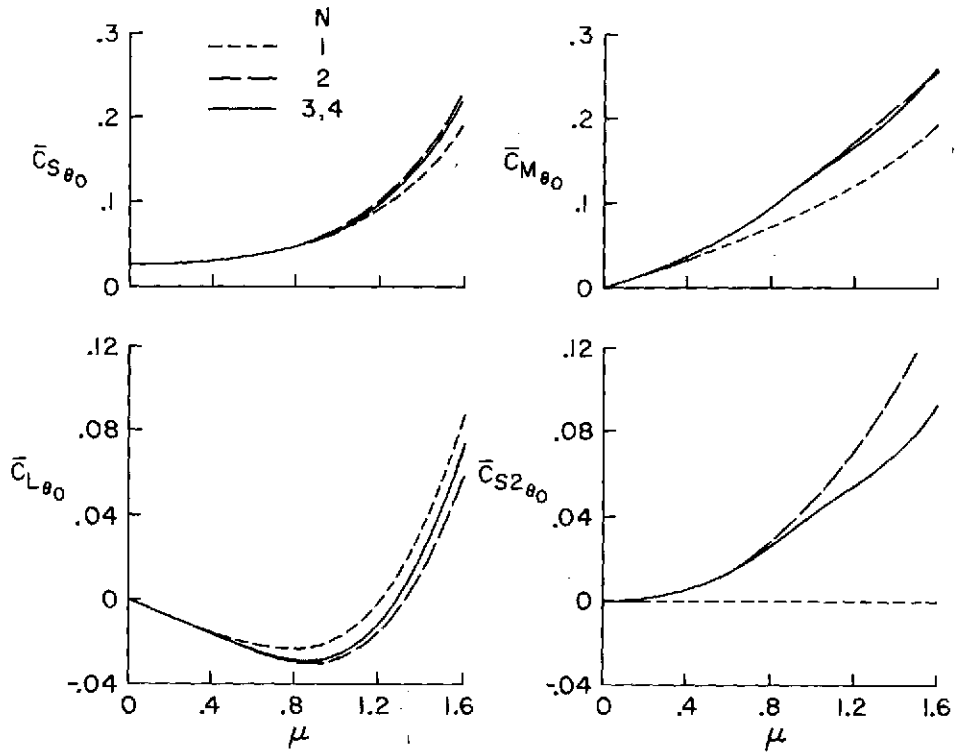

Figure 10.- Effect of number of harmonics on response of rigid hinged blade; $e = 0$, $e_{rc} = 0$, $B = 0.97$, $p = 1.15$, $\gamma = 4$, $\theta_{q_1} = 0$.

rotor thrust), n harmonics are required for $\mu < 0.4$, n + 1 harmonics are required for $0.4 < \mu < 1.0$, and n + 2 harmonics are required for $\mu > 1.0$. For response derivatives in the nonrotating system (i.e., rotor pitch and roll hub moments), n + 1, n + 2, and n + 3 harmonics are required for $\mu < 0.4$, $0.4 < \mu < 1.0$, and $\mu > 1.0$, respectively. Of course, for individual derivatives under special assumptions, fewer harmonics may sometimes be adequate; but, in general, the above requirements are necessary to ensure reasonable accuracy.

Azimuth increment— In obtaining the Fourier components of the equation coefficients, the integrals in equation (30) are numerically evaluated using a finite number (IN) of azimuthal increments. The number of increments can influence the results. Figure 11 illustrates the effect of the number of azimuthal increments. A reduction from 32 to 12 increments seems to have little effect on the derivatives calculated with three harmonics. The change from 12 to 7 increments, however, has a significant effect. In general, although only 2N + 1 azimuthal increments are required to define N Fourier coefficients, the higher harmonics of the response derivatives may be in error if additional increments are not taken. It is preferable to use twice the required minimum number of increments. For example, for the derivative $\partial(a_2)\bar{C}_S/\partial\theta_0$ at $\mu < 1.0$, it is advisable that $N = 3$ and $IN = 14$.

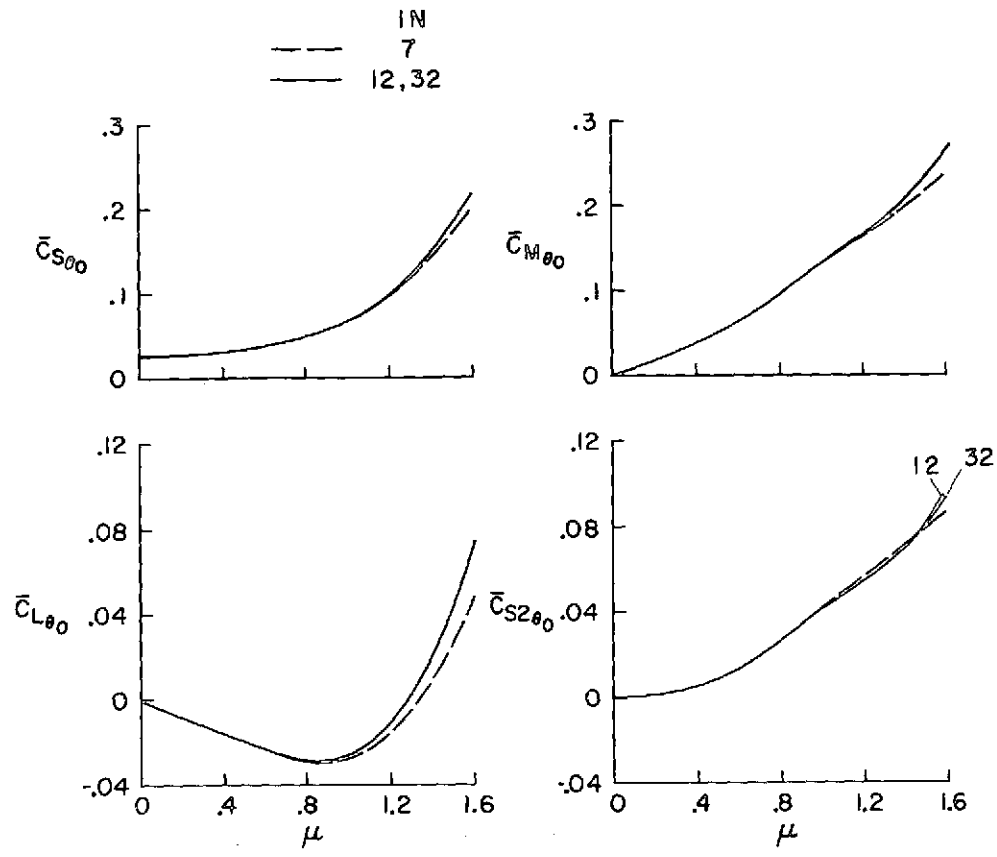

Figure 11.- Effect of number of azimuthal increments on response of rigid hinged blade; $e_{\gamma} = 0$, $e_{rc} = 0$, $B = 0.97$, $P = 1.15$, $\gamma = 4$, $\theta_{q_1} = 0$.

Aerodynamic Approximations

Compressibility— When the blade chord and lift-curve slope vary with radius and azimuth, an average Lock number γ is defined and the radial and azimuthal variations in γ are accounted for by the parameter $s(r,\psi)$. For example, the Prandtl-Glauert compressibility correction gives a variation in lift-curve slope:

$$s = \frac{\operatorname{sgn}(U_y)}{\sqrt{1 - M^2(r,\psi)}} \tag{55}$$

where M is the local blade section Mach number. Figure 12 gives response derivatives for three cases: first, with no compressibility correction $s = \pm 1$; second, with s determined by the Mach number at $\bar{r} = 3/4$, $\psi = 0$; and, third, with the full radial and azimuthal variation for M and s. In each case, the Mach number at $\bar{r} = 1.0$ and $\psi = 90°$ is maintained at 0.9 for all advance ratios. Completely neglecting compressibility results in considerable error. In hover, the correction using the Mach number at $\bar{r} = 3/4$ gives accurate results, but is increasingly in error as advance ratio

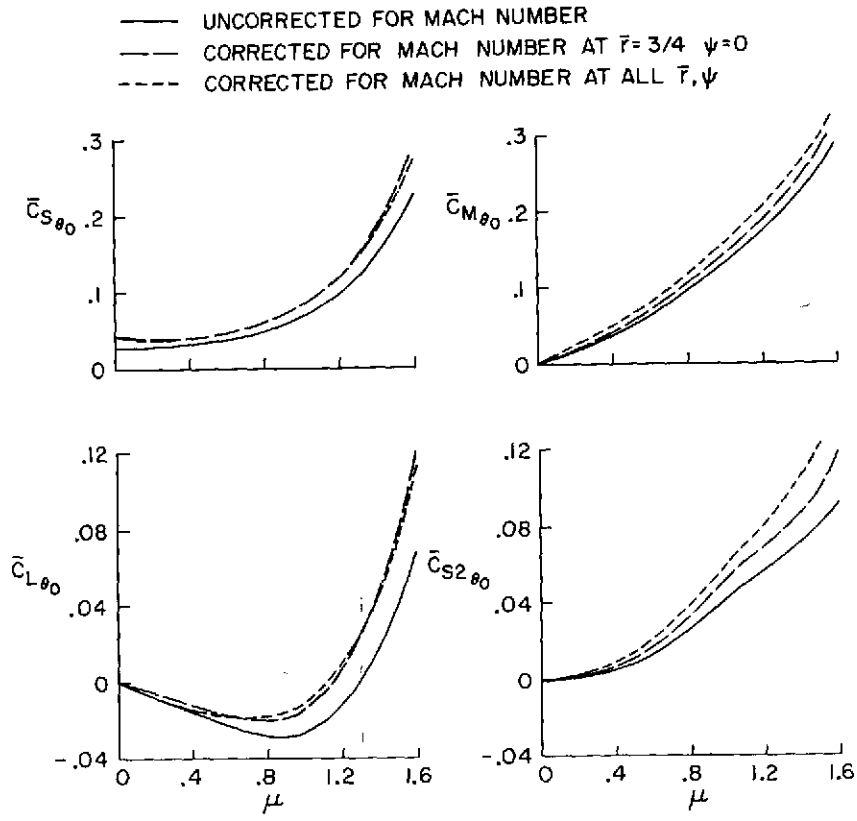

Figure 12.- Effect of compressibility on response of rigid hinged blade; advancing tip Mach number = 0.9, e = 0, e_{rc} = 0, B = 0.97, P = 1.15, γ = 4, θ_{q_1} = 0.

increases (especially for the higher harmonics of the response). For pitch and roll hub moments at moderate advance ratio and high Mach number, the azimuthal variation of Mach number is required.

Reversed flow assumptions— When a rotor is in forward flight, certain portions of the rotor disk will experience reversed flow. That is, during some portion of the azimuthal sweep, some or all radial positions will encounter airflow directed toward the trailing edge of the blade. This phenomenon can cause localized blade stall or reversed lift forces. For very low advance ratios, this effect is usually ignored. However, at higher advance ratios it must be considered. Figure 13 compares three cases: (1) assuming no reversed flow (s = 1), which implies that the direction of the lift force is not reversed when the relative fluid velocity is directed toward the blade trailing edge; (2) neglecting lift for reversed flow (s = 1, s = 0), which implies that all lift is lost when the relative velocity reverses; and (3) full reversed flow (s = ±1), which implies that the direction of the lift force reverses when the relative velocity reverses. For advance ratios less than 0.6, results for the three cases are nearly identical, but above this advance ratio large differences exist. With no reversed flow, the response

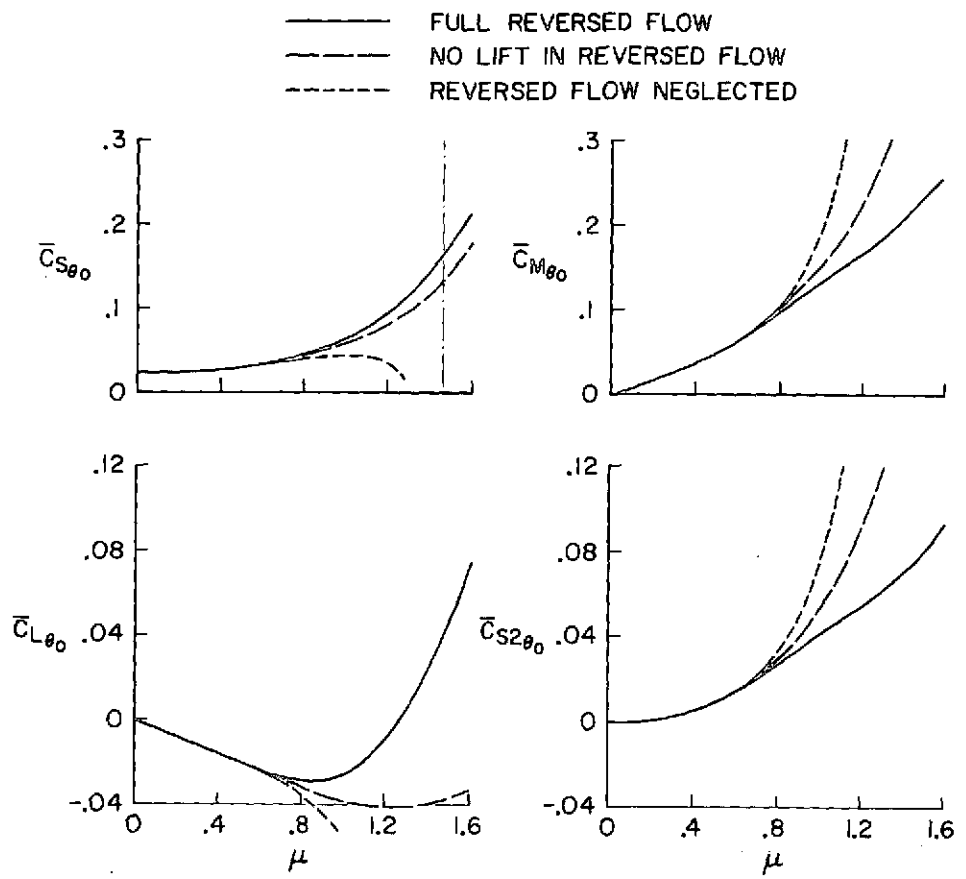

Figure 13.- Effect of reversed flow on response of rigid hinged blade; e = 0, e_{rc} = 0, B = 0.97, P = 1.15, γ = 4, θ_{q_1} = 0.

derivatives become infinite at an advance ratio of about 1.4. This "instability" is solely a result of neglecting reversed flow and does not appear when full reversed flow is considered. For an advance ratio greater than 0.6, full reversed flow is required.

Tip loss and root cutout— The parameter s can also be used to account for losses of lift at the blade tip and root. These effects are treated by setting s equal to zero where the blade is assumed to develop no lift:

$$s = 0 \quad \text{for:} \quad \bar{r} > B \ , \ \bar{r} < e_{rc} \tag{56}$$

The tip loss factor B accounts for the finite aspect ratio of a rotor blade by neglecting the lift beyond some radial station near the tip. Actually, the tip loss factor is not an independent parameter and can be entirely accounted for by redefining R in the dimensionless coefficients. However, the tip loss factor is usually treated as an independent parameter and this practice is followed here. Figure 14 shows that tip loss is significant for all rotor harmonics, even at low advance ratios.

Rotor blades also lose lift because of incomplete airfoil sections near the blade root. Although root cutout is often neglected because of the low

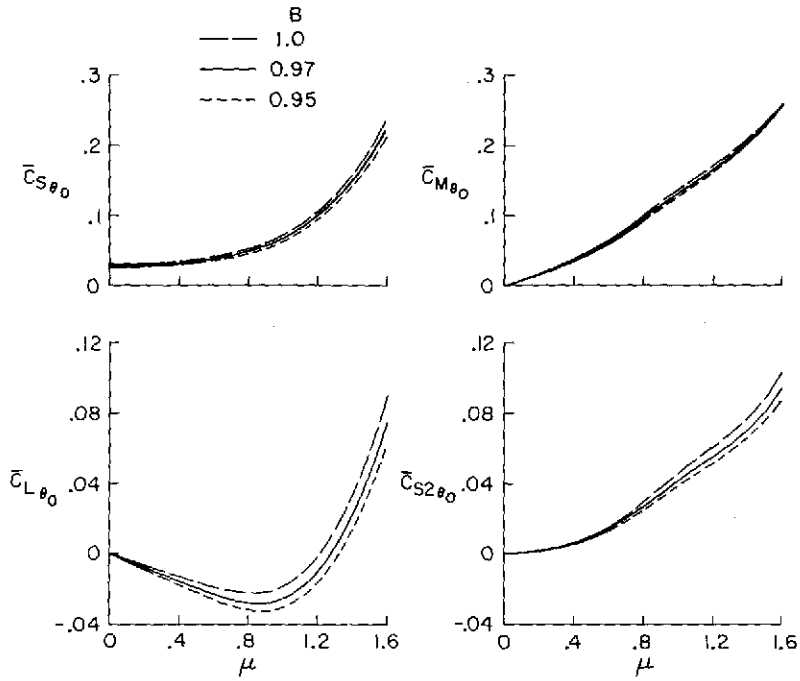

Figure 14.- Effect of tip loss factor on response of rigid hinged blade; $e = 0$, $e_{rc} = 0$, $P = 1.15$, $\gamma = 4$, $\theta_{q_1} = 0$.

dynamic pressure near the root (and because of the small area affected), it nevertheless affects rotor response at high advance ratios. Figure 15 shows the effect of root cutout. For $\mu < 1.0$, root cutout has a small, although noticeable, effect. At higher advance ratios, the effect becomes more pronounced and should not be ignored.

Structural Approximations

Mode shape— The bending mode shapes of a flexible rotor blade are functions of bending stiffness distribution EI, mass distribution m, and rotor angular velocity Ω. Figure 16 illustrates the variation of the first bending mode shape for a uniform cantilever blade as the similarity parameter $EI/m\Omega^2R^4$ varies from 0 to ∞. For small values of EI or large values of Ω, the mode shape approaches a straight line, and the rotating frequency P approaches unity. Conversely, for large values of EI and small values of Ω, the mode shape approaches the nonrotating beam mode shape and P approaches ∞.

The blade mode shape influences the flapping response by determining the aerodynamic, inertial, and elastic integrals that define the coefficients of the equations of motion. The aerodynamic loading in particular depends directly on the amplitude and slope of the mode shape (eq. (26)). Therefore, when a single modal function ϕ_j is used to calculate response derivatives, the choice of that modal function can significantly affect the results.

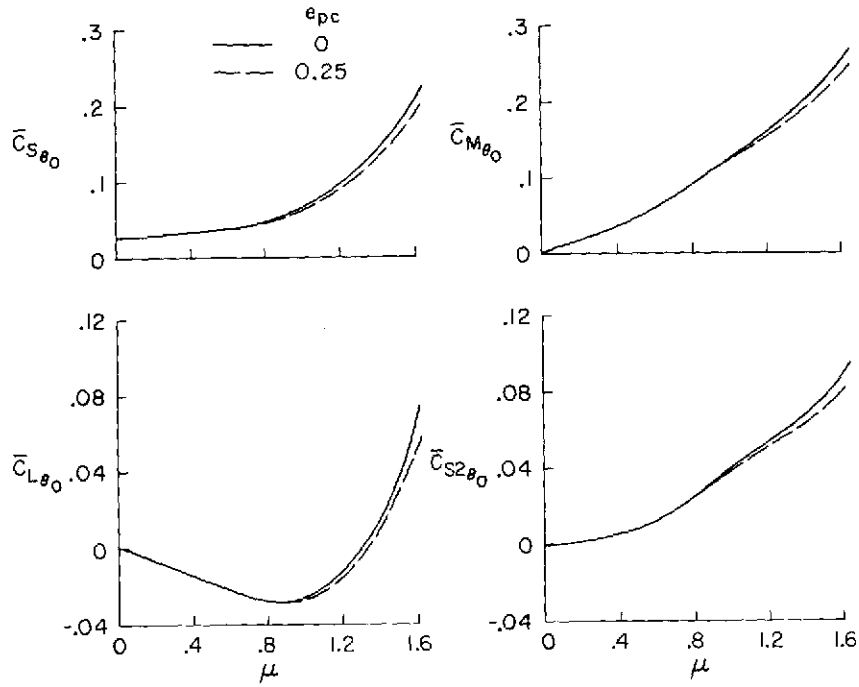

Figure 15.- Effect of root cutout on response of rigid hinged blade; e = 0, B = 0.97, P = 1.15, γ = 4, θ_{q_1} = 0.

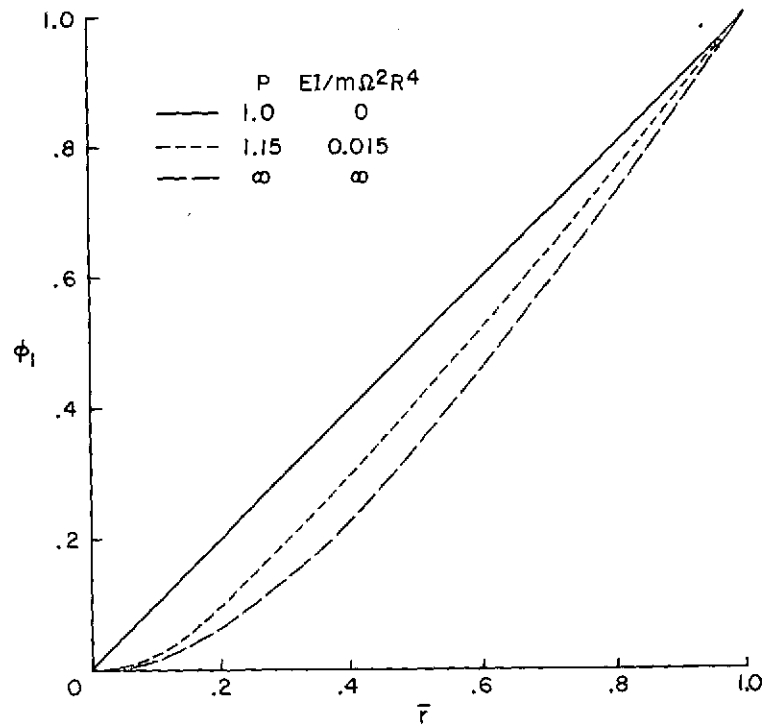

Figure 16.- First bending mode shapes for a uniform cantilever blade.

Figure 17 compares three different single-mode results over a range of flap frequencies from $P = 1.0$ to 1.8 and $\mu = 1.0$. The first result uses the first rotating mode shape (at each value of P) for the modal function. The second result is calculated using the nonrotating mode shape at all values of P. The proper rotating frequency is maintained by varying the similarity parameter $EI/m\Omega^2R^4$ appropriately. The third result is calculated using the straight line mode shape of a rigid, hinged blade with offset $e = 0.25$. This offset gives a good approximation for the nonrotating mode. For this case, K_β is varied to obtain the appropriate rotating frequency. (At P values below 1.09 and 1.22, respectively, the second and third cases require negative values of EI or K_β.) The figures clearly show that the two approximations are adequate for $P > 1.50$. At low values of P where the actual mode shape approaches a straight line passing through the axis of rotation, the nonrotating

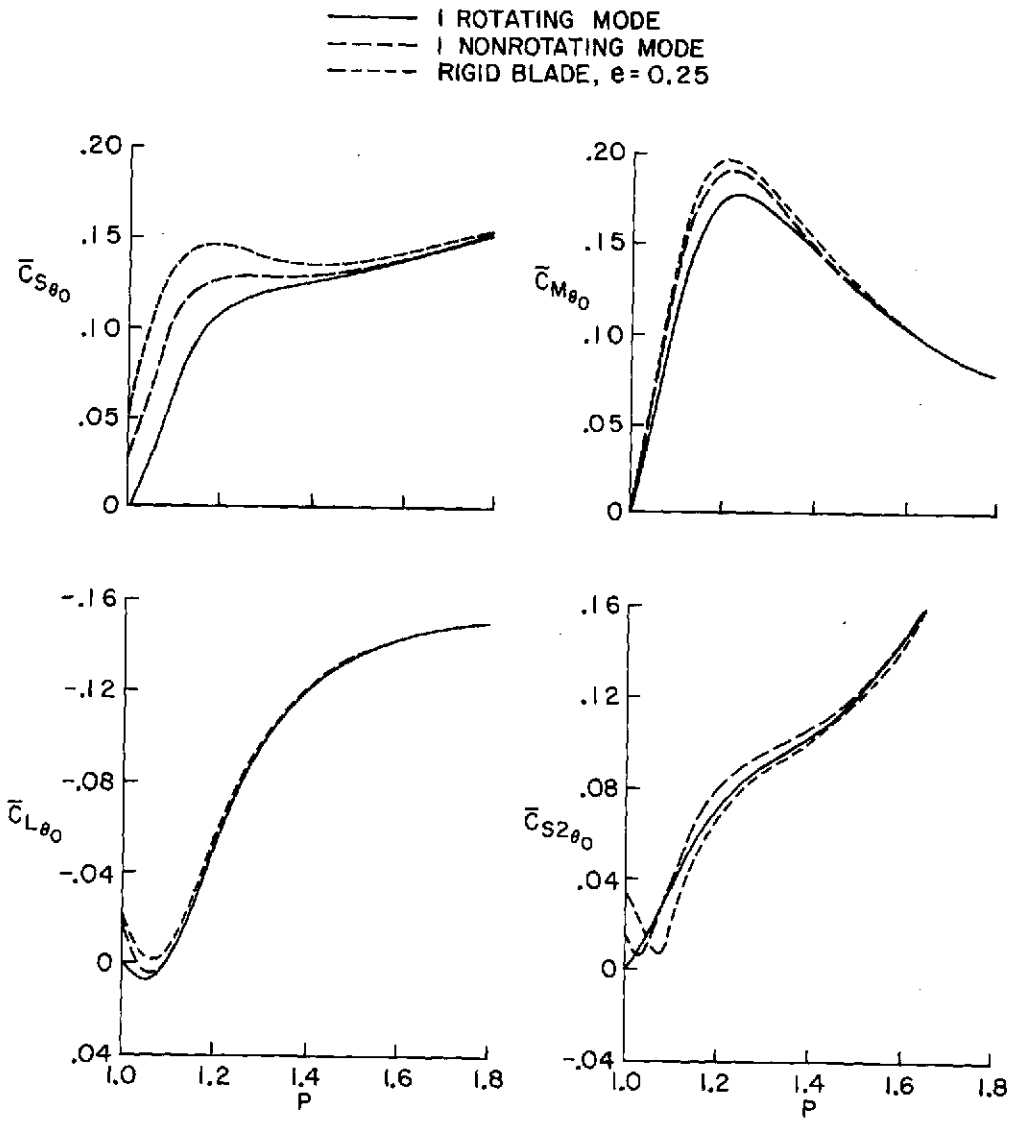

Figure 17.- Effect of mode shape on response of uniform blade as a function of flap frequency; $e_{rc} = 0.25$, $B = 0.97$, $\mu = 1.0$, $\gamma = 4$, $\theta_{q_1} = 0$.

approximations are much less accurate, although the offset hinged, rigid blade would give good results for low P if the offset e were varied as a function of P.

In figure 18, the same comparison is given for various values of μ at P = 1.15. At advance ratios below 0.4, there is little difference between the results. At higher advance ratios, however, there are large differences between the three modal representations. In figure 19, the differences between modal assumptions are examined in more detail. For the first curve, the nonrotating mode shape is used as the modal function in the aerodynamic and inertial integrals. For the second curve, the straight line mode shape with offset is used as the modal function in the aerodynamic and inertial integrals. For the third curve, the nonrotating mode shape is used in the inertial integrals and the straight line mode shape is used for the aerodynamic integrals. This figure shows that the major effect of mode shape results from the aerodynamic integrals rather than the inertial integrals because the first derivative of the mode shape (ϕ_j') strongly influences the periodic terms in D_{ij}^K, Q_{ij}^K, and W_{ij}^K. The mode shape, therefore, must be modeled closely for slope as well as for deflection.

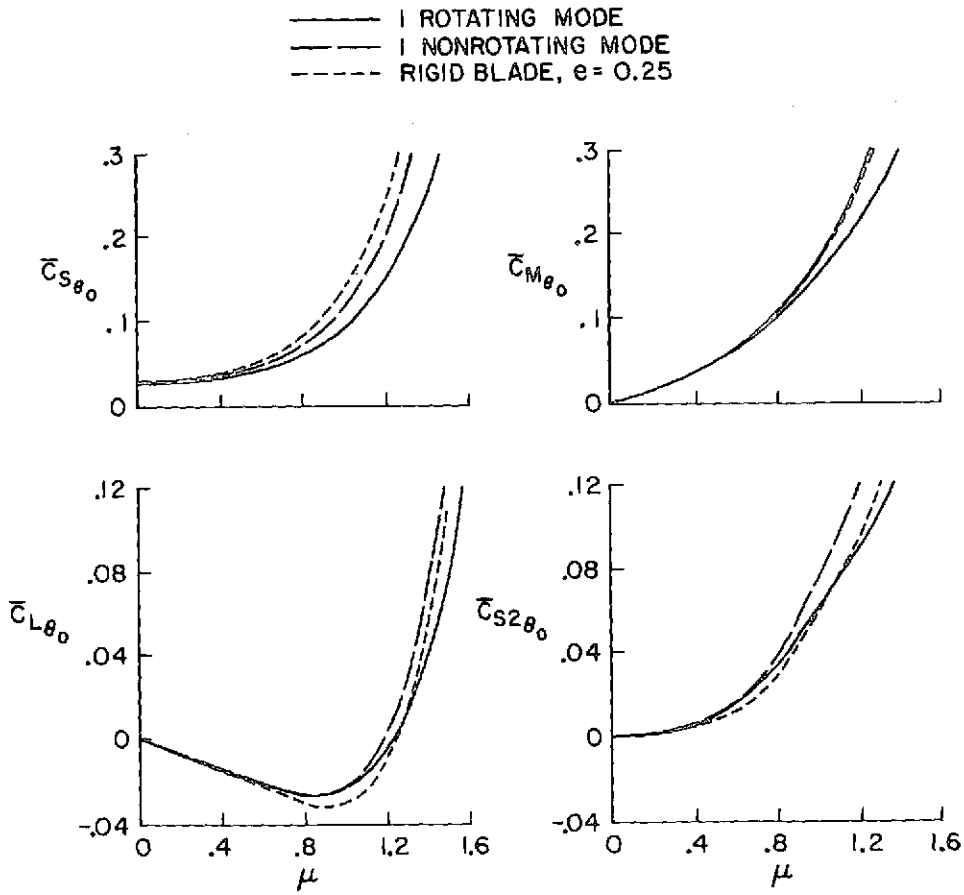

Figure 18.- Effect of mode shape on response of uniform blade as a function of advance ratio; e_{rc} = 0.25, B = 0.97, P = 1.15, γ = 4, θ_{q_1} = 0.

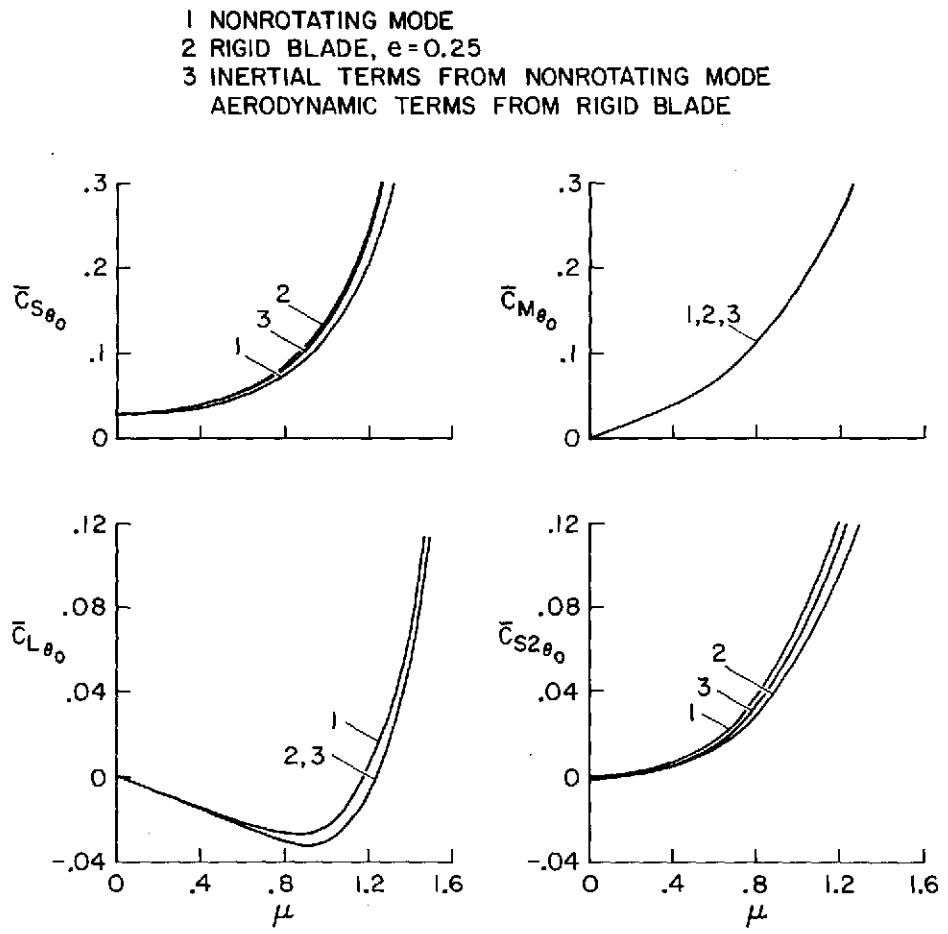

Figure 19.- Relative importance of inertial and aerodynamic contributions to the response of uniform blade; B = 0.97, e_{rc} = 0.25, P = 1.15, γ = 4, θ_{q_1} = 0.

Number of modes— Because of the periodic nature of the aerodynamic terms in the blade equations, even the rotor response to steady control inputs is time-varying. This implies that no single mode shape can completely represent the blade motion at all azimuths. Mathematically, this phenomenon can be attributed to the fact that steady control inputs produce unsteady aerodynamic blade forces at integer multiple frequencies of the rotor speed. Thus, any higher modes with frequencies in the range of aerodynamic excitation will contribute to the rotor response. In addition, even the exact rotating mode shapes (which represent uncoupled degrees of freedom for a rotor in a vacuum) become coupled in the rotor equations because of the aerodynamic terms. It follows that, when the higher-order modes participate in the response, they do more than merely superpose their own contributions. The higher modes actually couple with the first mode, altering its response as well.

Figure 20 compares results calculated using as many as four rotating modes. Below an advance ratio of 0.6, the higher modes are not important. As

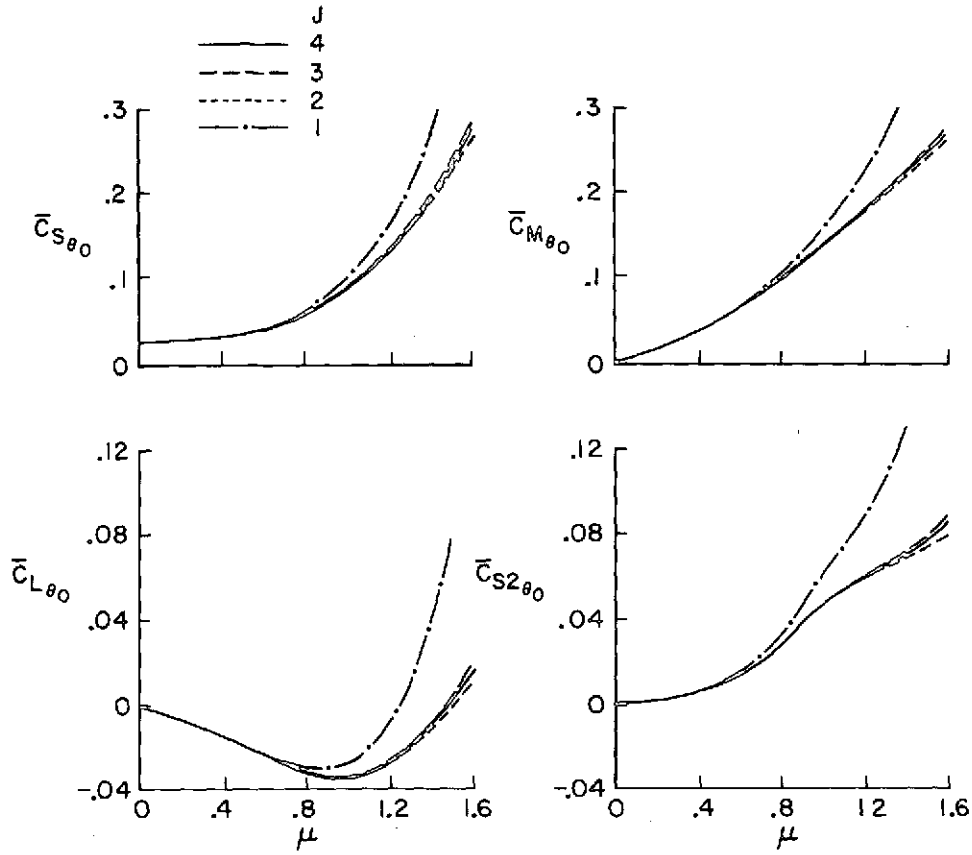

Figure 20.- Effect of number of modal coordinates on response of uniform blade, rotating modes; B = 0.97, e_{rc} = 0, P = 1.15 γ = 4, θ_{q_1} = 0.

the advance ratio is increased, however, the second and third modes begin to influence the response. For any given advance ratio, however, the solution converges as the number of modes becomes large. The two-mode solution is a good approximation up to μ = 1.2, and the three-mode solution is accurate to μ = 1.6. Convergence for blades with arbitrary mass and stiffness distributions is not as easily generalized and will depend on the proximity of the higher blade frequencies to the integer multiple aerodynamic forcing frequencies.

Nonrotating modes— Although the use of the exact rotating modes is desirable for rapid convergence, the use of such modes can be inconvenient and cumbersome for practical use. When the uncoupled rotating modes are used as modal functions, a different set of mode shapes must be used at every value of P (or rotor speed) for which the response is desired. This means that many preliminary calculations must be performed for a range of P values before the response derivatives can be determined. This problem may be circumvented by use of a convenient set of linearly independent functions as modal functions for all values of P. Although these functions must necessarily be highly coupled over part of the P range (so that an eigenvalue problem must still be solved to determine the exact value of P), they

nevertheless have the advantage of being independent of the rotor operating condition.

A convenient choice for such modal functions is the set of nonrotating mode shapes for a uniform beam. The nonrotating modes have the advantage of being the limiting case of the uniform rotating modes as $P \to \infty$. In figure 21, response derivatives are presented using one, two, and three nonrotating modes as modal functions, together with the result using four rotating modes from figure 20. As previously noted, a single nonrotating mode as a modal function is only valid up to $\mu = 0.4$. The two-mode solution, however, is somewhat better and is accurate up to $\mu = 0.8$. The three-mode solution gives excellent results up to $\mu = 1.4$. Therefore, although the nonrotating modes converge more slowly to the proper solution than do the rotating modes, they converge rapidly enough to make them of practical use.

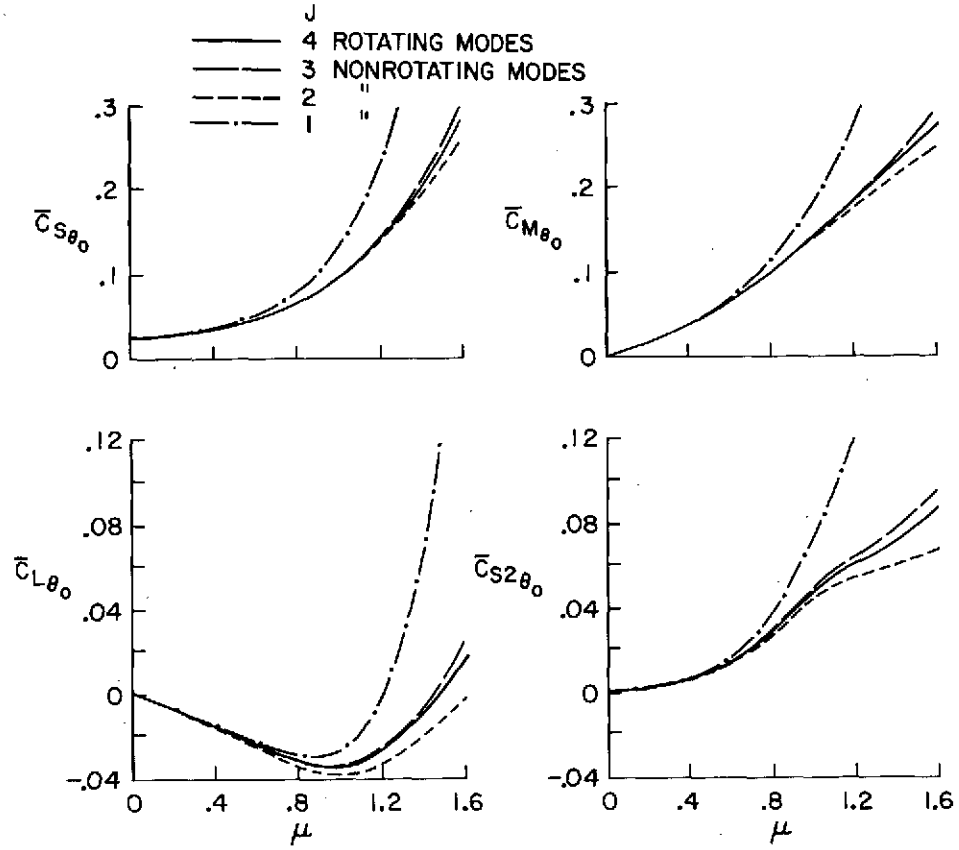

Figure 21.- Effect of number of modal coordinates on response of uniform blades, nonrotating modes; $B = 0.97$, $e_{rc} = 0$, $P = 1.15$, $\gamma = 4$, $\theta_{q_1} = 0$.

CONCLUDING REMARKS

In this report, the linear equations of motion for the flapping response of an elastic rotor blade in forward flight were derived, and a generalized harmonic balance method for solving these equations was formulated. The basic response characteristics of the hingeless rotor were examined in terms of the

main system parameters and the sensitivity of the derivatives to the mathematical model was investigated. Comprehensive figures and tables were presented in an appendix to facilitate rapid estimation of twelve hingeless rotor derivatives.

The use of a simplified mathematical model for this study was discussed in detail. The main purpose was to simplify the problem in order to permit investigation of the fundamental behavior of a wide variety of hingeless rotor configurations. Therefore, it is pertinent to review the assumptions of the mathematical model. Only flap bending deflections were considered. Torsion and lead-lag bending were not included. Linear quasisteady aerodynamics were used, without stall or nonuniform downwash. These assumptions are satisfactory for the purposes stated previously. Refinements to the mathematical model (treated in appendix A) include unsteady aerodynamics, rotor hub motions, and nonuniform downwash.

It is appropriate to review a few of the findings regarding basic hingeless rotor response. The simplest behavior is evident in the control power derivatives in hover. Depending only on the parameter $C = 8(P^2 - 1)/\gamma$ (for a rigid blade without hinge offset), the magnitude and phase of the dimensionless response to cyclic pitch vary from 0 to 1/16 and 90° to 0°, respectively, as C varies from 0 to ∞. Simplified closed-form expressions for the derivatives in forward flight were given and are valid for low advance ratios. At low advance ratios, the basic behavior is little different from that exhibited in hover. The derivatives are quite sensitive to flap frequency. For hingeless rotors with moderate values of P, large pitch and roll coupling can exist and static angle-of-attack instability can be pronounced. However, these undesirable properties can be minimized by proper selection of the basic configuration properties (including pitch-flap coupling).

The hingeless rotor flapping response was found to be sensitive to the mathematical modeling in the following respects. For $\mu > 0.4$, the number of harmonics retained in the analysis should be larger by 2 than the highest response harmonic of interest, and the number of azimuthal points chosen to define the harmonic coefficients should be twice the minimum number $(2N + 1)$ needed to define N harmonic coefficients.

The radial and azimuthal variations of compressibility were found to be important for an advancing tip Mach number of 0.9. Reversed flow effects may be neglected below $\mu = 0.6$; however, they are very important for higher advance ratios. The tip loss factor is important for all advance ratios, but root cutout is only important above $\mu = 1.0$.

For uniform stiffness rotor blades, at $\mu = 0.8$, mode shape effects are unimportant above $P = 1.5$, but approximate mode shapes are increasingly inaccurate as P is reduced. For $P = 1.15$, approximate mode shapes are accurate below $\mu = 0.4$, but accurate modes are required for higher μ. The effect of mode shape approximations was found to influence mainly the aerodynamic forces. The rigid, hinged, spring-restrained blade approximation is only useful for low advance ratios. If possible, elastic cantilever modes should be used.

The second and higher elastic bending modes are unimportant below $\mu = 0.6$. Two modes and three modes are adequate up to $\mu = 1.2$ and 1.6, respectively. Approximate nonrotating modes were found to be useful and accurate. One, two, and three nonrotating modes were adequate up to $\mu = 0.4$, 0.8, and 1.4, respectively.

Ames Research Center
National Aeronautics and Space Administration

and

Army Air Mobility R&D Laboratory
Moffett Field, Calif. 94035, Sept. 18, 1974

APPENDIX A

EXTENSIONS OF THE BLADE FLAPPING EQUATIONS

The blade flapping equations given by equation (29) are sufficient to determine basic steady-state rotor response derivatives. However, these equations may be easily extended to incorporate unsteady airfoil aerodynamics, induced downwash (steady and unsteady), rotor hub motion, built-in blade preshape, and unsteady harmonic control excitations. The extended equations can also be solved by the generalized harmonic balance method.

The additional effects considered in this appendix can be significant if a more thorough treatment of hingeless rotor response is required, including, for example, downwash aerodynamics, rotor shaft angular rate derivatives, and dynamic response of rotors. A detailed treatment and discussion of the behavior of the extended equations is beyond the scope of this report; however, it is not difficult to include the equations as a convenient addition to the basic development. Results using the equations in this appendix are available, however, in references 7 and 20.

Unsteady Hub Motions

The Lagrangian of a rotating beam performing roll (α_s), pitch (α_c), and plunge (z) motions at the hub is given by

$$J_L = \int_\varepsilon^R \left\{ \frac{1}{2} m \left[\frac{d\psi}{dt} r + w\left(\frac{d\alpha_s}{dt} r \cos\phi - \frac{d\alpha_c}{dt} r \sin\phi \right) \right]^2 \right.$$
$$+ \frac{1}{2} m \left(\frac{\partial w}{\partial t} - \frac{dz}{dt} - \frac{d\alpha_s}{dt} r \sin\phi - \frac{d\alpha_c}{dt} r \cos\phi \right)^2 - mgw$$
$$\left. - \frac{1}{2} (EI) \left(\frac{\partial^2 w}{\partial r^2} \right)^2 - \frac{1}{2} T_r \left(\frac{\partial w}{\partial r} + \frac{\partial w_o}{\partial r} \right)^2 \right\} dr - \frac{1}{2} K_\beta \left(\frac{\partial w}{\partial r} \right)^2_{r=\varepsilon} \qquad (A1)$$

which is identical to equation (1) except for the addition of roll rate ($d\alpha_s/dt$), pitch rate ($d\alpha_c/dt$), plunge rate (dz/dt), built-in blade preshape (w_o), and local acceleration of gravity (g). (The blade deformation w is defined as the displacement with respect to w_o so that the blade vertical position is $w + w_o$.) Correspondingly, the left-hand side of equation (2) will take on the additional terms:

$$\int_{\varepsilon}^{R}\left[m\frac{d^2z}{dt^2}+m\frac{d^2\alpha_s}{dt^2}r\sin\psi+2m\frac{d\alpha_s}{dt}\frac{d\psi}{dt}r\cos\psi+m\frac{d^2\alpha_c}{dt^2}r\cos\psi\right.$$

$$\left.-2m\frac{d\alpha_c}{dt}\frac{d\psi}{dt}r\sin\psi-mg+\frac{d}{dr}\left(T_r\frac{dw_o}{dr}\right)\right]dr\,\delta w-T_r\left(\frac{dw_o}{dr}\right)\delta w\Big|_{\varepsilon}^{R} \qquad (A2)$$

and the right-hand side of equation (7) will contain the additional forcing functions:

$$R\int_{\varepsilon}^{R}m\left(-g+\frac{d^2z}{dt^2}+\frac{d^2\alpha_s}{dt^2}r\sin\psi+2\frac{d\alpha_s}{dt}\Omega r\cos\psi+\frac{d^2\alpha_c}{dt^2}r\cos\psi\right.$$

$$\left.-2\frac{d\alpha_c}{dt}\Omega r\sin\psi\right)dr-\Omega^2R^2\int_{\varepsilon}^{R}\left(mr\phi_i\frac{d\phi_o}{dr}-\phi_i\frac{d^2\phi_o}{dr^2}\int_{r}^{R}m\eta\,d\eta\right)dr\,q_o$$

$$-\Omega^2R^2\left(\phi_i\frac{d\phi_o}{dr}\int_{r}^{R}m\eta\,d\eta\right)\Big|_{\varepsilon}^{R}q_o \qquad (A3a)$$

where ϕ_o and q_o represent the built-in blade preshape:

$$w_o = R\phi_o q_o \qquad (A3b)$$

With the additional definitions,

$$\left.\begin{aligned}
&g_o \equiv \frac{g}{\Omega^2R}-\frac{\ddot{z}}{R}\,,\quad g_s \equiv 2\dot{\alpha}_c-\ddot{\alpha}_s\,,\quad g_c \equiv -2\dot{\alpha}_s-\ddot{\alpha}_c\\
&\bar{m} \equiv \frac{1}{\rho acR}\int_0^1 m\,d\bar{r}\,,\quad S_y \equiv \frac{1}{\rho acR}\int_0^1 m\bar{r}\,d\bar{r}\,,\quad m_{yy} \equiv \frac{1}{\rho acR}\int_0^1 m\bar{r}^2\,d\bar{r} \equiv \frac{1}{\gamma}\\
&m_{yo} \equiv \frac{1}{\rho acR}\int_0^1 m\bar{r}\phi_o\,d\bar{r}\,,\quad P_{oi} \equiv \frac{1}{\rho acR}\int_e^1\left(\phi_i'\phi_o'\int_{\bar{r}}^1 m\eta\,d\eta\right)d\bar{r}
\end{aligned}\right\} \qquad (A4)$$

the blade flapping equations (eq. 8) become

$$\sum_{j=1}^{J}\left[m_{ij}\ddot{q}_j+(P_{ij}+K_{ij})q_j\right]=\int_e^1\phi_i\bar{F}\,dr+P_{oi}q_o-S_ig_o$$

$$-m_{yi}(g_s\sin\psi+g_c\cos\psi)\,,\qquad i=1,J \qquad (A5)$$

Similarly, the shear and moment equations (eq. 13a) become

$$\left.\begin{aligned}
\bar{C}_V &= -\sum_{j=1}^{J} S_j \ddot{q}_j + \int_0^1 \bar{F}\, d\bar{r} - mg_o - S_y(g_s \sin\psi + g_c \cos\psi) \\
\bar{C}_S &= -\sum_{j=1}^{J} m_{yj}(\ddot{q}_j + q_j) + \int_0^1 \bar{F}\bar{r}\, d\bar{r} - S_y g_o - m_{yy}(g_s \sin\psi + g_c \cos\psi) \\
&\quad - m_{yo} q_o
\end{aligned}\right\} \tag{A6}$$

Unsteady Aerodynamics

The effects of classical, two-dimensional, unsteady aerodynamics can be included in equation (22) by simply assigning to the three angle-of-attack components three individual complex parameters $s_\theta(r,\psi)$, $s_u(r,\psi)$, and $s_w(r,\psi)$ in place of $s(r,\psi)$. These parameters will depend on the reduced frequency k. The aerodynamic loading in equation (22) becomes

$$F = \frac{\rho a c}{2}\left[s_\theta(U_y{}^2\theta) - s_u(U_y \bar{U}_z) - s_w\left(U_y \frac{dw}{dt}\right)\right] \tag{A7}$$

where $\bar{U}_z \equiv U_z - (dw/dt)$. One example of expressions for s may be obtained from Theodorsen's theory, reference 21. From that theory,

$$\left.\begin{aligned}
s_\theta &= \frac{\pm\bar{c}}{c}\left\{C(k) + k^2\left(\frac{e_{ac}}{2} - \frac{1}{4}\right) + ik\left[\frac{1}{2} + C(k)\left(1 - 2\,\frac{e_{ac}}{2}\right)\right]\right\} \\
s_u &= \frac{\pm\bar{c}}{c} C(k), \quad s_w = \frac{\pm\bar{c}}{c}\left[C(k) + \frac{ik}{2}\right]
\end{aligned}\right\} \tag{A8}$$

where e_{ac} is the aerodynamic offset (which may be different for regions of forward and reversed flow), k is the local reduced frequency $\Omega\bar{c}(\omega \pm n)/2U_y$, and C(k) is the Theodorsen function. (More exact formulations for s can be treated in a similar manner.) This makes s_θ, s_u, s_w complex functions of r, ψ, the frequency of the excitation ω, and the harmonic number n. Furthermore, equation (A8) must include a superposition of all harmonics of the blade motion. The generalized harmonic balance method developed in appendix B provides the proper value of reduced frequency k to be used for each superposed harmonic in the equations.

The effects of unsteady hub motions and blade preshape can be included in equation (25) by writing more complete expressions for θ and $\bar{U}_z$. Specifically, blade twist can be added to the blade pitch angle θ in equation (24).

$$\theta_{twist} = \theta_t P_t(\bar{r}) \tag{A9a}$$

where P_t is an arbitrary pretwist shape (e.g., for linear twist $P_t = \bar{r} - 3/4$) and θ_t is the magnitude of the pretwist. The velocity U_z is also generalized to include the effects of induced inflow velocity ν, plunge, pitch, roll, and blade preshape w_o.

$$\begin{aligned} U_z \equiv \frac{dw}{dt} + \overline{U}_z &= \frac{dw}{dt} + V_z - V_x\left(\frac{dw}{dr} + \frac{dw_o}{dr}\right)\cos\psi \\ &= \frac{dw}{dt} + \nu - \frac{dz}{dt} - \frac{d\alpha_s}{dt} r \sin\psi - \frac{d\alpha_c}{dt} r \cos\psi - V_\infty \sin(\alpha_c) \\ &\quad + V_\infty \cos(\alpha_c)\left(\frac{dw}{dr} + \frac{dw_o}{dr}\right)\cos\psi \end{aligned} \tag{A9b}$$

Equation (25) therefore becomes

$$\begin{aligned} \overline{F} = \frac{1}{2}\Bigg\{ & s_\theta(\bar{r} + \mu \sin\psi)^2 \left[\theta_o + \theta_s \sin\psi + \theta_c \cos\psi + \theta_t P_t(\bar{r}) + \sum_{j=1}^{J} \theta_{q_j} q_j\right] \\ & - s_u(\bar{r} + \mu \sin\psi)\left[\lambda(r,\psi) + \mu \cos\psi \sum_{j=1}^{J} \phi_j' q_j\right]\Bigg\} \\ & - s_w(\bar{r} + \mu \sin\psi) \sum_{j=1}^{J} \phi_j \dot{q}_j \end{aligned} \tag{A10a}$$

where

$$\mu \equiv \frac{V_\infty \cos(\alpha_c)}{\Omega R} \tag{A10b}$$

$$\begin{aligned} \lambda(r,\psi) \equiv & \frac{\nu(r,\psi) - (dz/dt) - V_\infty \sin\alpha_c}{\Omega R} \\ & - \dot{\alpha}_s \bar{r} \sin\psi - \dot{\alpha}_c \bar{r} \cos\psi \end{aligned} \tag{A10c}$$

Final Equations

Although equation (A10) is in a readily usable form, a few additional definitions render it more tractable for use in the blade equations. First, the inflow distribution is expressed as an expansion in functions of $\bar{r}$ and ψ:

$$\lambda(r,\psi) = \lambda_o P_1(\bar{r}) + \sum_{n=1}^{I} [\lambda_{ns} P_{2n}(\bar{r}) \sin(n\psi) + \lambda_{nc} P_{2n+1}(\bar{r}) \cos(n\psi)] \tag{A11}$$

Second, a new set of generalized control variables θ_k is defined with $K = 9 + 2I$:

$$\left.\begin{aligned} &\theta_1 \equiv \theta_o\ ,\quad \theta_2 \equiv \theta_s\ ,\quad \theta_3 \equiv \theta_c\ ,\quad \theta_4 \equiv \theta_t\ ,\quad \theta_5 \equiv q_o\ ,\quad \theta_6 \equiv g_o\ ,\quad \theta_7 \equiv g_s \\ &\theta_8 \equiv g_c\ ,\quad \theta_q \equiv \lambda_o\ ,\quad \theta_{8+2i} \equiv \lambda_{is}\ ,\quad \theta_{q+2i} \equiv \lambda_{ic}\ ,\quad i = 1, I \end{aligned}\right\} \tag{A12}$$

Third, several new V functions are defined for equation (28):

$$\left.\begin{aligned} V_4 &\equiv V_1 P_t(\bar{r}) \\ V_5 &\equiv -\left[\frac{\mu\bar{r}\cos(\psi)}{2} + \frac{\mu^2 \sin(2\psi)}{4}\right]\phi_o'(\bar{r}) \\ V_6 &\equiv V_7 = V_8 = 0 \\ V_{q+2j} &\equiv -\left[\frac{\bar{r}}{2} + \frac{\mu \sin(\psi)}{2}\right] P_{2j+1} \cos(j\psi)\ , \qquad j = 0, I \\ V_{8+2j} &\equiv -\left[\frac{\bar{r}}{2} + \frac{\mu \sin(\psi)}{2}\right] P_{2j} \sin(j\psi)\ , \qquad j = 1, I \end{aligned}\right\} \tag{A13}$$

The resultant form of the forcing function becomes

$$\bar{F} = \sum_{j=1}^{J} [-s_w V_C \phi_j \dot{q}_j - s_u (V_K \phi_j' + \theta_{q_j} V_1) q_j] + \sum_{i=1}^{4} s_\theta V_i \theta_i + \sum_{i=5}^{9+2I} s_w V_i \theta_i \tag{A14}$$

Equation (30) may then be extended by

$$
\left.
\begin{aligned}
D_{ij}^{C} &= \int_{e}^{1} s_w V_C \phi_i \phi_j \, d\bar{r} \\
D_{ij}^{K} &= \int_{e}^{1} s_u V_K \phi_i \phi_j' \, d\bar{r} \\
D_{ij}^{A} &= \int_{e}^{1} \theta_{q_j}(\bar{r}) s_\theta V_1 \phi_i \, d\bar{r} \\
D_{ij}^{V} &= \int_{e}^{1} s_\theta V_j \phi_i \, d\bar{r} , \qquad j = 1, 4 \\
D_{i5}^{V} &= \int_{e}^{1} s_u V_j \phi_i \, d\bar{r} - P_{oi} \\
D_{i6}^{V} &= -S_i \\
D_{i7}^{V} &= -m_{yi} \sin \psi \\
D_{i8}^{V} &= -m_{yi} \cos \psi \\
D_{ij}^{V} &= \int_{e}^{1} s_w V_j \phi_i \, d\bar{r} , \qquad j = q, q + 2I \\
Q_j^{C} &= \int_{e}^{1} s_w V_C \phi_j \bar{r} \, d\bar{r} \\
Q_j^{K} &= \int_{e}^{1} s_u V_K \phi_j' \bar{r} \, d\bar{r} \\
Q_j^{A} &= \int_{0}^{1} \theta_{q_j}(\bar{r}) s_\theta V_I \bar{r} \, d\bar{r}
\end{aligned}
\right\} \qquad \text{(A15)}
$$

(Continued)

$$
\left.
\begin{aligned}
Q_j^V &= \int_0^1 s_\theta V_j \bar{r}\, d\bar{r}\,, \qquad j = 1,\ 4 \\
Q_5^V &= \int_0^1 s_u V_5 \bar{r}\, d\bar{r} - m_{yo} \\
Q_6^V &= -S_y \\
Q_7^V &= -m_{yy} \sin\psi \\
Q_8^V &= -m_{yy} \cos\psi \\
Q_j^V &= \int_0^1 s_u V_j \bar{r}\, d\bar{r}\,, \qquad j = 9,\ 9 + 2I \\
W_j^C &= \int_e^1 s_w V_C \phi_j\, d\bar{r} \\
W_j^K &= \int_e^1 s_u V_K \phi_j'\, d\bar{r} \\
W_j^A &= \int_0^1 \theta q_j(\bar{r}) s_\theta V_1\, d\bar{r} \\
W_j^V &= \int_0^1 s_\theta V_j\, d\bar{r}\,, \qquad j = 1,\ 4
\end{aligned}
\right\} \qquad \text{(A15)}
$$

(Continued)

$$
\left.
\begin{aligned}
W_6^V &= -\bar{m} \\
W_7^V &= -S_y \sin\psi \\
W_8^V &= -S_y \cos\psi \\
W_j^V &= \int_0^1 s_u V_j \, d\bar{r} , \qquad j = 5,\ j = 9,\ 9 + 2I
\end{aligned}
\right\} \tag{A15}
$$

The resultant extended equations are identical in form to equations (29) except that the definitions for D, Q, and W are given by equation (A15).

Analysis

The formal solution to the unsteady flapping equations is obtained in a manner similar to that for the steady equations. Equation (36) is altered by the addition of a harmonic modulation of the forcing functions and Floquet's theorem still applies:

$$
\{\dot{x}\} - \left[\eta_j\right]\{x\} = \{U\}e^{i\omega\psi} \tag{A16}
$$

The solution for the q_j follows along the same line as equations (37) to (39):

$$
q_j = \sum_{m=1}^{2J} \sum_{k=-N}^{+N} \sum_{n=-N}^{+N} \frac{A_{jm,k} U_{m,n} e^{i(m+n+\omega)\psi}}{\omega + n - \eta_m} , \qquad j = 1,\ J \tag{A17}
$$

Therefore, Floquet theory establishes the existence of a solution to the unsteady flapping equations of the form

$$
q_j = \left[\sum_{n=0}^{N} (a_n)_{q_j} \cos(n\psi) + (b_n)_{q_j} \sin(n\psi)\right] e^{i\omega\psi} \tag{A18}
$$

The a_n and b_n terms are, in this case, complex quantities that indicate the magnitude and phase of each harmonic of the response. The harmonic balance procedures developed in appendix B include the case of the harmonic modulation $e^{i\omega\psi}$ so that the unsteady equations may also be solved by the harmonic balance method.

APPENDIX B

FOURIER OPERATIONS

As noted previously, the harmonic balance method quickly becomes cumbersome when several harmonics of the response or several degrees of freedom are treated for linear systems with periodic coefficient equations. This occurs because a large number of linear algebraic equations must be formed, and the coefficients of these equations depend, in a complicated manner, on the harmonics of the coefficients and on the number and type of the generalized coordinates. Practical numerical computations for solving these equations depend on an efficient method of obtaining the harmonic balance equations (such as the generalized matrix formulation described previously). To provide a complete development of the method, this appendix includes details of three of the basic elements of the generalized harmonic balance method of this report. The first concerns the formulation of several basic matrix operators from the definition of the Fourier series. The second is a matrix formulation for multiplying two Fourier series one of which has unknown coefficients. The third is a matrix formulation for multiplying two Fourier series having frequency-dependent coefficients.

Linear Operations

Basic identities— Given a function $f(\psi)$ periodic with 2π, the following coefficients are defined:

$$(a_n)_f = \frac{1}{\pi}\int_0^{2\pi} f(\psi)\cos(n\psi)d\psi\ , \qquad n = 1, \infty \tag{B1a}$$

$$(b_n)_f = \frac{1}{\pi}\int_0^{2\pi} f(\psi)\sin(n\psi)d\psi\ , \qquad n = 1, \infty \tag{B1b}$$

$$(a_o)_f = \frac{1}{2\pi}\int_0^{2\pi} f(\psi)d\psi \tag{B1c}$$

$$(b_o)_f = 0 \tag{B1d}$$

$$f,n = \frac{(a_n)_f - i(b_n)_f}{2}\ , \qquad n = 1, \infty \tag{B1e}$$

$$f,-n = \frac{(a_n)_f + i(b_n)_f}{2}\ , \qquad n = 1, \infty \tag{B1f}$$

$$f,0 = (a_o)_f \tag{B1g}$$

It follows from equations (B1) (ref. 22) that

$$f(\psi) = \sum_{n=0}^{\infty} (a_n)_f \cos(n\psi) + (b_n)_f \sin(n\psi) = \sum_{n=-\infty}^{\infty} f,n\, e^{in\psi} \tag{B1h}$$

The terms $(a_n)_f$ and $(b_n)_f$ are called the Fourier coefficients of $f(\psi)$, and the terms f,n are called the complex Fourier coefficients of f.

There is also an interesting summation relation that has important applications in periodic systems with multiple, time-lagging components; that is, if there are b components at equally spaced intervals in the period

$$\psi_k = \psi_1 + (k - 1)\frac{2\pi}{b}$$

then the following identities hold:

$$\frac{1}{b}\sum_{k=1}^{b} \cos(n\psi_k) = \begin{cases} 0 \text{ if } n \text{ is not an integer multiple of } b \\ \cos(n\psi_1) \text{ if } n \text{ is an integer multiple of } b \end{cases} \tag{B2a}$$

$$\frac{1}{b}\sum_{k=1}^{b} \sin(n\psi_1) = \begin{cases} 0 \text{ if } n \text{ is not an integer multiple of } b \\ \sin(n\psi_1) \text{ if } n \text{ is an integer multiple of } b \end{cases} \tag{B2b}$$

Phase change— It is often useful to be able to express the Fourier series of $f(\psi + \Delta)$ as a function of the Fourier series for $f(\psi)$. In particular, if $f(\psi)$ is expressed as a truncated Fourier series

$$f(\psi) = \sum_{n=0}^{N} (a_n)_f \cos(n\psi) + (b_n)_f \sin(n\psi) \tag{B3}$$

then the objective is to be able to express $g(\psi) = f(\psi + \Delta)$ as

$$g(\psi) = \sum_{n=0}^{N} (a_n)_g \cos(n\psi) + (b_n)_g \sin(n\psi) \tag{B4}$$

where $(a_n)_g$ and $(b_n)_g$ are functions of $(a_n)_f$ and $(b_n)_f$. Applying the definition of $g(\psi)$ to equation (B3) implies that

$$g(\psi) = \sum_{n=0}^{N} (a_n)_f \cos[n(\psi + \Delta)] + (b_n)_f \sin[n(\psi + \Delta)]$$

$$= \sum_{n=0}^{N} [(a_n)_f \cos(n\Delta) + (b_n)_f \sin(n\Delta)]\cos(n\psi)$$

$$+ [-(a_n)_f \sin(n\Delta) + (b_n)_f \cos(n\Delta)]\sin(n\psi) \qquad \text{(B5)}$$

A comparison of equations (B4) and (B5) shows that

$$(a_n)_g = (a_n)_f \cos(n\Delta) + (b_n)_f \sin(n\Delta)$$

$$(b_n)_g = -(a_n)_f \sin(n\Delta) + (b_n)_f \cos(n\Delta)$$

which, in matrix form, yields the basic identity:

$$\begin{Bmatrix} a_n \\ b_n \end{Bmatrix}_g = [\Phi(\Delta)] \begin{Bmatrix} a_n \\ b_n \end{Bmatrix}_f \qquad \text{(B6a)}$$

where

$$[\Phi(\Delta)] \equiv \left[\begin{array}{ccc|ccc} 1 & & & 0 & & \\ & \cos(\Delta) & & & \sin(\Delta) & \\ & & \ddots & & & \ddots \\ & & \cos(N\Delta) & & & \sin(N\Delta) \\ \hline 0 & & & 1 & & \\ & -\sin(\Delta) & & & \cos(\Delta) & \\ & & \ddots & & & \ddots \\ & & -\sin(N\Delta) & & & \cos(N\Delta) \end{array}\right] \qquad \text{(B6b)}$$

The matrix $[\Phi]$ is an order $2(N+1)$ phase shift matrix. It can easily be seen from its structure that

$$[\Phi(\Delta_1 + \Delta_2)] = [\Phi(\Delta_1)][\Phi(\Delta_2)] = [\Phi(\Delta_2)][\Phi(\Delta_1)]$$

Derivative— It is also necessary to be able to express the Fourier series of the derivative of a function $f(\psi)$ in terms of the Fourier series of the original function $f(\psi)$; that is, if

$$\frac{df}{d\psi} = \dot{f} = \sum_{n=0}^{N} (a_n)_{\dot{f}} \cos(n\psi) + (b_n)_{\dot{f}} \sin(n\psi) \tag{B7}$$

then the task is to determine $(a_n)_{\dot{f}}$ and $(b_n)_{\dot{f}}$ as functions of $(a_n)_f$ and $(b_n)_f$. Applying the definition of $\dot{f}$ to equation (B3) implies that

$$\dot{f} = \sum_{n=0}^{N} -n(a_n)_f \sin(n\psi) + n(b_n)_f \cos(n\psi) \tag{B8}$$

A comparison of equations (B7) and (B8) yields

$$(a_n)_{\dot{f}} = n(b_n)_f$$

$$(b_n)_{\dot{f}} = -n(a_n)_f$$

which, in matrix form, is

$$\begin{Bmatrix} a_n \\ b_n \end{Bmatrix}_{\dot{f}} = [\square] \begin{Bmatrix} a_n \\ b_n \end{Bmatrix}_f \tag{B9a}$$

where

$$[\square] = \left[\begin{array}{ccc|ccc} & & & 0 & & \\ & & & & 1 & \\ & 0 & & & & \ddots \\ & & & & & \\ & & & & & N \\ \hline 0 & & & & & \\ & -1 & & & & \\ & & \ddots & & 0 & \\ & & & & & \\ & & -N & & & \end{array}\right] \tag{B9b}$$

From equations (B9a,b), it can be inferred that the Kth derivative of $f(\psi)$, $\overset{K}{f}(\psi)$, has Fourier coefficients given by

$$\begin{Bmatrix} a_n \\ b_n \end{Bmatrix}^K_f = [\square^K] \begin{Bmatrix} a_n \\ b_n \end{Bmatrix}_f \tag{B10a}$$

where

$$[\square^K] = [\square]^K \tag{B10b}$$

It is easily shown that $[\square]^K$ has the simple form

$$[\square^K] = \begin{cases} \begin{bmatrix} 0 & & & & 0 \\ 1 & \ddots & & & \\ & \ddots & & & \\ & & N^K & & \\ \hline & & & 0 & \\ & & & -1 & \ddots \\ 0 & & & & \ddots \\ & & & & -N^K \end{bmatrix}, & \begin{bmatrix} & & & 0 & \\ & & & 1 & \ddots \\ 0 & & & & \ddots \\ & & & & N^K \\ \hline & & & 0 & \\ & & & -1 & \ddots \\ 0 & & & & \ddots \\ & & & & -N^K \end{bmatrix}, \\ K = 0, 4, 8, \ldots & K = 1, 5, 9, \ldots \\ \begin{bmatrix} 0 & & & & 0 \\ -1 & \ddots & & & \\ & \ddots & & & \\ & & -N^K & & \\ \hline & & & 0 & \\ & & & -1 & \ddots \\ 0 & & & & \ddots \\ & & & & -N^K \end{bmatrix}, & \begin{bmatrix} & & & 0 & \\ & & & -1 & \ddots \\ 0 & & & & \ddots \\ & & & & -N^K \\ \hline & & & 0 & \\ & & & 1 & \ddots \\ 0 & & & & \ddots \\ & & & & N^K \end{bmatrix}, \\ K = 2, 6, 10, \ldots & K = 3, 7, 11, \ldots \end{cases} \tag{B10c}$$

When $f(\psi)$ is modulated by the harmonic function $e^{i\omega\psi}$,

$$f(\psi) = \sum_{n=0}^{N} [(a_n)_f \cos(n\psi) + (b_n)_f \sin(n\psi)]e^{i\omega\psi}$$

then $\dot{f}$ becomes

$$f(\psi) = \sum_{n=0}^{\infty} \left\{[n(b_n)_f + i\omega(a_n)_f]\cos(n\psi) + [-n(a_n)_f + i\omega(b_n)_f]\sin(n\psi)\right\}e^{i\omega\psi}$$

The derivative rule of equation (B10) can be generalized, in this case, to

$$\left\{\begin{matrix} a_n \\ b_n \end{matrix}\right\}_{\substack{K \\ f}} = \left[\square + i\omega I_{2(N+1)}\right]^K \left\{\begin{matrix} a_n \\ b_n \end{matrix}\right\}_f$$

Product of Two Series

Problem statement— A central element in the generalized harmonic balance method is the multiplication of two Fourier series in symbolic form, to yield the Fourier series of the product as a matrix function of the two original Fourier series coefficients including the case when one of the original series is unknown. In other words, given two Fourier series expansions,

$$f(\psi) = \sum_{k=0}^{N} a_k \cos(k\psi) + b_k \sin(k\psi) \qquad \text{(B11a)}$$

$$g(\psi) = \sum_{j=0}^{N} A_j \cos(j\psi) + B_j \sin(j\psi) \qquad \text{(B11b)}$$

and the product expansion,

$$h(\psi) = g(\psi)f(\psi) = \sum_{n=0}^{N} \alpha_n \cos(n\psi) + \beta_n \sin(n\psi) \qquad \text{(B11c)}$$

it is desired to find α_n and β_n as functions of a_k, b_k, A_j, and B_j. Applying the definition of $h(\psi)$ gives the Fourier product:

$$h(\psi) = \sum_{j=0}^{N}\sum_{k=0}^{N} A_j a_k \cos(j\psi)\cos(k\psi) + A_j b_k \cos(j\psi)\sin(k\psi)$$

$$+ B_j a_k \sin(j\psi)\cos(k\psi) + B_j b_k \sin(j\psi)\sin(k\psi)$$

Use of the basic trigonometric identities yields

$$h(\psi) = \frac{1}{2}\sum_{j=0}^{N}\sum_{k=0}^{N} [A_j a_k - B_j b_k]\cos[(j + k)\psi] + [A_j a_k + B_j b_k]\cos[(j - k)\psi]$$

$$+ [B_j a_k + A_j b_k]\sin[(j + k)\psi] + [B_j a_k - A_j b_k]\sin[(j - k)\psi] \quad \text{(B11d)}$$

The terms with equal ψ multipliers must be isolated so that α_n and β_n may be found; that is, for each value of n ($n = 0, N$), the values of j and k must be found so that $j + k = n$, $j - k = n$, or $k - j = n$.

Matrix definitions— The first matrices to be defined are square triangular matrices defined as simple functions of a column array x_k, $k = 0, N$:

$$\left.\begin{aligned}
\left[\begin{smallmatrix} & 0 \\ x & \end{smallmatrix}\right] &\equiv \begin{bmatrix} x_0 & 0 & 0 & \cdots & 0 & 0 \\ x_1 & x_0 & 0 & \cdots & 0 & 0 \\ x_2 & x_1 & x_0 & \cdots & 0 & 0 \\ \cdot & \cdot & \cdot & & \cdot & \cdot \\ \cdot & \cdot & \cdot & & \cdot & \cdot \\ \cdot & \cdot & \cdot & & \cdot & \cdot \\ \cdot & \cdot & \cdot & & \cdot & \cdot \\ x_N & x_{N-1} & x_{N-2} & \cdots & x_1 & x_0 \end{bmatrix}, \\
\left[\begin{smallmatrix} x & \\ & 0 \end{smallmatrix}\right] &\equiv \begin{bmatrix} x_0 & x_1 & x_2 & \cdots & x_{N-1} & x_N \\ x_1 & x_2 & x_3 & \cdots & x_N & 0 \\ x_2 & x_3 & x_4 & \cdots & 0 & 0 \\ \cdot & \cdot & \cdot & & \cdot & \cdot \\ \cdot & \cdot & \cdot & & \cdot & \cdot \\ \cdot & \cdot & \cdot & & \cdot & \cdot \\ \cdot & \cdot & \cdot & & \cdot & \cdot \\ x_N & 0 & 0 & \cdots & 0 & 0 \end{bmatrix}, \\
\left[\begin{smallmatrix} & x \\ 0 & \end{smallmatrix}\right] &\equiv \left[\begin{smallmatrix} & 0 \\ x & \end{smallmatrix}\right]^T, \qquad [x_0] \equiv \begin{bmatrix} x_0 & 0 & \cdots & 0 \\ 0 & 0 & \cdots & 0 \\ \cdot & \cdot & & \\ \cdot & \cdot & & \\ 0 & 0 & \cdots & 0 \end{bmatrix}
\end{aligned}\right\} \quad \text{(B12)}$$

If the rows and columns of these matrices are ordered row number = n(0,N) column number = j(0,N), and if the subscript of x is called k, it follows that for all nonzero elements of $\begin{bmatrix} \diagdown & 0 \\ x & \end{bmatrix}$, $j + k = n$; of $\begin{bmatrix} x & \diagup \\ & 0 \end{bmatrix}$, $k - j = n$; and of $\begin{bmatrix} \diagdown & x \\ 0 & \end{bmatrix}$, $j - k = n$. Thus, these matrices are important in combining like terms of a Fourier product.

If the properties of the triangular matrices are applied to equation (B11d), it is possible to collect terms of constant harmonics. For example, if the contributions of A_j to the $\cos(n\psi)$ coefficients (α_n) are considered, it can be seen that

$$\underset{\text{due to } A_j}{\{\alpha_n\}} = \frac{1}{2}\left\langle \underset{j+k=n}{\begin{bmatrix} \diagdown & 0 \\ a & \end{bmatrix}} + \underset{j-k=n}{\begin{bmatrix} \diagdown & a \\ 0 & \end{bmatrix}} + \underset{k-j=n}{\begin{bmatrix} a & \diagup \\ & 0 \end{bmatrix}} - \underset{\substack{\text{correction for } j=k,\ n=0 \\ \text{counted twice}}}{\begin{bmatrix} a_0 & a_1 & \cdots & a_N \\ 0 & 0 & & 0 \\ \vdots & \vdots & & \vdots \\ 0 & 0 & \cdots & 0 \end{bmatrix}} \right\rangle \{A_j\}$$

The nth row of the column α_n is seen to be the sum of all coefficients for $j + k = n$, $j - k = n$, or $k - j = n$ from equation (A11). (The last matrix term is a correction since, for $n = 0$, there should be only one contribution since $j - k = 0$ or $k - j = 0$ is the same term from equation (B11).) If one defines $\bar{\alpha}_0 \equiv 2\alpha_0$, the symmetry property of the bracket term can be preserved ($\begin{bmatrix} a & \diagup \\ & 0 \end{bmatrix}^T = \begin{bmatrix} a & \diagup \\ & 0 \end{bmatrix}$, $\begin{bmatrix} \diagdown & 0 \\ a & \end{bmatrix}^T = \begin{bmatrix} \diagdown & a \\ 0 & \end{bmatrix}$). Although it is known that $\beta_0 = b_0 = B_0 = 0$, by equation (B1d), it is also advantageous from a symmetry standpoint to maintain the β_0 row and B_0 column in the matrices by simply defining $\beta_0 \equiv a_0 B_0 = 0$. When this is done, the α_n and β_n coefficients (as found in eq. (B11)) can be collected symbolically:

$$\begin{Bmatrix} 2\alpha_0 \\ \alpha_1 \\ \cdot \\ \cdot \\ \cdot \\ \alpha_N \end{Bmatrix} = \frac{1}{2} \left\langle + \begin{bmatrix} 0 & \\ a & \ddots \end{bmatrix} + \begin{bmatrix} a & \\ 0 & \ddots \end{bmatrix} + \begin{bmatrix} & a \\ \ddots & 0 \end{bmatrix} + [a_0] \right\rangle \begin{Bmatrix} A_0 \\ A_1 \\ \cdot \\ \cdot \\ \cdot \\ A_N \end{Bmatrix}$$

$$+ \frac{1}{2} \left\langle - \begin{bmatrix} 0 & \\ b & \ddots \end{bmatrix} + \begin{bmatrix} b & \\ 0 & \ddots \end{bmatrix} + \begin{bmatrix} & b \\ \ddots & 0 \end{bmatrix} - [b_0] \right\rangle \begin{Bmatrix} B_0 \\ B_1 \\ \cdot \\ \cdot \\ \cdot \\ B_N \end{Bmatrix}$$

$$\equiv [P^{++}(a)]\{A\} + [P^{+-}(b)]\{B\} \tag{B13a}$$

$$\begin{Bmatrix} \beta_0 \\ \beta_1 \\ \cdot \\ \cdot \\ \cdot \\ \beta_N \end{Bmatrix} = \frac{1}{2} \left\langle + \begin{bmatrix} 0 & \\ b & \ddots \end{bmatrix} - \begin{bmatrix} b & \\ 0 & \ddots \end{bmatrix} + \begin{bmatrix} & b \\ \ddots & 0 \end{bmatrix} - [b_0] \right\rangle \begin{Bmatrix} A_0 \\ A_1 \\ \cdot \\ \cdot \\ \cdot \\ A_N \end{Bmatrix}$$

$$+ \frac{1}{2} \left\langle + \begin{bmatrix} 0 & \\ a & \ddots \end{bmatrix} + \begin{bmatrix} a & \\ 0 & \ddots \end{bmatrix} - \begin{bmatrix} & a \\ \ddots & 0 \end{bmatrix} + [a_0] \right\rangle \begin{Bmatrix} B_0 \\ B_1 \\ \cdot \\ \cdot \\ \cdot \\ B_N \end{Bmatrix}$$

$$\equiv [P^{-+}(b)]\{A\} + [P^{--}(a)]\{B\} \tag{B13b}$$

Fourier product matrix— If the above results are combined in matrix form, a complete matrix method is obtained for symbolically multiplying two Fourier series in the frequency domain:

$$\begin{Bmatrix} 2\alpha_0 \\ \alpha_1 \\ \cdot \\ \cdot \\ \alpha_N \\ \beta_0 \\ \beta_1 \\ \cdot \\ \cdot \\ \beta_N \end{Bmatrix} = \left[\begin{array}{c|c} P^{++}(a) & P^{+-}(b) \\ \hline P^{-+}(b) & P^{--}(a) \end{array}\right] \begin{Bmatrix} A_0 \\ A_1 \\ \cdot\cdot \\ \cdot\cdot \\ A_N \\ B_0 \\ B_1 \\ \cdot \\ \cdot \\ B_N \end{Bmatrix} \equiv [\bar{\Pi}(f)] \begin{Bmatrix} A_j \\ \\ B_j \end{Bmatrix} \tag{B14}$$

The matrix $[\bar{\Pi}]$, called the modified Fourier product matrix, is a square symmetric matrix. Its first row (or column) is just $\begin{Bmatrix} a \\ b \end{Bmatrix}_f$ and its (N+1) row (or column) has all zeroes except an a_0 on the diagonal. If f is a known function (with known Fourier series) and if g is an unknown periodic function (whose Fourier coefficients are unknowns A_j, B_j), then equation (B14) represents the symbolic multiplication to obtain the Fourier series for $h = g \cdot f$. In this case, $[\bar{\Pi}(f)]$ is a known matrix formed by the algorithm in equations (B13a,b).

When the first row of $[\bar{\Pi}]$ is multiplied by 1/2, the new matrix is called $[\Pi]$, the Fourier product matrix. It follows that

$$\begin{Bmatrix} \alpha_n \\ \beta_n \end{Bmatrix}_h = [\Pi(f)] \begin{Bmatrix} A_j \\ B_j \end{Bmatrix}_g \tag{B15}$$

It can be shown from the structure of Π that

$$[\Pi(f_1 + xf_2)] = [\Pi(f_1)] + x[\Pi(f_2)]$$

$$[\Pi(f_1 \cdot f_2)] = [\Pi(f_1)] \cdot [\Pi(f_2)] = [\Pi(f_2)] \cdot [\Pi(f_1)]$$

so that $[\Pi]$ is a linear commutative operator.

Product of Two Fourier Series with Frequency-Dependent Coefficients

When the Fourier coefficients of the functions $f(\psi)$ and $h(\psi)$ (eq. (B11)) are functions of the frequency content of $h(\psi)$ itself, then the Fourier product matrix $[\Pi(f)]$ in equation (B15) must be altered to take this frequency dependence into account. First, the j and $j + N$ rows of equation (B15) are rewritten:

$$\begin{Bmatrix} \alpha_j \\ \beta_j \end{Bmatrix} = \begin{bmatrix} <\Pi_j(f)> \\ <\Pi_{j+N}(f)> \end{bmatrix} \begin{Bmatrix} A \\ B \end{Bmatrix} \tag{B16}$$

These two equations are the result of a harmonic balance of the function product and result from the single equation:

$$[\alpha_j \cos(j\psi) + \beta_j \sin(j\psi)]e^{i\omega\psi} = <\Pi_j(f)>\begin{Bmatrix} A \\ B \end{Bmatrix}\cos(j\psi)e^{i\omega\psi} + <\Pi_{j+N}(f)>\begin{Bmatrix} A \\ B \end{Bmatrix}\sin(j\psi)e^{i\omega\psi} \tag{B17}$$

where the possibility of a harmonic modulation of $h(\psi)$ and $g(\psi)$ has been allowed. The only two frequencies possible in equation (B17) are $\omega + j$ and $\omega - j$. Therefore, two possible values may exist for each α_j, β_j, and Π_{ji}:

$$\left.\begin{aligned} \Pi_{ji}(f)\big|_{\omega+j} &\equiv \overset{+}{\Pi}_{ji}, \qquad \Pi_{ji}(f)\big|_{\omega-j} \equiv \overset{-}{\Pi}_{ji} \\ \alpha_j(h)\big|_{\omega+j} &\equiv \overset{+}{\alpha}_j, \qquad \alpha_j(h)\big|_{\omega-j} \equiv \overset{-}{\alpha}_j \\ \beta_j(h)\big|_{\omega+j} &\equiv \overset{+}{\beta}_j, \qquad \beta_j(h)\big|_{\omega-j} \equiv \overset{-}{\beta}_j \end{aligned}\right\} \tag{B18}$$

When equation (B17) is separated into frequency components, with each f and h given the value corresponding to that frequency, the resultant equation is

$$\frac{1}{2}(\overset{+}{\alpha}_j - i\overset{+}{\beta}_j)e^{i(\omega+j)\psi} + \frac{1}{2}(\overset{-}{\alpha}_j + i\overset{-}{\beta}_j)e^{i(\omega-j)\psi} = \frac{1}{2}[<\overset{+}{\Pi}_j> - i<\overset{-}{\Pi}_j>]\begin{Bmatrix} A \\ B \end{Bmatrix}e^{i(\omega+j)\psi} + \frac{1}{2}[<\overset{+}{\Pi}_{j+n}> + i<\overset{-}{\Pi}_{j+n}>]\begin{Bmatrix} A \\ B \end{Bmatrix}e^{i(\omega-j)\psi} \tag{B19}$$

The resultant harmonic balance including frequency dependence is

$$\frac{1}{2}\begin{Bmatrix} \overset{+}{\alpha}_j + \overset{-}{\alpha}_j - i(\overset{+}{\beta}_j - \overset{-}{\beta}_j) \\ \overset{+}{\beta}_j + \overset{-}{\beta}_j + i(\overset{+}{\alpha}_j - \overset{-}{\alpha}_j) \end{Bmatrix} = \frac{1}{2}\begin{bmatrix} \langle \overset{+}{\Pi}_j + \overset{-}{\Pi}_j \rangle - i\langle \overset{+}{\Pi}_{j+n} - \overset{-}{\Pi}_{j+n} \rangle \\ \langle \overset{+}{\Pi}_{j+n} + \overset{-}{\Pi}_{j+n} \rangle + i\langle \overset{+}{\Pi}_j - \overset{-}{\Pi}_j \rangle \end{bmatrix}\begin{Bmatrix} A \\ B \end{Bmatrix} \quad (B20)$$

which is written as

$$\begin{Bmatrix} \tilde{\alpha}_j \\ \beta_j \end{Bmatrix} = [\tilde{\Pi}]\begin{Bmatrix} A \\ B \end{Bmatrix} \quad (B21)$$

where the tilda marking indicates the operation:

$$\{\tilde{\ }\} \equiv \frac{1}{2}\begin{bmatrix} I_{N+1} & -iI_{N+1} \\ iI_{N+1} & I_{N+1} \end{bmatrix}\{\ \}_{\omega+j} + \frac{1}{2}\begin{bmatrix} I_{N+1} & iI_{N+1} \\ -iI_{N+1} & I_{N+1} \end{bmatrix}\{\ \}_{\omega-j} \quad (B22)$$

When there is no j dependence, the tilda transformation is

$$\{\tilde{\ }\} = \{\ \}_{\omega+j} = \{\ \}_{\omega-j} \quad (B23)$$

When $\omega = 0$, the values at $\omega \pm j$ are complex conjugates so that

$$\{\tilde{\ }\} = \mathrm{Re}\{\ \}_j + \begin{bmatrix} 0 & I_{N+1} \\ -I_{N+1} & 0 \end{bmatrix}\mathrm{Im}\{\ \}_j \quad (B24)$$

a real operation. In general, however, the tilda operation implies complex quantities in the harmonic balance.

APPENDIX C

FIGURES AND TABLES FOR ROTOR DERIVATIVES

Twelve basic rotor derivatives are included in this appendix: thrust, pitch moment, and roll moment with respect to collective pitch, longitudinal cyclic pitch, lateral cyclic pitch, and shaft angle of attack. There are four main independent variables or system parameters: the configuration parameters P, γ, and θ_{q_1} and the advance ratio μ. Figures and tables of these derivatives are presented for a sufficient range of system parameters to be of use in obtaining rapid estimates of these derivatives. The charts also give additional qualitative insight into the behavior of hingeless rotor derivatives.

The results are calculated using the following mathematical model. The rotor blade is of uniform mass and stiffness and is represented by two elastic bending modes. The modes and frequencies are given by the uniform approximation of reference 23, which yields modal functions for the rotating blade that give a smooth variation in mode shape as the fundamental flap frequency varies from 1.0 to ∞. That is, the modes transition smoothly from Legendre polynomials for $P = 1.0$ to nonrotating cantilever beam modes at $P = \infty$. A root hinge is not included ($K_\beta = \infty$), the root cutout is zero, and the tip loss factor $B = 0.97$. Full reversed flow effects are included and compressibility is neglected. Three harmonics of blade response are retained ($N = 3$) and the number of azimuthal increments is $IN = 32$.

When pitch-flap coupling is included, the blade pitch angle produced by the the first and second mode flap bending is apportioned according to the ratio

$$\frac{\theta_{q_2}}{\theta_{q_1}} = 0.16 \tag{C1}$$

which is the ratio of the modal deflections (for nonrotating cantilever modes) in the limit as the blade root is approached, i.e.,

$$\lim_{\bar{r} \to 0} \frac{\phi_2(\bar{r})}{\phi_1(\bar{r})} = 0.16 \tag{C2}$$

This apportionment is based on the assumption that pitch-flap coupling is produced by a pitch link mechanism that moves vertically to change the blade pitch by rotating a pitch horn (lever arm) extending in a chordwise direction from the blade. The kinematic boundary condition of this mechanism requires that the blade must pitch when vertical bending deflections occur at the radial location of the pitch link. The ratio of pitch-flap coupling of two bending modes is therefore equal to the ratio of their modal deflections.

Figures 22 to 37 are charts of the rotor derivatives calculated according to the above mathematical model for Lock numbers of 5 and 10, advance ratios $0 < \mu < 1.0$, flap frequencies $1 < P < \infty$, and pitch-flap coupling $-3.0 < \theta_{q_1} < 0.8$. Larger positive values of pitch-flap coupling were not included because of flapping instability at high advance ratios. The thrust derivatives are plotted as a function of P for several values of μ. At low advance ratios there is little variation with P as noted previously. At higher advance ratios several variations occur. Near $P \approx 1.2$, $\gamma = 5$, the thrust derivatives increase due to the effects of mode shape, reversed flow, and second harmonic response. For low values of P, the variation in bending mode shape with P is also significant. The small increase in thrust for $P \approx 2.2$ occurs when the first flap bending mode is in resonance with second harmonic aerodynamic forces. The small perturbation of $\bar{C}_{T_{\theta_o}}$ at $P = 1.1$ and $\mu = 1.0$ occurs when the second flap bending mode is in resonance with third harmonic aerodynamic forces.

The pitch and roll moment derivatives are plotted using orthogonal axes so that pitch-roll coupling variations can be easily observed. At zero advance ratio these derivatives form a semi-circle as discussed previously. These semi-circles generally expand and distort as the advance ratio increases above zero. For $P = 0$, the rotor moment derivatives are zero and for $P = \infty$, the pitch and roll derivatives are uncoupled at all advance ratios. The variation in pitch-roll coupling with advance ratio can be observed by the deviation of P = constant curves from straight lines through the origin. The effects of the second flap bending mode and the second and third harmonic of aerodynamic forces also produce changes in the rotor moment derivatives similar to those discussed above for the thrust derivatives.

The rotor moment derivatives as a function of pitch-flap coupling are given in the form of magnitude and phase primarily to illustrate how such coupling may be used to modify the rotor response magnitude and reduce phase variations with advance ratio. The plots show that pitch-flap coupling alone cannot give a phase angle for the moments that is independent of advance ratio for all derivatives. A small amount of positive pitch-flap coupling can decrease the moment phasing below 20°, but at the expense of destabilizing the rotor by increasing the thrust and pitch-up derivatives. Negative pitch-flap coupling, on the other hand, decreases the thrust and pitch-up derivatives but increases the phase change over the advance ratio range $0 < \mu < 1.0$. Thus, while pitch-flap coupling is a powerful design parameter, by itself it is not adequate for completely uncoupling the pitch and roll moment derivatives at all advance ratios.

Tables 2 through 49 include numerical values for the derivatives plotted in the above figures.

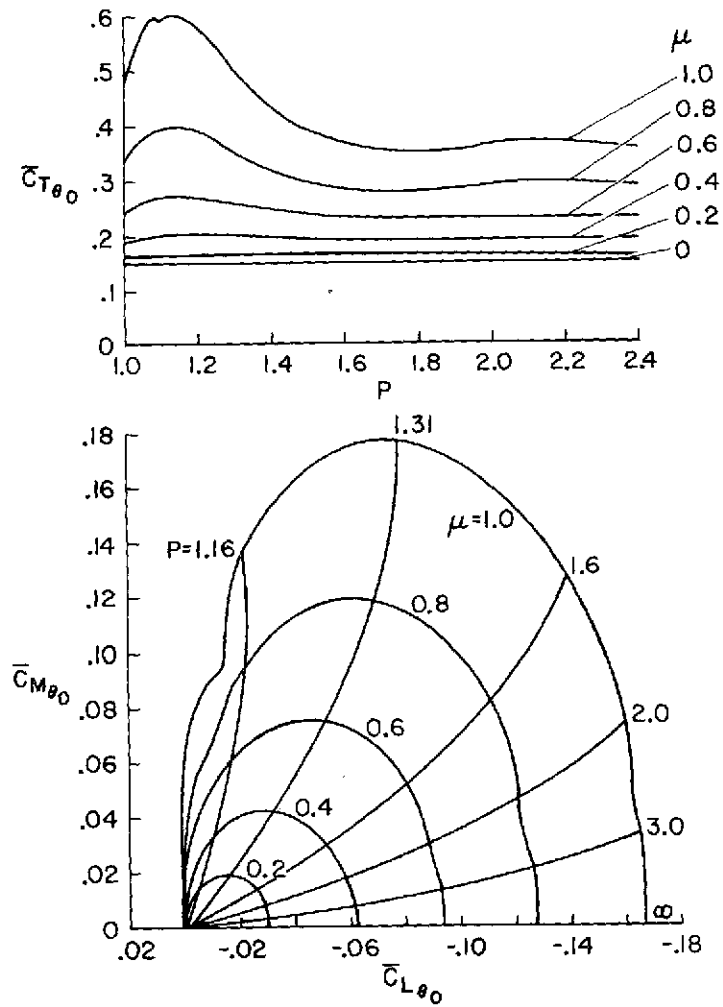

Figure 22.— Response derivatives with respect to θ_0, $\gamma = 5$, $\theta_{q_1} = 0$.

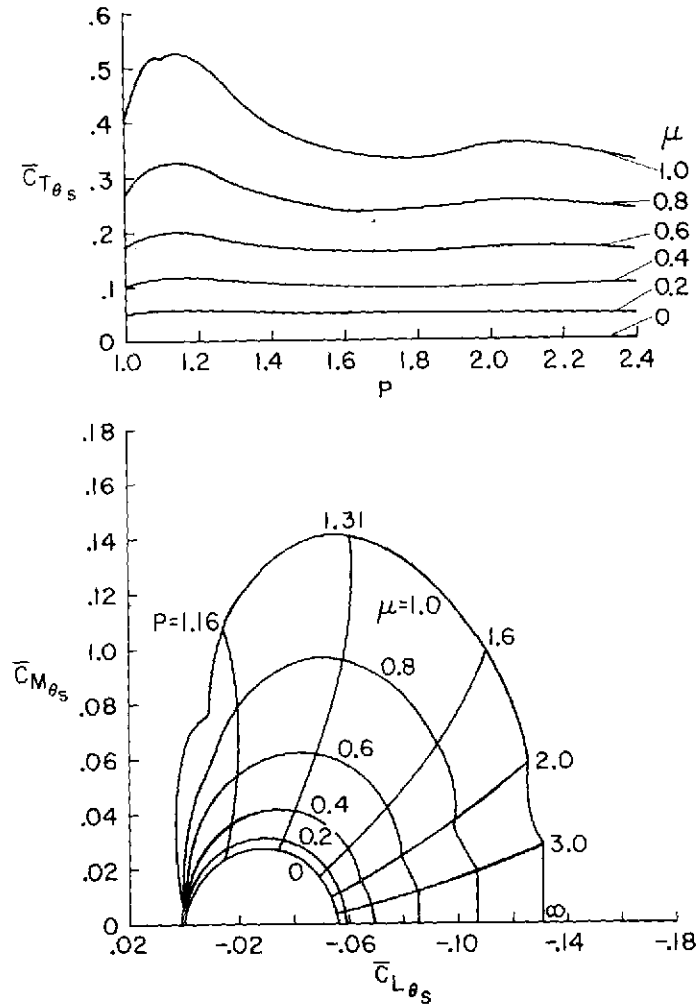

Figure 23.— Response derivatives with respect to θ_s, $\gamma = 5$, $\theta_{q_1} = 0$.

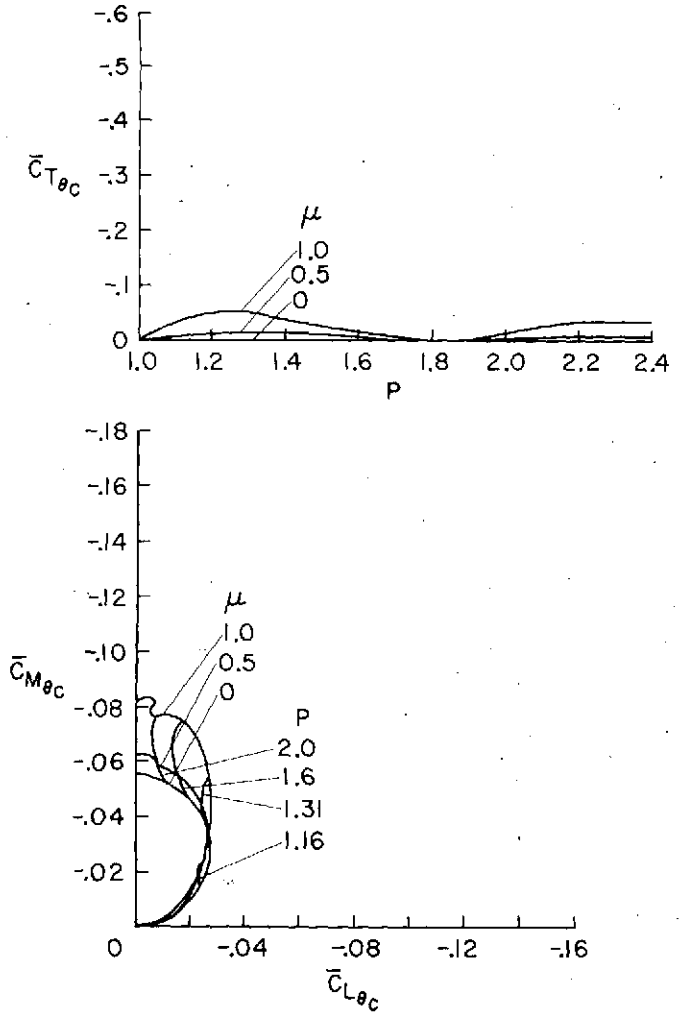

Figure 24.— Response derivatives with respect to θ_C, $\gamma = 5$, $\theta_{q_1} = 0$.

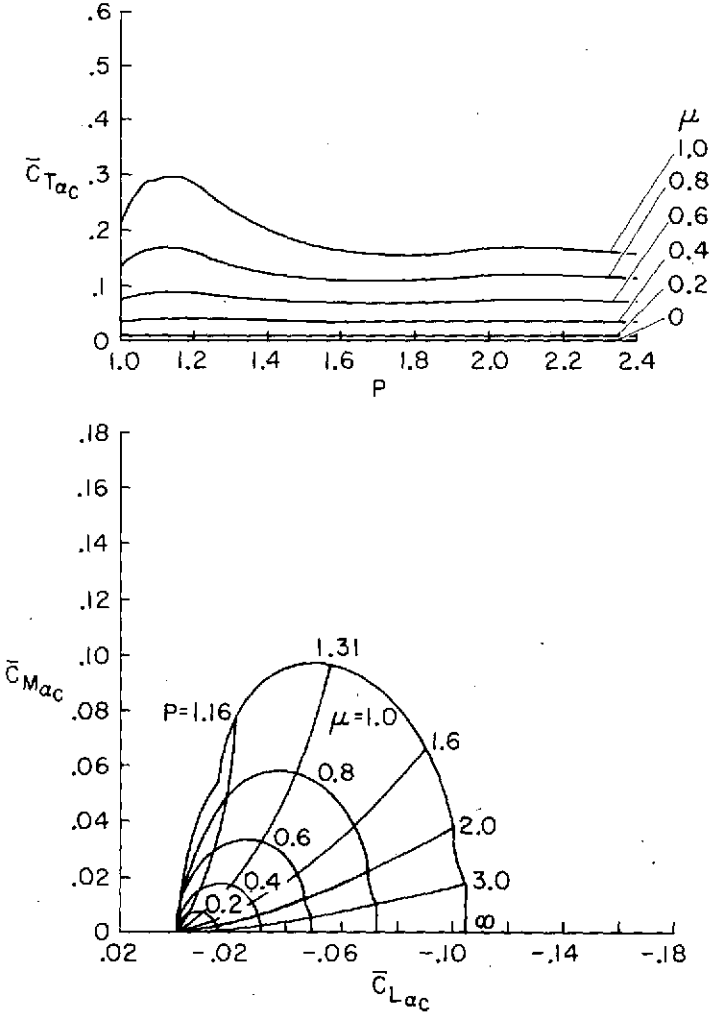

Figure 25.— Response derivatives with respect to α_C, $\gamma = 5$, $\theta_{q_1} = 0$.

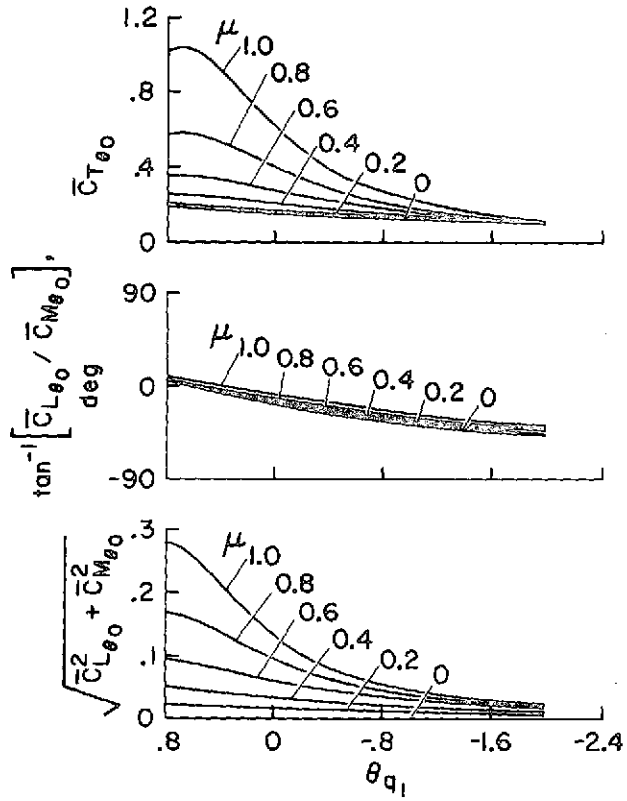

Figure 26.— Response derivatives with respect to θ_O, P = 1.15, γ = 5.

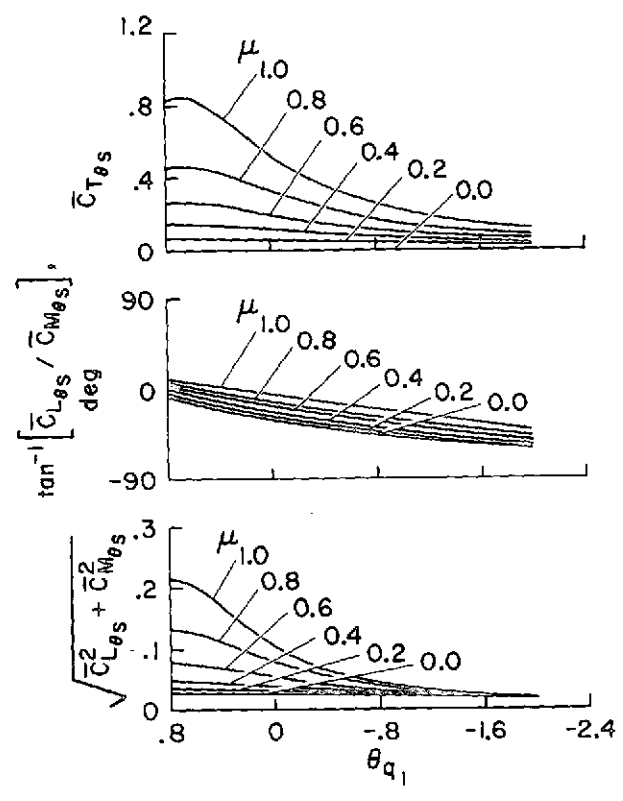

Figure 27.— Response derivatives with respect to θ_S, P = 1.15, γ = 5.

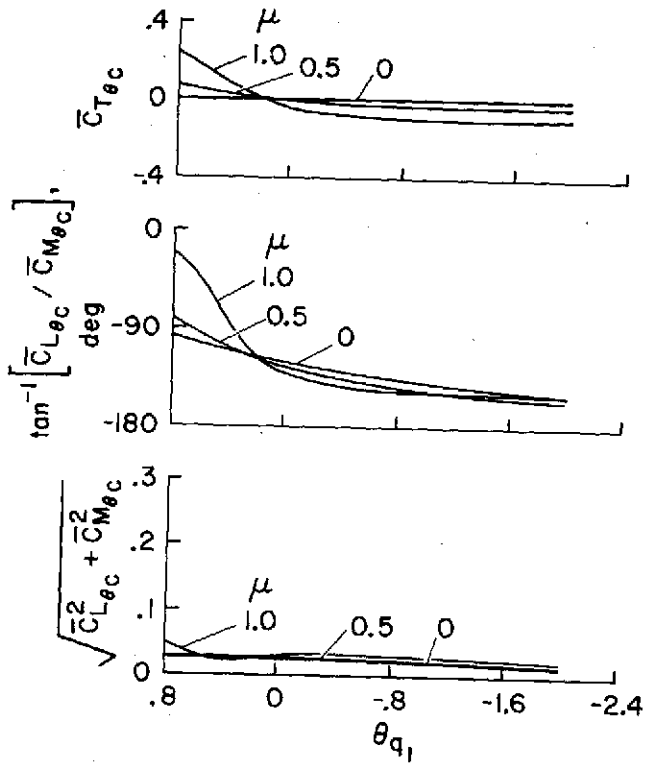

Figure 28.— Response derivatives with respect to θ_c, P = 1.15, γ = 5.

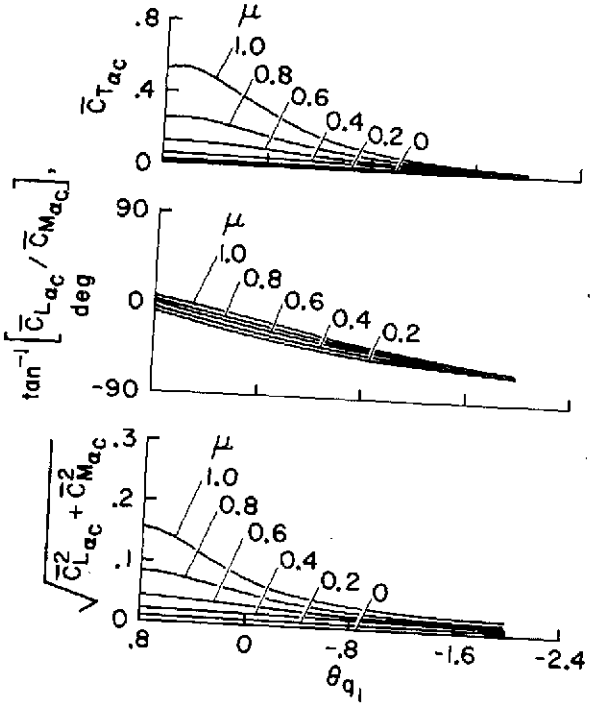

Figure 29.— Response derivatives with respect to α_c, P = 1.15, γ = 5.

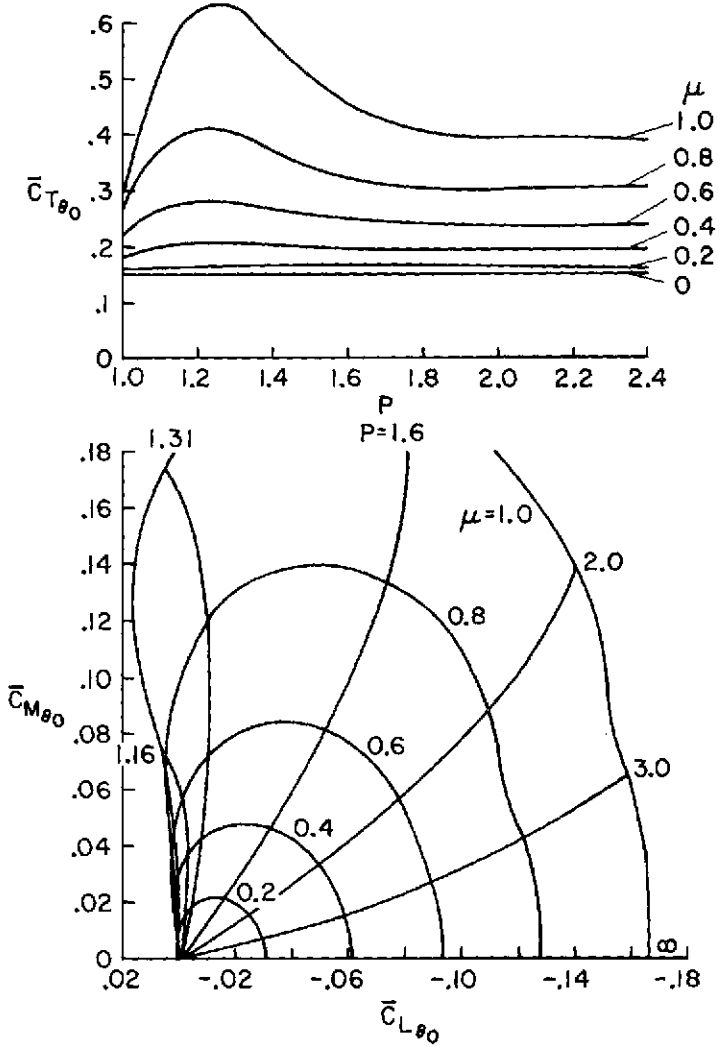

Figure 30.— Response derivatives with respect to θ_o, $\gamma = 10$, $\theta_{q_1} = 0$.

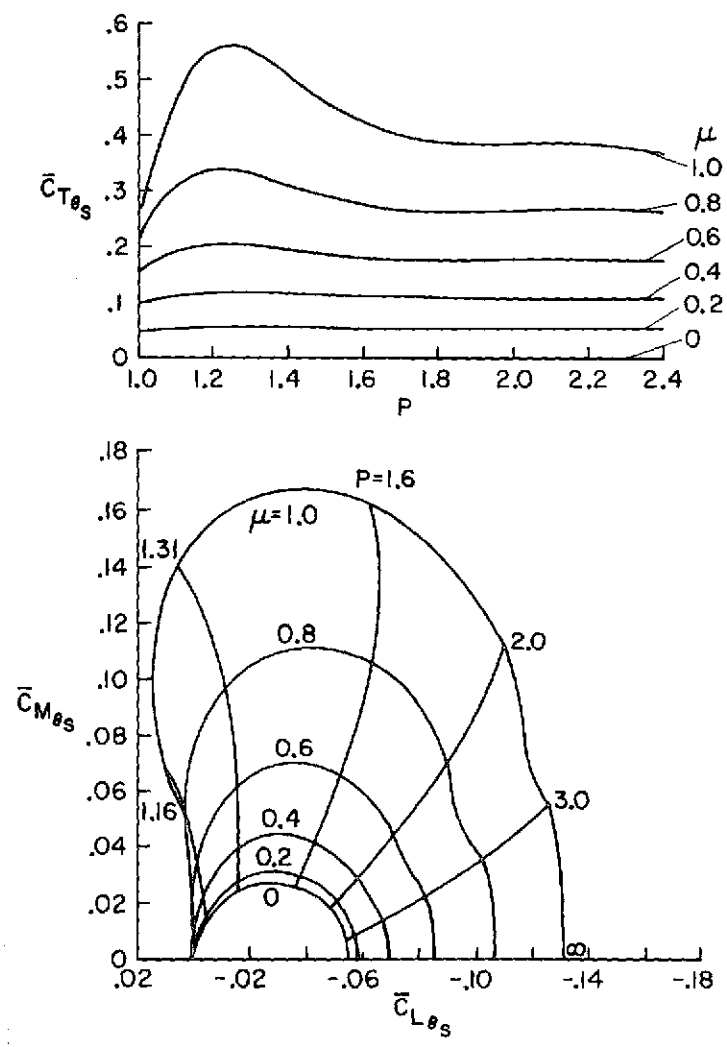

Figure 31.— Response derivatives with respect to θ_s, $\gamma = 10$, $\theta_{q_1} = 0$.

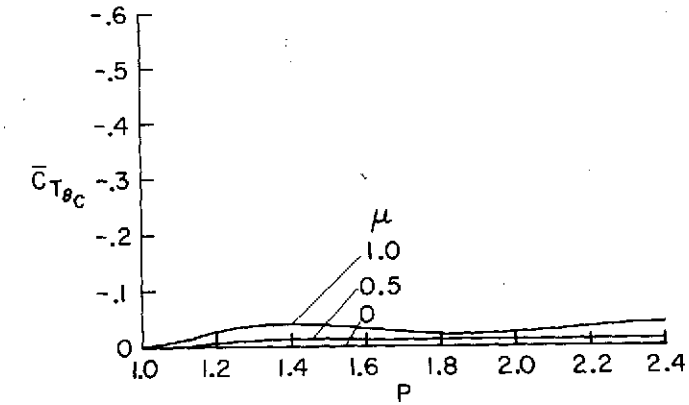

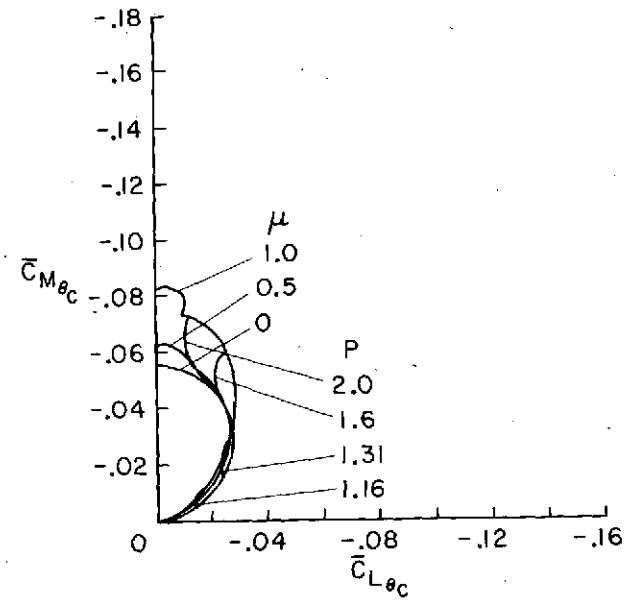

Figure 32.— Response derivatives with respect to θ_c, $\gamma = 10$, $\theta_{q_1} = 0$.

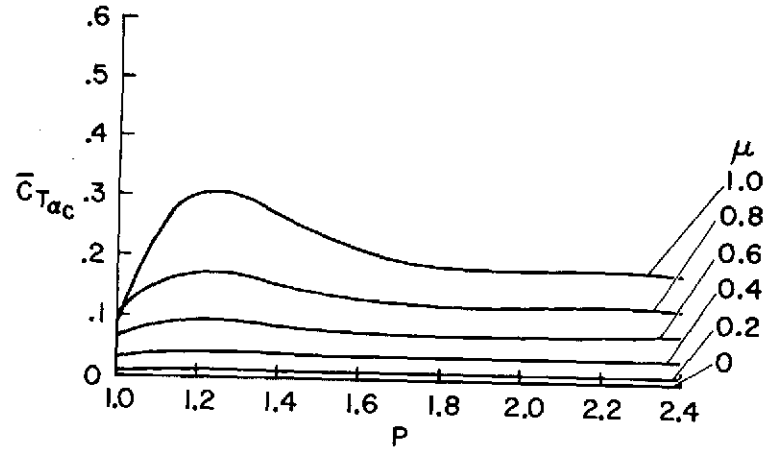

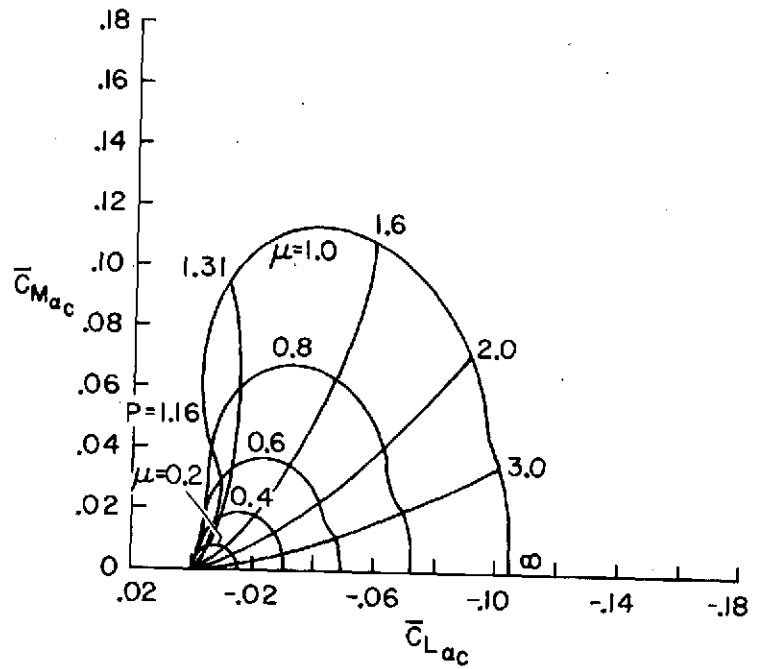

Figure 33.— Response derivatives with respect to α_c, $\gamma = 10$, $\theta_{q_1} = 0$.

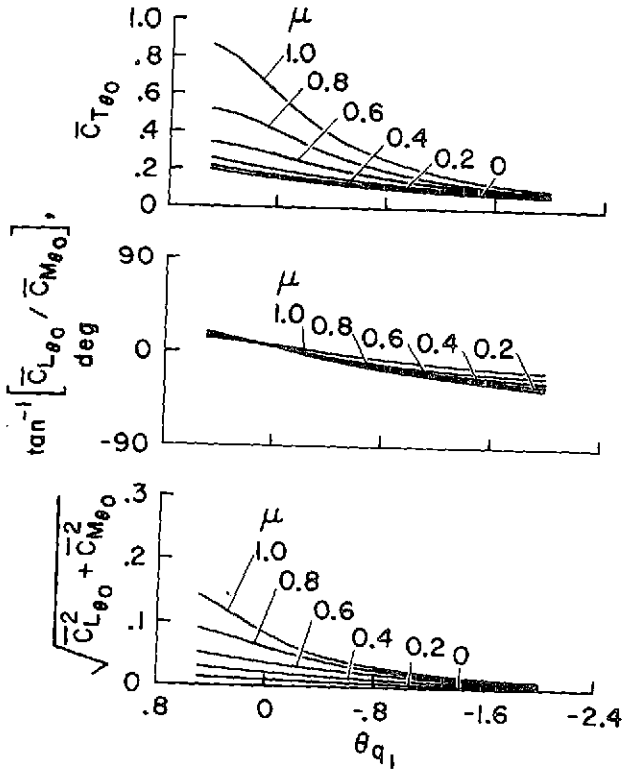

Figure 34.— Response derivatives with respect to θ_o, P = 1.15, γ = 10.

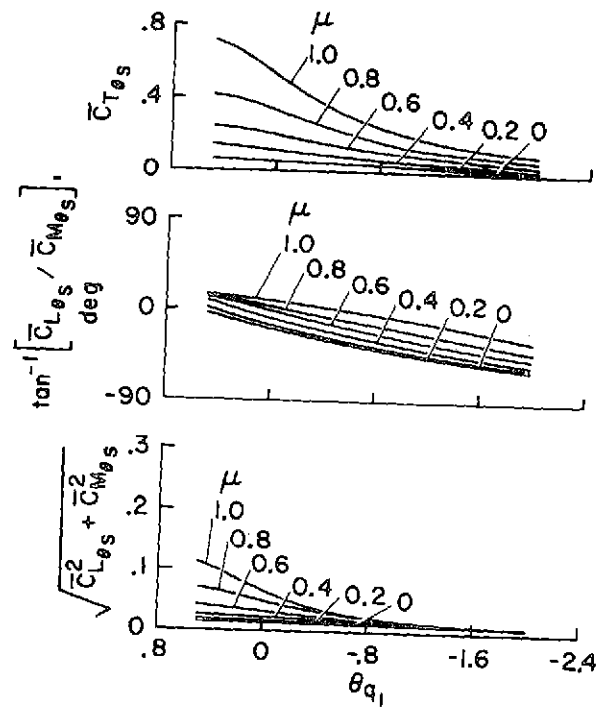

Figure 35.— Response derivatives with respect to θ_s, P = 1.15, γ = 10.

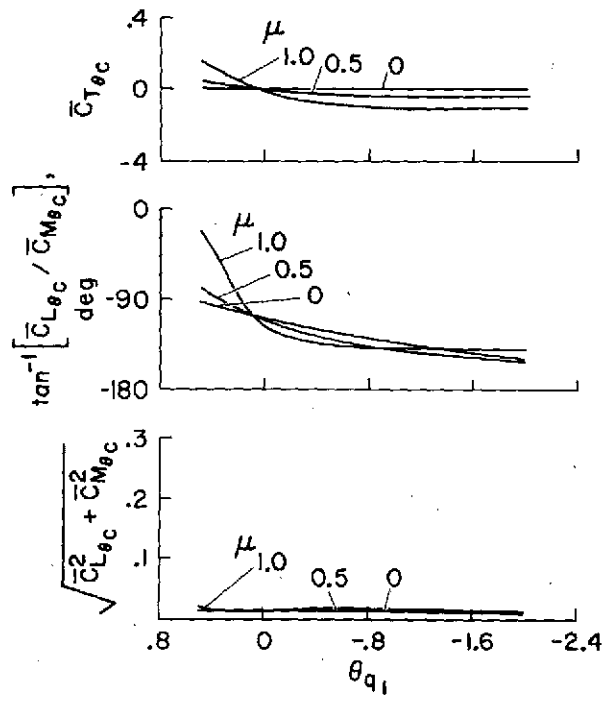

Figure 36.— Response derivatives with respect to θ_c, P = 1.15, γ = 10.

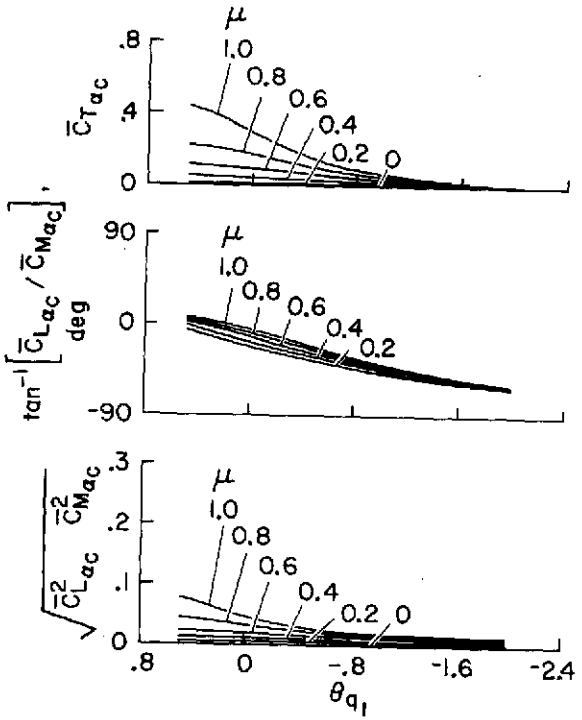

Figure 37.— Response derivatives with respect to α_c, P = 1.15, γ = 10.

TABLE 2.– THRUST DERIVATIVE, $\bar{C}_{T_{\theta_0}}$, $\gamma = 5$, $\theta_{q_1} = 0$

p \ μ	0.0000	0.1000	0.2000	0.3000	0.4000	0.5000	0.6000	0.7000	0.8000	0.9000	1.0000
1.00	0.1521	0.1543	0.1610	0.1723	0.1888	0.2115	0.2419	0.2819	0.3332	0.3972	0.4773
1.02	0.1521	0.1545	0.1619	0.1742	0.1922	0.2170	0.2503	0.2945	0.3522	0.4229	0.5112
1.04	0.1521	0.1548	0.1627	0.1761	0.1956	0.2225	0.2587	0.3069	0.3707	0.4503	0.5515
1.08	0.1521	0.1551	0.1641	0.1791	0.2007	0.2301	0.2694	0.3218	0.3912	0.4816	0.5962
1.12	0.1521	0.1553	0.1647	0.1803	0.2025	0.2327	0.2730	0.3266	0.3970	0.4874	0.5972
1.16	0.1521	0.1553	0.1649	0.1806	0.2027	0.2325	0.2720	0.3243	0.3937	0.4847	0.5994
1.20	0.1521	0.1553	0.1647	0.1802	0.2018	0.2305	0.2680	0.3174	0.3827	0.4690	0.5798
1.24	0.1521	0.1552	0.1644	0.1794	0.2002	0.2275	0.2627	0.3082	0.3680	0.4469	0.5492
1.28	0.1521	0.1551	0.1641	0.1785	0.1985	0.2243	0.2570	0.2988	0.3528	0.4236	0.5156
1.34	0.1521	0.1550	0.1635	0.1773	0.1960	0.2198	0.2493	0.2860	0.3323	0.3919	0.4691
1.40	0.1521	0.1549	0.1631	0.1762	0.1939	0.2161	0.2431	0.2757	0.3160	0.3668	0.4317
1.50	0.1521	0.1547	0.1625	0.1749	0.1913	0.2117	0.2368	0.2641	0.2976	0.3384	0.3892
1.60	0.1521	0.1546	0.1621	0.1740	0.1898	0.2090	0.2315	0.2573	0.2871	0.3222	0.3647
1.70	0.1521	0.1546	0.1619	0.1734	0.1888	0.2076	0.2294	0.2541	0.2820	0.3143	0.3524
1.80	0.1521	0.1545	0.1617	0.1732	0.1884	0.2072	0.2290	0.2537	0.2814	0.3129	0.3496
1.90	0.1521	0.1545	0.1616	0.1731	0.1885	0.2077	0.2303	0.2561	0.2851	0.3177	0.3547
2.00	0.1521	0.1545	0.1616	0.1731	0.1888	0.2087	0.2325	0.2602	0.2914	0.3261	0.3647
2.10	0.1521	0.1545	0.1615	0.1731	0.1889	0.2092	0.2337	0.2625	0.2952	0.3314	0.3709
2.20	0.1521	0.1545	0.1615	0.1729	0.1886	0.2087	0.2330	0.2614	0.2938	0.3295	0.3682
2.60	0.1521	0.1544	0.1613	0.1724	0.1873	0.2058	0.2276	0.2524	0.2798	0.3095	0.3408
3.00	0.1521	0.1544	0.1613	0.1722	0.1868	0.2047	0.2257	0.2493	0.2752	0.3034	0.3335
5.00	0.1521	0.1544	0.1612	0.1720	0.1864	0.2039	0.2242	0.2469	0.2715	0.2976	0.3268
∞	0.1521	0.1544	0.1612	0.1720	0.1863	0.2038	0.2241	0.2466	0.2710	0.2969	0.3238

TABLE 3.— ROLL MOMENT DERIVATIVE, $\overline{C}_{L_{\theta_o}}$, $\gamma = 5$, $\theta_{q_1} = 0$

P \ μ	0.0000	0.1000	0.2000	0.3000	0.4000	0.5000	0.6000	0.7000	0.8000	0.9000	1.0000
1.00	0.0000	-0.0000	-0.0000	-0.0000	-0.0000	-0.0000	-0.0000	-0.0000	-0.0000	-0.0000	-0.0000
1.02	-0.0000	0.0001	0.0002	0.0004	0.0005	0.0006	0.0006	0.0008	0.0009	0.0013	0.0017
1.04	-0.0000	0.0001	0.0002	0.0003	0.0003	0.0003	0.0003	0.0004	0.0007	0.0013	0.0022
1.08	-0.0000	-0.0004	-0.0009	-0.0015	-0.0020	-0.0027	-0.0032	-0.0041	-0.0051	-0.0061	-0.0081
1.12	-0.0000	-0.0014	-0.0029	-0.0044	-0.0059	-0.0077	-0.0092	-0.0111	-0.0131	-0.0142	-0.0142
1.16	-0.0000	-0.0027	-0.0054	-0.0082	-0.0110	-0.0140	-0.0168	-0.0197	-0.0222	-0.0229	-0.0208
1.20	-0.0000	-0.0042	-0.0084	-0.0126	-0.0169	-0.0214	-0.0259	-0.0304	-0.0344	-0.0362	-0.0343
1.24	-0.0000	-0.0056	-0.0113	-0.0170	-0.0228	-0.0290	-0.0352	-0.0415	-0.0473	-0.0510	-0.0506
1.28	-0.0000	-0.0070	-0.0140	-0.0211	-0.0284	-0.0360	-0.0439	-0.0519	-0.0596	-0.0653	-0.0669
1.34	-0.0000	-0.0087	-0.0174	-0.0263	-0.0355	-0.0450	-0.0549	-0.0652	-0.0753	-0.0839	-0.0886
1.40	-0.0000	-0.0100	-0.0202	-0.0305	-0.0410	-0.0520	-0.0636	-0.0756	-0.0875	-0.0984	-0.1059
1.50	-0.0000	-0.0117	-0.0234	-0.0353	-0.0476	-0.0603	-0.0735	-0.0874	-0.1016	-0.1151	-0.1262
1.60	-0.0000	-0.0127	-0.0255	-0.0384	-0.0517	-0.0654	-0.0798	-0.0948	-0.1102	-0.1255	-0.1391
1.70	-0.0000	-0.0134	-0.0268	-0.0405	-0.0544	-0.0687	-0.0837	-0.0994	-0.1157	-0.1321	-0.1475
1.80	-0.0000	-0.0138	-0.0277	-0.0418	-0.0561	-0.0708	-0.0861	-0.1022	-0.1190	-0.1363	-0.1533
1.90	-0.0000	-0.0141	-0.0284	-0.0426	-0.0571	-0.0720	-0.0873	-0.1035	-0.1206	-0.1386	-0.1573
2.00	-0.0000	-0.0144	-0.0288	-0.0432	-0.0577	-0.0725	-0.0878	-0.1038	-0.1209	-0.1394	-0.1597
2.10	-0.0000	-0.0145	-0.0291	-0.0436	-0.0582	-0.0730	-0.0881	-0.1039	-0.1208	-0.1394	-0.1607
2.20	-0.0000	-0.0147	-0.0293	-0.0440	-0.0587	-0.0735	-0.0886	-0.1043	-0.1211	-0.1396	-0.1609
2.60	-0.0000	-0.0149	-0.0299	-0.0449	-0.0600	-0.0753	-0.0909	-0.1070	-0.1239	-0.1421	-0.1623
3.00	0.0000	-0.0150	-0.0301	-0.0453	-0.0606	-0.0761	-0.0920	-0.1086	-0.1261	-0.1449	-0.1652
5.00	0.0000	-0.0151	-0.0304	-0.0457	-0.0611	-0.0768	-0.0930	-0.1097	-0.1273	-0.1460	-0.1661
∞	0.0000	-0.0152	-0.0304	-0.0457	-0.0612	-0.0769	-0.0930	-0.1098	-0.1274	-0.1461	-0.1662

TABLE 4.– PITCH MOMENT DERIVATIVE, $\bar{C}_{M_{\theta_o}}$, $\gamma = 5$, $\theta_{q_1} = 0$

P \ μ	0.0000	0.1000	0.2000	0.3000	0.4000	0.5000	0.6000	0.7000	0.8000	0.9000	1.0000
1.00	-0.0000	-0.0000	0.0000	0.0000	0.0000	-0.0000	0.0000	-0.0000	-0.0000	-0.0000	-0.0000
1.02	-0.0000	0.0011	0.0023	0.0036	0.0050	0.0065	0.0083	0.0103	0.0125	0.0148	0.0172
1.04	0.0000	0.0023	0.0046	0.0072	0.0101	0.0133	0.0170	0.0214	0.0263	0.0316	0.0375
1.08	0.0000	0.0045	0.0092	0.0143	0.0201	0.0269	0.0350	0.0450	0.0577	0.0726	0.0897
1.12	0.0000	0.0063	0.0129	0.0202	0.0284	0.0380	0.0492	0.0622	0.0770	0.0919	0.1056
1.16	0.0000	0.0077	0.0158	0.0247	0.0349	0.0467	0.0609	0.0774	0.0961	0.1159	0.1349
1.20	-0.0000	0.0086	0.0177	0.0277	0.0392	0.0526	0.0688	0.0878	0.1098	0.1338	0.1580
1.24	-0.0000	0.0091	0.0188	0.0294	0.0415	0.0558	0.0730	0.0934	0.1172	0.1438	0.1715
1.28	-0.0000	0.0093	0.0191	0.0299	0.0423	0.0568	0.0743	0.0951	0.1195	0.1472	0.1767
1.34	-0.0000	0.0091	0.0188	0.0294	0.0415	0.0557	0.0726	0.0929	0.1168	0.1442	0.1741
1.40	-0.0000	0.0087	0.0179	0.0279	0.0394	0.0528	0.0687	0.0877	0.1101	0.1360	0.1648
1.50	-0.0000	0.0077	0.0159	0.0248	0.0349	0.0466	0.0605	0.0769	0.0964	0.1191	0.1448
1.60	-0.0000	0.0068	0.0140	0.0217	0.0305	0.0406	0.0525	0.0665	0.0832	0.1029	0.1255
1.70	-0.0000	0.0060	0.0122	0.0190	0.0266	0.0352	0.0454	0.0574	0.0717	0.0888	0.1087
1.80	-0.0000	0.0052	0.0108	0.0167	0.0232	0.0306	0.0393	0.0495	0.0619	0.0768	0.0946
1.90	-0.0000	0.0046	0.0095	0.0147	0.0204	0.0268	0.0342	0.0430	0.0537	0.0669	0.0829
2.00	-0.0000	0.0041	0.0085	0.0131	0.0182	0.0238	0.0304	0.0380	0.0474	0.0590	0.0736
2.10	-0.0000	0.0037	0.0076	0.0118	0.0164	0.0216	0.0276	0.0346	0.0430	0.0534	0.0664
2.20	-0.0000	0.0033	0.0069	0.0107	0.0150	0.0199	0.0255	0.0320	0.0397	0.0491	0.0607
2.60	-0.0000	0.0023	0.0048	0.0075	0.0106	0.0142	0.0184	0.0234	0.0292	0.0361	0.0441
3.00	-0.0000	0.0017	0.0035	0.0055	0.0079	0.0106	0.0139	0.0178	0.0224	0.0277	0.0339
5.00	-0.0000	0.0005	0.0012	0.0019	0.0027	0.0036	0.0046	0.0059	0.0073	0.0090	0.0109
∞	-0.0000	-0.0000	-0.0000	0.0000	0.0000	0.0000	0.0000	0.0000	0.0000	0.0000	0.0000

TABLE 5.— THRUST DERIVATIVE, $\bar{C}_{T_{\theta_s}}$, $\gamma = 5$, $\theta_{q_1} = 0$

μ / p	0.0000	0.1000	0.2000	0.3000	0.4000	0.5000	0.6000	0.7000	0.8000	0.9000	1.0000
1.00	-0.0000	0.0236	0.0479	0.0737	0.1021	0.1344	0.1722	0.2174	0.2717	0.3370	0.4176
1.02	-0.0000	0.0244	0.0495	0.0762	0.1058	0.1397	0.1798	0.2283	0.2874	0.3581	0.4462
1.04	-0.0000	0.0251	0.0510	0.0787	0.1094	0.1450	0.1873	0.2392	0.3036	0.3820	0.4806
1.08	-0.0000	0.0262	0.0533	0.0822	0.1144	0.1519	0.1968	0.2524	0.3224	0.4105	0.5199
1.12	-0.0000	0.0266	0.0541	0.0834	0.1160	0.1537	0.1993	0.2559	0.3270	0.4156	0.5214
1.16	-0.0000	0.0266	0.0541	0.0834	0.1158	0.1531	0.1979	0.2534	0.3239	0.4134	0.5238
1.20	-0.0000	0.0264	0.0536	0.0826	0.1145	0.1508	0.1940	0.2472	0.3145	0.4005	0.5085
1.24	-0.0000	0.0261	0.0530	0.0815	0.1127	0.1479	0.1892	0.2394	0.3023	0.3826	0.4843
1.28	-0.0000	0.0258	0.0523	0.0803	0.1107	0.1448	0.1842	0.2314	0.2898	0.3638	0.4577
1.34	-0.0000	0.0253	0.0513	0.0787	0.1081	0.1407	0.1776	0.2209	0.2733	0.3367	0.4211
1.40	-0.0000	0.0249	0.0505	0.0774	0.1061	0.1374	0.1725	0.2128	0.2606	0.3191	0.3921
1.50	-0.0000	0.0245	0.0496	0.0758	0.1037	0.1339	0.1669	0.2041	0.2469	0.2978	0.3600
1.60	-0.0000	0.0242	0.0490	0.0750	0.1025	0.1321	0.1643	0.1999	0.2401	0.2870	0.3431
1.70	-0.0000	0.0240	0.0487	0.0746	0.1021	0.1317	0.1639	0.1992	0.2386	0.2837	0.3369
1.80	-0.0000	0.0239	0.0486	0.0746	0.1025	0.1326	0.1655	0.2015	0.2415	0.2869	0.3393
1.90	-0.0000	0.0239	0.0486	0.0749	0.1034	0.1345	0.1688	0.2066	0.2485	0.2953	0.3486
2.00	-0.0000	0.0238	0.0486	0.0751	0.1042	0.1363	0.1720	0.2118	0.2559	0.3048	0.3592
2.10	-0.0000	0.0238	0.0485	0.0749	0.1039	0.1361	0.1721	0.2123	0.2572	0.3068	0.3613
2.20	-0.0000	0.0237	0.0483	0.0744	0.1028	0.1341	0.1690	0.2080	0.2514	0.2996	0.3523
2.60	-0.0000	0.0236	0.0478	0.0729	0.0995	0.1280	0.1590	0.1928	0.2299	0.2706	0.3151
3.00	-0.0000	0.0236	0.0476	0.0725	0.0986	0.1265	0.1566	0.1894	0.2255	0.2656	0.3104
5.00	-0.0000	0.0235	0.0475	0.0722	0.0981	0.1255	0.1547	0.1863	0.2206	0.2579	0.2987
∞	0.0000	0.0235	0.0475	0.0722	0.0980	0.1254	0.1546	0.1860	0.2201	0.2572	0.2977

TABLE 6.— ROLL MOMENT DERIVATIVE, $\bar{C}_{L_{\theta_s}}$, $\gamma = 5$, $\theta_{q_1} = 0$

P \ μ	0.0000	0.1000	0.2000	0.3000	0.4000	0.5000	0.6000	0.7000	0.8000	0.9000	1.0000
1.00	-0.0000	-0.0000	-0.0000	-0.0000	-0.0000	-0.0000	-0.0000	-0.0000	-0.0000	-0.0000	-0.0000
1.02	-0.0003	-0.0002	-0.0002	-0.0001	-0.0000	0.0000	0.0002	0.0005	0.0009	0.0016	0.0024
1.04	-0.0012	-0.0011	-0.0011	-0.0010	-0.0009	-0.0006	-0.0003	0.0001	0.0009	0.0021	0.0037
1.08	-0.0048	-0.0048	-0.0048	-0.0048	-0.0047	-0.0047	-0.0044	-0.0043	-0.0040	-0.0036	-0.0038
1.12	-0.0096	-0.0097	-0.0098	-0.0099	-0.0101	-0.0105	-0.0106	-0.0109	-0.0111	-0.0105	-0.0086
1.16	-0.0152	-0.0153	-0.0155	-0.0160	-0.0166	-0.0175	-0.0183	-0.0190	-0.0193	-0.0180	-0.0140
1.20	-0.0208	-0.0210	-0.0215	-0.0224	-0.0236	-0.0252	-0.0269	-0.0286	-0.0298	-0.0291	-0.0250
1.24	-0.0261	-0.0264	-0.0272	-0.0284	-0.0303	-0.0326	-0.0354	-0.0384	-0.0408	-0.0414	-0.0382
1.28	-0.0308	-0.0312	-0.0322	-0.0339	-0.0363	-0.0395	-0.0432	-0.0473	-0.0511	-0.0531	-0.0514
1.34	-0.0365	-0.0370	-0.0383	-0.0406	-0.0438	-0.0480	-0.0530	-0.0586	-0.0641	-0.0682	-0.0689
1.40	-0.0409	-0.0414	-0.0430	-0.0457	-0.0495	-0.0545	-0.0604	-0.0672	-0.0741	-0.0800	-0.0828
1.50	-0.0457	-0.0464	-0.0483	-0.0515	-0.0560	-0.0618	-0.0689	-0.0769	-0.0855	-0.0935	-0.0992
1.60	-0.0487	-0.0494	-0.0515	-0.0550	-0.0600	-0.0663	-0.0740	-0.0828	-0.0923	-0.1017	-0.1095
1.70	-0.0506	-0.0514	-0.0536	-0.0572	-0.0623	-0.0689	-0.0769	-0.0862	-0.0964	-0.1068	-0.1163
1.80	-0.0519	-0.0526	-0.0548	-0.0585	-0.0637	-0.0703	-0.0784	-0.0879	-0.0985	-0.1097	-0.1209
1.90	-0.0527	-0.0535	-0.0556	-0.0593	-0.0643	-0.0708	-0.0788	-0.0882	-0.0990	-0.1109	-0.1238
2.00	-0.0533	-0.0541	-0.0562	-0.0597	-0.0646	-0.0709	-0.0786	-0.0878	-0.0985	-0.1108	-0.1252
2.10	-0.0538	-0.0545	-0.0566	-0.0602	-0.0651	-0.0713	-0.0788	-0.0877	-0.0981	-0.1104	-0.1253
2.20	-0.0541	-0.0548	-0.0571	-0.0607	-0.0658	-0.0721	-0.0797	-0.0885	-0.0987	-0.1106	-0.1251
2.60	-0.0547	-0.0556	-0.0581	-0.0622	-0.0678	-0.0748	-0.0830	-0.0924	-0.1028	-0.1142	-0.1266
3.00	-0.0550	-0.0559	-0.0584	-0.0627	-0.0686	-0.0760	-0.0849	-0.0952	-0.1065	-0.1187	-0.1312
5.00	-0.0552	-0.0561	-0.0587	-0.0631	-0.0690	-0.0764	-0.0853	-0.0953	-0.1063	-0.1182	-0.1303
∞	-0.0553	-0.0562	-0.0588	-0.0631	-0.0691	-0.0765	-0.0853	-0.0954	-0.1064	-0.1182	-0.1305

TABLE 7.- PITCH MOMENT DERIVATIVE, $\bar{C}_{M_{\theta_s}}$, $\gamma = 5$, $\theta_{q_1} = 0$

p \ μ	0.0000	0.1000	0.2000	0.3000	0.4000	0.5000	0.6000	0.7000	0.8000	0.9000	1.0000
1.00	-0.0000	0.0000	0.0000	-0.0000	0.0000	0.0000	0.0000	-0.0000	-0.0000	-0.0000	-0.0000
1.02	0.0039	0.0040	0.0043	0.0048	0.0055	0.0064	0.0075	0.0088	0.0102	0.0118	0.0135
1.04	0.0078	0.0080	0.0086	0.0096	0.0110	0.0129	0.0153	0.0182	0.0216	0.0255	0.0298
1.08	0.0147	0.0151	0.0163	0.0183	0.0213	0.0254	0.0309	0.0381	0.0476	0.0591	0.0723
1.12	0.0202	0.0208	0.0225	0.0254	0.0298	0.0356	0.0433	0.0526	0.0634	0.0746	0.0846
1.16	0.0241	0.0248	0.0269	0.0306	0.0360	0.0433	0.0531	0.0651	0.0790	0.0939	0.1080
1.20	0.0263	0.0271	0.0295	0.0337	0.0398	0.0482	0.0594	0.0733	0.0899	0.1082	0.1265
1.24	0.0272	0.0281	0.0306	0.0350	0.0416	0.0506	0.0624	0.0774	0.0955	0.1160	0.1372
1.28	0.0271	0.0280	0.0306	0.0351	0.0418	0.0509	0.0630	0.0783	0.0970	0.1184	0.1413
1.34	0.0259	0.0267	0.0293	0.0337	0.0402	0.0491	0.0609	0.0758	0.0941	0.1155	0.1390
1.40	0.0240	0.0248	0.0272	0.0314	0.0375	0.0459	0.0570	0.0710	0.0882	0.1086	0.1314
1.50	0.0207	0.0214	0.0235	0.0271	0.0325	0.0398	0.0493	0.0615	0.0765	0.0945	0.1152
1.60	0.0177	0.0183	0.0201	0.0232	0.0278	0.0340	0.0421	0.0525	0.0654	0.0812	0.0996
1.70	0.0152	0.0157	0.0172	0.0199	0.0237	0.0290	0.0359	0.0447	0.0558	0.0696	0.0861
1.80	0.0131	0.0135	0.0149	0.0171	0.0204	0.0249	0.0307	0.0382	0.0478	0.0600	0.0749
1.90	0.0114	0.0118	0.0130	0.0150	0.0178	0.0217	0.0267	0.0332	0.0415	0.0523	0.0658
2.00	0.0100	0.0104	0.0115	0.0134	0.0161	0.0196	0.0241	0.0299	0.0372	0.0467	0.0589
2.10	0.0089	0.0093	0.0104	0.0123	0.0149	0.0184	0.0227	0.0281	0.0348	0.0431	0.0539
2.20	0.0079	0.0083	0.0094	0.0113	0.0139	0.0173	0.0216	0.0267	0.0330	0.0405	0.0498
2.60	0.0053	0.0056	0.0064	0.0079	0.0099	0.0126	0.0160	0.0202	0.0252	0.0308	0.0373
3.00	0.0039	0.0041	0.0047	0.0057	0.0072	0.0093	0.0119	0.0152	0.0191	0.0236	0.0288
5.00	0.0013	0.0013	0.0015	0.0019	0.0023	0.0030	0.0037	0.0047	0.0057	0.0070	0.0085
∞	0.0000	0.0000	0.0000	0.0000	0.0000	0.0000	0.0000	0.0000	0.0000	0.0000	0.0000

TABLE 8.— THRUST DERIVATIVE, $\bar{C}_{T_{\theta_c}}$, $\gamma = 5$, $\theta_{q_1} = 0$

P \ μ	0.0000	0.1000	0.2000	0.3000	0.4000	0.5000	0.6000	0.7000	0.8000	0.9000	1.0000
1.00	0.0000	0.0000	-0.0000	-0.0000	-0.0000	-0.0000	-0.0001	-0.0002	-0.0004	-0.0006	-0.0009
1.02	0.0000	-0.0000	-0.0000	-0.0001	-0.0003	-0.0006	-0.0011	-0.0018	-0.0028	-0.0040	-0.0055
1.04	0.0000	-0.0001	-0.0003	-0.0006	-0.0011	-0.0018	-0.0028	-0.0042	-0.0061	-0.0085	-0.0115
1.08	0.0000	-0.0007	-0.0014	-0.0023	-0.0034	-0.0048	-0.0068	-0.0096	-0.0132	-0.0183	-0.0251
1.12	0.0000	-0.0012	-0.0025	-0.0039	-0.0056	-0.0078	-0.0109	-0.0150	-0.0200	-0.0266	-0.0340
1.16	0.0000	-0.0017	-0.0034	-0.0053	-0.0075	-0.0103	-0.0141	-0.0191	-0.0257	-0.0341	-0.0439
1.20	0.0000	-0.0020	-0.0041	-0.0063	-0.0087	-0.0118	-0.0159	-0.0214	-0.0287	-0.0383	-0.0497
1.24	0.0000	-0.0022	-0.0045	-0.0068	-0.0094	-0.0125	-0.0165	-0.0220	-0.0294	-0.0393	-0.0515
1.28	0.0000	-0.0023	-0.0046	-0.0069	-0.0094	-0.0124	-0.0162	-0.0214	-0.0284	-0.0380	-0.0501
1.34	0.0000	-0.0023	-0.0045	-0.0067	-0.0090	-0.0115	-0.0147	-0.0190	-0.0250	-0.0334	-0.0446
1.40	0.0000	-0.0022	-0.0043	-0.0062	-0.0081	-0.0101	-0.0125	-0.0158	-0.0207	-0.0277	-0.0374
1.50	0.0000	-0.0019	-0.0037	-0.0052	-0.0065	-0.0076	-0.0087	-0.0105	-0.0133	-0.0180	-0.0252
1.60	0.0000	-0.0016	-0.0031	-0.0042	-0.0049	-0.0051	-0.0052	-0.0056	-0.0067	-0.0095	-0.0147
1.70	0.0000	-0.0014	-0.0026	-0.0033	-0.0035	-0.0031	-0.0023	-0.0015	-0.0014	-0.0027	-0.0065
1.80	0.0000	-0.0012	-0.0022	-0.0027	-0.0025	-0.0017	-0.0004	0.0010	0.0019	0.0013	-0.0018
1.90	0.0000	-0.0011	-0.0019	-0.0024	-0.0023	-0.0017	-0.0006	0.0006	0.0013	0.0005	-0.0030
2.00	0.0000	-0.0010	-0.0019	-0.0026	-0.0032	-0.0035	-0.0038	-0.0042	-0.0051	-0.0074	-0.0123
2.10	0.0000	-0.0009	-0.0019	-0.0031	-0.0045	-0.0063	-0.0086	-0.0113	-0.0148	-0.0193	-0.0257
2.20	0.0000	-0.0008	-0.0019	-0.0033	-0.0053	-0.0080	-0.0116	-0.0159	-0.0212	-0.0273	-0.0347
2.60	0.0000	-0.0005	-0.0013	-0.0025	-0.0042	-0.0065	-0.0095	-0.0132	-0.0174	-0.0220	-0.0268
3.00	0.0000	-0.0004	-0.0009	-0.0017	-0.0028	-0.0044	-0.0063	-0.0085	-0.0110	-0.0136	-0.0159
5.00	0.0000	-0.0001	-0.0003	-0.0005	-0.0008	-0.0013	-0.0019	-0.0027	-0.0037	-0.0049	-0.0065
∞	-0.0000	-0.0000	-0.0000	0.0000	0.0000	0.0000	0.0000	0.0000	0.0000	0.0000	0.0000

TABLE 9.— ROLL MOMENT DERIVATIVE, $\bar{C}_{L_{\theta_c}}$, $\gamma = 5$, $\theta_{q_1} = 0$

p \ μ	0.0000	0.1000	0.2000	0.3000	0.4000	0.5000	0.6000	0.7000	0.8000	0.9000	1.0000
1.00	0.0000	0.0000	-0.0000	0.0000	0.0000	0.0000	0.0000	0.0000	0.0000	0.0000	0.0000
1.02	-0.0039	-0.0039	-0.0039	-0.0039	-0.0039	-0.0039	-0.0039	-0.0039	-0.0039	-0.0039	-0.0040
1.04	-0.0078	-0.0078	-0.0078	-0.0078	-0.0078	-0.0077	-0.0077	-0.0077	-0.0078	-0.0078	-0.0079
1.08	-0.0147	-0.0147	-0.0146	-0.0146	-0.0145	-0.0145	-0.0145	-0.0145	-0.0145	-0.0146	-0.0146
1.12	-0.0202	-0.0202	-0.0201	-0.0200	-0.0199	-0.0197	-0.0196	-0.0195	-0.0192	-0.0193	-0.0196
1.16	-0.0241	-0.0241	-0.0240	-0.0239	-0.0237	-0.0234	-0.0233	-0.0231	-0.0231	-0.0234	-0.0242
1.20	-0.0263	-0.0263	-0.0262	-0.0260	-0.0258	-0.0255	-0.0252	-0.0251	-0.0251	-0.0257	-0.0269
1.24	-0.0272	-0.0272	-0.0270	-0.0268	-0.0265	-0.0261	-0.0258	-0.0255	-0.0256	-0.0263	-0.0280
1.28	-0.0271	-0.0271	-0.0269	-0.0266	-0.0263	-0.0258	-0.0254	-0.0250	-0.0250	-0.0258	-0.0278
1.34	-0.0259	-0.0258	-0.0256	-0.0253	-0.0248	-0.0242	-0.0236	-0.0232	-0.0231	-0.0239	-0.0261
1.40	-0.0240	-0.0239	-0.0237	-0.0233	-0.0228	-0.0221	-0.0214	-0.0208	-0.0207	-0.0214	-0.0238
1.50	-0.0207	-0.0206	-0.0203	-0.0199	-0.0192	-0.0184	-0.0176	-0.0168	-0.0166	-0.0174	-0.0199
1.60	-0.0177	-0.0176	-0.0173	-0.0167	-0.0160	-0.0151	-0.0142	-0.0134	-0.0131	-0.0138	-0.0164
1.70	-0.0152	-0.0150	-0.0147	-0.0142	-0.0134	-0.0124	-0.0114	-0.0105	-0.0102	-0.0108	-0.0135
1.80	-0.0131	-0.0130	-0.0127	-0.0121	-0.0113	-0.0102	-0.0091	-0.0082	-0.0077	-0.0083	-0.0109
1.90	-0.0114	-0.0113	-0.0110	-0.0105	-0.0097	-0.0087	-0.0077	-0.0066	-0.0060	-0.0064	-0.0086
2.00	-0.0100	-0.0100	-0.0098	-0.0094	-0.0088	-0.0081	-0.0072	-0.0063	-0.0055	-0.0054	-0.0066
2.10	-0.0089	-0.0089	-0.0088	-0.0087	-0.0084	-0.0081	-0.0075	-0.0069	-0.0062	-0.0056	-0.0055
2.20	-0.0079	-0.0080	-0.0080	-0.0080	-0.0080	-0.0080	-0.0078	-0.0075	-0.0070	-0.0063	-0.0052
2.60	-0.0053	-0.0054	-0.0054	-0.0056	-0.0058	-0.0061	-0.0064	-0.0067	-0.0069	-0.0068	-0.0059
3.00	-0.0039	-0.0039	-0.0039	-0.0040	-0.0042	-0.0044	-0.0047	-0.0051	-0.0055	-0.0057	-0.0054
5.00	-0.0013	-0.0013	-0.0013	-0.0013	-0.0013	-0.0013	-0.0013	-0.0012	-0.0011	-0.0010	-0.0008
∞	-0.0000	-0.0000	-0.0000	-0.0000	-0.0000	-0.0000	-0.0000	-0.0000	-0.0000	-0.0000	-0.0000

TABLE 10.— PITCH MOMENT DERIVATIVE, $\bar{C}_{M_{\theta_c}}$, $\gamma = 5$, $\theta_{q_1} = 0$

p \ μ	0.0000	0.1000	0.2000	0.3000	0.4000	0.5000	0.6000	0.7000	0.8000	0.9000	1.0000
1.00	-0.0000	-0.0000	0.0000	-0.0000	-0.0000	-0.0000	-0.0000	-0.0000	-0.0000	-0.0000	-0.0000
1.02	-0.0003	-0.0003	-0.0003	-0.0003	-0.0003	-0.0003	-0.0003	-0.0003	-0.0003	-0.0003	-0.0003
1.04	-0.0012	-0.0012	-0.0012	-0.0012	-0.0013	-0.0013	-0.0014	-0.0014	-0.0015	-0.0015	-0.0015
1.08	-0.0048	-0.0048	-0.0049	-0.0050	-0.0052	-0.0055	-0.0058	-0.0063	-0.0071	-0.0076	-0.0082
1.12	-0.0096	-0.0097	-0.0099	-0.0102	-0.0106	-0.0112	-0.0118	-0.0127	-0.0137	-0.0142	-0.0143
1.16	-0.0152	-0.0153	-0.0156	-0.0161	-0.0168	-0.0178	-0.0189	-0.0202	-0.0216	-0.0226	-0.0229
1.20	-0.0208	-0.0210	-0.0214	-0.0221	-0.0232	-0.0245	-0.0262	-0.0281	-0.0301	-0.0317	-0.0326
1.24	-0.0261	-0.0263	-0.0269	-0.0278	-0.0291	-0.0308	-0.0329	-0.0353	-0.0379	-0.0402	-0.0417
1.28	-0.0308	-0.0310	-0.0317	-0.0327	-0.0343	-0.0363	-0.0388	-0.0416	-0.0446	-0.0474	-0.0495
1.34	-0.0365	-0.0368	-0.0375	-0.0388	-0.0405	-0.0428	-0.0457	-0.0489	-0.0524	-0.0558	-0.0585
1.40	-0.0409	-0.0411	-0.0419	-0.0433	-0.0452	-0.0476	-0.0507	-0.0541	-0.0579	-0.0616	-0.0648
1.50	-0.0457	-0.0460	-0.0469	-0.0483	-0.0503	-0.0528	-0.0560	-0.0596	-0.0635	-0.0675	-0.0711
1.60	-0.0487	-0.0490	-0.0499	-0.0513	-0.0533	-0.0558	-0.0589	-0.0625	-0.0664	-0.0705	-0.0744
1.70	-0.0506	-0.0509	-0.0517	-0.0531	-0.0550	-0.0574	-0.0604	-0.0639	-0.0678	-0.0720	-0.0761
1.80	-0.0519	-0.0521	-0.0529	-0.0541	-0.0559	-0.0581	-0.0609	-0.0642	-0.0681	-0.0724	-0.0768
1.90	-0.0527	-0.0530	-0.0536	-0.0547	-0.0562	-0.0582	-0.0607	-0.0638	-0.0675	-0.0720	-0.0768
2.00	-0.0533	-0.0535	-0.0541	-0.0550	-0.0563	-0.0581	-0.0603	-0.0631	-0.0667	-0.0713	-0.0766
2.10	-0.0538	-0.0540	-0.0545	-0.0554	-0.0567	-0.0583	-0.0604	-0.0631	-0.0666	-0.0712	-0.0767
2.20	-0.0541	-0.0543	-0.0549	-0.0559	-0.0573	-0.0590	-0.0612	-0.0640	-0.0674	-0.0718	-0.0774
2.60	-0.0547	-0.0550	-0.0558	-0.0571	-0.0589	-0.0612	-0.0640	-0.0671	-0.0708	-0.0750	-0.0800
3.00	-0.0550	-0.0553	-0.0561	-0.0576	-0.0596	-0.0622	-0.0655	-0.0693	-0.0736	-0.0784	-0.0836
5.00	-0.0552	-0.0555	-0.0564	-0.0579	-0.0599	-0.0624	-0.0655	-0.0691	-0.0731	-0.0774	-0.0824
∞	-0.0553	-0.0556	-0.0565	-0.0579	-0.0599	-0.0625	-0.0655	-0.0691	-0.0730	-0.0774	-0.0821

TABLE 11.— THRUST DERIVATIVE, $\bar{C}_{T_{\alpha_c}}$, $\gamma = 5$, $\theta_{q_1} = 0$

p \ μ	0.0000	0.1000	0.2000	0.3000	0.4000	0.5000	0.6000	0.7000	0.8000	0.9000	1.0000
1.00	0.0000	0.0023	0.0088	0.0193	0.0334	0.0513	0.0735	0.1005	0.1331	0.1719	0.2184
1.02	0.0000	0.0024	0.0093	0.0202	0.0351	0.0541	0.0778	0.1072	0.1440	0.1874	0.2391
1.04	0.0000	0.0025	0.0097	0.0211	0.0367	0.0568	0.0820	0.1137	0.1541	0.2034	0.2639
1.08	0.0000	0.0026	0.0102	0.0224	0.0389	0.0602	0.0870	0.1210	0.1645	0.2201	0.2905
1.12	0.0000	0.0027	0.0104	0.0228	0.0396	0.0611	0.0882	0.1226	0.1667	0.2232	0.2932
1.16	0.0000	0.0027	0.0104	0.0228	0.0394	0.0606	0.0872	0.1208	0.1641	0.2204	0.2928
1.20	0.0000	0.0026	0.0103	0.0225	0.0388	0.0595	0.0850	0.1169	0.1578	0.2110	0.2803
1.24	0.0000	0.0026	0.0102	0.0221	0.0380	0.0579	0.0823	0.1122	0.1499	0.1986	0.2622
1.28	0.0000	0.0026	0.0100	0.0217	0.0372	0.0564	0.0795	0.1075	0.1420	0.1859	0.2429
1.34	0.0000	0.0025	0.0097	0.0211	0.0360	0.0543	0.0759	0.1013	0.1317	0.1692	0.2167
1.40	0.0000	0.0025	0.0095	0.0206	0.0351	0.0527	0.0731	0.0966	0.1237	0.1562	0.1962
1.50	0.0000	0.0024	0.0093	0.0201	0.0341	0.0509	0.0701	0.0914	0.1151	0.1420	0.1735
1.60	0.0000	0.0024	0.0092	0.0197	0.0335	0.0500	0.0685	0.0888	0.1107	0.1345	0.1611
1.70	0.0000	0.0023	0.0091	0.0196	0.0333	0.0496	0.0681	0.0880	0.1092	0.1316	0.1556
1.80	0.0000	0.0023	0.0090	0.0195	0.0333	0.0498	0.0685	0.0889	0.1103	0.1325	0.1555
1.90	0.0000	0.0023	0.0090	0.0196	0.0335	0.0505	0.0699	0.0911	0.1136	0.1366	0.1600
2.00	0.0000	0.0023	0.0090	0.0196	0.0338	0.0512	0.0713	0.0937	0.1175	0.1419	0.1662
2.10	0.0000	0.0023	0.0090	0.0196	0.0337	0.0512	0.0716	0.0943	0.1188	0.1439	0.1688
2.20	0.0000	0.0023	0.0089	0.0195	0.0334	0.0506	0.0704	0.0926	0.1164	0.1410	0.1654
2.60	0.0000	0.0023	0.0089	0.0191	0.0325	0.0484	0.0663	0.0857	0.1059	0.1264	0.1466
3.00	0.0000	0.0023	0.0088	0.0190	0.0322	0.0478	0.0652	0.0839	0.1034	0.1233	0.1435
5.00	0.0000	0.0023	0.0088	0.0189	0.0320	0.0473	0.0644	0.0825	0.1011	0.1194	0.1370
∞	0.0000	0.0023	0.0088	0.0189	0.0320	0.0473	0.0643	0.0824	0.1008	0.1190	0.1364

TABLE 12.— ROLL MOMENT DERIVATIVE, $\bar{C}_{L_{\alpha_c}}$, $\gamma = 5$, $\theta_{q_1} = 0$

p \ μ	0.0000	0.1000	0.2000	0.3000	0.4000	0.5000	0.6000	0.7000	0.8000	0.9000	1.0000
1.00	0.0000	-0.0000	-0.0000	-0.0000	-0.0000	-0.0000	-0.0000	-0.0000	-0.0000	-0.0000	-0.0000
1.02	0.0000	-0.0000	-0.0001	-0.0002	-0.0003	-0.0004	-0.0006	-0.0007	-0.0009	-0.0011	-0.0013
1.04	0.0000	-0.0002	-0.0005	-0.0007	-0.0010	-0.0013	-0.0016	-0.0020	-0.0025	-0.0028	-0.0031
1.08	0.0000	-0.0008	-0.0016	-0.0024	-0.0032	-0.0041	-0.0049	-0.0061	-0.0075	-0.0090	-0.0113
1.12	0.0000	-0.0014	-0.0029	-0.0043	-0.0058	-0.0073	-0.0087	-0.0105	-0.0125	-0.0143	-0.0158
1.16	0.0000	-0.0022	-0.0044	-0.0066	-0.0087	-0.0109	-0.0132	-0.0157	-0.0183	-0.0203	-0.0212
1.20	0.0000	-0.0030	-0.0059	-0.0089	-0.0118	-0.0149	-0.0181	-0.0216	-0.0252	-0.0284	-0.0300
1.24	0.0000	-0.0037	-0.0074	-0.0110	-0.0147	-0.0186	-0.0228	-0.0274	-0.0323	-0.0368	-0.0398
1.28	0.0000	-0.0043	-0.0086	-0.0129	-0.0173	-0.0220	-0.0271	-0.0327	-0.0387	-0.0447	-0.0494
1.34	0.0000	-0.0051	-0.0102	-0.0153	-0.0206	-0.0262	-0.0323	-0.0392	-0.0469	-0.0548	-0.0619
1.40	0.0000	-0.0056	-0.0113	-0.0171	-0.0230	-0.0293	-0.0363	-0.0442	-0.0530	-0.0625	-0.0717
1.50	0.0000	-0.0063	-0.0126	-0.0191	-0.0257	-0.0329	-0.0408	-0.0498	-0.0600	-0.0713	-0.0830
1.60	0.0000	-0.0067	-0.0134	-0.0203	-0.0274	-0.0351	-0.0435	-0.0531	-0.0641	-0.0766	-0.0901
1.70	0.0000	-0.0069	-0.0140	-0.0211	-0.0284	-0.0363	-0.0451	-0.0551	-0.0666	-0.0799	-0.0947
1.80	0.0000	-0.0071	-0.0143	-0.0215	-0.0290	-0.0371	-0.0460	-0.0561	-0.0680	-0.0819	-0.0978
1.90	0.0000	-0.0072	-0.0145	-0.0218	-0.0294	-0.0374	-0.0463	-0.0565	-0.0685	-0.0828	-0.0998
2.00	0.0000	-0.0073	-0.0146	-0.0220	-0.0295	-0.0375	-0.0463	-0.0563	-0.0683	-0.0829	-0.1009
2.10	0.0000	-0.0073	-0.0147	-0.0221	-0.0297	-0.0377	-0.0463	-0.0563	-0.0681	-0.0828	-0.1012
2.20	0.0000	-0.0074	-0.0148	-0.0223	-0.0299	-0.0380	-0.0467	-0.0566	-0.0684	-0.0829	-0.1013
2.60	0.0000	-0.0075	-0.0150	-0.0227	-0.0306	-0.0390	-0.0481	-0.0584	-0.0703	-0.0847	-0.1022
3.00	0.0000	-0.0075	-0.0151	-0.0228	-0.0309	-0.0394	-0.0488	-0.0595	-0.0720	-0.0868	-0.1046
5.00	0.0000	-0.0076	-0.0152	-0.0230	-0.0311	-0.0397	-0.0492	-0.0599	-0.0723	-0.0869	-0.1043
∞	0.0000	-0.0076	-0.0152	-0.0230	-0.0311	-0.0397	-0.0493	-0.0600	-0.0724	-0.0870	-0.1043

TABLE 13.— PITCH MOMENT DERIVATIVE, $\bar{C}_{M_{\alpha_c}}$, $\gamma = 5$, $\theta_{q_1} = 0$

P \ μ	0.0000	0.1000	0.2000	0.3000	0.4000	0.5000	0.6000	0.7000	0.8000	0.9000	1.0000
1.00	0.0000	0.0000	-0.0000	-0.0000	-0.0000	-0.0000	0.0000	-0.0000	-0.0000	0.0000	-0.0000
1.02	0.0000	0.0005	0.0011	0.0017	0.0024	0.0032	0.0042	0.0054	0.0068	0.0083	0.0100
1.04	0.0000	0.0010	0.0022	0.0034	0.0048	0.0065	0.0085	0.0110	0.0140	0.0175	0.0215
1.08	0.0000	0.0020	0.0041	0.0064	0.0092	0.0126	0.0168	0.0222	0.0292	0.0381	0.0492
1.12	0.0000	0.0027	0.0056	0.0089	0.0128	0.0174	0.0234	0.0306	0.0393	0.0493	0.0597
1.16	0.0000	0.0032	0.0067	0.0106	0.0154	0.0211	0.0285	0.0377	0.0489	0.0620	0.0762
1.20	0.0000	0.0035	0.0073	0.0117	0.0169	0.0234	0.0317	0.0422	0.0553	0.0709	0.0885
1.24	0.0000	0.0036	0.0076	0.0121	0.0176	0.0244	0.0331	0.0443	0.0584	0.0755	0.0952
1.28	0.0000	0.0036	0.0075	0.0121	0.0176	0.0244	0.0333	0.0446	0.0590	0.0767	0.0974
1.34	0.0000	0.0034	0.0072	0.0115	0.0168	0.0235	0.0320	0.0429	0.0569	0.0743	0.0950
1.40	0.0000	0.0032	0.0067	0.0107	0.0156	0.0218	0.0298	0.0400	0.0530	0.0694	0.0891
1.50	0.0000	0.0027	0.0057	0.0092	0.0135	0.0188	0.0256	0.0344	0.0457	0.0600	0.0775
1.60	0.0000	0.0023	0.0049	0.0079	0.0115	0.0160	0.0218	0.0293	0.0389	0.0513	0.0665
1.70	0.0000	0.0020	0.0042	0.0067	0.0098	0.0136	0.0185	0.0249	0.0331	0.0438	0.0573
1.80	0.0000	0.0017	0.0036	0.0058	0.0084	0.0116	0.0158	0.0212	0.0283	0.0377	0.0496
1.90	0.0000	0.0015	0.0031	0.0050	0.0073	0.0101	0.0137	0.0183	0.0244	0.0326	0.0433
2.00	0.0000	0.0013	0.0028	0.0045	0.0065	0.0090	0.0122	0.0163	0.0217	0.0289	0.0385
2.10	0.0000	0.0011	0.0025	0.0040	0.0059	0.0083	0.0113	0.0151	0.0200	0.0264	0.0349
2.20	0.0000	0.0010	0.0022	0.0037	0.0055	0.0077	0.0106	0.0142	0.0187	0.0245	0.0320
2.60	0.0000	0.0007	0.0015	0.0025	0.0038	0.0055	0.0077	0.0105	0.0140	0.0183	0.0236
3.00	0.0000	0.0005	0.0011	0.0018	0.0028	0.0041	0.0058	0.0080	0.0108	0.0141	0.0180
5.00	0.0000	0.0001	0.0003	0.0006	0.0009	0.0013	0.0018	0.0025	0.0033	0.0043	0.0054
∞	0.0000	0.0000	0.0000	0.0000	0.0000	0.0000	0.0000	0.0000	0.0000	0.0000	0.0000

TABLE 14.— THRUST DERIVATIVE, $\bar{C}_{T_{\theta_o}}$, $\gamma = 5$, $P = 1.15$

θ_{q_1} \ μ	0.0000	0.1000	0.2000	0.3000	0.4000	0.5000	0.6000	0.7000	0.8000	0.9000	1.0000
0.80	0.1890	0.1933	0.2057	0.2265	0.2565	0.2984	0.3576	0.4436	0.5699	0.7555	1.0101
0.70	0.1835	0.1878	0.2005	0.2218	0.2527	0.2960	0.3574	0.4465	0.5772	0.7691	1.0318
0.60	0.1782	0.1825	0.1952	0.2166	0.2476	0.2911	0.3528	0.4419	0.5716	0.7604	1.0167
0.50	0.1732	0.1775	0.1900	0.2110	0.2415	0.2841	0.3443	0.4305	0.5546	0.7327	0.9712
0.40	0.1685	0.1726	0.1848	0.2051	0.2345	0.2755	0.3328	0.4140	0.5290	0.6912	0.9050
0.30	0.1641	0.1680	0.1796	0.1990	0.2269	0.2656	0.3192	0.3938	0.4979	0.6417	0.8282
0.20	0.1599	0.1636	0.1746	0.1928	0.2190	0.2549	0.3041	0.3715	0.4639	0.5889	0.7488
0.10	0.1559	0.1594	0.1696	0.1866	0.2109	0.2439	0.2884	0.3484	0.4292	0.5366	0.6721
0.00	0.1521	0.1553	0.1649	0.1806	0.2028	0.2327	0.2726	0.3254	0.3954	0.4869	0.6012
-0.10	0.1484	0.1514	0.1602	0.1746	0.1949	0.2218	0.2571	0.3033	0.3635	0.4410	0.5374
-0.20	0.1450	0.1477	0.1558	0.1689	0.1871	0.2112	0.2423	0.2823	0.3339	0.3994	0.4807
-0.30	0.1417	0.1442	0.1515	0.1634	0.1797	0.2010	0.2282	0.2628	0.3068	0.3623	0.4309
-0.40	0.1385	0.1408	0.1474	0.1581	0.1726	0.1914	0.2151	0.2448	0.2823	0.3292	0.3874
-0.50	0.1355	0.1376	0.1435	0.1530	0.1659	0.1824	0.2029	0.2284	0.2603	0.3000	0.3494
-0.60	0.1326	0.1345	0.1398	0.1483	0.1596	0.1740	0.1917	0.2134	0.2405	0.2742	0.3162
-0.70	0.1298	0.1315	0.1363	0.1437	0.1537	0.1661	0.1813	0.1998	0.2228	0.2514	0.2873
-0.80	0.1272	0.1287	0.1329	0.1394	0.1481	0.1589	0.1718	0.1875	0.2070	0.2313	0.2619
-0.90	0.1246	0.1259	0.1297	0.1354	0.1429	0.1521	0.1631	0.1764	0.1928	0.2134	0.2397
-1.00	0.1222	0.1233	0.1266	0.1316	0.1380	0.1459	0.1551	0.1663	0.1801	0.1976	0.2201
-1.10	0.1198	0.1208	0.1237	0.1280	0.1334	0.1401	0.1478	0.1571	0.1688	0.1835	0.2028
-1.40	0.1133	0.1139	0.1157	0.1183	0.1215	0.1251	0.1293	0.1344	0.1410	0.1498	0.1619
-3.00	0.0877	0.0875	0.0869	0.0857	0.0840	0.0819	0.0795	0.0774	0.0758	0.0754	0.0766
-∞	0.0000	0.0000	0.0000	0.0000	0.0000	0.0000	0.0000	0.0000	0.0000	0.0000	0.0000

TABLE 15.— ROLL MOMENT DERIVATIVE, $\overline{C}_{L_{\theta_o}}$, $\gamma = 5$, $P = 1.15$

θ_{q_1} \ μ	0.0000	0.1000	0.2000	0.3000	0.4000	0.5000	0.6000	0.7000	0.8000	0.9000	1.0000
0.80	-0.0000	0.0009	0.0019	0.0031	0.0046	0.0063	0.0094	0.0129	0.0178	0.0264	0.0398
0.70	-0.0000	0.0003	0.0007	0.0012	0.0020	0.0029	0.0049	0.0074	0.0109	0.0179	0.0298
0.60	-0.0000	-0.0002	-0.0004	-0.0004	-0.0003	-0.0002	0.0007	0.0020	0.0042	0.0094	0.0193
0.50	-0.0000	-0.0007	-0.0014	-0.0020	-0.0025	-0.0031	-0.0030	-0.0028	-0.0019	0.0016	0.0094
0.40	-0.0000	-0.0011	-0.0023	-0.0034	-0.0045	-0.0057	-0.0063	-0.0071	-0.0073	-0.0051	0.0008
0.30	-0.0000	-0.0015	-0.0031	-0.0046	-0.0062	-0.0079	-0.0092	-0.0106	-0.0117	-0.0106	-0.0061
0.20	-0.0000	-0.0019	-0.0037	-0.0057	-0.0076	-0.0097	-0.0115	-0.0135	-0.0151	-0.0149	-0.0115
0.10	-0.0000	-0.0021	-0.0043	-0.0065	-0.0087	-0.0112	-0.0133	-0.0157	-0.0177	-0.0180	-0.0155
0.00	-0.0000	-0.0024	-0.0048	-0.0072	-0.0097	-0.0123	-0.0147	-0.0173	-0.0195	-0.0202	-0.0183
-0.10	-0.0000	-0.0025	-0.0051	-0.0077	-0.0104	-0.0132	-0.0158	-0.0184	-0.0207	-0.0216	-0.0202
-0.20	-0.0000	-0.0027	-0.0054	-0.0081	-0.0109	-0.0138	-0.0164	-0.0192	-0.0215	-0.0224	-0.0213
-0.30	-0.0000	-0.0028	-0.0056	-0.0084	-0.0113	-0.0142	-0.0169	-0.0196	-0.0218	-0.0228	-0.0220
-0.40	-0.0000	-0.0029	-0.0058	-0.0086	-0.0115	-0.0144	-0.0171	-0.0197	-0.0219	-0.0229	-0.0223
-0.50	-0.0000	-0.0029	-0.0058	-0.0088	-0.0116	-0.0145	-0.0171	-0.0197	-0.0218	-0.0228	-0.0223
-0.60	-0.0000	-0.0029	-0.0059	-0.0088	-0.0116	-0.0145	-0.0170	-0.0195	-0.0215	-0.0224	-0.0221
-0.70	-0.0000	-0.0029	-0.0059	-0.0088	-0.0116	-0.0144	-0.0168	-0.0192	-0.0211	-0.0220	-0.0218
-0.80	-0.0000	-0.0029	-0.0059	-0.0087	-0.0115	-0.0142	-0.0166	-0.0188	-0.0206	-0.0215	-0.0214
-0.90	-0.0000	-0.0029	-0.0058	-0.0086	-0.0113	-0.0140	-0.0163	-0.0184	-0.0200	-0.0209	-0.0209
-1.00	-0.0000	-0.0029	-0.0057	-0.0085	-0.0112	-0.0137	-0.0159	-0.0179	-0.0195	-0.0203	-0.0203
-1.10	-0.0000	-0.0028	-0.0057	-0.0084	-0.0109	-0.0134	-0.0155	-0.0174	-0.0189	-0.0197	-0.0198
-1.40	-0.0000	-0.0027	-0.0053	-0.0079	-0.0102	-0.0124	-0.0143	-0.0159	-0.0171	-0.0179	-0.0180
-3.00	-0.0000	-0.0018	-0.0035	-0.0051	-0.0065	-0.0076	-0.0085	-0.0093	-0.0098	-0.0100	-0.0101
$-\infty$	0.0000	0.0000	0.0000	0.0000	0.0000	0.0000	0.0000	0.0000	0.0000	0.0000	0.0000

TABLE 16.— PITCH MOMENT DERIVATIVE, $\bar{C}_{M_{\theta_o}}$, $\gamma = 5$, $P = 1.15$

θ_{q_1} \ μ	0.0000	0.1000	0.2000	0.3000	0.4000	0.5000	0.6000	0.7000	0.8000	0.9000	1.0000
0.80	0.0000	0.0108	0.0223	0.0352	0.0506	0.0695	0.0935	0.1249	0.1657	0.2165	0.2746
0.70	0.0000	0.0104	0.0216	0.0342	0.0492	0.0677	0.0914	0.1224	0.1626	0.2126	0.2695
0.60	0.0000	0.0101	0.0208	0.0330	0.0474	0.0653	0.0882	0.1179	0.1562	0.2032	0.2559
0.50	0.0000	0.0097	0.0200	0.0316	0.0454	0.0624	0.0840	0.1118	0.1471	0.1897	0.2362
0.40	0.0000	0.0092	0.0191	0.0301	0.0431	0.0591	0.0792	0.1047	0.1364	0.1737	0.2133
0.30	0.0000	0.0088	0.0181	0.0285	0.0408	0.0556	0.0740	0.0969	0.1249	0.1568	0.1896
0.20	0.0000	0.0083	0.0171	0.0269	0.0383	0.0519	0.0687	0.0891	0.1133	0.1401	0.1669
0.10	0.0000	0.0078	0.0161	0.0253	0.0359	0.0483	0.0634	0.0813	0.1021	0.1244	0.1461
0.00	0.0000	0.0074	0.0152	0.0237	0.0335	0.0448	0.0583	0.0740	0.0917	0.1102	0.1277
-0.10	0.0000	0.0070	0.0143	0.0222	0.0312	0.0414	0.0534	0.0671	0.0823	0.0976	0.1118
-0.20	0.0000	0.0065	0.0134	0.0207	0.0290	0.0383	0.0489	0.0609	0.0738	0.0865	0.0980
-0.30	0.0000	0.0061	0.0125	0.0193	0.0269	0.0353	0.0448	0.0552	0.0662	0.0768	0.0863
-0.40	0.0000	0.0057	0.0117	0.0180	0.0249	0.0326	0.0410	0.0501	0.0595	0.0684	0.0762
-0.50	0.0000	0.0054	0.0109	0.0168	0.0231	0.0300	0.0376	0.0455	0.0536	0.0612	0.0677
-0.60	0.0000	0.0050	0.0102	0.0157	0.0215	0.0277	0.0345	0.0415	0.0485	0.0549	0.0604
-0.70	0.0000	0.0047	0.0096	0.0146	0.0199	0.0256	0.0317	0.0378	0.0439	0.0494	0.0541
-0.80	0.0000	0.0044	0.0089	0.0136	0.0185	0.0237	0.0291	0.0346	0.0400	0.0447	0.0487
-0.90	0.0000	0.0041	0.0084	0.0127	0.0172	0.0220	0.0268	0.0317	0.0364	0.0406	0.0440
-1.00	0.0000	0.0039	0.0078	0.0119	0.0161	0.0204	0.0248	0.0292	0.0333	0.0370	0.0400
-1.10	0.0000	0.0036	0.0073	0.0111	0.0150	0.0189	0.0229	0.0269	0.0306	0.0338	0.0364
-1.40	0.0000	0.0030	0.0061	0.0091	0.0122	0.0153	0.0184	0.0214	0.0241	0.0264	0.0283
-3.00	0.0000	0.0013	0.0026	0.0039	0.0052	0.0064	0.0076	0.0088	0.0099	0.0110	0.0119
-∞	0.0000	0.0000	0.0000	0.0000	0.0000	0.0000	0.0000	0.0000	0.0000	0.0000	0.0000

TABLE 17.— THRUST DERIVATIVE, $\bar{C}_{T_{\theta_s}}$, $\gamma = 5$, $P = 1.15$

θ_{q_1} \ μ	0.0000	0.1000	0.2000	0.3000	0.4000	0.5000	0.6000	0.7000	0.8000	0.9000	1.0000
0.80	-0.0000	0.0346	0.0703	0.1081	0.1502	0.1994	0.2609	0.3430	0.4561	0.6149	0.8246
0.70	-0.0000	0.0341	0.0693	0.1071	0.1493	0.1992	0.2624	0.3469	0.4638	0.6281	0.8453
0.60	-0.0000	0.0334	0.0680	0.1052	0.1471	0.1969	0.2600	0.3446	0.4611	0.6238	0.8375
0.50	-0.0000	0.0325	0.0662	0.1026	0.1436	0.1925	0.2544	0.3367	0.4491	0.6042	0.8056
0.40	-0.0000	0.0315	0.0642	0.0994	0.1392	0.1864	0.2459	0.3243	0.4300	0.5734	0.7570
0.30	-0.0000	0.0304	0.0619	0.0958	0.1340	0.1791	0.2355	0.3087	0.4061	0.5357	0.6994
0.20	-0.0000	0.0292	0.0594	0.0918	0.1283	0.1710	0.2237	0.2913	0.3796	0.4950	0.6390
0.10	-0.0000	0.0279	0.0568	0.0877	0.1222	0.1623	0.2112	0.2729	0.3523	0.4542	0.5801
0.00	-0.0000	0.0266	0.0541	0.0835	0.1160	0.1534	0.1985	0.2545	0.3254	0.4151	0.5252
-0.10	-0.0000	0.0254	0.0515	0.0792	0.1097	0.1446	0.1859	0.2366	0.2998	0.3788	0.4752
-0.20	-0.0000	0.0241	0.0489	0.0750	0.1036	0.1359	0.1738	0.2195	0.2759	0.3456	0.4306
-0.30	-0.0000	0.0229	0.0463	0.0709	0.0976	0.1276	0.1622	0.2035	0.2539	0.3157	0.3910
-0.40	-0.0000	0.0217	0.0438	0.0670	0.0919	0.1197	0.1513	0.1887	0.2339	0.2890	0.3562
-0.50	-0.0000	0.0205	0.0414	0.0632	0.0865	0.1122	0.1412	0.1751	0.2158	0.2661	0.3255
-0.60	-0.0000	0.0194	0.0392	0.0597	0.0814	0.1052	0.1318	0.1626	0.1994	0.2439	0.2984
-0.70	-0.0000	0.0184	0.0370	0.0563	0.0766	0.0986	0.1231	0.1512	0.1846	0.2250	0.2746
-0.80	-0.0000	0.0174	0.0350	0.0531	0.0721	0.0926	0.1151	0.1408	0.1713	0.2081	0.2534
-0.90	-0.0000	0.0164	0.0331	0.0501	0.0679	0.0869	0.1077	0.1314	0.1593	0.1930	0.2347
-1.00	-0.0000	0.0155	0.0313	0.0473	0.0640	0.0817	0.1010	0.1228	0.1485	0.1795	0.2179
-1.10	-0.0000	0.0147	0.0296	0.0447	0.0603	0.0769	0.0948	0.1150	0.1387	0.1673	0.2030
-1.40	-0.0000	0.0125	0.0251	0.0379	0.0509	0.0645	0.0790	0.0953	0.1144	0.1375	0.1664
-3.00	-0.0000	0.0060	0.0119	0.0178	0.0237	0.0297	0.0359	0.0428	0.0509	0.0604	0.0720
-∞	0.0000	0.0000	0.0000	0.0000	0.0000	0.0000	0.0000	0.0000	0.0000	0.0000	0.0000

TABLE 18.— ROLL MOMENT DERIVATIVE, $\overline{C}_{L_{\theta_s}}$, $\gamma = 5$, $P = 1.15$

θ_{q_1} \ μ	0.0000	0.1000	0.2000	0.3000	0.4000	0.5000	0.6000	0.7000	0.8000	0.9000	1.0000
0.80	-0.0040	-0.0038	-0.0031	-0.0020	-0.0003	0.0016	0.0049	0.0088	0.0140	0.0222	0.0343
0.70	-0.0057	-0.0055	-0.0050	-0.0041	-0.0029	-0.0013	0.0011	0.0042	0.0084	0.0156	0.0266
0.60	-0.0072	-0.0071	-0.0067	-0.0062	-0.0053	-0.0042	-0.0023	-0.0001	0.0030	0.0088	0.0184
0.50	-0.0087	-0.0086	-0.0084	-0.0080	-0.0075	-0.0069	-0.0057	-0.0042	-0.0020	0.0025	0.0107
0.40	-0.0100	-0.0099	-0.0098	-0.0097	-0.0095	-0.0093	-0.0086	-0.0078	-0.0064	-0.0029	0.0038
0.30	-0.0111	-0.0111	-0.0111	-0.0112	-0.0112	-0.0114	-0.0111	-0.0109	-0.0101	-0.0074	-0.0017
0.20	-0.0121	-0.0122	-0.0123	-0.0125	-0.0127	-0.0131	-0.0132	-0.0134	-0.0131	-0.0110	-0.0062
0.10	-0.0130	-0.0131	-0.0132	-0.0135	-0.0139	-0.0145	-0.0149	-0.0153	-0.0153	-0.0137	-0.0095
0.00	-0.0137	-0.0138	-0.0140	-0.0144	-0.0149	-0.0157	-0.0162	-0.0168	-0.0170	-0.0156	-0.0120
-0.10	-0.0143	-0.0144	-0.0147	-0.0151	-0.0157	-0.0165	-0.0172	-0.0179	-0.0181	-0.0170	-0.0137
-0.20	-0.0148	-0.0149	-0.0152	-0.0157	-0.0163	-0.0172	-0.0179	-0.0186	-0.0189	-0.0178	-0.0149
-0.30	-0.0152	-0.0153	-0.0156	-0.0161	-0.0168	-0.0176	-0.0184	-0.0191	-0.0193	-0.0184	-0.0156
-0.40	-0.0155	-0.0156	-0.0159	-0.0164	-0.0171	-0.0179	-0.0186	-0.0193	-0.0195	-0.0186	-0.0161
-0.50	-0.0157	-0.0158	-0.0161	-0.0166	-0.0172	-0.0181	-0.0188	-0.0194	-0.0196	-0.0187	-0.0163
-0.60	-0.0158	-0.0159	-0.0162	-0.0167	-0.0173	-0.0181	-0.0188	-0.0194	-0.0195	-0.0186	-0.0164
-0.70	-0.0158	-0.0159	-0.0162	-0.0167	-0.0173	-0.0181	-0.0187	-0.0192	-0.0193	-0.0184	-0.0164
-0.80	-0.0158	-0.0159	-0.0162	-0.0167	-0.0173	-0.0180	-0.0185	-0.0190	-0.0190	-0.0182	-0.0163
-0.90	-0.0158	-0.0159	-0.0161	-0.0166	-0.0172	-0.0178	-0.0183	-0.0187	-0.0187	-0.0179	-0.0161
-1.00	-0.0157	-0.0158	-0.0160	-0.0165	-0.0170	-0.0176	-0.0181	-0.0184	-0.0184	-0.0176	-0.0159
-1.10	-0.0156	-0.0156	-0.0159	-0.0163	-0.0168	-0.0174	-0.0178	-0.0181	-0.0180	-0.0173	-0.0156
-1.40	-0.0151	-0.0151	-0.0153	-0.0157	-0.0161	-0.0166	-0.0169	-0.0171	-0.0169	-0.0162	-0.0148
-3.00	-0.0116	-0.0116	-0.0117	-0.0119	-0.0121	-0.0123	-0.0124	-0.0124	-0.0123	-0.0120	-0.0115
$-\infty$	0.0000	0.0000	0.0000	0.0000	0.0000	0.0000	0.0000	0.0000	0.0000	0.0000	0.0000

TABLE 19.— PITCH MOMENT DERIVATIVE, $\bar{C}_{M_{\theta_s}}$, $\gamma = 5$, $P = 1.15$

θ_{q_1} \ μ	0.0000	0.1000	0.2000	0.3000	0.4000	0.5000	0.6000	0.7000	0.8000	0.9000	1.0000
0.80	0.0306	0.0317	0.0350	0.0408	0.0496	0.0619	0.0789	0.1018	0.1320	0.1696	0.2115
0.70	0.0301	0.0311	0.0344	0.0400	0.0486	0.0607	0.0775	0.1002	0.1301	0.1673	0.2087
0.60	0.0294	0.0304	0.0335	0.0390	0.0473	0.0589	0.0751	0.0969	0.1255	0.1607	0.1992
0.50	0.0286	0.0296	0.0325	0.0377	0.0455	0.0566	0.0719	0.0924	0.1188	0.1507	0.1849
0.40	0.0277	0.0286	0.0314	0.0362	0.0436	0.0539	0.0681	0.0868	0.1106	0.1386	0.1678
0.30	0.0266	0.0275	0.0301	0.0346	0.0415	0.0509	0.0639	0.0807	0.1016	0.1256	0.1499
0.20	0.0256	0.0263	0.0288	0.0329	0.0392	0.0478	0.0596	0.0745	0.0926	0.1127	0.1325
0.10	0.0244	0.0252	0.0274	0.0312	0.0369	0.0447	0.0552	0.0682	0.0837	0.1005	0.1165
0.00	0.0233	0.0239	0.0260	0.0295	0.0347	0.0417	0.0509	0.0623	0.0755	0.0894	0.1023
-0.10	0.0221	0.0227	0.0246	0.0278	0.0325	0.0387	0.0469	0.0567	0.0679	0.0794	0.0898
-0.20	0.0210	0.0216	0.0232	0.0261	0.0303	0.0359	0.0431	0.0516	0.0611	0.0706	0.0791
-0.30	0.0199	0.0204	0.0219	0.0245	0.0283	0.0332	0.0396	0.0469	0.0549	0.0629	0.0698
-0.40	0.0188	0.0193	0.0207	0.0230	0.0264	0.0308	0.0363	0.0427	0.0495	0.0562	0.0619
-0.50	0.0178	0.0182	0.0194	0.0215	0.0246	0.0285	0.0334	0.0389	0.0447	0.0503	0.0550
-0.60	0.0168	0.0172	0.0183	0.0202	0.0229	0.0264	0.0307	0.0355	0.0405	0.0452	0.0492
-0.70	0.0159	0.0162	0.0172	0.0189	0.0214	0.0244	0.0283	0.0324	0.0368	0.0408	0.0441
-0.80	0.0150	0.0153	0.0162	0.0177	0.0199	0.0227	0.0260	0.0297	0.0335	0.0369	0.0397
-0.90	0.0141	0.0144	0.0152	0.0166	0.0186	0.0211	0.0240	0.0273	0.0305	0.0335	0.0359
-1.00	0.0133	0.0136	0.0143	0.0156	0.0174	0.0196	0.0222	0.0251	0.0279	0.0305	0.0326
-1.10	0.0126	0.0128	0.0135	0.0147	0.0163	0.0182	0.0206	0.0231	0.0256	0.0279	0.0297
-1.40	0.0106	0.0108	0.0113	0.0122	0.0134	0.0148	0.0166	0.0184	0.0201	0.0216	0.0228
-3.00	0.0048	0.0049	0.0050	0.0053	0.0056	0.0059	0.0064	0.0069	0.0072	0.0074	0.0074
$-\infty$	0.0000	0.0000	0.0000	0.0000	0.0000	0.0000	0.0000	0.0000	0.0000	0.0000	0.0000

TABLE 20.— THRUST DERIVATIVE, $\bar{C}_{T_{\theta_c}}$, $\gamma = 5$, $P = 1.15$

θ_{q_1} \ μ	0.0000	0.1000	0.2000	0.3000	0.4000	0.5000	0.6000	0.7000	0.8000	0.9000	1.0000
0.80	0.0000	0.0123	0.0249	0.0380	0.0520	0.0675	0.0862	0.1097	0.1412	0.1854	0.2447
0.70	0.0000	0.0100	0.0203	0.0311	0.0427	0.0556	0.0712	0.0909	0.1173	0.1546	0.2051
0.60	0.0000	0.0078	0.0160	0.0245	0.0336	0.0438	0.0560	0.0713	0.0918	0.1206	0.1600
0.50	0.0000	0.0058	0.0119	0.0182	0.0250	0.0325	0.0413	0.0521	0.0665	0.0865	0.1140
0.40	0.0000	0.0040	0.0081	0.0125	0.0171	0.0220	0.0275	0.0341	0.0427	0.0545	0.0712
0.30	0.0000	0.0023	0.0047	0.0073	0.0098	0.0124	0.0150	0.0179	0.0214	0.0263	0.0338
0.20	0.0000	0.0008	0.0017	0.0026	0.0033	0.0039	0.0040	0.0037	0.0031	0.0025	0.0027
0.10	0.0000	-0.0004	-0.0009	-0.0014	-0.0022	-0.0034	-0.0054	-0.0083	-0.0121	-0.0170	-0.0221
0.00	0.0000	-0.0016	-0.0032	-0.0050	-0.0071	-0.0098	-0.0134	-0.0182	-0.0245	-0.0325	-0.0417
-0.10	0.0000	-0.0025	-0.0052	-0.0080	-0.0112	-0.0151	-0.0200	-0.0264	-0.0344	-0.0446	-0.0568
-0.20	0.0000	-0.0034	-0.0069	-0.0106	-0.0147	-0.0195	-0.0254	-0.0329	-0.0422	-0.0540	-0.0683
-0.30	0.0000	-0.0041	-0.0083	-0.0127	-0.0176	-0.0231	-0.0298	-0.0380	-0.0481	-0.0610	-0.0769
-0.40	0.0000	-0.0047	-0.0095	-0.0145	-0.0199	-0.0260	-0.0332	-0.0419	-0.0527	-0.0663	-0.0833
-0.50	0.0000	-0.0052	-0.0104	-0.0159	-0.0217	-0.0283	-0.0359	-0.0449	-0.0561	-0.0702	-0.0880
-0.60	0.0000	-0.0056	-0.0112	-0.0170	-0.0232	-0.0300	-0.0379	-0.0472	-0.0585	-0.0729	-0.0914
-0.70	0.0000	-0.0059	-0.0118	-0.0179	-0.0243	-0.0314	-0.0394	-0.0488	-0.0602	-0.0748	-0.0937
-0.80	0.0000	-0.0061	-0.0123	-0.0186	-0.0252	-0.0323	-0.0404	-0.0498	-0.0613	-0.0761	-0.0953
-0.90	0.0000	-0.0063	-0.0126	-0.0191	-0.0258	-0.0330	-0.0411	-0.0505	-0.0620	-0.0768	-0.0963
-1.00	0.0000	-0.0064	-0.0129	-0.0194	-0.0262	-0.0334	-0.0415	-0.0508	-0.0623	-0.0771	-0.0968
-1.10	0.0000	-0.0065	-0.0130	-0.0196	-0.0264	-0.0337	-0.0417	-0.0509	-0.0623	-0.0771	-0.0970
-1.40	0.0000	-0.0065	-0.0131	-0.0197	-0.0264	-0.0334	-0.0412	-0.0502	-0.0612	-0.0760	-0.0961
-3.00	0.0000	-0.0051	-0.0101	-0.0151	-0.0203	-0.0257	-0.0318	-0.0391	-0.0488	-0.0624	-0.0820
$-\infty$	0.0000	0.0000	0.0000	0.0000	0.0000	0.0000	0.0000	0.0000	0.0000	0.0000	0.0000

TABLE 21.— ROLL MOMENT DERIVATIVE, $\bar{C}_{L_{\theta_c}}$, $\gamma = 5$, $P = 1.15$

θ_{a_1} \ μ	0.0000	0.1000	0.2000	0.3000	0.4000	0.5000	0.6000	0.7000	0.8000	0.9000	1.0000
0.80	-0.0306	-0.0305	-0.0302	-0.0296	-0.0290	-0.0280	-0.0269	-0.0255	-0.0237	-0.0212	-0.0177
0.70	-0.0301	-0.0300	-0.0298	-0.0294	-0.0289	-0.0282	-0.0275	-0.0265	-0.0252	-0.0235	-0.0208
0.60	-0.0294	-0.0294	-0.0292	-0.0289	-0.0286	-0.0281	-0.0276	-0.0270	-0.0261	-0.0250	-0.0232
0.50	-0.0286	-0.0286	-0.0284	-0.0282	-0.0280	-0.0277	-0.0274	-0.0270	-0.0264	-0.0258	-0.0247
0.40	-0.0277	-0.0276	-0.0276	-0.0274	-0.0272	-0.0270	-0.0268	-0.0265	-0.0262	-0.0259	-0.0254
0.30	-0.0267	-0.0266	-0.0266	-0.0264	-0.0263	-0.0260	-0.0259	-0.0258	-0.0255	-0.0255	-0.0254
0.20	-0.0256	-0.0255	-0.0255	-0.0254	-0.0252	-0.0250	-0.0249	-0.0248	-0.0246	-0.0247	-0.0249
0.10	-0.0244	-0.0244	-0.0243	-0.0242	-0.0241	-0.0238	-0.0238	-0.0236	-0.0235	-0.0237	-0.0242
0.00	-0.0233	-0.0233	-0.0232	-0.0231	-0.0229	-0.0226	-0.0225	-0.0224	-0.0223	-0.0226	-0.0232
-0.10	-0.0221	-0.0221	-0.0220	-0.0219	-0.0217	-0.0214	-0.0213	-0.0211	-0.0211	-0.0214	-0.0222
-0.20	-0.0210	-0.0210	-0.0209	-0.0207	-0.0205	-0.0202	-0.0201	-0.0199	-0.0198	-0.0203	-0.0212
-0.30	-0.0199	-0.0199	-0.0198	-0.0196	-0.0194	-0.0191	-0.0189	-0.0187	-0.0187	-0.0192	-0.0202
-0.40	-0.0188	-0.0188	-0.0187	-0.0185	-0.0183	-0.0179	-0.0178	-0.0176	-0.0176	-0.0181	-0.0192
-0.50	-0.0178	-0.0177	-0.0176	-0.0174	-0.0172	-0.0169	-0.0167	-0.0166	-0.0166	-0.0171	-0.0183
-0.60	-0.0168	-0.0167	-0.0166	-0.0164	-0.0162	-0.0159	-0.0157	-0.0156	-0.0156	-0.0162	-0.0175
-0.70	-0.0158	-0.0158	-0.0157	-0.0155	-0.0153	-0.0149	-0.0148	-0.0147	-0.0148	-0.0154	-0.0167
-0.80	-0.0150	-0.0149	-0.0148	-0.0146	-0.0144	-0.0141	-0.0139	-0.0138	-0.0139	-0.0146	-0.0160
-0.90	-0.0141	-0.0141	-0.0140	-0.0138	-0.0135	-0.0132	-0.0131	-0.0131	-0.0132	-0.0139	-0.0154
-1.00	-0.0133	-0.0133	-0.0132	-0.0130	-0.0128	-0.0125	-0.0124	-0.0123	-0.0125	-0.0133	-0.0147
-1.10	-0.0126	-0.0125	-0.0124	-0.0122	-0.0120	-0.0118	-0.0117	-0.0117	-0.0119	-0.0127	-0.0142
-1.40	-0.0106	-0.0106	-0.0105	-0.0103	-0.0101	-0.0099	-0.0099	-0.0100	-0.0103	-0.0112	-0.0127
-3.00	-0.0048	-0.0048	-0.0048	-0.0047	-0.0047	-0.0046	-0.0048	-0.0051	-0.0057	-0.0067	-0.0082
$-\infty$	0.0000	0.0000	0.0000	0.0000	0.0000	0.0000	0.0000	0.0000	0.0000	0.0000	0.0000

TABLE 22.– PITCH MOMENT DERIVATIVE, $\bar{C}_{M_{\theta_c}}$, $\gamma = 5$, $P = 1.15$

θ_{q_1} \ μ	0.0000	0.1000	0.2000	0.3000	0.4000	0.5000	0.6000	0.7000	0.8000	0.9000	1.0000
0.80	-0.0040	-0.0037	-0.0028	-0.0012	0.0011	0.0043	0.0090	0.0152	0.0234	0.0342	0.0470
0.70	-0.0057	-0.0054	-0.0047	-0.0035	-0.0017	0.0008	0.0045	0.0094	0.0160	0.0248	0.0353
0.60	-0.0072	-0.0071	-0.0065	-0.0057	-0.0043	-0.0025	0.0001	0.0038	0.0086	0.0152	0.0232
0.50	-0.0087	-0.0086	-0.0082	-0.0077	-0.0068	-0.0056	-0.0038	-0.0014	0.0017	0.0062	0.0118
0.40	-0.0100	-0.0099	-0.0097	-0.0095	-0.0090	-0.0084	-0.0075	-0.0062	-0.0044	-0.0017	0.0018
0.30	-0.0111	-0.0111	-0.0111	-0.0110	-0.0110	-0.0109	-0.0106	-0.0102	-0.0096	-0.0083	-0.0062
0.20	-0.0121	-0.0122	-0.0123	-0.0124	-0.0126	-0.0130	-0.0132	-0.0136	-0.0138	-0.0135	-0.0125
0.10	-0.0130	-0.0131	-0.0133	-0.0136	-0.0140	-0.0147	-0.0154	-0.0162	-0.0171	-0.0174	-0.0172
0.00	-0.0137	-0.0138	-0.0141	-0.0145	-0.0152	-0.0161	-0.0171	-0.0183	-0.0195	-0.0203	-0.0206
-0.10	-0.0143	-0.0144	-0.0148	-0.0153	-0.0161	-0.0172	-0.0184	-0.0198	-0.0213	-0.0224	-0.0229
-0.20	-0.0148	-0.0149	-0.0153	-0.0159	-0.0168	-0.0180	-0.0193	-0.0209	-0.0225	-0.0237	-0.0244
-0.30	-0.0152	-0.0153	-0.0157	-0.0164	-0.0173	-0.0186	-0.0200	-0.0216	-0.0233	-0.0245	-0.0253
-0.40	-0.0155	-0.0156	-0.0160	-0.0167	-0.0177	-0.0190	-0.0204	-0.0220	-0.0237	-0.0250	-0.0257
-0.50	-0.0157	-0.0158	-0.0162	-0.0169	-0.0179	-0.0192	-0.0207	-0.0223	-0.0239	-0.0251	-0.0259
-0.60	-0.0158	-0.0159	-0.0163	-0.0170	-0.0180	-0.0193	-0.0207	-0.0223	-0.0239	-0.0251	-0.0258
-0.70	-0.0158	-0.0160	-0.0164	-0.0171	-0.0181	-0.0193	-0.0207	-0.0222	-0.0238	-0.0249	-0.0256
-0.80	-0.0158	-0.0160	-0.0164	-0.0171	-0.0180	-0.0192	-0.0206	-0.0220	-0.0235	-0.0246	-0.0252
-0.90	-0.0158	-0.0159	-0.0163	-0.0170	-0.0179	-0.0191	-0.0204	-0.0218	-0.0232	-0.0242	-0.0248
-1.00	-0.0157	-0.0158	-0.0162	-0.0169	-0.0178	-0.0189	-0.0201	-0.0215	-0.0228	-0.0238	-0.0244
-1.10	-0.0156	-0.0157	-0.0161	-0.0167	-0.0176	-0.0187	-0.0199	-0.0211	-0.0224	-0.0233	-0.0239
-1.40	-0.0151	-0.0152	-0.0155	-0.0161	-0.0169	-0.0178	-0.0189	-0.0200	-0.0211	-0.0218	-0.0223
-3.00	-0.0116	-0.0117	-0.0119	-0.0122	-0.0127	-0.0132	-0.0138	-0.0144	-0.0151	-0.0155	-0.0157
$-\infty$	0.0000	0.0000	0.0000	0.0000	0.0000	0.0000	0.0000	0.0000	0.0000	0.0000	0.0000

TABLE 23.— THRUST DERIVATIVE, $\bar{C}_{T_{\alpha_c}}$, $\gamma = 5$, $P = 1.15$

θ_{q_1} \ μ	0.0000	0.1000	0.2000	0.3000	0.4000	0.5000	0.6000	0.7000	0.8000	0.9000	1.0000
0.80	0.0000	0.0034	0.0135	0.0297	0.0521	0.0813	0.1200	0.1731	0.2491	0.3618	0.5231
0.70	0.0000	0.0034	0.0134	0.0296	0.0520	0.0815	0.1209	0.1754	0.2535	0.3696	0.5357
0.60	0.0000	0.0034	0.0132	0.0292	0.0513	0.0806	0.1198	0.1740	0.2514	0.3656	0.5277
0.50	0.0000	0.0033	0.0129	0.0285	0.0501	0.0788	0.1169	0.1693	0.2435	0.3515	0.5025
0.40	0.0000	0.0032	0.0125	0.0276	0.0485	0.0761	0.1126	0.1621	0.2313	0.3300	0.4656
0.30	0.0000	0.0031	0.0121	0.0265	0.0465	0.0727	0.1071	0.1530	0.2160	0.3040	0.4225
0.20	0.0000	0.0029	0.0116	0.0254	0.0443	0.0690	0.1009	0.1429	0.1993	0.2761	0.3778
0.10	0.0000	0.0028	0.0110	0.0241	0.0420	0.0650	0.0943	0.1322	0.1821	0.2484	0.3345
0.00	0.0000	0.0027	0.0104	0.0228	0.0395	0.0608	0.0876	0.1215	0.1652	0.2219	0.2943
-0.10	0.0000	0.0025	0.0099	0.0215	0.0371	0.0567	0.0810	0.1111	0.1491	0.1974	0.2579
-0.20	0.0000	0.0024	0.0093	0.0202	0.0346	0.0527	0.0746	0.1013	0.1342	0.1751	0.2255
-0.30	0.0000	0.0023	0.0088	0.0189	0.0323	0.0488	0.0685	0.0921	0.1205	0.1551	0.1970
-0.40	0.0000	0.0021	0.0082	0.0177	0.0300	0.0451	0.0628	0.0836	0.1081	0.1372	0.1719
-0.50	0.0000	0.0020	0.0077	0.0165	0.0279	0.0416	0.0575	0.0757	0.0969	0.1213	0.1499
-0.60	0.0000	0.0019	0.0072	0.0154	0.0259	0.0384	0.0526	0.0686	0.0868	0.1073	0.1307
-0.70	0.0000	0.0018	0.0068	0.0143	0.0240	0.0354	0.0481	0.0621	0.0777	0.0948	0.1138
-0.80	0.0000	0.0016	0.0063	0.0133	0.0222	0.0326	0.0439	0.0562	0.0696	0.0837	0.0989
-0.90	0.0000	0.0015	0.0059	0.0124	0.0206	0.0300	0.0401	0.0509	0.0623	0.0739	0.0858
-1.00	0.0000	0.0014	0.0055	0.0116	0.0190	0.0276	0.0366	0.0461	0.0557	0.0651	0.0741
-1.10	0.0000	0.0014	0.0052	0.0108	0.0176	0.0254	0.0335	0.0417	0.0498	0.0573	0.0638
-1.40	0.0000	0.0011	0.0042	0.0087	0.0140	0.0198	0.0255	0.0308	0.0353	0.0383	0.0392
-3.00	0.0000	0.0005	0.0016	0.0030	0.0042	0.0050	0.0050	0.0037	0.0005	-0.0052	-0.0147
$-\infty$	0.0000	0.0000	0.0000	0.0000	0.0000	0.0000	0.0000	0.0000	0.0000	0.0000	0.0000

TABLE 24.— ROLL MOMENT DERIVATIVE, $\overline{C}_{L_{\alpha_c}}$, $\gamma = 5$, $P = 1.15$

θ_{q_1} \ μ	0.0000	0.1000	0.2000	0.3000	0.4000	0.5000	0.6000	0.7000	0.8000	0.9000	1.0000
0.80	0.0000	-0.0007	-0.0013	-0.0017	-0.0018	-0.0016	-0.0008	0.0003	0.0023	0.0064	0.0135
0.70	0.0000	-0.0009	-0.0018	-0.0025	-0.0029	-0.0031	-0.0028	-0.0022	-0.0010	0.0019	0.0079
0.60	0.0000	-0.0011	-0.0022	-0.0032	-0.0039	-0.0045	-0.0047	-0.0048	-0.0044	-0.0025	0.0020
0.50	0.0000	-0.0013	-0.0026	-0.0038	-0.0048	-0.0058	-0.0065	-0.0071	-0.0075	-0.0067	-0.0035
0.40	0.0000	-0.0015	-0.0030	-0.0044	-0.0056	-0.0069	-0.0080	-0.0092	-0.0103	-0.0103	-0.0084
0.30	0.0000	-0.0017	-0.0033	-0.0049	-0.0064	-0.0079	-0.0094	-0.0110	-0.0125	-0.0133	-0.0124
0.20	0.0000	-0.0018	-0.0036	-0.0053	-0.0070	-0.0088	-0.0105	-0.0124	-0.0143	-0.0156	-0.0155
0.10	0.0000	-0.0019	-0.0038	-0.0057	-0.0075	-0.0094	-0.0114	-0.0135	-0.0157	-0.0174	-0.0178
0.00	0.0000	-0.0020	-0.0040	-0.0060	-0.0079	-0.0100	-0.0120	-0.0143	-0.0167	-0.0186	-0.0195
-0.10	0.0000	-0.0021	-0.0042	-0.0062	-0.0083	-0.0104	-0.0125	-0.0149	-0.0173	-0.0194	-0.0206
-0.20	0.0000	-0.0022	-0.0043	-0.0064	-0.0085	-0.0107	-0.0129	-0.0153	-0.0177	-0.0199	-0.0213
-0.30	0.0000	-0.0022	-0.0044	-0.0066	-0.0087	-0.0109	-0.0131	-0.0155	-0.0180	-0.0202	-0.0218
-0.40	0.0000	-0.0022	-0.0045	-0.0067	-0.0088	-0.0110	-0.0132	-0.0156	-0.0180	-0.0203	-0.0220
-0.50	0.0000	-0.0023	-0.0045	-0.0067	-0.0089	-0.0111	-0.0133	-0.0156	-0.0180	-0.0202	-0.0220
-0.60	0.0000	-0.0023	-0.0045	-0.0068	-0.0089	-0.0111	-0.0133	-0.0156	-0.0179	-0.0201	-0.0220
-0.70	0.0000	-0.0023	-0.0046	-0.0068	-0.0089	-0.0111	-0.0132	-0.0154	-0.0177	-0.0199	-0.0218
-0.80	0.0000	-0.0023	-0.0045	-0.0067	-0.0089	-0.0110	-0.0131	-0.0153	-0.0175	-0.0197	-0.0216
-0.90	0.0000	-0.0023	-0.0045	-0.0067	-0.0088	-0.0109	-0.0129	-0.0151	-0.0173	-0.0194	-0.0214
-1.00	0.0000	-0.0023	-0.0045	-0.0067	-0.0087	-0.0108	-0.0128	-0.0149	-0.0170	-0.0191	-0.0211
-1.10	0.0000	-0.0022	-0.0045	-0.0066	-0.0086	-0.0106	-0.0126	-0.0146	-0.0167	-0.0188	-0.0209
-1.40	0.0000	-0.0022	-0.0043	-0.0064	-0.0083	-0.0102	-0.0120	-0.0139	-0.0159	-0.0179	-0.0200
-3.00	0.0000	-0.0017	-0.0034	-0.0049	-0.0064	-0.0078	-0.0092	-0.0106	-0.0121	-0.0138	-0.0156
$-\infty$	0.0000	0.0000	0.0000	0.0000	0.0000	0.0000	0.0000	0.0000	0.0000	0.0000	0.0000

TABLE 25.— PITCH MOMENT DERIVATIVE, $\bar{C}_{M_{\alpha_c}}$, $\gamma = 5$, $P = 1.15$

ϑ_{q_1} \ μ	0.0000	0.1000	0.2000	0.3000	0.4000	0.5000	0.6000	0.7000	0.8000	0.9000	1.0000
0.80	0.0000	0.0041	0.0087	0.0141	0.0210	0.0301	0.0424	0.0594	0.0827	0.1141	0.1534
0.70	0.0000	0.0040	0.0085	0.0139	0.0207	0.0295	0.0417	0.0584	0.0814	0.1124	0.1508
0.60	0.0000	0.0039	0.0083	0.0135	0.0201	0.0287	0.0404	0.0565	0.0784	0.1077	0.1435
0.50	0.0000	0.0038	0.0081	0.0131	0.0194	0.0276	0.0387	0.0538	0.0741	0.1007	0.1327
0.40	0.0000	0.0037	0.0078	0.0126	0.0186	0.0263	0.0366	0.0505	0.0689	0.0924	0.1200
0.30	0.0000	0.0036	0.0075	0.0120	0.0177	0.0248	0.0344	0.0469	0.0632	0.0836	0.1069
0.20	0.0000	0.0034	0.0072	0.0115	0.0167	0.0233	0.0320	0.0432	0.0575	0.0748	0.0942
0.10	0.0000	0.0033	0.0068	0.0109	0.0158	0.0218	0.0297	0.0396	0.0520	0.0666	0.0826
0.00	0.0000	0.0031	0.0065	0.0103	0.0148	0.0203	0.0274	0.0361	0.0468	0.0591	0.0723
-0.10	0.0000	0.0029	0.0061	0.0097	0.0139	0.0189	0.0252	0.0329	0.0420	0.0524	0.0633
-0.20	0.0000	0.0028	0.0058	0.0091	0.0130	0.0175	0.0232	0.0299	0.0377	0.0465	0.0556
-0.30	0.0000	0.0026	0.0055	0.0085	0.0121	0.0162	0.0213	0.0272	0.0339	0.0414	0.0490
-0.40	0.0000	0.0025	0.0051	0.0080	0.0113	0.0150	0.0195	0.0247	0.0306	0.0369	0.0434
-0.50	0.0000	0.0023	0.0048	0.0075	0.0105	0.0139	0.0179	0.0225	0.0276	0.0330	0.0385
-0.60	0.0000	0.0022	0.0045	0.0070	0.0098	0.0129	0.0165	0.0205	0.0250	0.0297	0.0344
-0.70	0.0000	0.0021	0.0043	0.0066	0.0092	0.0120	0.0152	0.0188	0.0227	0.0267	0.0309
-0.80	0.0000	0.0020	0.0040	0.0062	0.0085	0.0111	0.0140	0.0172	0.0206	0.0242	0.0278
-0.90	0.0000	0.0018	0.0038	0.0058	0.0080	0.0103	0.0130	0.0158	0.0188	0.0220	0.0252
-1.00	0.0000	0.0017	0.0036	0.0055	0.0075	0.0096	0.0120	0.0146	0.0172	0.0201	0.0229
-1.10	0.0000	0.0016	0.0034	0.0051	0.0070	0.0090	0.0111	0.0134	0.0158	0.0184	0.0209
-1.40	0.0000	0.0014	0.0028	0.0043	0.0058	0.0073	0.0090	0.0107	0.0125	0.0144	0.0163
-3.00	0.0000	0.0006	0.0012	0.0019	0.0025	0.0031	0.0038	0.0044	0.0051	0.0061	0.0073
$-\infty$	0.0000	0.0000	0.0000	0.0000	0.0000	0.0000	0.0000	0.0000	0.0000	0.0000	0.0000

TABLE 26.— THRUST DERIVATIVE, $\overline{C}_{T_{\theta_0}}$, $\gamma = 10$, $\theta_{q_1} = 0$

p \ μ	0.0000	0.1000	0.2000	0.3000	0.4000	0.5000	0.6000	0.7000	0.8000	0.9000	1.0000
1.00	0.1521	0.1540	0.1598	0.1694	0.1829	0.2007	0.2226	0.2479	0.2740	0.2954	0.3039
1.02	0.1521	0.1542	0.1606	0.1713	0.1866	0.2072	0.2323	0.2633	0.3003	0.3282	0.3390
1.04	0.1521	0.1545	0.1617	0.1736	0.1908	0.2141	0.2430	0.2794	0.3249	0.3654	0.3828
1.08	0.1521	0.1550	0.1637	0.1779	0.1981	0.2252	0.2595	0.3034	0.3578	0.4211	0.4819
1.12	0.1521	0.1553	0.1647	0.1801	0.2021	0.2316	0.2704	0.3207	0.3843	0.4620	0.5469
1.16	0.1521	0.1554	0.1654	0.1817	0.2047	0.2357	0.2768	0.3310	0.4013	0.4908	0.5973
1.20	0.1521	0.1555	0.1658	0.1825	0.2062	0.2378	0.2797	0.3353	0.4089	0.5050	0.6239
1.24	0.1521	0.1556	0.1659	0.1829	0.2067	0.2383	0.2799	0.3353	0.4091	0.5072	0.6317
1.28	0.1521	0.1556	0.1659	0.1828	0.2064	0.2375	0.2781	0.3319	0.4039	0.5006	0.6257
1.34	0.1521	0.1555	0.1657	0.1822	0.2051	0.2348	0.2731	0.3230	0.3898	0.4802	0.5997
1.40	0.1521	0.1555	0.1654	0.1813	0.2032	0.2313	0.2667	0.3122	0.3723	0.4539	0.5637
1.50	0.1521	0.1553	0.1646	0.1796	0.1998	0.2251	0.2561	0.2945	0.3440	0.4109	0.5027
1.60	0.1521	0.1551	0.1639	0.1780	0.1968	0.2200	0.2476	0.2808	0.3226	0.3776	0.4543
1.70	0.1521	0.1550	0.1634	0.1768	0.1946	0.2164	0.2420	0.2720	0.3085	0.3562	0.4222
1.80	0.1521	0.1549	0.1629	0.1758	0.1931	0.2141	0.2388	0.2675	0.3016	0.3450	0.4042
1.90	0.1521	0.1548	0.1626	0.1752	0.1921	0.2131	0.2377	0.2664	0.3000	0.3417	0.3971
2.00	0.1521	0.1547	0.1624	0.1748	0.1916	0.2127	0.2380	0.2670	0.3019	0.3435	0.3968
2.10	0.1521	0.1546	0.1622	0.1745	0.1913	0.2127	0.2386	0.2682	0.3050	0.3472	0.3992
2.20	0.1521	0.1546	0.1621	0.1742	0.1910	0.2126	0.2389	0.2703	0.3070	0.3497	0.4003
2.60	0.1521	0.1545	0.1616	0.1733	0.1893	0.2097	0.2345	0.2636	0.2970	0.3342	0.3746
3.00	0.1521	0.1545	0.1614	0.1727	0.1879	0.2070	0.2297	0.2557	0.2850	0.3172	0.3510
5.00	0.1521	0.1544	0.1612	0.1720	0.1865	0.2042	0.2247	0.2477	0.2728	0.2996	0.3270
∞	0.1521	0.1544	0.1612	0.1720	0.1863	0.2038	0.2241	0.2466	0.2710	0.2969	0.3238

TABLE 27.— ROLL MOMENT DERIVATIVE, $\bar{C}_{L_{\theta_o}}$, $\gamma = 10$, $\theta_{q_1} = 0$

p \ μ	0.0000	0.1000	0.2000	0.3000	0.4000	0.5000	0.6000	0.7000	0.8000	0.9000	1.0000
1.00	0.0000	-0.0000	-0.0000	-0.0000	-0.0000	-0.0000	-0.0000	-0.0000	-0.0000	-0.0000	-0.0000
1.02	-0.0000	0.0002	0.0004	0.0005	0.0006	0.0007	0.0006	0.0005	0.0003	-0.0004	-0.0018
1.04	-0.0000	0.0003	0.0007	0.0010	0.0012	0.0013	0.0012	0.0011	0.0008	-0.0001	-0.0023
1.08	-0.0000	0.0004	0.0008	0.0012	0.0015	0.0016	0.0020	0.0019	0.0014	0.0004	-0.0026
1.12	-0.0000	0.0004	0.0009	0.0013	0.0018	0.0020	0.0027	0.0029	0.0027	0.0028	0.0024
1.16	-0.0000	0.0003	0.0007	0.0011	0.0016	0.0019	0.0028	0.0036	0.0046	0.0072	0.0113
1.20	-0.0000	0.0000	0.0001	0.0002	0.0005	0.0007	0.0013	0.0023	0.0041	0.0084	0.0160
1.24	-0.0000	-0.0004	-0.0009	-0.0012	-0.0015	-0.0017	-0.0016	-0.0009	0.0009	0.0060	0.0159
1.28	-0.0000	-0.0011	-0.0023	-0.0033	-0.0043	-0.0053	-0.0059	-0.0061	-0.0048	0.0002	0.0112
1.34	-0.0000	-0.0024	-0.0047	-0.0071	-0.0094	-0.0119	-0.0143	-0.0163	-0.0167	-0.0131	-0.0020
1.40	-0.0000	-0.0037	-0.0075	-0.0113	-0.0152	-0.0193	-0.0236	-0.0278	-0.0306	-0.0293	-0.0199
1.50	-0.0000	-0.0059	-0.0120	-0.0181	-0.0246	-0.0315	-0.0390	-0.0467	-0.0536	-0.0569	-0.0520
1.60	-0.0000	-0.0079	-0.0159	-0.0241	-0.0326	-0.0419	-0.0519	-0.0626	-0.0729	-0.0803	-0.0804
1.70	-0.0000	-0.0094	-0.0190	-0.0288	-0.0390	-0.0500	-0.0619	-0.0746	-0.0875	-0.0983	-0.1028
1.80	-0.0000	-0.0107	-0.0215	-0.0324	-0.0439	-0.0560	-0.0691	-0.0833	-0.0979	-0.1112	-0.1197
1.90	-0.0000	-0.0116	-0.0233	-0.0352	-0.0474	-0.0603	-0.0742	-0.0891	-0.1048	-0.1201	-0.1320
2.00	-0.0000	-0.0123	-0.0247	-0.0372	-0.0500	-0.0634	-0.0776	-0.0928	-0.1091	-0.1257	-0.1405
2.10	-0.0000	-0.0129	-0.0258	-0.0388	-0.0520	-0.0655	-0.0798	-0.0951	-0.1115	-0.1288	-0.1460
2.20	-0.0000	-0.0133	-0.0266	-0.0400	-0.0534	-0.0672	-0.0814	-0.0965	-0.1128	-0.1303	-0.1491
2.60	-0.0000	-0.0143	-0.0285	-0.0428	-0.0571	-0.0714	-0.0858	-0.1007	-0.1164	-0.1336	-0.1534
3.00	-0.0000	-0.0147	-0.0294	-0.0441	-0.0589	-0.0739	-0.0891	-0.1048	-0.1213	-0.1391	-0.1590
5.00	0.0000	-0.0151	-0.0303	-0.0455	-0.0609	-0.0766	-0.0927	-0.1094	-0.1270	-0.1457	-0.1659
∞	0.0000	-0.0152	-0.0304	-0.0457	-0.0612	-0.0769	-0.0930	-0.1098	-0.1274	-0.1461	-0.1662

TABLE 28.— PITCH MOMENT DERIVATIVE, $\bar{C}_{M_{\theta_o}}$, $\gamma = 10$, $\theta_{q_1} = 0$

p \ μ	0.0000	0.1000	0.2000	0.3000	0.4000	0.5000	0.6000	0.7000	0.8000	0.9000	1.0000
1.00	-0.0000	0.0000	0.0000	0.0000	0.0000	0.0000	-0.0000	-0.0000	-0.0000	-0.0000	-0.0000
1.02	0.0000	0.0006	0.0012	0.0019	0.0027	0.0035	0.0045	0.0056	0.0069	0.0081	0.0091
1.04	0.0000	0.0012	0.0025	0.0039	0.0055	0.0073	0.0094	0.0118	0.0145	0.0174	0.0202
1.08	0.0000	0.0026	0.0054	0.0084	0.0118	0.0159	0.0203	0.0259	0.0334	0.0408	0.0480
1.12	0.0000	0.0039	0.0080	0.0125	0.0176	0.0238	0.0305	0.0389	0.0494	0.0589	0.0669
1.16	0.0000	0.0050	0.0104	0.0163	0.0230	0.0310	0.0404	0.0516	0.0646	0.0771	0.0878
1.20	0.0000	0.0062	0.0127	0.0200	0.0283	0.0383	0.0503	0.0646	0.0812	0.0980	0.1129
1.24	0.0000	0.0072	0.0149	0.0234	0.0332	0.0451	0.0594	0.0768	0.0971	0.1184	0.1379
1.28	0.0000	0.0081	0.0167	0.0263	0.0375	0.0509	0.0674	0.0875	0.1110	0.1365	0.1602
1.34	-0.0000	0.0091	0.0189	0.0297	0.0424	0.0577	0.0765	0.0996	0.1269	0.1571	0.1861
1.40	-0.0000	0.0098	0.0203	0.0319	0.0455	0.0619	0.0821	0.1068	0.1363	0.1694	0.2020
1.50	-0.0000	0.0103	0.0212	0.0333	0.0473	0.0642	0.0847	0.1099	0.1399	0.1744	0.2096
1.60	-0.0000	0.0101	0.0208	0.0326	0.0462	0.0623	0.0818	0.1055	0.1340	0.1670	0.2022
1.70	-0.0000	0.0096	0.0197	0.0308	0.0434	0.0583	0.0760	0.0976	0.1236	0.1541	0.1877
1.80	-0.0000	0.0089	0.0183	0.0285	0.0400	0.0534	0.0693	0.0885	0.1117	0.1394	0.1710
1.90	-0.0000	0.0082	0.0168	0.0262	0.0366	0.0486	0.0626	0.0795	0.1000	0.1251	0.1545
2.00	-0.0000	0.0075	0.0154	0.0239	0.0333	0.0440	0.0565	0.0714	0.0896	0.1119	0.1391
2.10	-0.0000	0.0069	0.0141	0.0219	0.0304	0.0401	0.0512	0.0644	0.0804	0.1005	0.1255
2.20	-0.0000	0.0063	0.0129	0.0200	0.0279	0.0367	0.0468	0.0587	0.0730	0.0910	0.1138
2.60	-0.0000	0.0045	0.0093	0.0145	0.0204	0.0271	0.0348	0.0439	0.0546	0.0675	0.0833
3.00	-0.0000	0.0034	0.0070	0.0109	0.0154	0.0207	0.0269	0.0344	0.0432	0.0535	0.0658
5.00	-0.0000	0.0011	0.0024	0.0038	0.0054	0.0072	0.0093	0.0118	0.0147	0.0180	0.0219
∞	-0.0000	-0.0000	-0.0000	0.0000	0.0000	0.0000	0.0000	0.0000	0.0000	0.0000	0.0000

TABLE 29.— THRUST DERIVATIVE, $\overline{C}_{T_{\theta_s}}$, $\gamma = 10$, $\theta_{q_1} = 0$

P \ μ	0.0000	0.1000	0.2000	0.3000	0.4000	0.5000	0.6000	0.7000	0.8000	0.9000	1.0000
1.00	-0.0000	0.0235	0.0475	0.0723	0.0986	0.1269	0.1574	0.1892	0.2207	0.2486	0.2678
1.02	-0.0000	0.0243	0.0491	0.0749	0.1026	0.1333	0.1662	0.2028	0.2428	0.2758	0.2985
1.04	-0.0000	0.0251	0.0507	0.0776	0.1068	0.1397	0.1758	0.2173	0.2651	0.3094	0.3467
1.08	-0.0000	0.0263	0.0534	0.0820	0.1135	0.1493	0.1905	0.2392	0.2967	0.3623	0.4277
1.12	-0.0000	0.0270	0.0548	0.0844	0.1171	0.1546	0.1994	0.2536	0.3195	0.3982	0.4848
1.16	-0.0000	0.0274	0.0556	0.0858	0.1192	0.1579	0.2044	0.2619	0.3337	0.4228	0.5283
1.20	-0.0000	0.0275	0.0559	0.0864	0.1202	0.1593	0.2065	0.2653	0.3399	0.4349	0.5513
1.24	-0.0000	0.0275	0.0559	0.0864	0.1203	0.1593	0.2063	0.2650	0.3401	0.4372	0.5588
1.28	-0.0000	0.0273	0.0557	0.0860	0.1197	0.1584	0.2046	0.2622	0.3360	0.4322	0.5548
1.34	-0.0000	0.0270	0.0551	0.0850	0.1181	0.1558	0.2002	0.2549	0.3248	0.4164	0.5351
1.40	-0.0000	0.0267	0.0543	0.0838	0.1161	0.1526	0.1950	0.2463	0.3111	0.3980	0.5073
1.50	-0.0000	0.0261	0.0530	0.0817	0.1128	0.1474	0.1867	0.2328	0.2896	0.3630	0.4602
1.60	-0.0000	0.0255	0.0519	0.0799	0.1102	0.1435	0.1805	0.2230	0.2738	0.3383	0.4236
1.70	-0.0000	0.0251	0.0511	0.0787	0.1085	0.1410	0.1769	0.2174	0.2647	0.3233	0.4001
1.80	-0.0000	0.0248	0.0505	0.0778	0.1074	0.1398	0.1755	0.2154	0.2612	0.3167	0.3879
1.90	-0.0000	0.0245	0.0500	0.0773	0.1070	0.1396	0.1757	0.2159	0.2617	0.3159	0.3830
2.00	-0.0000	0.0244	0.0497	0.0769	0.1067	0.1397	0.1764	0.2176	0.2642	0.3184	0.3844
2.10	-0.0000	0.0242	0.0494	0.0766	0.1064	0.1396	0.1769	0.2189	0.2665	0.3210	0.3854
2.20	-0.0000	0.0241	0.0492	0.0762	0.1058	0.1390	0.1764	0.2187	0.2666	0.3210	0.3837
2.60	-0.0000	0.0238	0.0484	0.0743	0.1024	0.1332	0.1674	0.2058	0.2487	0.2965	0.3492
3.00	-0.0000	0.0237	0.0479	0.0733	0.1002	0.1293	0.1611	0.1963	0.2354	0.2791	0.3278
5.00	-0.0000	0.0235	0.0475	0.0723	0.0982	0.1258	0.1552	0.1871	0.2219	0.2599	0.3018
∞	0.0000	0.0235	0.0475	0.0722	0.0980	0.1254	0.1546	0.1860	0.2201	0.2572	0.2977

TABLE 30.— ROLL MOMENT DERIVATIVE, $\bar{C}_{L_{\theta_s}}$, $\gamma = 10$, $\theta_{q_1} = 0$

p \ μ	0.0000	0.1000	0.2000	0.3000	0.4000	0.5000	0.6000	0.7000	0.8000	0.9000	1.0000
1.00	-0.0000	-0.0000	-0.0000	-0.0000	-0.0000	-0.0000	-0.0000	-0.0000	-0.0000	-0.0000	-0.0000
1.02	-0.0000	-0.0000	-0.0000	0.0000	0.0001	0.0002	0.0003	0.0003	0.0002	-0.0000	-0.0009
1.04	-0.0003	-0.0003	-0.0002	-0.0000	0.0001	0.0003	0.0005	0.0007	0.0007	0.0004	-0.0007
1.08	-0.0016	-0.0016	-0.0014	-0.0011	-0.0007	-0.0003	0.0004	0.0009	0.0013	0.0014	-0.0001
1.12	-0.0032	-0.0031	-0.0028	-0.0024	-0.0017	-0.0011	0.0000	0.0010	0.0019	0.0032	0.0042
1.16	-0.0052	-0.0050	-0.0047	-0.0041	-0.0032	-0.0023	-0.0008	0.0008	0.0029	0.0065	0.0115
1.20	-0.0076	-0.0075	-0.0071	-0.0064	-0.0055	-0.0045	-0.0029	-0.0008	0.0020	0.0072	0.0153
1.24	-0.0105	-0.0103	-0.0099	-0.0093	-0.0085	-0.0076	-0.0062	-0.0042	-0.0010	0.0049	0.0152
1.28	-0.0135	-0.0134	-0.0131	-0.0127	-0.0121	-0.0115	-0.0105	-0.0090	-0.0061	0.0000	0.0114
1.34	-0.0184	-0.0183	-0.0182	-0.0182	-0.0181	-0.0182	-0.0183	-0.0179	-0.0162	-0.0109	0.0006
1.40	-0.0231	-0.0232	-0.0233	-0.0237	-0.0244	-0.0254	-0.0266	-0.0278	-0.0277	-0.0242	-0.0138
1.50	-0.0302	-0.0304	-0.0311	-0.0322	-0.0340	-0.0365	-0.0398	-0.0434	-0.0464	-0.0465	-0.0396
1.60	-0.0360	-0.0364	-0.0374	-0.0392	-0.0419	-0.0457	-0.0506	-0.0562	-0.0618	-0.0652	-0.0624
1.70	-0.0405	-0.0409	-0.0423	-0.0446	-0.0480	-0.0526	-0.0586	-0.0657	-0.0732	-0.0792	-0.0803
1.80	-0.0439	-0.0444	-0.0459	-0.0485	-0.0524	-0.0575	-0.0642	-0.0722	-0.0810	-0.0891	-0.0935
1.90	-0.0464	-0.0469	-0.0486	-0.0514	-0.0555	-0.0609	-0.0679	-0.0763	-0.0860	-0.0955	-0.1030
2.00	-0.0483	-0.0488	-0.0506	-0.0535	-0.0577	-0.0633	-0.0703	-0.0788	-0.0887	-0.0993	-0.1092
2.10	-0.0497	-0.0503	-0.0521	-0.0551	-0.0594	-0.0649	-0.0718	-0.0802	-0.0901	-0.1012	-0.1129
2.20	-0.0508	-0.0514	-0.0533	-0.0564	-0.0607	-0.0663	-0.0731	-0.0812	-0.0909	-0.1021	-0.1148
2.60	-0.0532	-0.0539	-0.0561	-0.0597	-0.0647	-0.0708	-0.0780	-0.0862	-0.0954	-0.1060	-0.1185
3.00	-0.0542	-0.0550	-0.0574	-0.0614	-0.0669	-0.0738	-0.0820	-0.0914	-0.1018	-0.1132	-0.1255
5.00	-0.0552	-0.0560	-0.0586	-0.0629	-0.0688	-0.0763	-0.0851	-0.0951	-0.1062	-0.1181	-0.1303
∞	-0.0553	-0.0562	-0.0588	-0.0631	-0.0691	-0.0765	-0.0853	-0.0954	-0.1064	-0.1182	-0.1305

TABLE 31.— PITCH MOMENT DERIVATIVE, $\overline{C}_{M_{\theta_s}}$, $\gamma = 10$, $\theta_{q_1} = 0$

p \ μ	0.0000	0.1000	0.2000	0.3000	0.4000	0.5000	0.6000	0.7000	0.8000	0.9000	1.0000
1.00	0.0000	-0.0000	0.0000	0.0000	0.0000	0.0000	-0.0000	-0.0000	-0.0000	0.0000	0.0000
1.02	0.0020	0.0020	0.0022	0.0024	0.0028	0.0033	0.0039	0.0046	0.0054	0.0062	0.0070
1.04	0.0040	0.0041	0.0044	0.0050	0.0058	0.0068	0.0081	0.0097	0.0116	0.0136	0.0157
1.08	0.0078	0.0080	0.0088	0.0101	0.0119	0.0145	0.0175	0.0215	0.0271	0.0327	0.0384
1.12	0.0115	0.0119	0.0130	0.0149	0.0177	0.0215	0.0263	0.0323	0.0400	0.0473	0.0533
1.16	0.0150	0.0155	0.0170	0.0195	0.0232	0.0282	0.0348	0.0429	0.0526	0.0621	0.0702
1.20	0.0182	0.0188	0.0206	0.0237	0.0283	0.0347	0.0431	0.0536	0.0661	0.0790	0.0895
1.24	0.0209	0.0216	0.0237	0.0274	0.0329	0.0405	0.0506	0.0635	0.0789	0.0954	0.1106
1.28	0.0231	0.0239	0.0263	0.0305	0.0367	0.0453	0.0570	0.0719	0.0900	0.1099	0.1286
1.34	0.0255	0.0264	0.0291	0.0338	0.0409	0.0507	0.0640	0.0813	0.1024	0.1262	0.1494
1.40	0.0268	0.0277	0.0306	0.0357	0.0433	0.0538	0.0681	0.0866	0.1095	0.1357	0.1622
1.50	0.0271	0.0281	0.0311	0.0363	0.0440	0.0548	0.0694	0.0882	0.1117	0.1392	0.1682
1.60	0.0260	0.0269	0.0298	0.0348	0.0422	0.0525	0.0662	0.0840	0.1063	0.1329	0.1620
1.70	0.0242	0.0251	0.0277	0.0324	0.0392	0.0485	0.0610	0.0771	0.0975	0.1222	0.1503
1.80	0.0221	0.0229	0.0254	0.0296	0.0357	0.0441	0.0552	0.0696	0.0878	0.1104	0.1369
1.90	0.0201	0.0208	0.0231	0.0269	0.0324	0.0399	0.0497	0.0624	0.0785	0.0989	0.1237
2.00	0.0182	0.0189	0.0209	0.0245	0.0295	0.0362	0.0450	0.0561	0.0704	0.0886	0.1115
2.10	0.0165	0.0171	0.0191	0.0223	0.0270	0.0332	0.0411	0.0510	0.0637	0.0800	0.1009
2.20	0.0150	0.0156	0.0174	0.0205	0.0249	0.0307	0.0380	0.0471	0.0585	0.0731	0.0920
2.60	0.0104	0.0109	0.0124	0.0149	0.0186	0.0234	0.0295	0.0370	0.0460	0.0567	0.0697
3.00	0.0076	0.0080	0.0092	0.0112	0.0141	0.0180	0.0230	0.0292	0.0367	0.0454	0.0556
5.00	0.0026	0.0027	0.0031	0.0038	0.0047	0.0060	0.0075	0.0094	0.0116	0.0141	0.0172
∞	0.0000	0.0000	0.0000	0.0000	0.0000	0.0000	0.0000	0.0000	0.0000	0.0000	0.0000

TABLE 32.— THRUST DERIVATIVE, $\bar{C}_{T_{\theta_c}}$, $\gamma = 10$, $\theta_{q_1} = 0$

p \ μ	0.0000	0.1000	0.2000	0.3000	0.4000	0.5000	0.6000	0.7000	0.8000	0.9000	1.0000
1.00	0.0000	0.0000	-0.0000	-0.0000	-0.0000	-0.0000	-0.0001	-0.0003	-0.0006	-0.0011	-0.0018
1.02	0.0000	0.0000	0.0001	0.0001	0.0000	-0.0000	-0.0001	-0.0005	-0.0010	-0.0016	-0.0025
1.04	0.0000	0.0000	0.0000	-0.0000	-0.0001	-0.0004	-0.0006	-0.0011	-0.0018	-0.0026	-0.0039
1.08	0.0000	-0.0002	-0.0005	-0.0008	-0.0012	-0.0016	-0.0020	-0.0028	-0.0034	-0.0051	-0.0078
1.12	0.0000	-0.0005	-0.0011	-0.0017	-0.0024	-0.0033	-0.0044	-0.0059	-0.0075	-0.0098	-0.0123
1.16	0.0000	-0.0009	-0.0018	-0.0028	-0.0039	-0.0053	-0.0070	-0.0094	-0.0121	-0.0156	-0.0192
1.20	0.0000	-0.0012	-0.0025	-0.0038	-0.0053	-0.0071	-0.0094	-0.0124	-0.0163	-0.0211	-0.0263
1.24	0.0000	-0.0016	-0.0032	-0.0048	-0.0066	-0.0087	-0.0113	-0.0149	-0.0196	-0.0256	-0.0324
1.28	0.0000	-0.0019	-0.0037	-0.0056	-0.0076	-0.0098	-0.0127	-0.0166	-0.0218	-0.0288	-0.0369
1.34	0.0000	-0.0022	-0.0043	-0.0064	-0.0085	-0.0109	-0.0138	-0.0178	-0.0233	-0.0310	-0.0406
1.40	0.0000	-0.0024	-0.0047	-0.0069	-0.0090	-0.0112	-0.0139	-0.0176	-0.0229	-0.0306	-0.0408
1.50	0.0000	-0.0025	-0.0049	-0.0070	-0.0088	-0.0105	-0.0125	-0.0151	-0.0194	-0.0262	-0.0366
1.60	0.0000	-0.0024	-0.0047	-0.0066	-0.0080	-0.0091	-0.0102	-0.0117	-0.0146	-0.0203	-0.0299
1.70	0.0000	-0.0023	-0.0044	-0.0060	-0.0071	-0.0077	-0.0080	-0.0086	-0.0104	-0.0150	-0.0240
1.80	0.0000	-0.0021	-0.0040	-0.0055	-0.0063	-0.0066	-0.0065	-0.0066	-0.0078	-0.0118	-0.0205
1.90	0.0000	-0.0019	-0.0037	-0.0050	-0.0059	-0.0062	-0.0062	-0.0063	-0.0075	-0.0113	-0.0200
2.00	0.0000	-0.0018	-0.0034	-0.0048	-0.0059	-0.0066	-0.0071	-0.0079	-0.0097	-0.0140	-0.0230
2.10	0.0000	-0.0016	-0.0032	-0.0047	-0.0062	-0.0075	-0.0090	-0.0109	-0.0139	-0.0191	-0.0285
2.20	0.0000	-0.0015	-0.0031	-0.0047	-0.0066	-0.0087	-0.0112	-0.0144	-0.0188	-0.0251	-0.0348
2.60	0.0000	-0.0011	-0.0024	-0.0042	-0.0067	-0.0100	-0.0143	-0.0196	-0.0258	-0.0327	-0.0401
3.00	0.0000	-0.0008	-0.0018	-0.0032	-0.0052	-0.0079	-0.0113	-0.0153	-0.0198	-0.0244	-0.0287
5.00	0.0000	-0.0002	-0.0006	-0.0011	-0.0017	-0.0027	-0.0039	-0.0054	-0.0074	-0.0097	-0.0127
∞	-0.0000	-0.0000	-0.0000	0.0000	0.0000	0.0000	0.0000	0.0000	0.0000	0.0000	0.0000

TABLE 33.— ROLL MOMENT DERIVATIVE, $\bar{C}_{L_{\theta_c}}$, $\gamma = 10$, $\theta_{q_1} = 0$

p \ μ	0.0000	0.1000	0.2000	0.3000	0.4000	0.5000	0.6000	0.7000	0.8000	0.9000	1.0000
1.00	-0.0000	-0.0000	0.0000	-0.0000	0.0000	0.0000	0.0000	0.0000	0.0000	0.0000	-0.0000
1.02	-0.0020	-0.0020	-0.0019	-0.0019	-0.0019	-0.0019	-0.0019	-0.0019	-0.0019	-0.0020	-0.0020
1.04	-0.0040	-0.0039	-0.0039	-0.0039	-0.0039	-0.0039	-0.0039	-0.0039	-0.0039	-0.0039	-0.0039
1.08	-0.0078	-0.0078	-0.0078	-0.0077	-0.0077	-0.0076	-0.0076	-0.0076	-0.0075	-0.0075	-0.0075
1.12	-0.0115	-0.0115	-0.0115	-0.0114	-0.0113	-0.0112	-0.0112	-0.0111	-0.0109	-0.0108	-0.0108
1.16	-0.0150	-0.0150	-0.0150	-0.0149	-0.0148	-0.0147	-0.0146	-0.0145	-0.0144	-0.0144	-0.0145
1.20	-0.0182	-0.0182	-0.0182	-0.0181	-0.0179	-0.0178	-0.0177	-0.0176	-0.0176	-0.0178	-0.0183
1.24	-0.0209	-0.0209	-0.0209	-0.0208	-0.0206	-0.0204	-0.0203	-0.0202	-0.0203	-0.0208	-0.0216
1.28	-0.0231	-0.0231	-0.0231	-0.0229	-0.0228	-0.0225	-0.0224	-0.0223	-0.0224	-0.0231	-0.0244
1.34	-0.0255	-0.0255	-0.0254	-0.0252	-0.0249	-0.0246	-0.0243	-0.0242	-0.0243	-0.0252	-0.0271
1.40	-0.0268	-0.0268	-0.0266	-0.0264	-0.0260	-0.0256	-0.0251	-0.0248	-0.0249	-0.0259	-0.0283
1.50	-0.0271	-0.0271	-0.0268	-0.0265	-0.0259	-0.0252	-0.0244	-0.0237	-0.0236	-0.0246	-0.0277
1.60	-0.0260	-0.0259	-0.0256	-0.0251	-0.0243	-0.0233	-0.0222	-0.0212	-0.0209	-0.0218	-0.0251
1.70	-0.0242	-0.0241	-0.0237	-0.0231	-0.0222	-0.0210	-0.0196	-0.0184	-0.0177	-0.0184	-0.0218
1.80	-0.0221	-0.0220	-0.0216	-0.0210	-0.0200	-0.0186	-0.0171	-0.0156	-0.0147	-0.0152	-0.0184
1.90	-0.0201	-0.0200	-0.0196	-0.0189	-0.0179	-0.0166	-0.0150	-0.0134	-0.0122	-0.0124	-0.0152
2.00	-0.0182	-0.0181	-0.0178	-0.0172	-0.0162	-0.0150	-0.0135	-0.0118	-0.0105	-0.0104	-0.0126
2.10	-0.0165	-0.0164	-0.0161	-0.0156	-0.0149	-0.0138	-0.0125	-0.0110	-0.0097	-0.0092	-0.0106
2.20	-0.0150	-0.0149	-0.0147	-0.0144	-0.0138	-0.0131	-0.0120	-0.0108	-0.0097	-0.0090	-0.0094
2.60	-0.0104	-0.0104	-0.0105	-0.0105	-0.0106	-0.0108	-0.0110	-0.0112	-0.0113	-0.0111	-0.0102
3.00	-0.0076	-0.0077	-0.0077	-0.0078	-0.0081	-0.0084	-0.0089	-0.0095	-0.0101	-0.0104	-0.0100
5.00	-0.0026	-0.0026	-0.0026	-0.0026	-0.0026	-0.0026	-0.0026	-0.0025	-0.0023	-0.0021	-0.0017
∞	-0.0000	-0.0000	-0.0000	-0.0000	-0.0000	-0.0000	-0.0000	-0.0000	-0.0000	-0.0000	-0.0000

TABLE 34.— PITCH MOMENT DERIVATIVE, $\bar{C}_{M_{\theta_c}}$, $\gamma = 10$, $\theta_{q_1} = 0$

p \ μ	0.0000	0.1000	0.2000	0.3000	0.4000	0.5000	0.6000	0.7000	0.8000	0.9000	1.0000
1.00	-0.0000	-0.0000	-0.0000	-0.0000	-0.0000	-0.0000	-0.0000	-0.0000	-0.0000	-0.0000	-0.0000
1.02	-0.0000	-0.0000	-0.0000	-0.0000	-0.0000	-0.0000	-0.0000	-0.0000	-0.0000	-0.0000	-0.0000
1.04	-0.0003	-0.0003	-0.0003	-0.0003	-0.0003	-0.0003	-0.0003	-0.0004	-0.0004	-0.0004	-0.0004
1.08	-0.0016	-0.0016	-0.0016	-0.0017	-0.0017	-0.0018	-0.0018	-0.0019	-0.0022	-0.0023	-0.0023
1.12	-0.0032	-0.0032	-0.0033	-0.0034	-0.0034	-0.0037	-0.0038	-0.0041	-0.0047	-0.0048	-0.0047
1.16	-0.0052	-0.0052	-0.0053	-0.0055	-0.0057	-0.0061	-0.0064	-0.0069	-0.0075	-0.0077	-0.0076
1.20	-0.0076	-0.0077	-0.0078	-0.0081	-0.0085	-0.0091	-0.0097	-0.0104	-0.0112	-0.0117	-0.0116
1.24	-0.0104	-0.0105	-0.0108	-0.0112	-0.0118	-0.0125	-0.0135	-0.0146	-0.0157	-0.0165	-0.0166
1.28	-0.0135	-0.0136	-0.0140	-0.0145	-0.0153	-0.0164	-0.0177	-0.0192	-0.0207	-0.0219	-0.0222
1.34	-0.0183	-0.0185	-0.0189	-0.0197	-0.0208	-0.0223	-0.0241	-0.0262	-0.0284	-0.0302	-0.0309
1.40	-0.0231	-0.0233	-0.0238	-0.0248	-0.0262	-0.0280	-0.0303	-0.0329	-0.0357	-0.0381	-0.0392
1.50	-0.0302	-0.0305	-0.0312	-0.0324	-0.0341	-0.0363	-0.0391	-0.0424	-0.0458	-0.0490	-0.0508
1.60	-0.0360	-0.0363	-0.0371	-0.0384	-0.0402	-0.0427	-0.0457	-0.0492	-0.0531	-0.0567	-0.0592
1.70	-0.0405	-0.0408	-0.0415	-0.0428	-0.0447	-0.0472	-0.0502	-0.0538	-0.0578	-0.0618	-0.0649
1.80	-0.0439	-0.0441	-0.0449	-0.0461	-0.0479	-0.0502	-0.0532	-0.0567	-0.0607	-0.0649	-0.0686
1.90	-0.0464	-0.0466	-0.0473	-0.0485	-0.0501	-0.0522	-0.0549	-0.0583	-0.0622	-0.0666	-0.0708
2.00	-0.0483	-0.0485	-0.0491	-0.0502	-0.0516	-0.0536	-0.0560	-0.0591	-0.0628	-0.0673	-0.0721
2.10	-0.0497	-0.0499	-0.0505	-0.0514	-0.0528	-0.0545	-0.0567	-0.0595	-0.0630	-0.0676	-0.0728
2.20	-0.0508	-0.0510	-0.0515	-0.0525	-0.0537	-0.0553	-0.0574	-0.0599	-0.0632	-0.0677	-0.0732
2.60	-0.0532	-0.0534	-0.0541	-0.0552	-0.0567	-0.0585	-0.0607	-0.0634	-0.0665	-0.0706	-0.0759
3.00	-0.0542	-0.0544	-0.0552	-0.0565	-0.0584	-0.0608	-0.0637	-0.0672	-0.0712	-0.0758	-0.0811
5.00	-0.0552	-0.0554	-0.0563	-0.0578	-0.0598	-0.0623	-0.0654	-0.0690	-0.0731	-0.0776	-0.0827
∞	-0.0553	-0.0556	-0.0565	-0.0579	-0.0599	-0.0625	-0.0655	-0.0691	-0.0730	-0.0774	-0.0821

TABLE 35.— THRUST DERIVATIVE, $\bar{C}_{T_{\alpha_c}}$, $\gamma = 10$, $\theta_{q_1} = 0$

P \ μ	0.0000	0.1000	0.2000	0.3000	0.4000	0.5000	0.6000	0.7000	0.8000	0.9000	1.0000
1.00	0.0000	0.0022	0.0086	0.0184	0.0311	0.0461	0.0627	0.0795	0.0936	0.0997	0.0911
1.02	0.0000	0.0023	0.0090	0.0194	0.0331	0.0497	0.0683	0.0888	0.1115	0.1237	0.1159
1.04	0.0000	0.0024	0.0094	0.0204	0.0351	0.0532	0.0742	0.0984	0.1269	0.1491	0.1547
1.08	0.0000	0.0026	0.0102	0.0221	0.0382	0.0583	0.0825	0.1114	0.1453	0.1826	0.2160
1.12	0.0000	0.0027	0.0106	0.0230	0.0398	0.0611	0.0875	0.1199	0.1596	0.2069	0.2589
1.16	0.0000	0.0028	0.0108	0.0235	0.0407	0.0626	0.0900	0.1245	0.1680	0.2228	0.2889
1.20	0.0000	0.0028	0.0109	0.0237	0.0411	0.0632	0.0910	0.1262	0.1715	0.2301	0.3038
1.24	0.0000	0.0028	0.0109	0.0237	0.0410	0.0631	0.0907	0.1258	0.1712	0.2309	0.3078
1.28	0.0000	0.0028	0.0108	0.0236	0.0407	0.0625	0.0896	0.1239	0.1682	0.2271	0.3039
1.34	0.0000	0.0027	0.0106	0.0232	0.0400	0.0611	0.0871	0.1195	0.1610	0.2160	0.2891
1.40	0.0000	0.0027	0.0104	0.0227	0.0391	0.0595	0.0842	0.1143	0.1523	0.2024	0.2692
1.50	0.0000	0.0026	0.0101	0.0220	0.0377	0.0569	0.0796	0.1064	0.1389	0.1806	0.2363
1.60	0.0000	0.0025	0.0098	0.0213	0.0365	0.0549	0.0762	0.1006	0.1292	0.1644	0.2108
1.70	0.0000	0.0025	0.0096	0.0209	0.0357	0.0536	0.0742	0.0973	0.1234	0.1544	0.1944
1.80	0.0000	0.0024	0.0095	0.0206	0.0352	0.0529	0.0733	0.0959	0.1209	0.1498	0.1847
1.90	0.0000	0.0024	0.0094	0.0203	0.0349	0.0527	0.0732	0.0960	0.1210	0.1490	0.1826
2.00	0.0000	0.0024	0.0093	0.0202	0.0348	0.0527	0.0736	0.0969	0.1224	0.1504	0.1829
2.10	0.0000	0.0024	0.0092	0.0201	0.0347	0.0527	0.0739	0.0977	0.1239	0.1522	0.1841
2.20	0.0000	0.0023	0.0092	0.0200	0.0345	0.0526	0.0738	0.0979	0.1243	0.1528	0.1840
2.60	0.0000	0.0023	0.0090	0.0195	0.0334	0.0505	0.0701	0.0921	0.1158	0.1408	0.1665
3.00	0.0000	0.0023	0.0089	0.0192	0.0327	0.0489	0.0673	0.0874	0.1087	0.1310	0.1538
5.00	0.0000	0.0023	0.0088	0.0189	0.0320	0.0475	0.0646	0.0829	0.1018	0.1206	0.1388
∞	0.0000	0.0023	0.0088	0.0189	0.0320	0.0473	0.0643	0.0824	0.1008	0.1190	0.1364

TABLE 36.— ROLL MOMENT DERIVATIVE, $\bar{C}_{L_{\alpha_c}}$, $\gamma = 10$, $\theta_{q_1} = 0$

p \ μ	0.0000	0.1000	0.2000	0.3000	0.4000	0.5000	0.6000	0.7000	0.8000	0.9000	1.0000
1.00	0.0000	-0.0000	-0.0000	-0.0000	-0.0000	-0.0000	-0.0000	-0.0000	-0.0000	-0.0000	-0.0000
1.02	0.0000	-0.0000	-0.0001	-0.0001	-0.0002	-0.0004	-0.0006	-0.0009	-0.0014	-0.0023	-0.0038
1.04	0.0000	-0.0001	-0.0002	-0.0004	-0.0006	-0.0008	-0.0012	-0.0018	-0.0025	-0.0038	-0.0062
1.08	0.0000	-0.0003	-0.0007	-0.0011	-0.0014	-0.0019	-0.0023	-0.0031	-0.0042	-0.0058	-0.0088
1.12	0.0000	-0.0006	-0.0012	-0.0017	-0.0022	-0.0027	-0.0030	-0.0036	-0.0045	-0.0055	-0.0070
1.16	0.0000	-0.0009	-0.0017	-0.0024	-0.0030	-0.0036	-0.0039	-0.0042	-0.0046	-0.0043	-0.0032
1.20	0.0000	-0.0012	-0.0024	-0.0033	-0.0042	-0.0049	-0.0053	-0.0057	-0.0057	-0.0046	-0.0018
1.24	0.0000	-0.0016	-0.0031	-0.0044	-0.0056	-0.0066	-0.0074	-0.0080	-0.0081	-0.0067	-0.0029
1.28	0.0000	-0.0020	-0.0039	-0.0057	-0.0072	-0.0086	-0.0099	-0.0110	-0.0115	-0.0105	-0.0063
1.34	0.0000	-0.0026	-0.0052	-0.0076	-0.0099	-0.0121	-0.0142	-0.0164	-0.0181	-0.0182	-0.0146
1.40	0.0000	-0.0033	-0.0065	-0.0096	-0.0126	-0.0156	-0.0188	-0.0222	-0.0253	-0.0271	-0.0251
1.50	0.0000	-0.0042	-0.0084	-0.0126	-0.0167	-0.0211	-0.0259	-0.0312	-0.0369	-0.0417	-0.0431
1.60	0.0000	-0.0050	-0.0100	-0.0150	-0.0201	-0.0255	-0.0316	-0.0385	-0.0463	-0.0538	-0.0588
1.70	0.0000	-0.0056	-0.0112	-0.0168	-0.0226	-0.0288	-0.0358	-0.0439	-0.0532	-0.0628	-0.0709
1.80	0.0000	-0.0060	-0.0121	-0.0182	-0.0245	-0.0312	-0.0388	-0.0476	-0.0579	-0.0692	-0.0800
1.90	0.0000	-0.0064	-0.0128	-0.0192	-0.0258	-0.0328	-0.0408	-0.0500	-0.0609	-0.0734	-0.0864
2.00	0.0000	-0.0066	-0.0133	-0.0199	-0.0267	-0.0340	-0.0420	-0.0514	-0.0627	-0.0760	-0.0908
2.10	0.0000	-0.0068	-0.0136	-0.0205	-0.0274	-0.0348	-0.0429	-0.0523	-0.0636	-0.0773	-0.0935
2.20	0.0000	-0.0070	-0.0139	-0.0209	-0.0280	-0.0354	-0.0435	-0.0528	-0.0640	-0.0779	-0.0949
2.60	0.0000	-0.0073	-0.0146	-0.0219	-0.0294	-0.0372	-0.0457	-0.0551	-0.0662	-0.0799	-0.0973
3.00	0.0000	-0.0074	-0.0149	-0.0224	-0.0302	-0.0384	-0.0474	-0.0576	-0.0696	-0.0836	-0.1011
5.00	0.0000	-0.0075	-0.0152	-0.0229	-0.0310	-0.0396	-0.0491	-0.0598	-0.0722	-0.0868	-0.1042
∞	0.0000	-0.0076	-0.0152	-0.0230	-0.0311	-0.0397	-0.0493	-0.0600	-0.0724	-0.0870	-0.1043

TABLE 37.— PITCH MOMENT DERIVATIVE, $\bar{C}_{M_{\alpha_c}}$, $\gamma = 10$, $\theta_{q_1} = 0$

P \ μ	0.0000	0.1000	0.2000	0.3000	0.4000	0.5000	0.6000	0.7000	0.8000	0.9000	1.0000
1.00	0.0000	-0.0000	-0.0000	-0.0000	0.0000	0.0000	-0.0000	-0.0000	-0.0000	-0.0000	0.0000
1.02	0.0000	0.0002	0.0005	0.0008	0.0012	0.0017	0.0022	0.0028	0.0036	0.0043	0.0049
1.04	0.0000	0.0005	0.0011	0.0017	0.0025	0.0034	0.0045	0.0059	0.0075	0.0092	0.0108
1.08	0.0000	0.0010	0.0022	0.0035	0.0051	0.0070	0.0094	0.0124	0.0163	0.0208	0.0255
1.12	0.0000	0.0015	0.0032	0.0052	0.0075	0.0105	0.0141	0.0186	0.0243	0.0304	0.0363
1.16	0.0000	0.0020	0.0042	0.0068	0.0099	0.0137	0.0186	0.0247	0.0322	0.0404	0.0485
1.20	0.0000	0.0024	0.0051	0.0082	0.0120	0.0168	0.0229	0.0308	0.0404	0.0514	0.0625
1.24	0.0000	0.0028	0.0059	0.0094	0.0139	0.0195	0.0268	0.0363	0.0481	0.0618	0.0760
1.28	0.0000	0.0031	0.0065	0.0105	0.0154	0.0218	0.0301	0.0409	0.0546	0.0708	0.0879
1.34	0.0000	0.0034	0.0071	0.0116	0.0171	0.0242	0.0336	0.0459	0.0617	0.0808	0.1013
1.40	0.0000	0.0036	0.0075	0.0122	0.0180	0.0256	0.0355	0.0487	0.0657	0.0864	0.1093
1.50	0.0000	0.0036	0.0076	0.0123	0.0182	0.0259	0.0359	0.0493	0.0665	0.0880	0.1123
1.60	0.0000	0.0034	0.0073	0.0118	0.0174	0.0246	0.0341	0.0467	0.0630	0.0836	0.1075
1.70	0.0000	0.0032	0.0067	0.0109	0.0161	0.0227	0.0313	0.0427	0.0575	0.0765	0.0993
1.80	0.0000	0.0029	0.0062	0.0099	0.0146	0.0205	0.0282	0.0383	0.0516	0.0688	0.0900
1.90	0.0000	0.0026	0.0056	0.0090	0.0132	0.0185	0.0253	0.0342	0.0460	0.0614	0.0810
2.00	0.0000	0.0024	0.0051	0.0082	0.0119	0.0167	0.0228	0.0306	0.0410	0.0548	0.0728
2.10	0.0000	0.0022	0.0046	0.0074	0.0109	0.0152	0.0206	0.0277	0.0369	0.0493	0.0656
2.20	0.0000	0.0020	0.0042	0.0068	0.0100	0.0139	0.0190	0.0254	0.0337	0.0447	0.0596
2.60	0.0000	0.0014	0.0029	0.0049	0.0073	0.0104	0.0144	0.0195	0.0259	0.0339	0.0441
3.00	0.0000	0.0010	0.0022	0.0036	0.0055	0.0080	0.0112	0.0154	0.0207	0.0271	0.0348
5.00	0.0000	0.0003	0.0007	0.0012	0.0018	0.0027	0.0037	0.0051	0.0067	0.0086	0.0110
∞	0.0000	0.0000	0.0000	0.0000	0.0000	0.0000	0.0000	0.0000	0.0000	0.0000	0.0000

TABLE 38.— THRUST DERIVATIVE, $\bar{C}_{T_{\theta_0}}$, $\gamma = 10$, $P = 1.15$

θ_{q_1} \ μ	0.0000	0.1000	0.2000	0.3000	0.4000	0.5000	0.6000	0.7000	0.8000	0.9000	1.0000
0.50	0.2013	0.2049	0.2154	0.2328	0.2580	0.2931	0.3423	0.4135	0.5164	0.6640	0.8594
0.40	0.1890	0.1927	0.2036	0.2216	0.2476	0.2837	0.3338	0.4051	0.5059	0.6471	0.8286
0.30	0.1782	0.1819	0.1928	0.2109	0.2369	0.2727	0.3221	0.3910	0.4863	0.6161	0.7783
0.20	0.1685	0.1722	0.1829	0.2006	0.2260	0.2607	0.3080	0.3727	0.4601	0.5759	0.7168
0.10	0.1599	0.1634	0.1737	0.1908	0.2150	0.2479	0.2922	0.3516	0.4299	0.5310	0.6513
0.00	0.1521	0.1554	0.1652	0.1813	0.2042	0.2349	0.2756	0.3290	0.3980	0.4850	0.5870
-0.10	0.1450	0.1481	0.1573	0.1724	0.1936	0.2218	0.2587	0.3061	0.3661	0.4404	0.5267
-0.20	0.1385	0.1414	0.1500	0.1639	0.1834	0.2090	0.2420	0.2837	0.3356	0.3987	0.4719
-0.30	0.1326	0.1353	0.1432	0.1560	0.1737	0.1967	0.2260	0.2624	0.3070	0.3607	0.4231
-0.40	0.1272	0.1297	0.1369	0.1485	0.1645	0.1851	0.2109	0.2425	0.2807	0.3266	0.3800
-0.50	0.1222	0.1244	0.1310	0.1415	0.1558	0.1741	0.1968	0.2241	0.2569	0.2962	0.3422
-0.60	0.1176	0.1196	0.1256	0.1350	0.1478	0.1639	0.1837	0.2073	0.2355	0.2693	0.3093
-0.70	0.1133	0.1151	0.1205	0.1289	0.1403	0.1545	0.1717	0.1921	0.2164	0.2455	0.2805
-0.80	0.1093	0.1110	0.1158	0.1233	0.1333	0.1458	0.1607	0.1784	0.1993	0.2246	0.2554
-0.90	0.1056	0.1071	0.1114	0.1181	0.1269	0.1378	0.1508	0.1660	0.1841	0.2062	0.2336
-1.00	0.1021	0.1035	0.1073	0.1132	0.1210	0.1305	0.1417	0.1548	0.1706	0.1900	0.2142
-1.10	0.0989	0.1001	0.1035	0.1087	0.1155	0.1238	0.1335	0.1448	0.1586	0.1756	0.1973
-1.20	0.0958	0.0969	0.0999	0.1045	0.1104	0.1176	0.1260	0.1358	0.1478	0.1630	0.1825
-1.40	0.0902	0.0911	0.0934	0.0970	0.1014	0.1068	0.1130	0.1204	0.1296	0.1417	0.1578
-2.00	0.0769	0.0772	0.0783	0.0797	0.0814	0.0834	0.0858	0.0889	0.0933	0.1001	0.1101
-3.00	0.0616	0.0617	0.0618	0.0618	0.0616	0.0614	0.0612	0.0615	0.0627	0.0657	0.0714
-10.00	0.0258	0.0257	0.0255	0.0249	0.0238	0.0222	0.0199	0.0173	0.0146	0.0131	0.0127
$-\infty$	0.0000	0.0000	0.0000	0.0000	0.0000	0.0000	0.0000	0.0000	0.0000	0.0000	0.0000

TABLE 39.— ROLL MOMENT DERIVATIVE, $\bar{C}_{L_{\theta_o}}$, γ = 10, P = 1.15

θ_{q_1} \ μ	0.0000	0.1000	0.2000	0.3000	0.4000	0.5000	0.6000	0.7000	0.8000	0.9000	1.0000
0.50	-0.0000	0.0022	0.0044	0.0067	0.0091	0.0113	0.0143	0.0174	0.0208	0.0262	0.0334
0.40	-0.0000	0.0017	0.0035	0.0054	0.0073	0.0091	0.0117	0.0143	0.0171	0.0217	0.0280
0.30	-0.0000	0.0013	0.0027	0.0042	0.0057	0.0071	0.0092	0.0113	0.0134	0.0173	0.0225
0.20	-0.0000	0.0010	0.0020	0.0031	0.0042	0.0052	0.0069	0.0084	0.0100	0.0131	0.0175
0.10	-0.0000	0.0006	0.0014	0.0021	0.0029	0.0035	0.0048	0.0058	0.0069	0.0094	0.0131
0.00	-0.0000	0.0004	0.0008	0.0012	0.0017	0.0020	0.0029	0.0036	0.0043	0.0063	0.0094
-0.10	-0.0000	0.0001	0.0003	0.0005	0.0007	0.0007	0.0013	0.0016	0.0021	0.0037	0.0064
-0.20	-0.0000	-0.0000	-0.0000	-0.0001	-0.0001	-0.0003	-0.0000	0.0000	0.0003	0.0016	0.0039
-0.30	-0.0000	-0.0002	-0.0004	-0.0006	-0.0008	-0.0012	-0.0011	-0.0011	-0.0010	-0.0000	0.0020
-0.40	-0.0000	-0.0003	-0.0007	-0.0011	-0.0015	-0.0019	-0.0020	-0.0022	-0.0022	-0.0012	0.0005
-0.50	-0.0000	-0.0005	-0.0010	-0.0015	-0.0020	-0.0025	-0.0027	-0.0030	-0.0030	-0.0022	-0.0006
-0.60	-0.0000	-0.0006	-0.0012	-0.0018	-0.0024	-0.0030	-0.0033	-0.0036	-0.0037	-0.0030	-0.0015
-0.70	-0.0000	-0.0007	-0.0014	-0.0020	-0.0027	-0.0034	-0.0037	-0.0040	-0.0042	-0.0035	-0.0022
-0.80	-0.0000	-0.0007	-0.0015	-0.0022	-0.0029	-0.0036	-0.0040	-0.0044	-0.0045	-0.0039	-0.0027
-0.90	-0.0000	-0.0008	-0.0016	-0.0024	-0.0031	-0.0038	-0.0042	-0.0046	-0.0048	-0.0042	-0.0031
-1.00	-0.0000	-0.0008	-0.0017	-0.0025	-0.0032	-0.0040	-0.0044	-0.0048	-0.0049	-0.0044	-0.0034
-1.10	-0.0000	-0.0008	-0.0017	-0.0025	-0.0033	-0.0040	-0.0045	-0.0048	-0.0050	-0.0046	-0.0036
-1.20	-0.0000	-0.0009	-0.0017	-0.0026	-0.0033	-0.0041	-0.0045	-0.0049	-0.0050	-0.0046	-0.0037
-1.40	-0.0000	-0.0009	-0.0018	-0.0026	-0.0034	-0.0041	-0.0045	-0.0048	-0.0050	-0.0046	-0.0039
-2.00	-0.0000	-0.0008	-0.0016	-0.0024	-0.0031	-0.0037	-0.0041	-0.0043	-0.0045	-0.0042	-0.0037
-3.00	-0.0000	-0.0006	-0.0013	-0.0019	-0.0024	-0.0029	-0.0032	-0.0035	-0.0036	-0.0036	-0.0033
-10.00	-0.0000	-0.0001	-0.0003	-0.0005	-0.0008	-0.0010	-0.0013	-0.0016	-0.0019	-0.0020	-0.0020
-∞	0.0000	0.0000	0.0000	0.0000	0.0000	0.0000	0.0000	0.0000	0.0000	0.0000	0.0000

TABLE 40.— PITCH MOMENT DERIVATIVE, $\bar{C}_{M_{\theta_o}}$, $\gamma = 10$, $P = 1.15$

θ_{q_1} \ μ	0.0000	0.1000	0.2000	0.3000	0.4000	0.5000	0.6000	0.7000	0.8000	0.9000	1.0000
0.50	0.0000	0.0060	0.0123	0.0194	0.0275	0.0376	0.0497	0.0658	0.0875	0.1126	0.1400
0.40	0.0000	0.0058	0.0119	0.0187	0.0266	0.0364	0.0481	0.0635	0.0837	0.1065	0.1301
0.30	0.0000	0.0055	0.0114	0.0179	0.0255	0.0348	0.0460	0.0603	0.0787	0.0986	0.1181
0.20	0.0000	0.0053	0.0109	0.0171	0.0243	0.0331	0.0435	0.0565	0.0729	0.0898	0.1055
0.10	0.0000	0.0050	0.0103	0.0162	0.0230	0.0312	0.0407	0.0525	0.0667	0.0808	0.0932
0.00	0.0000	0.0048	0.0098	0.0153	0.0216	0.0292	0.0379	0.0483	0.0606	0.0721	0.0819
-0.10	0.0000	0.0045	0.0092	0.0144	0.0203	0.0272	0.0351	0.0442	0.0547	0.0642	0.0718
-0.20	0.0000	0.0042	0.0087	0.0135	0.0190	0.0253	0.0323	0.0403	0.0492	0.0570	0.0630
-0.30	0.0000	0.0040	0.0082	0.0127	0.0177	0.0234	0.0297	0.0367	0.0443	0.0506	0.0554
-0.40	0.0000	0.0037	0.0077	0.0118	0.0164	0.0216	0.0272	0.0333	0.0398	0.0451	0.0489
-0.50	0.0000	0.0035	0.0072	0.0110	0.0153	0.0200	0.0249	0.0303	0.0358	0.0402	0.0433
-0.60	0.0000	0.0033	0.0067	0.0103	0.0142	0.0184	0.0229	0.0275	0.0324	0.0361	0.0386
-0.70	0.0000	0.0031	0.0063	0.0096	0.0131	0.0170	0.0210	0.0251	0.0293	0.0325	0.0346
-0.80	0.0000	0.0029	0.0058	0.0089	0.0122	0.0157	0.0193	0.0229	0.0266	0.0293	0.0311
-0.90	0.0000	0.0027	0.0055	0.0083	0.0113	0.0145	0.0177	0.0210	0.0242	0.0266	0.0282
-1.00	0.0000	0.0025	0.0051	0.0077	0.0105	0.0135	0.0163	0.0193	0.0222	0.0243	0.0256
-1.10	0.0000	0.0023	0.0048	0.0072	0.0098	0.0125	0.0151	0.0177	0.0203	0.0222	0.0234
-1.20	0.0000	0.0022	0.0044	0.0067	0.0091	0.0116	0.0140	0.0164	0.0187	0.0204	0.0215
-1.40	0.0000	0.0019	0.0039	0.0059	0.0079	0.0100	0.0121	0.0141	0.0161	0.0175	0.0184
-2.00	0.0000	0.0013	0.0027	0.0041	0.0054	0.0069	0.0083	0.0097	0.0110	0.0121	0.0127
-3.00	0.0000	0.0008	0.0016	0.0024	0.0033	0.0043	0.0053	0.0063	0.0073	0.0081	0.0086
-10.00	0.0000	0.0001	0.0002	0.0004	0.0006	0.0008	0.0010	0.0013	0.0015	0.0016	0.0017
$-\infty$	0.0000	0.0000	0.0000	0.0000	0.0000	0.0000	0.0000	0.0000	0.0000	0.0000	0.0000

TABLE 41.— THRUST DERIVATIVE, $\bar{C}_{T_{\theta_s}}$, $\gamma = 10$, $P = 1.15$

θ_{q_1} \ μ	0.0000	0.1000	0.2000	0.3000	0.4000	0.5000	0.6000	0.7000	0.8000	0.9000	1.0000
0.50	0.0000	0.0351	0.0707	0.1076	0.1475	0.1929	0.2481	0.3200	0.4165	0.5483	0.7182
0.40	0.0000	0.0336	0.0679	0.1039	0.1432	0.1885	0.2439	0.3155	0.4107	0.5383	0.6987
0.30	0.0000	0.0320	0.0649	0.0997	0.1380	0.1824	0.2366	0.3063	0.3973	0.5168	0.6632
0.20	0.0000	0.0305	0.0618	0.0952	0.1321	0.1749	0.2271	0.2932	0.3782	0.4872	0.6180
0.10	-0.0000	0.0289	0.0587	0.0904	0.1256	0.1664	0.2158	0.2776	0.3555	0.4533	0.5688
0.00	-0.0000	0.0273	0.0555	0.0855	0.1188	0.1572	0.2034	0.2603	0.3309	0.4178	0.5194
-0.10	-0.0000	0.0257	0.0522	0.0805	0.1118	0.1477	0.1905	0.2425	0.3060	0.3829	0.4724
-0.20	-0.0000	0.0242	0.0491	0.0756	0.1048	0.1382	0.1776	0.2247	0.2816	0.3499	0.4291
-0.30	-0.0000	0.0226	0.0460	0.0708	0.0980	0.1288	0.1649	0.2076	0.2586	0.3193	0.3899
-0.40	-0.0000	0.0212	0.0430	0.0661	0.0913	0.1198	0.1527	0.1914	0.2372	0.2914	0.3548
-0.50	-0.0000	0.0198	0.0401	0.0616	0.0850	0.1112	0.1412	0.1762	0.2175	0.2663	0.3236
-0.60	-0.0000	0.0185	0.0374	0.0574	0.0790	0.1031	0.1305	0.1623	0.1997	0.2438	0.2959
-0.70	-0.0000	0.0172	0.0348	0.0534	0.0733	0.0955	0.1206	0.1495	0.1835	0.2236	0.2713
-0.80	-0.0000	0.0160	0.0324	0.0496	0.0681	0.0885	0.1115	0.1379	0.1689	0.2056	0.2495
-0.90	-0.0000	0.0149	0.0302	0.0461	0.0632	0.0821	0.1031	0.1273	0.1558	0.1895	0.2300
-1.00	-0.0000	0.0139	0.0281	0.0429	0.0587	0.0761	0.0955	0.1177	0.1439	0.1751	0.2126
-1.10	-0.0000	0.0130	0.0262	0.0399	0.0546	0.0707	0.0885	0.1090	0.1333	0.1621	0.1970
-1.20	-0.0000	0.0121	0.0244	0.0372	0.0508	0.0657	0.0822	0.1011	0.1236	0.1505	0.1830
-1.40	-0.0000	0.0105	0.0212	0.0323	0.0440	0.0569	0.0711	0.0875	0.1070	0.1304	0.1588
-2.00	-0.0000	0.0071	0.0143	0.0218	0.0296	0.0382	0.0477	0.0588	0.0724	0.0886	0.1078
-3.00	-0.0000	0.0040	0.0082	0.0124	0.0168	0.0217	0.0272	0.0339	0.0422	0.0519	0.0625
-10.00	-0.0000	0.0005	0.0010	0.0017	0.0024	0.0033	0.0044	0.0063	0.0090	0.0121	0.0124
$-\infty$	0.0000	0.0000	0.0000	0.0000	0.0000	0.0000	0.0000	0.0000	0.0000	0.0000	0.0000

TABLE 42.— ROLL MOMENT DERIVATIVE, $\bar{C}_{L_{\theta_s}}$, $\gamma = 10$, $P = 1.15$

θ_{q_1} \ μ	0.0000	0.1000	0.2000	0.3000	0.4000	0.5000	0.6000	0.7000	0.8000	0.9000	1.0000
0.50	-0.0006	-0.0003	0.0005	0.0019	0.0038	0.0060	0.0091	0.0125	0.0163	0.0220	0.0291
0.40	-0.0015	-0.0012	-0.0005	0.0007	0.0023	0.0042	0.0070	0.0100	0.0134	0.0184	0.0249
0.30	-0.0023	-0.0021	-0.0015	-0.0004	0.0009	0.0025	0.0049	0.0075	0.0104	0.0149	0.0206
0.20	-0.0032	-0.0030	-0.0024	-0.0016	-0.0004	0.0008	0.0029	0.0051	0.0076	0.0115	0.0166
0.10	-0.0039	-0.0038	-0.0033	-0.0026	-0.0016	-0.0006	0.0011	0.0029	0.0050	0.0084	0.0130
0.00	-0.0046	-0.0045	-0.0042	-0.0036	-0.0028	-0.0019	-0.0004	0.0010	0.0028	0.0058	0.0099
-0.10	-0.0053	-0.0052	-0.0049	-0.0044	-0.0038	-0.0031	-0.0019	-0.0006	0.0009	0.0036	0.0073
-0.20	-0.0058	-0.0058	-0.0055	-0.0052	-0.0047	-0.0041	-0.0031	-0.0020	-0.0006	0.0017	0.0052
-0.30	-0.0063	-0.0063	-0.0061	-0.0058	-0.0054	-0.0050	-0.0041	-0.0032	-0.0019	0.0002	0.0034
-0.40	-0.0068	-0.0067	-0.0066	-0.0064	-0.0061	-0.0057	-0.0050	-0.0041	-0.0030	-0.0009	0.0020
-0.50	-0.0071	-0.0071	-0.0070	-0.0068	-0.0066	-0.0063	-0.0057	-0.0049	-0.0038	-0.0018	0.0008
-0.60	-0.0074	-0.0074	-0.0073	-0.0072	-0.0070	-0.0068	-0.0062	-0.0055	-0.0045	-0.0026	-0.0000
-0.70	-0.0076	-0.0076	-0.0076	-0.0075	-0.0073	-0.0072	-0.0067	-0.0060	-0.0050	-0.0033	-0.0008
-0.80	-0.0078	-0.0078	-0.0078	-0.0077	-0.0076	-0.0075	-0.0070	-0.0064	-0.0054	-0.0038	-0.0014
-0.90	-0.0079	-0.0079	-0.0079	-0.0079	-0.0078	-0.0077	-0.0072	-0.0066	-0.0057	-0.0042	-0.0020
-1.00	-0.0080	-0.0080	-0.0080	-0.0080	-0.0079	-0.0078	-0.0074	-0.0068	-0.0060	-0.0045	-0.0024
-1.10	-0.0081	-0.0081	-0.0081	-0.0081	-0.0080	-0.0079	-0.0075	-0.0070	-0.0061	-0.0047	-0.0028
-1.20	-0.0081	-0.0081	-0.0081	-0.0081	-0.0081	-0.0080	-0.0076	-0.0071	-0.0063	-0.0049	-0.0031
-1.40	-0.0080	-0.0080	-0.0081	-0.0081	-0.0080	-0.0080	-0.0077	-0.0072	-0.0064	-0.0052	-0.0036
-2.00	-0.0075	-0.0075	-0.0076	-0.0076	-0.0076	-0.0076	-0.0073	-0.0069	-0.0063	-0.0054	-0.0043
-3.00	-0.0064	-0.0064	-0.0064	-0.0064	-0.0065	-0.0065	-0.0063	-0.0060	-0.0056	-0.0050	-0.0043
-10.00	-0.0025	-0.0025	-0.0025	-0.0025	-0.0025	-0.0025	-0.0024	-0.0022	-0.0020	-0.0017	-0.0017
-∞	0.0000	0.0000	0.0000	0.0000	0.0000	0.0000	0.0000	0.0000	0.0000	0.0000	0.0000

TABLE 43.— PITCH MOMENT DERIVATIVE, $\overline{C}_{M_{\theta_s}}$, $\gamma = 10$, $P = 1.15$

θ_{q_1} \ μ	0.0000	0.1000	0.2000	0.3000	0.4000	0.5000	0.6000	0.7000	0.8000	0.9000	1.0000
0.50	0.0155	0.0161	0.0180	0.0212	0.0259	0.0325	0.0412	0.0530	0.0692	0.0881	0.1087
0.40	0.0154	0.0160	0.0178	0.0209	0.0254	0.0318	0.0402	0.0515	0.0667	0.0839	0.1017
0.30	0.0152	0.0158	0.0175	0.0204	0.0247	0.0308	0.0387	0.0493	0.0631	0.0781	0.0929
0.20	0.0150	0.0155	0.0171	0.0198	0.0239	0.0296	0.0369	0.0465	0.0588	0.0716	0.0835
0.10	0.0146	0.0151	0.0166	0.0191	0.0229	0.0281	0.0348	0.0434	0.0541	0.0647	0.0742
0.00	0.0142	0.0146	0.0160	0.0184	0.0218	0.0266	0.0326	0.0402	0.0493	0.0581	0.0654
-0.10	0.0137	0.0141	0.0154	0.0175	0.0207	0.0250	0.0304	0.0370	0.0447	0.0518	0.0575
-0.20	0.0132	0.0136	0.0147	0.0167	0.0195	0.0233	0.0281	0.0338	0.0403	0.0461	0.0506
-0.30	0.0126	0.0130	0.0140	0.0158	0.0183	0.0217	0.0259	0.0309	0.0364	0.0411	0.0445
-0.40	0.0121	0.0124	0.0133	0.0149	0.0172	0.0202	0.0239	0.0281	0.0327	0.0366	0.0393
-0.50	0.0115	0.0118	0.0126	0.0140	0.0161	0.0187	0.0220	0.0256	0.0295	0.0326	0.0347
-0.60	0.0109	0.0111	0.0119	0.0132	0.0150	0.0174	0.0202	0.0233	0.0266	0.0292	0.0308
-0.70	0.0103	0.0105	0.0112	0.0124	0.0140	0.0161	0.0185	0.0212	0.0240	0.0262	0.0275
-0.80	0.0098	0.0100	0.0106	0.0116	0.0130	0.0149	0.0170	0.0194	0.0217	0.0235	0.0245
-0.90	0.0092	0.0094	0.0099	0.0109	0.0121	0.0138	0.0157	0.0177	0.0197	0.0212	0.0220
-1.00	0.0087	0.0089	0.0094	0.0102	0.0113	0.0127	0.0144	0.0162	0.0179	0.0192	0.0198
-1.10	0.0082	0.0083	0.0088	0.0095	0.0105	0.0118	0.0133	0.0148	0.0163	0.0174	0.0178
-1.20	0.0077	0.0079	0.0083	0.0089	0.0098	0.0109	0.0123	0.0136	0.0149	0.0158	0.0161
-1.40	0.0069	0.0070	0.0073	0.0078	0.0086	0.0094	0.0105	0.0116	0.0125	0.0132	0.0133
-2.00	0.0049	0.0049	0.0051	0.0054	0.0058	0.0062	0.0068	0.0073	0.0077	0.0079	0.0077
-3.00	0.0029	0.0029	0.0030	0.0030	0.0032	0.0033	0.0036	0.0037	0.0038	0.0036	0.0032
-10.00	0.0003	0.0003	0.0003	0.0002	0.0002	0.0002	0.0002	0.0002	0.0001	-0.0000	-0.0002
$-\infty$	0.0000	0.0000	0.0000	0.0000	0.0000	0.0000	0.0000	0.0000	0.0000	0.0000	0.0000

TABLE 44.— THRUST DERIVATIVE, $\bar{C}_{T_{\theta_c}}$, $\gamma = 10$, $P = 1.15$

θ_{q_1} \ μ	0.0000	0.1000	0.2000	0.3000	0.4000	0.5000	0.6000	0.7000	0.8000	0.9000	1.0000
0.50	0.0000	0.0087	0.0175	0.0265	0.0359	0.0460	0.0580	0.0730	0.0926	0.1190	0.1530
0.40	0.0000	0.0064	0.0129	0.0195	0.0265	0.0342	0.0433	0.0545	0.0691	0.0884	0.1128
0.30	0.0000	0.0042	0.0086	0.0131	0.0178	0.0230	0.0291	0.0365	0.0460	0.0582	0.0737
0.20	0.0000	0.0023	0.0047	0.0072	0.0098	0.0127	0.0159	0.0197	0.0245	0.0305	0.0383
0.10	0.0000	0.0006	0.0013	0.0020	0.0027	0.0033	0.0039	0.0045	0.0053	0.0062	0.0078
0.00	0.0000	-0.0008	-0.0016	-0.0025	-0.0035	-0.0048	-0.0064	-0.0085	-0.0110	-0.0141	-0.0174
-0.10	0.0000	-0.0021	-0.0042	-0.0064	-0.0090	-0.0118	-0.0153	-0.0196	-0.0246	-0.0309	-0.0378
-0.20	0.0000	-0.0032	-0.0064	-0.0098	-0.0135	-0.0178	-0.0228	-0.0287	-0.0357	-0.0443	-0.0540
-0.30	0.0000	-0.0041	-0.0082	-0.0126	-0.0174	-0.0226	-0.0289	-0.0361	-0.0445	-0.0548	-0.0669
-0.40	0.0000	-0.0048	-0.0098	-0.0149	-0.0204	-0.0266	-0.0337	-0.0419	-0.0514	-0.0629	-0.0767
-0.50	0.0000	-0.0054	-0.0110	-0.0167	-0.0229	-0.0297	-0.0375	-0.0463	-0.0566	-0.0692	-0.0844
-0.60	0.0000	-0.0059	-0.0119	-0.0182	-0.0248	-0.0321	-0.0403	-0.0497	-0.0605	-0.0738	-0.0902
-0.70	0.0000	-0.0063	-0.0126	-0.0192	-0.0263	-0.0339	-0.0424	-0.0521	-0.0634	-0.0773	-0.0947
-0.80	0.0000	-0.0065	-0.0132	-0.0200	-0.0273	-0.0352	-0.0439	-0.0538	-0.0654	-0.0798	-0.0980
-0.90	0.0000	-0.0067	-0.0135	-0.0206	-0.0280	-0.0360	-0.0449	-0.0549	-0.0667	-0.0815	-0.1005
-1.00	0.0000	-0.0068	-0.0138	-0.0209	-0.0284	-0.0365	-0.0454	-0.0555	-0.0674	-0.0826	-0.1022
-1.10	0.0000	-0.0069	-0.0139	-0.0211	-0.0286	-0.0367	-0.0457	-0.0558	-0.0678	-0.0832	-0.1034
-1.20	0.0000	-0.0069	-0.0139	-0.0211	-0.0286	-0.0367	-0.0456	-0.0557	-0.0678	-0.0834	-0.1041
-1.40	0.0000	-0.0068	-0.0137	-0.0208	-0.0282	-0.0361	-0.0449	-0.0549	-0.0671	-0.0830	-0.1045
-2.00	0.0000	-0.0061	-0.0123	-0.0186	-0.0253	-0.0325	-0.0405	-0.0500	-0.0619	-0.0781	-0.1008
-3.00	0.0000	-0.0047	-0.0095	-0.0144	-0.0196	-0.0254	-0.0320	-0.0401	-0.0509	-0.0667	-0.0898
-10.00	0.0000	-0.0012	-0.0025	-0.0038	-0.0053	-0.0071	-0.0095	-0.0129	-0.0190	-0.0304	-0.0507
$-\infty$	0.0000	0.0000	0.0000	0.0000	0.0000	0.0000	0.0000	0.0000	0.0000	0.0000	0.0000

TABLE 45.– ROLL MOMENT DERIVATIVE, $\bar{C}_{L_{\theta_c}}$, $\gamma = 10$, $P = 1.15$

θ_{a_1} \ μ	0.0000	0.1000	0.2000	0.3000	0.4000	0.5000	0.6000	0.7000	0.8000	0.9000	1.0000
0.50	-0.0155	-0.0154	-0.0151	-0.0147	-0.0141	-0.0134	-0.0126	-0.0117	-0.0106	-0.0093	-0.0076
0.40	-0.0154	-0.0154	-0.0151	-0.0148	-0.0144	-0.0138	-0.0132	-0.0126	-0.0118	-0.0108	-0.0097
0.30	-0.0152	-0.0152	-0.0150	-0.0148	-0.0145	-0.0141	-0.0137	-0.0132	-0.0127	-0.0120	-0.0113
0.20	-0.0150	-0.0149	-0.0148	-0.0147	-0.0145	-0.0142	-0.0139	-0.0136	-0.0132	-0.0129	-0.0124
0.10	-0.0146	-0.0146	-0.0145	-0.0144	-0.0143	-0.0141	-0.0139	-0.0137	-0.0135	-0.0133	-0.0132
0.00	-0.0142	-0.0142	-0.0141	-0.0141	-0.0140	-0.0138	-0.0138	-0.0137	-0.0135	-0.0135	-0.0136
-0.10	-0.0137	-0.0137	-0.0137	-0.0136	-0.0136	-0.0134	-0.0135	-0.0134	-0.0133	-0.0135	-0.0138
-0.20	-0.0132	-0.0132	-0.0132	-0.0131	-0.0131	-0.0130	-0.0130	-0.0131	-0.0131	-0.0133	-0.0137
-0.30	-0.0126	-0.0126	-0.0126	-0.0126	-0.0126	-0.0125	-0.0126	-0.0126	-0.0127	-0.0130	-0.0136
-0.40	-0.0121	-0.0120	-0.0120	-0.0120	-0.0120	-0.0119	-0.0120	-0.0121	-0.0122	-0.0127	-0.0134
-0.50	-0.0115	-0.0115	-0.0115	-0.0114	-0.0114	-0.0114	-0.0115	-0.0116	-0.0118	-0.0123	-0.0131
-0.60	-0.0109	-0.0109	-0.0109	-0.0109	-0.0109	-0.0108	-0.0109	-0.0111	-0.0113	-0.0119	-0.0129
-0.70	-0.0103	-0.0103	-0.0103	-0.0103	-0.0103	-0.0102	-0.0104	-0.0106	-0.0108	-0.0115	-0.0125
-0.80	-0.0098	-0.0097	-0.0097	-0.0097	-0.0097	-0.0097	-0.0099	-0.0101	-0.0104	-0.0111	-0.0122
-0.90	-0.0092	-0.0092	-0.0092	-0.0092	-0.0092	-0.0092	-0.0093	-0.0096	-0.0099	-0.0107	-0.0119
-1.00	-0.0087	-0.0087	-0.0087	-0.0087	-0.0087	-0.0087	-0.0089	-0.0091	-0.0095	-0.0103	-0.0116
-1.10	-0.0082	-0.0082	-0.0082	-0.0082	-0.0082	-0.0082	-0.0084	-0.0087	-0.0091	-0.0099	-0.0113
-1.20	-0.0077	-0.0077	-0.0077	-0.0077	-0.0077	-0.0077	-0.0079	-0.0082	-0.0087	-0.0096	-0.0110
-1.40	-0.0069	-0.0069	-0.0068	-0.0068	-0.0069	-0.0069	-0.0071	-0.0075	-0.0079	-0.0089	-0.0104
-2.00	-0.0048	-0.0048	-0.0048	-0.0048	-0.0049	-0.0049	-0.0052	-0.0056	-0.0062	-0.0073	-0.0089
-3.00	-0.0029	-0.0029	-0.0028	-0.0028	-0.0029	-0.0029	-0.0032	-0.0035	-0.0041	-0.0053	-0.0070
-10.00	-0.0003	-0.0003	-0.0003	-0.0002	-0.0002	-0.0003	-0.0004	-0.0006	-0.0010	-0.0018	-0.0033
-∞	0.0000	0.0000	0.0000	0.0000	0.0000	0.0000	0.0000	0.0000	0.0000	0.0000	0.0000

TABLE 46.— PITCH MOMENT DERIVATIVE, $\bar{C}_{M_{\theta_c}}$, $\gamma = 10$, $P = 1.15$

θ_{c_1} \ μ	0.0000	0.1000	0.2000	0.3000	0.4000	0.5000	0.6000	0.7000	0.8000	0.9000	1.0000
0.50	-0.0006	-0.0005	-0.0001	0.0005	0.0014	0.0027	0.0045	0.0068	0.0097	0.0136	0.0179
0.40	-0.0015	-0.0014	-0.0011	-0.0007	-0.0000	0.0008	0.0021	0.0037	0.0057	0.0084	0.0113
0.30	-0.0023	-0.0023	-0.0021	-0.0018	-0.0014	-0.0009	-0.0001	0.0007	0.0019	0.0035	0.0054
0.20	-0.0032	-0.0031	-0.0031	-0.0029	-0.0028	-0.0026	-0.0022	-0.0018	-0.0014	-0.0006	0.0003
0.10	-0.0039	-0.0039	-0.0039	-0.0040	-0.0040	-0.0041	-0.0041	-0.0041	-0.0043	-0.0041	-0.0036
0.00	-0.0046	-0.0047	-0.0047	-0.0049	-0.0051	-0.0054	-0.0057	-0.0061	-0.0067	-0.0069	-0.0067
-0.10	-0.0053	-0.0053	-0.0054	-0.0057	-0.0060	-0.0066	-0.0070	-0.0077	-0.0086	-0.0090	-0.0091
-0.20	-0.0058	-0.0059	-0.0061	-0.0064	-0.0068	-0.0075	-0.0081	-0.0090	-0.0100	-0.0106	-0.0107
-0.30	-0.0063	-0.0064	-0.0066	-0.0070	-0.0075	-0.0082	-0.0090	-0.0099	-0.0111	-0.0117	-0.0119
-0.40	-0.0068	-0.0068	-0.0071	-0.0075	-0.0080	-0.0088	-0.0096	-0.0107	-0.0118	-0.0125	-0.0127
-0.50	-0.0071	-0.0072	-0.0074	-0.0079	-0.0085	-0.0093	-0.0101	-0.0112	-0.0124	-0.0130	-0.0132
-0.60	-0.0074	-0.0075	-0.0077	-0.0082	-0.0088	-0.0097	-0.0105	-0.0116	-0.0127	-0.0133	-0.0135
-0.70	-0.0076	-0.0077	-0.0080	-0.0084	-0.0090	-0.0099	-0.0107	-0.0117	-0.0128	-0.0134	-0.0136
-0.80	-0.0078	-0.0079	-0.0081	-0.0086	-0.0092	-0.0100	-0.0109	-0.0118	-0.0129	-0.0134	-0.0136
-0.90	-0.0079	-0.0080	-0.0083	-0.0087	-0.0093	-0.0101	-0.0109	-0.0118	-0.0129	-0.0134	-0.0135
-1.00	-0.0080	-0.0081	-0.0083	-0.0088	-0.0094	-0.0102	-0.0109	-0.0118	-0.0128	-0.0133	-0.0133
-1.10	-0.0081	-0.0081	-0.0084	-0.0088	-0.0094	-0.0101	-0.0109	-0.0117	-0.0127	-0.0131	-0.0131
-1.20	-0.0081	-0.0081	-0.0084	-0.0088	-0.0093	-0.0101	-0.0108	-0.0116	-0.0125	-0.0129	-0.0129
-1.40	-0.0080	-0.0081	-0.0083	-0.0087	-0.0092	-0.0099	-0.0105	-0.0112	-0.0121	-0.0124	-0.0124
-2.00	-0.0075	-0.0076	-0.0077	-0.0080	-0.0084	-0.0090	-0.0095	-0.0100	-0.0106	-0.0109	-0.0106
-3.00	-0.0064	-0.0064	-0.0065	-0.0067	-0.0070	-0.0074	-0.0077	-0.0081	-0.0085	-0.0085	-0.0081
-10.00	-0.0025	-0.0025	-0.0025	-0.0026	-0.0026	-0.0026	-0.0027	-0.0028	-0.0029	-0.0029	-0.0027
$-\infty$	0.0000	0.0000	0.0000	0.0000	0.0000	0.0000	0.0000	0.0000	0.0000	0.0000	0.0000

TABLE 47.— THRUST DERIVATIVE, $\bar{C}_{T_{\alpha_c}}$, γ = 10, P = 1.15

θ_{q_1} \ μ	0.0000	0.1000	0.2000	0.3000	0.4000	0.5000	0.6000	0.7000	0.8000	0.9000	1.0000
0.50	0.0000	0.0034	0.0133	0.0290	0.0501	0.0772	0.1119	0.1583	0.2220	0.3127	0.4362
0.40	0.0000	0.0033	0.0129	0.0282	0.0489	0.0756	0.1100	0.1556	0.2177	0.3043	0.4188
0.30	0.0000	0.0032	0.0124	0.0272	0.0473	0.0732	0.1065	0.1503	0.2088	0.2884	0.3906
0.20	0.0000	0.0030	0.0119	0.0261	0.0453	0.0700	0.1017	0.1427	0.1965	0.2675	0.3561
0.10	0.0000	0.0029	0.0113	0.0248	0.0430	0.0663	0.0959	0.1336	0.1820	0.2439	0.3192
0.00	0.0000	0.0028	0.0108	0.0234	0.0406	0.0623	0.0896	0.1237	0.1664	0.2197	0.2829
-0.10	0.0000	0.0026	0.0101	0.0220	0.0380	0.0581	0.0829	0.1134	0.1508	0.1961	0.2486
-0.20	0.0000	0.0024	0.0095	0.0206	0.0354	0.0538	0.0762	0.1032	0.1356	0.1739	0.2174
-0.30	0.0000	0.0023	0.0089	0.0192	0.0328	0.0496	0.0697	0.0935	0.1213	0.1535	0.1893
-0.40	0.0000	0.0021	0.0083	0.0178	0.0303	0.0455	0.0635	0.0842	0.1082	0.1350	0.1644
-0.50	0.0000	0.0020	0.0077	0.0165	0.0279	0.0416	0.0576	0.0757	0.0961	0.1185	0.1425
-0.60	0.0000	0.0019	0.0072	0.0152	0.0256	0.0380	0.0521	0.0678	0.0853	0.1039	0.1232
-0.70	0.0000	0.0017	0.0066	0.0140	0.0235	0.0346	0.0470	0.0607	0.0755	0.0908	0.1062
-0.80	0.0000	0.0016	0.0061	0.0129	0.0215	0.0314	0.0424	0.0542	0.0667	0.0793	0.0913
-0.90	0.0000	0.0015	0.0057	0.0119	0.0196	0.0285	0.0382	0.0484	0.0589	0.0691	0.0782
-1.00	0.0000	0.0014	0.0052	0.0109	0.0179	0.0259	0.0343	0.0431	0.0519	0.0600	0.0666
-1.10	0.0000	0.0013	0.0048	0.0101	0.0164	0.0235	0.0309	0.0383	0.0457	0.0519	0.0563
-1.20	0.0000	0.0012	0.0045	0.0092	0.0149	0.0213	0.0277	0.0341	0.0401	0.0447	0.0472
-1.40	0.0000	0.0010	0.0038	0.0078	0.0125	0.0174	0.0223	0.0267	0.0305	0.0326	0.0318
-2.00	0.0000	0.0007	0.0025	0.0048	0.0073	0.0095	0.0111	0.0119	0.0114	0.0084	0.0013
-3.00	0.0000	0.0004	0.0014	0.0024	0.0030	0.0030	0.0019	-0.0004	-0.0046	-0.0123	-0.0255
-10.00	0.0000	0.0002	0.0006	0.0004	-0.0010	-0.0043	-0.0098	-0.0180	-0.0290	-0.0433	-0.0629
$-\infty$	0.0000	0.0000	0.0000	0.0000	0.0000	0.0000	0.0000	0.0000	0.0000	0.0000	0.0000

TABLE 48.— ROLL MOMENT DERIVATIVE, $\bar{C}_{L_{\alpha_c}}$, $\gamma = 10$, $P = 1.15$

θ_{q_1} \ μ	0.0000	0.1000	0.2000	0.3000	0.4000	0.5000	0.6000	0.7000	0.8000	0.9000	1.0000
0.50	0.0000	-0.0002	-0.0004	-0.0004	-0.0000	0.0003	0.0013	0.0024	0.0036	0.0060	0.0095
0.40	0.0000	-0.0004	-0.0007	-0.0008	-0.0006	-0.0004	0.0002	0.0009	0.0018	0.0037	0.0064
0.30	0.0000	-0.0005	-0.0009	-0.0012	-0.0012	-0.0012	-0.0008	-0.0004	0.0000	0.0013	0.0034
0.20	0.0000	-0.0006	-0.0011	-0.0015	-0.0018	-0.0020	-0.0018	-0.0017	-0.0016	-0.0008	0.0005
0.10	0.0000	-0.0007	-0.0014	-0.0019	-0.0023	-0.0027	-0.0028	-0.0029	-0.0031	-0.0028	-0.0019
0.00	0.0000	-0.0008	-0.0016	-0.0022	-0.0028	-0.0033	-0.0036	-0.0040	-0.0045	-0.0045	-0.0040
-0.10	0.0000	-0.0009	-0.0017	-0.0025	-0.0032	-0.0039	-0.0043	-0.0049	-0.0056	-0.0059	-0.0058
-0.20	0.0000	-0.0010	-0.0019	-0.0028	-0.0035	-0.0043	-0.0050	-0.0057	-0.0065	-0.0070	-0.0072
-0.30	0.0000	-0.0010	-0.0020	-0.0030	-0.0038	-0.0047	-0.0055	-0.0063	-0.0073	-0.0079	-0.0083
-0.40	0.0000	-0.0011	-0.0021	-0.0032	-0.0041	-0.0051	-0.0059	-0.0069	-0.0079	-0.0087	-0.0092
-0.50	0.0000	-0.0011	-0.0022	-0.0033	-0.0043	-0.0053	-0.0062	-0.0073	-0.0083	-0.0092	-0.0099
-0.60	0.0000	-0.0012	-0.0023	-0.0034	-0.0045	-0.0055	-0.0065	-0.0076	-0.0087	-0.0097	-0.0105
-0.70	0.0000	-0.0012	-0.0024	-0.0035	-0.0046	-0.0057	-0.0067	-0.0078	-0.0089	-0.0100	-0.0110
-0.80	0.0000	-0.0012	-0.0024	-0.0036	-0.0047	-0.0058	-0.0068	-0.0080	-0.0091	-0.0102	-0.0113
-0.90	0.0000	-0.0012	-0.0025	-0.0036	-0.0047	-0.0059	-0.0069	-0.0081	-0.0093	-0.0104	-0.0116
-1.00	0.0000	-0.0012	-0.0025	-0.0037	-0.0048	-0.0059	-0.0070	-0.0081	-0.0094	-0.0106	-0.0118
-1.10	0.0000	-0.0012	-0.0025	-0.0037	-0.0048	-0.0059	-0.0070	-0.0082	-0.0094	-0.0106	-0.0120
-1.20	0.0000	-0.0012	-0.0025	-0.0037	-0.0048	-0.0060	-0.0070	-0.0082	-0.0094	-0.0107	-0.0121
-1.40	0.0000	-0.0012	-0.0025	-0.0037	-0.0048	-0.0059	-0.0070	-0.0082	-0.0094	-0.0107	-0.0122
-2.00	0.0000	-0.0012	-0.0023	-0.0035	-0.0045	-0.0056	-0.0067	-0.0078	-0.0091	-0.0106	-0.0123
-3.00	0.0000	-0.0010	-0.0020	-0.0030	-0.0040	-0.0050	-0.0060	-0.0072	-0.0087	-0.0104	-0.0124
-10.00	0.0000	-0.0005	-0.0011	-0.0017	-0.0025	-0.0034	-0.0045	-0.0058	-0.0074	-0.0092	-0.0111
$-\infty$	0.0000	0.0000	0.0000	0.0000	0.0000	0.0000	0.0000	0.0000	0.0000	0.0000	0.0000

TABLE 49.– PITCH MOMENT DERIVATIVE, $\bar{C}_{M_{\alpha_c}}$, γ = 10, P = 1.15

θ_{q_1} \ μ	0.0000	0.1000	0.2000	0.3000	0.4000	0.5000	0.6000	0.7000	0.8000	0.9000	1.0000
0.50	0.0000	0.0021	0.0044	0.0073	0.0109	0.0157	0.0220	0.0307	0.0428	0.0582	0.0767
0.40	0.0000	0.0021	0.0044	0.0072	0.0107	0.0154	0.0215	0.0298	0.0411	0.0552	0.0714
0.30	0.0000	0.0020	0.0043	0.0070	0.0105	0.0149	0.0207	0.0285	0.0388	0.0513	0.0649
0.20	0.0000	0.0020	0.0042	0.0069	0.0101	0.0143	0.0197	0.0268	0.0361	0.0468	0.0580
0.10	0.0000	0.0019	0.0041	0.0066	0.0097	0.0136	0.0186	0.0250	0.0331	0.0422	0.0513
0.00	0.0000	0.0019	0.0040	0.0064	0.0093	0.0129	0.0175	0.0232	0.0302	0.0377	0.0451
-0.10	0.0000	0.0018	0.0038	0.0061	0.0088	0.0121	0.0163	0.0213	0.0273	0.0336	0.0396
-0.20	0.0000	0.0017	0.0037	0.0058	0.0083	0.0114	0.0151	0.0195	0.0246	0.0299	0.0348
-0.30	0.0000	0.0017	0.0035	0.0055	0.0078	0.0106	0.0139	0.0178	0.0222	0.0266	0.0306
-0.40	0.0000	0.0016	0.0033	0.0052	0.0074	0.0099	0.0128	0.0162	0.0200	0.0237	0.0270
-0.50	0.0000	0.0015	0.0031	0.0049	0.0069	0.0092	0.0118	0.0148	0.0180	0.0211	0.0240
-0.60	0.0000	0.0014	0.0030	0.0046	0.0065	0.0085	0.0109	0.0135	0.0162	0.0189	0.0214
-0.70	0.0000	0.0013	0.0028	0.0043	0.0060	0.0079	0.0100	0.0123	0.0147	0.0171	0.0192
-0.80	0.0000	0.0013	0.0026	0.0041	0.0056	0.0073	0.0092	0.0113	0.0134	0.0154	0.0173
-0.90	0.0000	0.0012	0.0025	0.0038	0.0053	0.0068	0.0085	0.0103	0.0122	0.0140	0.0157
-1.00	0.0000	0.0011	0.0023	0.0036	0.0049	0.0063	0.0079	0.0095	0.0111	0.0128	0.0143
-1.10	0.0000	0.0011	0.0022	0.0034	0.0046	0.0059	0.0073	0.0087	0.0102	0.0117	0.0131
-1.20	0.0000	0.0010	0.0021	0.0031	0.0043	0.0055	0.0068	0.0081	0.0094	0.0108	0.0121
-1.40	0.0000	0.0009	0.0018	0.0028	0.0038	0.0048	0.0059	0.0070	0.0081	0.0092	0.0105
-2.00	0.0000	0.0006	0.0013	0.0019	0.0026	0.0033	0.0040	0.0048	0.0056	0.0065	0.0076
-3.00	0.0000	0.0003	0.0008	0.0012	0.0017	0.0021	0.0027	0.0032	0.0038	0.0047	0.0059
-10.00	0.0000	0.0000	0.0001	0.0002	0.0003	0.0005	0.0008	0.0011	0.0014	0.0018	0.0025
$-\infty$	0.0000	0.0000	0.0000	0.0000	0.0000	0.0000	0.0000	0.0000	0.0000	0.0000	0.0000

REFERENCES

1. Payne, P. R.: A Stiff Hinged Helicopter Rotor. Aircraft Engineering, vol. 27, no. 321, Nov. 1955, pp. 358–370.

2. Young, Maurice I.: A Simplified Theory of Hingeless Rotors With Application to Tandem Helicopters. Proceedings of the 18th Annual National Forum of the American Helicopter Society, Washington, D. C., May 1962, pp. 38–45.

3. Sissingh, G. J.: Dynamics of Rotors Operating at High Advance Ratios. J. Amer. Helicopter Soc., vol. 13, no. 3, July 1968, pp. 56–63.

4. Bramwell, A. R. S.: A Method for Calculating the Stability and Control Derivatives of Helicopters With Hingeless Rotors. Research Memorandum Aero 69/4, Dept. of Aeronautics, The City University, London, 1969.

5. Shupe, N. K.: A Study of the Dynamic Motions of Hingeless Rotored Helicopters. Ph.D. Thesis, Princeton Univ., Sept. 1972; also R&D Tech. Rept. ECOM-3323 (AD 71302).

6. Curtiss, H. C., Jr.; and Shupe, N. K.: A Stability and Control Theory for Hingeless Rotors. Proceedings of the 27th Annual National Forum of the American Helicopter Society, Washington, D. C., Aug. 1971.

7. Ormiston, Robert A.; and Peters, David A.: Hingeless Helicopter Rotor Response With Nonuniform Inflow and Elastic Blade Bending. J. Aircraft, vol. 9, no. 10, Oct. 1972, pp. 730–736.

8. Sissingh, G. J.; and Kuczynski, W. A.: Investigations of the Effect of Blade Torsion on the Dynamics of the Flapping Motion. J. Amer. Helicopter Soc., vol. 15, no. 2, April 1970, pp. 2–9.

9. Hohenemser, K. H.; and Yin, S. K.: On the Question of Adequate Hingeless Rotor Modeling in Flight Dynamics. Preprint 732, presented at the 29th Annual National Forum of the American Helicopter Society, Washington, D. C., May 1973.

10. Huber, H. B.: Effect of Torsion-Flap-Lag Coupling on Hingeless Rotor Stability. Preprint 731, presented at the 29th Annual National Forum of the American Helicopter Society, Washington, D. C., May 1973.

11. Wheatley, John B.: An Aerodynamic Analysis of the Autogiro Rotor With a Comparison Between Calculated and Experimental Results. NACA Rept. 487, 1934.

12. Bailey, F. J., Jr.: A Simplified Theoretical Method of Determining the Characteristics of a Lifting Rotor in Forward Flight. NACA Rept. 716, 1941.

13. Gessow, Alfred; and Myers, G. C., Jr.: Aerodynamics of the Helicopter. The MacMillan Co., New York, 1952.

14. Seckel, E.; and Curtiss, H. C., Jr.: Aerodynamic Characteristics of Helicopter Rotors. Dept. of Aerospace and Mechanical Sciences Rept. 659, Princeton Univ., Dec. 1963.

15. Arcidiacano, P. J.; Jenney, D. S.; and Smith, A. F.: A Linearized Theory for the Estimation of Helicopter Characteristics at Advance Ratios Above 1.0. Proceedings of the 195h Annual National Forum of the American Helicopter Society, Washington, D. C., May 1963.

16. Bielewa, R. L.: A Second Order Non-Linear Theory of the Aeroelastic Properties of Helicopter Rotor Blades in Forward Flight. Ph.D. Thesis, Massachusetts Institute of Technology, 1965.

17. Houbolt, John C.; and Brooks, George W.: Differential Equations of Motion for Combined Flapwise Bending, Chordwise Bending, and Torsion of Twisted Nonuniform Rotor Blades. NACA Rept. 1346, Oct. 1956.

18. Meirovitch, Leonard: Analytical Methods in Vibrations. The MacMillan Co., New York, 1967.

19. Peters, D. A.; and Hohenemser, K. H.: Application of the Floquet Transition Matrix to Problems of Lifting Rotor Stability. J. Amer. Helicopter Soc., vol. 16, no. 2, April 1971.

20. Peters, D. A.: Hingeless Rotor Frequency Response With Unsteady Inflow. Proceedings of Specialists' Meeting on Rotorcraft Dynamics, American Helicopter Society and NASA/Ames Research Center, Moffett Field, Calif., Feb. 13–15, 1974, p. 12.

21. Bisplinghoff, Raymond L.; Ashley, Holt; and Halfman, Robert L.: Aeroelasticity. Addison Wesley Pub. Co., Cambridge, Mass., 1955.

22. Hildebrand, F. B.: Advanced Calculus for Applications. Prentice Hall, Englewood Cliffs, New Jersey, 1962.

23. Peters, D. A.: An Approximate Solution for the Free Vibrations of Rotating Uniform Cantilever Beams. NASA TM X-62,299, Sept. 1973.